



**ELECTRO-PULSE-ENHANCED  
CANCER THERAPY**

**BERTIL R. R. PERSSON**

# Electro-Pulse- Enhanced Cancer Therapy



# Electro-Pulse- Enhanced Cancer Therapy

By

Bertil R.R. Persson

**Cambridge  
Scholars  
Publishing**



Electro-Pulse-Enhanced Cancer Therapy

By Bertil R.R. Persson

This book first published 2020

Cambridge Scholars Publishing

Lady Stephenson Library, Newcastle upon Tyne, NE6 2PA, UK

British Library Cataloguing in Publication Data

A catalogue record for this book is available from the British Library

Copyright © 2020 by Bertil R.R. Persson

All rights for this book reserved. No part of this book may be reproduced, stored in a retrieval system, or transmitted, in any form or by any means, electronic, mechanical, photocopying, recording or otherwise, without the prior permission of the copyright owner.

ISBN (10): 1-5275-4627-6

ISBN (13): 978-1-5275-4627-1

# TABLE OF CONTENTS

Abstract .....	vi
Acknowledgements .....	viii
Chapter I .....	1
Introduction	
Chapter II.....	5
Biophysical Principles of <i>EpECT</i>	
Chapter III .....	26
Electro- Dosimetry	
Chapter IV .....	55
Gamma Camera Studies of Electro-Pulse Enhanced Drug Uptake	
Chapter V .....	69
Preclinical Studies of Electro-Pulse Enhanced Therapy	
Chapter VI.....	89
Clinical Studies of Electro-Pulse-Enhanced Chemotherapy	
Chapter VII.....	148
Safety of Electro Enhanced Chemotherapy	
Chapter VIII .....	157
New Dimensions for Electro-Pulse-Enhanced Cancer-Therapy	
References .....	170
Index .....	202

# ABSTRACT

This book is a summary of my 30 years' experience of electro-pulse-enhanced-therapy in the treatment of malignant tumours.

The first chapter is a short history of the discoveries that led to the clinical use of electro-pulse-enhanced cancer therapy (EpECT). In the late 1960s, Sale found that the action of inducing short electric pulses upon biological cell membranes made them transiently permeable without damaging the membrane structures. In the 1970s, Zimmermann observed that red blood cells began to lose haemoglobin after exposure to a pulsed electric field that exceeded a certain threshold. Exposure to short electrical pulses with amplitudes between 4 and 6 kV/cm resulted in the cells melting together into larger cells containing several nuclei. In the 1980s, Neumann and Wong demonstrated that electrical field-mediated transfer of DNA into cells is a handy technique, simple and easy to apply for DNA transfection. Okino and Mohri reported in 1987 the possibility of using the electroporation effect for enhanced transport of the anticancer drug Bleomycin across the cell membrane. The first clinical trial with EECT was performed on head and neck tumours by L. Mir and colleagues in France, 1991.

The second chapter describes the electrochemical and biophysical principles of the action of high voltage electrical pulses applied to human cells and tissues. The creation of channels in the cell-membrane, usually called electroporation, is the main phenomenon considered in electro-enhanced chemotherapy. However, electrochemical processes may also be involved.

My profession is in medical radiation physics, where radiation dosimetry is the most critical issue in radiation therapy. Thus, I considered it essential to know for certain the amount of energy delivered to the patient in electro-pulse enhanced cancer therapy as well.

The third chapter describes the measurement of the change in the electrical impedance of the tissue as an excellent way to estimate the energy delivered to the tissue through exposure to electrical high voltage pulses.

Another branch of my profession is the use of radio-pharmaceuticals to study the morphology and function of various human organs. As such, the fourth chapter describes the use of radioactive labelled drugs and gamma-camera recording to explore the enhanced uptake of drugs after exposure to electric pulses. Multivariate statistical methods are used to predict the

dependence of drug uptake in the exposed and non-exposed tissue on several variables

The fifth chapter summarizes the results of numerous preclinical studies of electro-pulse enhanced cancer therapy. Bleomycin and Cis-platinum are the drugs mainly used in clinical applications of such therapy. The results of extensive preclinical studies are shown to indicate promising combinations of electro-pulse chemotherapy with established immune therapy and radiation therapy regimes.

As mentioned above, the first clinical trial using Bleomycin and electric pulse treatment (called “electro-chemotherapy” (ECT)) was performed on head and neck tumours by Mir and colleagues in France in 1991. In the following years (up until 2018), clinical trials have treated more than 1500 patients with malignant melanoma, Kaposi’s sarcoma, breast cancer, squamous cell carcinoma, and basal cell carcinoma. The sixth chapter reviews and analyses the clinical results of these trials.

The seventh section discusses the safety concerns that must be taken into account when treating patients with high voltage electrical pulses.

The eighth, and final, part of the book presents a summary of potential new dimensions in electro-pulse enhanced Cancer therapy.



## ACKNOWLEDGEMENTS

This book is dedicated to my collaborators in the field of electro-pulse-enhanced cancer therapy (EpECT) over the past 30 years: Leif G. Salford, MD, Professor of Neuro Surgery at Lund University, who opened his laboratory for the first experiments with malignant glioma implanted in rat brains; Louis Mir who supported us with a French electroporation device for animal experiments which led to the publication of “A new brain tumour therapy with EpECT”; Per Henriksson for the “Zero Weed” adventure; Maria Danfelter MSc, for her dedicated pioneering work with cell survival; Per Engström, PhD, for his eminent pre-clinical pioneering work, a strong thesis, and for conducting the first clinical operations with EpECT; Catrin Bauréus-Koch, PhD, for her dedicated work in the extensive rat experiments using radiation and immune therapy combinations, and her exquisite thesis; Gustaf Grafström, PhD, for his skilful operations in the extensive rat experiments; Susanne Strömblad and Catarina Blennow, for their skilful technical assistance in the animal experiments and histology preparations; Bernt Böhmer, engineer and entrepreneur, for his skilful constructions and manufacturing of our various electro-pulse devices; Anders Johnsson, for promoting the gamma camera experiments, and Mohan Frick for bringing electro-pulse-enhanced cancer therapy to the market.

The authors wish to thank the QuickField support team for the temporary license of the program, Version 6.3.2 (Tera Analysis Ltd. <http://quickfield.com>), without which this work summarized in chapter 3.5 could not have been performed.

# CHAPTER I

## INTRODUCTION

### 1.1 ELECTROPORATION OF BIOLOGICAL CELL MEMBRANES

In the late 1960s, Sale found that the action of short electric pulses upon biological cell membranes made them transiently permeable without damaging the membrane structures.<sup>1</sup> When he applied high electric fields up to 25 kV/cm to suspensions of the cells, the potential difference across the membrane of the spherical cell increased. This phenomenon caused conformational changes to occur in the membrane structure, resulting in the loss of its semipermeable properties and lysis of the cells.<sup>2</sup>

Another researcher later found that electric impulses cause transient permeability changes in the membranes of vesicles storing biogenic amines which may lead to stimulated neuro-humoral secretion.<sup>3</sup> Studies of cell membranes in *Escherichia coli* B163 and B525 demonstrated dielectric breakdown using a Coulter counter, with hydrodynamic jet currents focusing close to the orifice of the counter. By plotting the relative pulse height for compensated amplification of a certain size of the cells against increasing detector current, the transcellular ion flow showed differences for the potassium-deficient mutant B525 in comparison with the wild-type B163, indicating a change in the membrane structure of B525.<sup>4</sup>

Researchers also observed that red blood cells began to lose haemoglobin after exposure to a pulsed electric field when the strength of the field exceeded a certain threshold. The haemoglobin fraction found in the supernatant was designed against the outer electric field strength, and resulted in the classic sigmoid curve characterizing the dielectric decomposition of mammalian cell membranes. They discovered that very short (<1ms), high voltage pulses can dramatically increase the permeability of cell membranes.<sup>5</sup>

Reversible electrical degradation of cell membranes is the fundamental cause of electro-permeabilization (also referred to as electro-injection or electroporation). Local degradation of the cell membrane occurs when the membrane potential exceeds 1V at room temperature and 2V at 4°C. The

breakdown voltage depends on the duration of the pulse. A short pulse ( $<1 \mu\text{s}$ ) causes transient decomposition at 1V, while a pulse of a longer duration than 10ms causes transient decomposition at 0.5 V. At pulses over 50-100  $\mu\text{s}$ , degradation causes irreversible cellular membrane destruction, leading to cell death.<sup>5,6,7,8,9,10</sup>

## 1.2 ELECTROFUSION OF BIOLOGICAL CELLS

Exposure of the microorganism *Dictyostelium discoidea* to short (40ps) electrical pulses with amplitudes between 4 and 6 kV/cm resulted in the cells melting together, forming larger cells containing more than 40 nuclei of cells evenly as they lyse.<sup>11</sup>

Red blood cells exposed to an electrically flawed AC with an amplitude of 2.5kV/cm and frequencies between 0.5 and 2 MHz were found to form chains of cells between the electrodes which remain after exposure, and which might lead to a possibility of cell fusion.<sup>12</sup> Zimmerman and colleagues applied this phenomenon to the inclusion of cells of various origins utilizing electrical degradation of cell membranes. This experiment resulted in hybrid cells that joined the properties of two varied cells into a single cell.<sup>13,14,15,16,17,18,19</sup>

The fusion rate of yeast cells treated with polyethylene glycol and  $\text{Ca}^{2+}$  ions and exposed to a high electric field (2.5 - 5 kV.cm<sup>-1</sup>) increased by a factor of about 200 for different strains of yeast *saccharomyces cerevisiae*, as opposed to fusion without electric field exposure. This method enables the production of a large number of cell hybrids for various purposes.<sup>20,21</sup>

## 1.3 ELECTRO-PULSE ENHANCED DNA TRANSFECTION

Compared to biochemical techniques, electric field mediated transfer of DNA into cells is beneficial, and simple and easy to apply for DNA transfection.<sup>22</sup> When exposing plasmid DNA containing the herpes simplex thymidine kinase (TK) gene and mouse L-cells lacking the TK gene, to electrical fields (8 kV/cm, 5 $\mu\text{s}$ ), a strong expression of TK-DNA was found in the mouse cells.<sup>23</sup> A possible model for the transfer of DNA-plasmids into cells by electroporation is an electro diffusive migration of DNA through the electroporated membrane.<sup>24</sup>

The effects of exposure of biological cells to high-voltage electric pulses have so far been explored in terms of electrofusion used for the production of cell hybrids and monoclonal antibody production, or electroporation induced DNA transport across the cell membrane.<sup>11,25,22,23 5521</sup>

## 1.4 ELECTRO-PULSE ENHANCED CHEMO-THERAPY *EpEChT*

Okino and Mohri (1987) first reported the possibility of using the electroporation effect for enhanced transport of the anticancer drug across the cell membrane.<sup>26</sup> They treated hepatocellular carcinoma (AH-109A) in rats through an administration of 5 mg of Bleomycin intra-muscularly and exposed the tumours to an electric pulse with an amplitude of 5 kV/cm and a duration of 2 ms. Four days after the treatment, the tumour size had decreased significantly, while tumours treated with electric impulses or Bleomycin alone showed no decrease in growth. Okino and Mohri suggested that electro-enhanced chemotherapy should produce better results than chemotherapy alone.<sup>26,27</sup>

## 1.5 CLINICAL ELECTRO ENHANCED CHEMO-THERAPY (*EpECT*)

The first clinical trial with *EpECT* was performed on head and neck tumours by Mir and colleagues in France in 1991.<sup>28</sup> In 1998 the Swedish Radiologist Dr Nordenström at the Karolinska Institute in Stockholm, developed electrochemical therapy (EChT) as a minimally invasive electrotherapeutic technique, using direct current for the treatment of cancer and haemangioma tumours.<sup>29</sup>

Application of electric pulses in vivo used to augment the chemotherapeutic efficiency in cancer treatment has commonly been referred to as electrochemotherapy and is abbreviated as ECT. However, this abbreviation is also associated with electro-convulsive therapy, as used in psychiatry for the treatment of depression. In this book, *EpECT* is used as an abbreviation for *electro-pulse-enhanced cancer therapy*, while electro-pulse enhanced chemotherapy is abbreviated as *EpEChT*.<sup>30</sup> This latter is a mode of *EpECT* tumour treatment that has been employed mostly for subcutaneous and cutaneous malignancies.<sup>31,32</sup> However, it is also employed to treat soft-tissue sarcomas<sup>33</sup>, glioma in the brain<sup>34</sup>, liver tumours<sup>35,36,37</sup> and tumours in the pancreas,<sup>38</sup> and has shown auspicious results.

In electro-pulse enhanced chemotherapy treatment, only cells exposed to strong electric fields respond immediately. The permeabilized tumour cells become much more accessible to hydrophilic molecules since the lipophilic membrane barrier generally rejects these. Bleomycin, a very toxic anticancer agent, has proven to be a particularly efficient drug in *EpEChT*, and is by far the most often used, but Cisplatin, another anticancer agent, has also been found to be effective.

Chapter II reviews the electrochemical and biophysical principles of pore formation. In the clinical use of electro-pulse-enhanced chemotherapy, it is important to control the exposure of the patient to an electric field.

Chapter III discusses electro-dosimetry, the measurements of the absorbed energy in a tumour through the electric pulse treatment.

In Chapter IV, radioactive tracers and gamma-camera measurements are employed to explore the effect of the enhanced accumulation of administered drugs in the treatment area.

In Chapter V, various preclinical studies of electro-enhanced cancer therapy are reviewed, as are trials using both Bleomycin, Cis-Platin and other drugs, as well as their combinations.

In chapter VI clinical studies of electro-enhanced cancer therapy using various devices are reviewed, considering both Bleomycin, Cis-Platin, other drugs, and their combinations.

The safety aspects of performing clinical electro-enhanced cancer therapy are discussed in chapter VII. The closing chapters then detail new dimensions of EpECT to summarize the clinical potential in applying electro-pulse treatment to enhance the effect of established cancer therapy regimes.

# CHAPTER II

## BIOPHYSICAL PRINCIPLES OF *EPECT*

### 2.1 CELL MEMBRANE

Cell membranes with a thickness of about 7 to 10 nano-m enclose all single cells in the body. The cell membrane is made up of a double layer of phosphorous glycerides, consisting of phosphoric acid and fatty acids (see Figure 2-1a). The end of these molecules with the hydrophilic phosphoric acid (which attracts water) cover each side of the cell membrane, while the other ends of long-chain hydrocarbon chains that are hydrophobic (water repellent) fill the space between the hydrophilic surface layers (see Figure 2-1b).

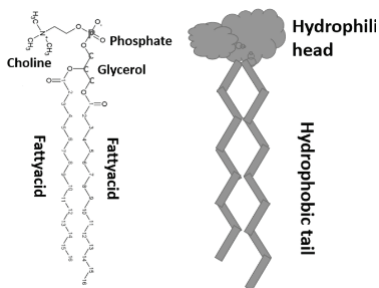


Figure 2-1a  
Phosphorous glycerides consisting of phosphoric acid and fatty acids

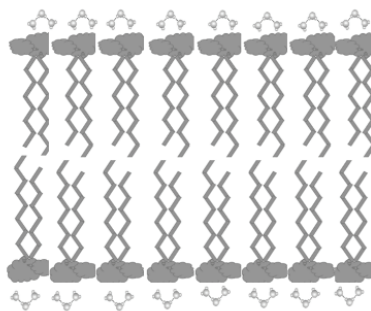


Figure 2-1b  
The hydrophilic phosphoric acid (which attracts water) covers each side of the cell membrane, while the other end of long fatty acid hydrocarbon chains that are hydrophobic (water repellent) fills the space between the surface layers.

This structure of the cell membrane creates an electrically insulating double layer of phosphorous glycerides. For the cell to communicate with the environment, there are a large number of various proteins embedded in

the cell membrane. A group of these proteins consists of channel proteins transporting distinct ions through their channels. The difference in concentrations of positive sodium, potassium, calcium ions and negative chloride ions on either side creates a membrane potential that is the basis for the emergence of bioelectric phenomena.

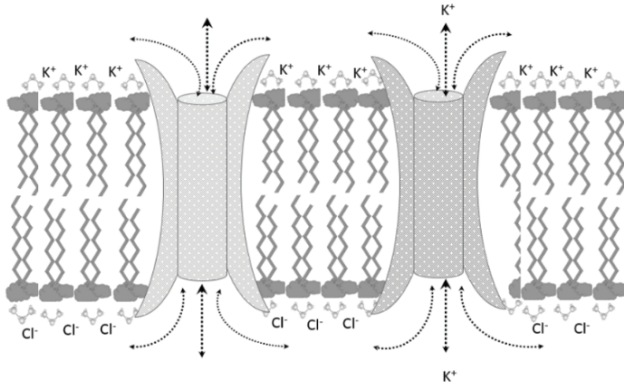


Figure. 2-2

The structure of a cell membrane consists of two lipid layers, with hydrophilic phosphate groups on the surface and hydrophobic fatty acid tails which fill the space inside the membrane. The channel protein embedded in the membrane transports sodium, potassium, calcium and chloride molecules through the membrane. This structure, with differences in ion concentrations on either side of the membrane, generates the membrane potential and the appearance of bioelectric phenomena.

## 2.2 MEMBRANE POTENTIAL

Differences in the concentrations of ions on opposite sides of a cellular membrane create an electrical potential called the Nernst potential ( $U_{ion}$ ), determined by the charge on the ion  $q_{ion}$  and the ion-concentrations on the inside and outside of the cell.

$$U_{ion} = \frac{R \cdot T}{q_{ion}} \ln \frac{\{\text{ion concentration outside the cell}\}}{\{\text{ion concentration inside the cell}\}} \quad \text{Eq. 2.1}$$

Sodium ( $\text{Na}^+$ ) and chloride ( $\text{Cl}^-$ ) ions appear in high concentrations on the extracellular side of the membrane and in low concentrations on the intracellular side. The concentration of potassium in normal rest conditions is usually about 30-50 times higher inside the cell compared to outside. Potassium ions, therefore, strive to flow out of the cell and accumulate on the outside of the membrane. As the negative charged  $q^-$  ions remain in the cell (mainly chloride), accumulating on the inside of the membrane, an electric field directed into the cell develops through the outflow of positively  $q^+$  charged potassium. This condition continues until the force created by the electric field ( $\vec{F} = \vec{E} \cdot q^+$ ), which is directed inwards, inhibits the outbound transport of potassium ions. The electric potential,  $\Phi$ , is the amount of work needed to move a positive unit charge,  $q^+ = 1$ , a distance  $\Delta\ell$  inside the electric field  $E$  without producing any acceleration. The work of moving the  $\text{K}^+$  ions a distance  $\Delta\ell$  in the  $E$  field inside the membrane is thus:

$$\vec{F} \cdot \Delta\ell = \vec{E} \cdot \Delta\ell \cdot q^+ = \Delta\Phi \quad \text{Eq. 2.2}$$

The potential energy  $\Delta\Phi$  is equal to the difference between the membrane potential  $\Phi_M$  and the Nernst potential for the potassium ion  $\Phi_K$ ,  $\Delta\Phi = \Phi_M - \Phi_K$ . At equilibrium, the potential energy is zero,  $\Delta\Phi = 0$  and  $\Phi_M = \Phi_K$ .

The general Nernst equation for an arbitrary ion  $\kappa$  is:

$$\Phi_i - \Phi_e = \Phi_\kappa = -\frac{R \cdot T}{q_\kappa \cdot F} \cdot \ln \frac{C_I^\kappa}{C_E^\kappa}; [V] \quad \text{Eq. 2.3}$$

where

$\Phi_i$  = potential on the inner side of the membrane;

$\Phi_e$  = potential on the external side of the membrane;

$\Phi_\kappa$  = equilibrium potential for the  $\kappa^{\text{th}}$  ion across the membrane  $\Phi_i - \Phi_e$  i.e., the Nernst potential  $U_\kappa$  [V];

$R$  = gas constant [8.314 J/(mole·degree Kelvin)];

$T$  = absolute temperature [degree Kelvin];

$q_\kappa$  = valence of the  $k^{\text{th}}$  ion;

$F$  = Faraday's constant [ $9.649 \cdot 10^4$  As/mole];

$C_I^\kappa$  = intracellular concentration of the  $\kappa^{\text{th}}$  ion;

$C_E^\kappa$  = extracellular concentration of the  $\kappa^{\text{th}}$  ion.

The potential that occurs is called the membrane potential, and is in the order of -40 mV to -70 mV. By introducing a temperature of 37 °C, which corresponds to  $T = 273 + 37$  °Kelvin,  $q=+1$  for the valence of the potassium ion, and replacing the natural logarithm ( $\ln$ ) with the tenth logarithm ( $\log_{10}$ ), the equation for a monovalent cation ( $q=+1$ ) can be written as:



$$\Phi = -61 \cdot \log_{10} \frac{C_I}{C_E} [mV] \quad \text{Eq. 2.4}$$

- The equilibrium's potential for potassium( $q=+1$ )  $\Phi_K$  is -88 mV at an intra-cellular potassium concentration of 140mM and an extracellular concentration of 5 mM.
- The equilibrium's potential for sodium( $q=+1$ ),  $\Phi_{Na}$ , is +61 mV at an intra-cellular sodium ion concentration of 14mM and an extracellular concentration of 140 mM.
- The equilibrium's potential for chloride( $q=-1$ ),  $\Phi_{Cl}$ , is -69 mV at an intra-cellular chloride ion concentration of 8mM and an extracellular concentration of 110 mM.
- The equilibrium's potential for calcium( $q=+2$ )  $\Phi_{Ca}$ , is +140 mV at an intra-cellular calcium ion concentration of 0.1  $\mu$ M and an extra-cellular concentration of 4mM

The interactions that generate the total rest potential are modelled by the Goldman equation, which is similar to the Nernst equation shown above. The Goldman equation considers the charges of the current ions as well as the difference between their internal and external concentrations. However, it also takes into account every  $\kappa^{\text{th}}$  ion's relative permeability  $P_K$  of the plasma membrane.

$$\Phi_M = \frac{R \cdot T}{F} \cdot \ln \left( \frac{P_K \cdot C_E^K + P_{Na} \cdot C_E^{Na} + P_{Cl} \cdot C_I^{Cl}}{P_K \cdot C_I^K + P_{Na} \cdot C_I^{Na} + P_{Cl} \cdot C_E^{Cl}} \right) \quad \text{Eq. 2.5}$$

In excitatory cells (nerve and muscle cells), the membrane potential is usually around -60 mV.

### 2.3 MEMBRANE EXPOSED TO ELECTRIC DC FIELD

The electric field  $E$  is written as the derivate of the electric potential,  $\Phi$ ,

$$E = -\frac{d\Phi}{dr} \text{ in vector form } \vec{E} = \text{grad}\Phi = \nabla\Phi \quad \text{Eq. 2.6}$$

Then, by Coulomb's and Gauss's laws, we get Poisson's equation

$$E = \frac{1}{4\pi \cdot \epsilon_0} \frac{q}{r^2} = -\frac{d\Phi}{dr} ; \frac{dE}{dr} = -\frac{d^2\Phi}{dr^2} \approx \frac{\rho}{\epsilon_0} ; \quad \text{Eq. 2.7}$$

$$\text{Alternatively, in vector sign } -\nabla^2\Phi = \frac{\rho}{\epsilon_0} ; \quad \text{Eq. 2.8}$$

where:

$\rho$  is the charge density (including bound charge)

$\epsilon_0$  is the permittivity =  $8.854187817... \times 10^{-12} \text{ F} \cdot \text{m}^{-1}$  (farads per metre).

When applying an external electric field, the superposed membrane potential is related to the charge density by Poisson's equation (as in Eq. 2.8). Where no charges are involved, solutions of the Laplace equation (Eq. 2.9) give the electric field in the extracellular and intracellular space.

$$\nabla^2 \Phi = 0 \quad \text{Eq. 2.9}$$

We assume that the model of a spherical cell according to Figure 2-3 has an inner radius **a** and an outer radius **b** with the membrane thickness **d**. The conductivity of the cell's internal material (cytoplasm) is  $\sigma_I$ , the cell membrane  $\sigma_M$  and the extracellular fluid  $\sigma_E$ .<sup>5</sup> The electrical potential in the corresponding areas is assumed to be  $\Phi_I$ ,  $\Phi_M$ , and  $\Phi_E$ .

Figure 2-3 shows a model of a cell as a layered lossless dielectric sphere subjected to a uniform electric field  $\vec{E} = E \cdot \vec{x}$ . The concentric outer shell and inner core have conductivities  $\sigma_I$  and  $\sigma_M$  respectively, and the outer radius is **b** and the inner radius **a**. The solutions to the Laplace equation (2.9) for the electric potentials in the three regions I, M and E are assumed to be as follows:

$$\Phi_E(r, \theta) = \left(-E \cdot r + \frac{B}{r^2}\right) \cdot \cos \theta; \text{ for } r > b \quad \text{Eq.2.10a}$$

$$\Phi_M(r, \theta) = \left(-B \cdot r + \frac{C}{r^2}\right) \cdot \cos \theta; \text{ for } b > r > a \quad \text{Eq.2.10b}$$

$$\Phi_I(r, \theta) = -D \cdot r \cdot \cos \theta; \text{ for } r < a \quad \text{Eq.2.10c}$$

where

$$\Phi_I=0, \Phi_M=A \cdot r \cdot \cos \theta, \text{ and } \Phi_E=\frac{B}{r^2} \cdot \cos \theta$$

The border conditions for the two interfaces  $r=a$  and  $r=b$  are as follows:

$$\Phi_I(a) = \Phi_M(a) \text{ and } \left(\sigma_I/a\right) \left(d\Phi_I/dr\right) = \left(\sigma_M/a\right) \left(d\Phi_M/dr\right) \quad \text{Eq. 2.11a}$$

$$\Phi_M(b) = \Phi_E(b) \text{ and } \left(\sigma_M/b\right) \left(d\Phi_M/dr\right) = \left(\sigma_E/b\right) \left(d\Phi_E/dr\right) \quad \text{Eq. 2.11b}$$

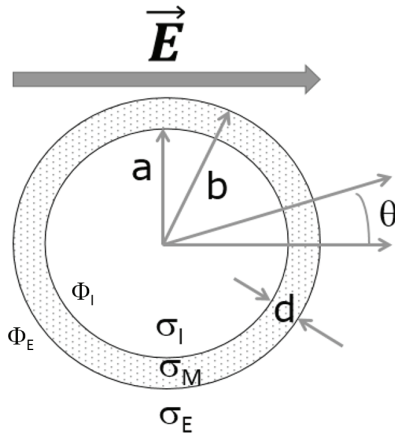


Figure 2-3

An applied external electric field  $\vec{E}$  on a spherical cell with the inner radius  $a$ , and the outer radius  $b$  with the membrane thickness  $d$ . The conductivity of the cell's internal material (cytoplasm) is  $\sigma_I$ , the cell membrane  $\sigma_M$  and the extracellular fluid  $\sigma_E$ .<sup>5</sup>

With these assumptions, the conductivity for the cytoplasm ' $\sigma_I$ ' is about the same as the extracellular space 'i.e.  $\approx \sigma_E$ ', and is much larger than the cell membrane 'i.e.  $\gg \sigma_M$ '. The Laplace equation gives the following expression for the part of the potential difference  $\Delta\Phi_M$  across the membrane depending upon the externally applied electric field  $E_0$ .<sup>5</sup>

$$\Delta\Phi_M = 1.5 \cdot b \cdot E_0 \cdot \cos \theta \quad \text{Eq.2.12}$$

If, for non-spherical cells, ' $1.5 \cdot \cos \theta$ ', is replaced by a form factor  $f$ , the equation for  $\Delta\Phi_M$  becomes:

$$\Delta\Phi_M = f \cdot b \cdot E_0 \quad \text{Eq.2.13}$$

For a cell with the shape of an ellipsoid of length  $L$  and width  $B$ , the form factor  $f$  becomes  $f = L / (L - 0.33 \cdot B)$ .<sup>5</sup> At an externally applied field strength of 4400 V/cm, which corresponds to a membrane potential of 1.5 V in bovine red blood cells with an average radius of 2.2  $\mu\text{m}$ , a dielectric degradation of the membrane occurred, which caused a 50% leakage of haemoglobin.<sup>5</sup> Cancer cells, which may be 10 times larger in diameter, can achieve the conditions for a dielectric breakdown at a membrane potential of 1.5 V, already around 400 V/cm.<sup>39,40</sup>

## 2.4 ELECTRIC PULSE PARAMETERS AND FREQUENCY

### 2.4.1 ELECTROPORATION WITH PULSED AC FIELDS

When an AC-field is applied to cell membranes, the induced trans-membrane potential becomes strongly dependent upon the frequency of the applied field; when the frequency approaches the relaxation time ' $\tau$ ' of the

membrane. Schwan (1983) derived a relationship from the basic electromagnetic theory for the calculation of the trans-membrane potential ' $\Delta\psi_{membrane}$ ' induced by an oscillating electric field ' $E_{applied}$ '.<sup>41</sup>

$$\Delta\psi_{membrane} = \frac{1.5 \cdot r \cdot E_{applied} \cdot \cos \theta}{\sqrt{1 + (\omega \cdot \tau)^2}} \quad \text{Eq.2.14}$$

$$\tau = r \cdot C_{membrane} \cdot (\rho_{internal} + \rho_{external}/2) \quad \text{Eq.2.15}$$

where

$\omega$	$\omega=2\pi f$ ; Angular frequency (rad.s <sup>-1</sup> )
$f$	Frequency (Hz)
$C_{membrane}$	Specific capacitance of the membrane (F.m <sup>-2</sup> )
$\rho_{internal}$	Resistivity of the internal medium ( $\Omega$ .m)
$\rho_{external}$	Resistivity of the external medium ( $\Omega$ .m)
$E_{applied}$	$=E_{applied}^0 \cdot \sin(\omega t)$ Applied field strength V.m <sup>-1</sup>
$t$	Time(s)
$r$	Radius of the cell

The maximum membrane potential induced by an applied AC field is:

$$\Delta\psi_{membrane}^{max} = \frac{1.5 \cdot r \cdot E_{applied}^0}{\sqrt{1 + (\omega \cdot \tau)^2}} \quad \text{Eq. 2.16}$$

$$\Delta\psi_{membrane}^{max} = \frac{1.5 \cdot r \cdot E_{applied}^0}{\sqrt{1 + (2\pi f \cdot \tau)^2}} \quad \text{Eq. 2.17}$$

The concept of electroporation using reactively-coupled AC-fields of kilohertz frequencies is attractive, because it may enable the use of non-invasive electrodes capable of producing electric fields of sufficient strength and depth in tissue to enhance cellular uptake of drugs, thus avoiding the need for invasive needle electrodes, and also reducing the likelihood of painful neural stimulation.

Under physiological conditions, a typical value of the capacitance of the cell membrane is in the order of  $C_m = 10^{-2}$  F.m<sup>-2</sup>. The values of the resistivity values  $\rho_{internal}$ ,  $\rho_{external}$  are in the order of 1  $\Omega$ .m. The typical radius 'r' of human cells are in the order of  $r = 10^{-6}$  -  $10^{-4}$  m. Thus, the frequency limits of the low-frequency potential ranges are in the order of  $10^2$ - $10^3$  kHz.

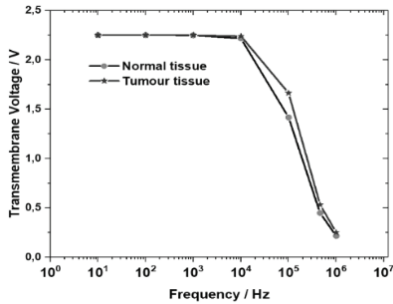


Figure 2-4a  
Theoretical calculation of electric-field induced trans-membrane potential, given an applied field strength of 1000 V/cm.

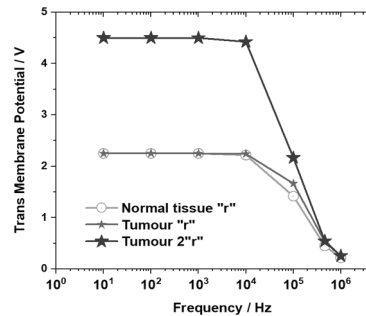


Figure 2-4b  
Theoretical calculation of electric-field induced trans-membrane potential, given an applied field strength of 1000 V/cm.

Grosse and Schwan (1992) presented a model for the calculation of cellular trans-membrane potential in the case of very weak electrolytes  $\rho \gg 1 \Omega \cdot \text{m}$ .<sup>42</sup> This model includes the effect of a variety of factors on transmembrane potential (see Figure 2-3), including medium conductivity and permittivity, cell membrane conductance and permittivity, surface admittance, and space charge effects. Measurements of the *ex vivo* electrical conductivity of a normal human liver and metastatic tumour tissue showed that the conductivity of tumour tissue was significantly higher over the entire frequency range (10 Hz to 1 MHz), with more pronounced differences at lower frequencies.<sup>43</sup>

The Foundation for Research on Information Technologies in Society (ITIS) has an excellent database for the dielectric properties of various human tissues:

<https://www.itis.ethz.ch/virtual-population/tissue-properties/database/dielectric-properties/>

In Table 2-1, the conductivity (S/m) and resistivity ( $\Omega \cdot \text{m}$ ) are given for muscle tissue derived from the ITIS database. According to reported experimental results, the values for tumours are predicted to differ from those for muscles by a factor of about 3 in the frequency range of 10-200 kHz.<sup>44,43</sup> Fitting actual ratios to frequency according to the data of Haemmerich et al. (2009) results in the following Gauss equation:

$$\frac{\sigma_{Tum}}{\sigma_{NT}} = 5.66756 - \frac{10.19901}{2.1077 \cdot \sqrt{\pi/2}} * e^{-2 * \left[ \frac{\log_{10}(f) - 5.73715}{2.1077} \right]^2} \quad \text{Eq. 2.18}$$

where:

$\sigma_{Tum}$	= Conductivity of tumour tissue;	S/m
$\sigma_{NT}$	= Conductivity of normal muscle tissue;	S/m
f	= Frequency;	Hz

In Table 2-1, the conductivity values for muscle tissue are derived from the ITIS database, and estimated values for tumour tissue are provided by applying the equation Eq. 2.18 to the muscle tissue data.

**Table 2-1**

The conductivity (S/m) and resistivity ( $\Omega.m$ ) for muscle and tumour tissue.

Frequency kHz	Muscle S/m	Tumour S/m	Muscle $\Omega.m$	Tumour $\Omega.m$
10	0.341	1.594	2.933	0.627
20	0.345	1.429	2.899	0.700
40	0.350	1.227	2.857	0.815
80	0.358	1.018	2.793	0.982
100	0.362	0.957	2.762	1.045
110	0.364	0.933	2.747	1.072
120	0.366	0.911	2.732	1.097
140	0.370	0.876	2.703	1.141
180	0.379	0.830	2.639	1.205
200	0.384	0.815	2.604	1.226

The equations for normal muscle tissue conductivity variation with frequency fitted to the data of the ITIS database in the frequency  $f$  interval 1 - 4000 Hz are as follows:

$$\sigma_m = 0.2 + 0.00003 \cdot f \text{ S/m} \quad \text{Eq.2.19}$$

In the frequency  $f$  interval 4000 – 200 000 Hz:

$$\sigma_m = 0.337 + 3.49 \cdot 10^{-7} \cdot f - 1.45 \cdot 10^{-12} \cdot f^2 + 4.49 \cdot 10^{-18} \cdot f^3 \text{ S/m} \quad \text{Eq.2.20}$$

In Figure 2-4a, calculations are based on Eq. 2.17 with data for normal tissue cellular radius  $r = 15 \mu\text{m}$ , and  $C_m = 0.001 \text{ F.m}^{-2}$ ;  $\rho_{in} = 10 \Omega.m$ ;  $\rho_{ex} = 15 \Omega.m$ . For tumour cellular radius  $r = 15 \mu\text{m}$ , and  $C_m = 0.001 \text{ F.m}^{-2}$ ;  $\rho_{in} = 3.3 \Omega.m$ ;  $\rho_{ex} = 15 \Omega.m$ .<sup>43</sup>

In Figure 2-4b, calculations are based on Eq. 2.17 with normal tissue data for cellular radius  $r = 15 \mu\text{m}$ .

$C_m = 0.001 \text{ F}\cdot\text{m}^{-2}$ ,  $\rho_{in} = 3.5\text{-}13 \Omega\cdot\text{m}$ ,  $\rho_{ex} = 15 \Omega\cdot\text{m}$ , and with tumour tissue data for cellular radius  $r = 15 \mu\text{m}$  or  $30 \mu\text{m}$ ,  $C_m = 0.001 \text{ F}\cdot\text{m}^{-2}$ ,  $\rho_{in} = 1.9\text{-}2.4 \Omega\cdot\text{m}$ , and  $\rho_{ex} = 15 \Omega\cdot\text{m}$ .<sup>43</sup>

In agreement with experimental findings, the theoretical model also predicts that a trans-membrane voltage of sufficient magnitude to cause electroporation appears at an applied field strength of 1200 V/cm at 20 kHz.<sup>45</sup>

A study by Chen et al. (2008) showed that 20–160 kHz in electric fields of peak amplitude 700–2000 V/cm, when applied as a series of short pulses, induce electroporation in cell membrane.<sup>46</sup> Increasing the field strength above 1100 V/cm results in higher cell electroporation efficiency, but increases cell death. In the study, total electroporation yield is only weakly dependent on the frequencies in the frequency range used, although the results suggest a peak of Calcein uptake at 60 kHz. For the parameter values chosen, AC and DC electroporation produced similar yields. Marszalek et al. (1990) studied electroporation in a murine myeloma cell line using AC fields, in the frequency range 100–300 kHz and with field strengths between 500 V/cm and 1500 V/cm.<sup>45</sup>

The study identified a threshold electric field around 600 V/cm using a single pulse of 200ms. However, the article gives no quantitative information about electroporation efficiency and cell viability. The threshold field strength for electroporation in the study of Marszalek et al. (1990) was approximately half of that found through the study by Chen et al. (2008).<sup>45,46</sup>

This result may be due to several factors, including differences in the conductivity of the extracellular medium, pulsing regime, the geometry of the electrodes, the chemistry used to detect electroporation, and cell lines.

The results of Chen et al. (2008) offer conclusive evidence of electroporation using pulsed with AC fields beyond the kilohertz range. The results also suggest an optimal frequency range of 40–120 kHz at a field strength of 1700 V/cm and total exposure time 40ms.<sup>46</sup>

Influenced by these findings of an optimal frequency window for electroporation achievements, the author analysed the frequency content of the various pulse sequences usually used in the protocols for electro-enhanced chemotherapy.

A recent investigation of electroporation with 5 ms bursts of sinusoidal signals in the frequency range of 8 -130 kHz showed that permeabilization appeared at about 100% up to 50 kHz, and then drastically decreased to

about zero above 130 kHz.<sup>47</sup> This result is in solid agreement with the results of the theoretical calculations displayed in Figure 2-4.

## 2.4.2 FOURIER ANALYSIS OF *EpECT* PULSES

The **Fourier analysis** decomposes a pulse  $V(t)$  in the time domain, into the frequencies  $f$  that make up a frequency distribution  $G(f)$ .

### A. A SINGLE RECTANGULAR PULSE

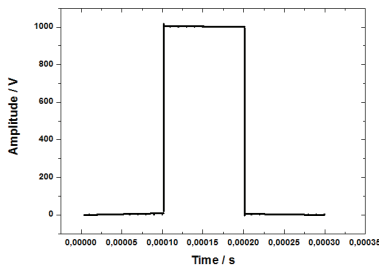


Figure 2-5a  
Single rectangular pulse of 1000 V amplitude, and 100 $\mu$ s pulse-length

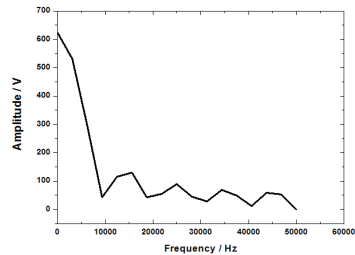


Figure 2-5b  
The positive frequency content of the single rectangular pulse in Figure 2-5a

The result of the Fourier analysis of a single rectangular pulse according to the ESOPE protocol displayed in Figure 2-5b shows that the main content of frequencies is in the low energy range  $< 1$  kHz. In the region of optimal electroporation (30- 120 kHz), there is only a minor content of frequencies.

### B. A PULSE-TRAIN OF RECTANGULAR PULSES

The result of the Fourier analysis of a pulse train of a rectangular pulse according to the ESOPE protocol displayed in Figure 2-6b shows that there is a peak at 5 kHz corresponding to the 200 $\mu$ s wavelength. There is, however, still a large amplitude at low frequencies, which causes nerve excitation and pain, which this study attempted to avoid by using a 5 kHz pulse-train. In the region of optimal electroporation 30 - 120 kHz, there is still only a minor content of frequencies.



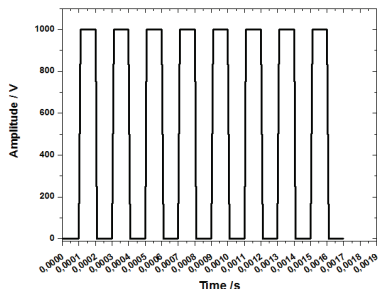


Figure 2-6a  
Pulse-train of 8 rectangular pulses of 1000 V amplitude, 100 $\mu$ s pulse-length and 200  $\mu$ s wave-length (5 kHz).

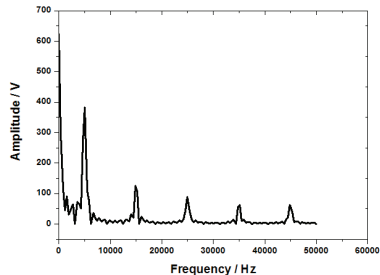


Figure 2-6b  
The positive frequency content of the pulse-train of 8 rectangular pulses in Figure 2-6a

The conductivity for healthy muscle tissue averaged over the positive frequency spectrum of Figure 2-6b for each pulse of the pulse train becomes 0.30 S/m. The specific energy thus delivered to a pulse train of 8 rectangular pulses of 1000 V amplitude and 100 $\mu$ s pulse-length is 2208 J/kg. By applying Eq.2.17, the conductivity of tumour tissue conductivity was estimated to be 1.68 S/m, and the specific energy delivered to a pulse train was put at 12514 J/kg.

### C. A SINGLE EXPONENTIALLY DECREASING PULSE

Figure 2-7b displays an exponentially decreasing pulse of 139  $\mu$ s half-time, 1000 V maximum amplitude, and 100 $\mu$ s pulse-length. The result of the Fourier analysis in Figure 2-7b shows that the main content of frequencies is in a broad peak around 7 kHz, with a substantial contribution in the region of optimal electroporation 30 - 120 kHz.

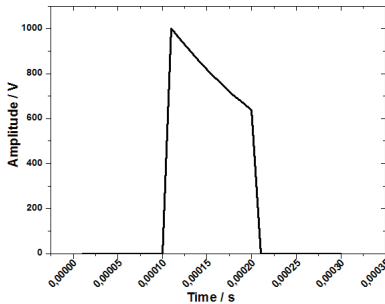


Figure 2-7a  
An exponentially decreasing pulse of 139  $\mu$ s half-time, 1000 V maximum amplitude, and 100 $\mu$ s pulse-length.

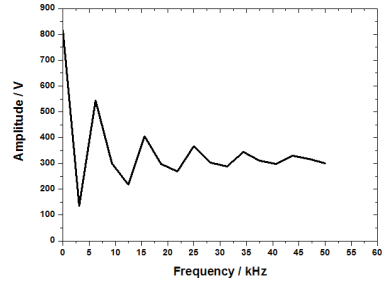


Figure 2-7b  
The positive frequency content of the single exponentially decreasing pulse in Figure 2-7a.

## D. A PULSE TRAIN OF EXPONENTIALLY DECREASING PULSE

Figure 2-8a displays a pulse-train of 8 exponentially decreasing pulses of 139  $\mu$ s half-time, 1000 V maximum amplitude, and 100  $\mu$ s pulse-length. The result of the Fourier analysis displayed in Figure 2-8b shows that the main content of frequencies is in a peak around 5 kHz corresponding to the pulse repetition frequency, and that there are several peaks with a minor contribution in the region of optimal electroporation 30- 120 kHz.

The conductivity for healthy muscle tissue averaged over the positive frequency spectrum of Figure 2-8b for each pulse of the pulse train becomes 0.34 S/m. The energy thus delivered to a pulse train of 8 exponentially decreasing pulses of 139  $\mu$ s half-time, 1000 V maximum amplitude, and 100  $\mu$ s pulse-length is 2030 J/kg. By applying Eq.2.17, the conductivity of tumour tissue conductivity was estimated at 1.94 S/m and the specific energy delivered to a pulse train was put at 11 500 J/kg.

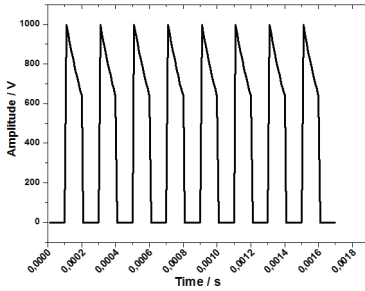


Figure 2-8a  
Pulse train of 8 exponentially decreasing pulses of 139  $\mu$ s half-time, 1000 V maximum amplitude and 100 $\mu$ s pulse-length.

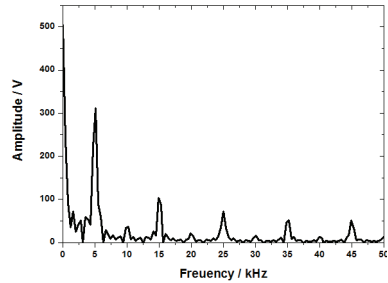


Figure 2-8b  
The positive frequency content of the exponentially decreasing pulse in Figure 2-8a.

### E. SINGLE SINUSOIDAL PULSE AT 10 kHz

Figure 2-9a displays a single sinusoidal pulse of  $\pm 1000$  V max amplitude and 9677.5 Hz frequency corresponding to 103  $\mu$ s pulse-length. The result of the Fourier analysis displayed in Figure 2-9b shows that the main content of frequencies is in a peak around 10 kHz, with a minor contribution of over-tones at a higher frequency.

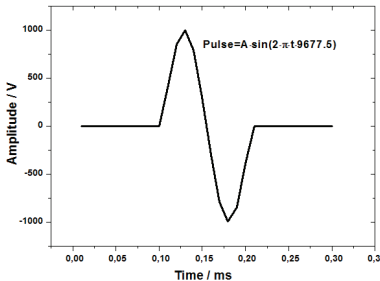


Figure 2-9a  
A sinusoidal pulse of  $\pm 1000$  V max amplitude and 9677.5 Hz frequency corresponding to 103  $\mu$ s pulse-length.

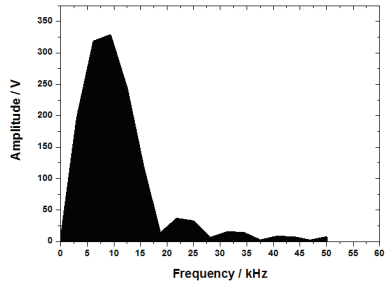


Figure 2-9b  
The positive frequency content of the sinusoidal pulse in Figure 2-9a.

## F. PULSE TRAIN OF 10 KHZ SINUSOIDAL PULSES

Figure 2-10a displays a pulse train of 8 sinusoidal pulses of  $\pm 1000$  V max amplitude and 9677.5 Hz frequency corresponding to 103  $\mu$ s pulse-length. The result of the Fourier analysis displayed in Figure 2-10b shows that the main content of frequencies is in one peak around 5 kHz corresponding to the pulse train frequency and another peak at 10 kHz corresponding to the frequency content of the single pulses. There is also a third peak corresponding to the overtone of the sinusoidal pulse. There are minor contributions in the regions of low frequencies  $< 1$  kHz and of optimal electroporation 30 - 120 kHz.

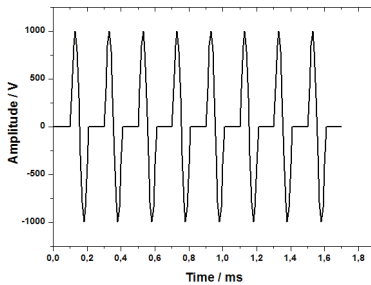


Figure 2-10a  
Pulse-train of 8 sinusoidal pulses of  $\pm 1000$  V max amplitude and 9677.5 Hz frequency corresponding to 100  $\mu$ s pulse-length.

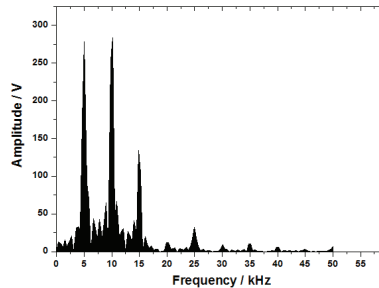


Figure 2-10b  
The positive frequency content of the pulse-train of 8 sinusoidal pulses in Figure 2-10a.

The conductivity for healthy muscle tissue averaged over the positive frequency spectrum of Figure 2-10b for each pulse of the pulse train becomes 0.34 S/m. The energy thus delivered to a pulse train of 8 sinusoidal pulses of  $\pm 1000$  V max amplitude and 9677.5 Hz frequency corresponding to 100  $\mu$ s pulse-length is 1409 J/kg. Thus, this pulse train must have 14 pulses to deliver the same energy as the ESOP protocol of 8 rectangular pulses of 100  $\mu$ s at 5 kHz.

## 2.5 ELECTRO-PORES CREATION AND EVOLUTION FOR DRUG DELIVERY

The application of external electrical fields to biological cells creates initially hydrophobic pores at a rate depending on the absorbed energy.<sup>48,49,50</sup> Smaller pores of radius  $r < 0.5$  nm are rapidly sealed, while

larger ones are stable hydrophilic pores with a radius  $> 0.8$  nm.<sup>51</sup> The rate of formation of such stable pores is modelled by the following equation.<sup>51,52</sup>

$$\frac{dN}{dt} = \alpha \cdot e^{(\Phi_M/\Phi_{Ep})^2} \cdot \left(1 - \frac{N}{N_{eq}(\Phi_M)}\right) \quad \text{Eq. 2.21}$$

where

$N$  = Pore density ( $\text{m}^{-2}$ )

$\alpha$  = Creation rate coefficient ( $1 \cdot 10^9 \text{ m}^{-2} \cdot \text{s}^{-1}$ )

$\Phi_M$  = Membrane potential

$\Phi_{Ep}$  = Threshold potential for electroporation  $\approx 258$  mV

$N_{eq}(\Phi_M)$  = Pore density at membrane potential  $\Phi_M$  given by Eq. 2.22

$N_0 = 1.5 \cdot 10^9 (\text{m}^{-2})$ .<sup>51</sup>

$$N_{eq}(\Phi_M) = N_0 \cdot e^{2.46 \cdot (\Phi_M/\Phi_{Ep})^2} \quad \text{Eq. 2.22}$$

The bilayer energy  $W_M$  of a membrane with  $K$  electro-pores of an initial radius  $r_j$  depends on the following parameters:<sup>53</sup>

1. Steric repulsion of lipid heads  $\sum_{j=1}^K \beta \cdot \left(\frac{r_s}{r_j}\right)^4$ ;
2. Edge energy of the pore perimeter  $\sum_{j=1}^K 2\pi\gamma r_j$ ;
3. The effect of the pores on the membrane tension ; where  $\sum_{j=1}^K -\pi \cdot \sigma_{eff}(A_p) \cdot r_j^2$  ;  $\sigma_{eff}(A_p)$  is a function of the combined area of pores  $A_p = \sum_{j=1}^K \pi r_j^2$ ;
4. Contribution to the membrane potential  $\sum_{j=1}^K \int_0^{r_j} F(r; \Phi_M) \cdot dr$ .

As the electro-pores expand their total area and ( $A_p = \sum_{j=1}^K \pi r_j^2$ ) increases, the effective membrane tension  $\sigma_{eff}$  felt by each pore decreases according to the equation:<sup>54</sup>

$$\sigma_{eff} = 2 \cdot \sigma' \cdot \frac{2 \cdot \sigma' - \sigma_o}{(1 - A_p/A_M)^2} \quad \text{Eq. 2.23}$$

where

$\sigma'$  is the specific tension energy ( $0.02 \text{ J} \cdot \text{m}^{-2}$ ) of the hydrocarbon-water;

$\sigma_o$  is the specific tension energy without pores ( $0.01 \text{ J} \cdot \text{m}^{-2}$ );

$A_M$  is the total area of the cell membrane ( $1.26 \cdot 10^{-9} \text{ m}^2$  of a cell with a  $10 \mu\text{m}$  radius).

The electric force  $F(r, \Phi_M)$  acting on a pore of a toroidal inner surface according to Fig 2-11 is given by Eq. 2.24.<sup>54</sup>

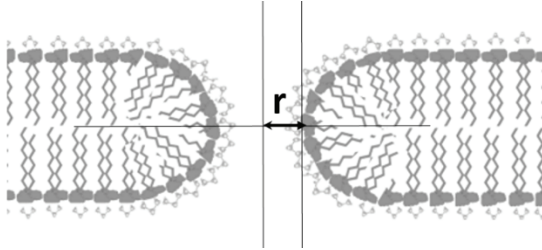


Figure 2-11  
Schematic illustration of an electro-pore of radius  $r$  in the cell membrane

$$F(r, \Phi_M) = \frac{F_{max}}{1 + \frac{0.97 \cdot 10^{-9}}{r + 0.31 \cdot 10^{-9}}} \cdot \Phi_M^2 \quad \text{Eq. 2.24}$$

where

$F_{max}$  is the maximum of electric force ( $0.7 \cdot 10^{-9} \text{ N} \cdot \text{V}^{-2}$  at  $\Phi_M = 1 \text{ V}$ ).

Thus the energy  $W$  of the entire membrane lipid bilayer is:<sup>54</sup>

$$W = \sum_{j=1}^K \left\{ \beta \cdot \left( \frac{r_s}{r_j} \right)^4 + 2\pi\gamma r_j - \pi \cdot \sigma_{eff}(A_p) \cdot r_j^2 + \int_0^{r_j} F(r_j \Phi_M) dr \right\} \quad \text{Eq. 2.25}$$

The radius of a pore with an initial radius  $r_j$  increases in size while the membrane energy is degrading according the following equation:

$$\frac{dr_j}{dt} = -\frac{D}{kT} \cdot \frac{dW_M}{dr_j} \cdot j = 1, 2, \dots, K \quad \text{Eq. 2.26}$$

where  $\frac{dW_M}{dr_j}$  is the rate of degrading the bilayer energy  $W_M$  of a membrane with  $K$  expanding electro-pores of an initial radius  $r_j$ .

## 2.6 DRUG DELIVERY THROUGH THE ELECTRO-PORES

The number of pores at the end of the electroporation pulse  $N_p$  is estimated by integrating the electro-pore density over the entire cell surface. Data on the effect of field strength from 130 V/cm to 1000 V/cm on a total number of pores distributed over the cell surface have been extracted from the diagrams in *Figure 8* of the work of Krassowska and Filev (2007).<sup>55</sup>

The average pore radius at the end of electroporation is assumed to be  $r_p$ , and thus the total cross-section area of electro-pores is  $A_p = K \cdot \pi \cdot r_p^2$ . As soon as the applied electroporation pulse ends, the created pores start to reseal at a first-order rate with mean decay time  $\tau_p$  in the order of seconds (*Figure 2-12*).

$$A_p = K \cdot \pi \cdot r_p^2 \cdot e^{-t/\tau_p} \quad \text{Eq. 2.27}$$

In an exploration of the enhanced uptake of the radioactive tracer in rats after applied electric pulses of 1000 V/cm field-strength and 100 $\mu$ s pulse-length, the relaxation time  $\tau$  of the bio-impedance was examined as well.<sup>56</sup> The radioactive tracer  $^{99m}\text{Tc-DTPA}$  was administered as a depot intramuscularly (i.m.) in the shoulder of Fischer-344 rats in several fractions of 50  $\mu$ l each, in 1-minute intervals. Treatment with electric pulses was performed with 2 needle electrodes separated by 8 mm and inserted in the right posterior thigh muscle, through which pulses of 600; 800; 1000; 1 200 V/cm field-strength (of 100, 250, and 500  $\mu$ s pulse-length) were applied. At 6 and 24 hours after electro pulse treatment, a gamma-camera recorded the distribution of  $^{99m}\text{Tc-DTPA}$  in the rats.

Before applying the pulse treatment, two measurements of the conductance performed at 2 and 20 kHz through the needle electrodes in the right posterior thigh muscle established the reference level  $G_{\text{before}}$ . Then, during the treatment, measurements of the conductance took place between each consecutive pulse ( $N_p = 2,4,6,10,12$ ) applied at 1s intervals.

After the last applied pulse, the final conductance  $G_{\text{after}}$  started to decrease and approach a plateau value. To study the relaxation of the created pores, the conductance measurements were continued 15 seconds after the last pulse at 1s intervals.

The plateau value relative to the conductivity  $G_{\text{after}}$  that was reached after 15s is a measure of the fraction of reversible electro-permeabilized cells. This value is of importance for the long-term transfer of exogenous substances to the cell and the outflow of immunogenic substances from the cell. Figure 2-12 displays the relaxation curve fitted to the following equation of single exponential decay:

$$G(t) = G_{\text{end}} \cdot (f_{\text{irr}} + f_{\text{rev}} \cdot \exp(-t/\tau_p)) \quad \text{Eq.2.28}$$

where

- $f_{\text{rev}}$  is the fraction of reversible electroporation;
- $f_{\text{irr}}$  is the fraction of irreversible electroporation;
- $\tau_p$  is the mean relaxation time.

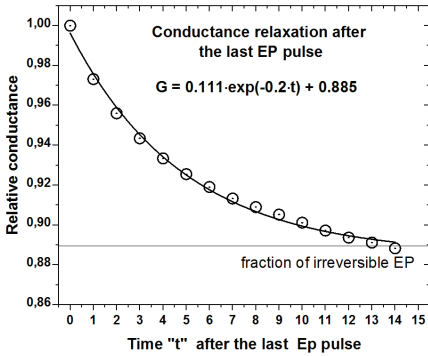


Figure 2-12  
 Conductance relaxation in seconds after application of 12 pulses with amplitude 1000 V/cm and pulse-length 100  $\mu$ s in a rat femur muscle.

Figure 2-12 shows that the conductance relaxation with a relaxation rate constant of  $0.2 \text{ s}^{-1}$  corresponding to a mean relaxation time or mean decay time  $\tau_p$  for the created pores is  $4.8 \pm 0.7 \text{ s}$ , and the fraction of reversible electro-permeabilized cells is 0.11 (11%).<sup>56</sup>

Directly after electroporation, the drug in the extracellular space has a concentration of  $C_{ex} = m_{ex} / V_{ex} \text{ (mol} \cdot \text{m}^{-3}\text{)}$ , and transfers into the cell interior to a concentration  $C_{in} = m_{in} / V_{in}$  dominantly due to diffusion according to Fick's law, if there is no ionic charge on the drug considered.<sup>57</sup>

$$J = dm_{in} / A_p \cdot dt = (D/d_M) \cdot (C_{ex} - C_{in}) \quad \text{Eq. 2.29}$$

where

$J$  is the flux of the drug through the cell membrane ( $\text{mole} \cdot \text{m}^{-2} \cdot \text{s}^{-1}$ );

$D$  is the diffusion coefficient of the drug ( $\text{m}^2/\text{s}$ );

$d_M$  is the thickness of the cell membrane;

$A_p$  is the total electro-pore area =  $K \cdot \pi \cdot r_p^2$ .

Eq. 2.30 thus gives the flow rate of the drug that enters a cell by diffusing through the aqueous pores across the cell membrane

$$dm_{in} / dt = (D/d_M) \cdot (C_{ex} - C_{in}) \cdot K \cdot \pi \cdot r_p^2 \cdot e^{-t/\tau_p} \quad \text{Eq.2.30}$$

where

$K$  is the total number of pores;

$r_p$  is the average pore radius.

$C_{ex} \gg C_{in}$  and  $C_{ex}$  are assumed to be approximately constant during the period  $T$  of drug accumulation to the cell (mole per cell) according to Eq. 2.31,

$$m_{in} = (D/d_M) \cdot C_{ex} \cdot K \cdot \pi \cdot r_p^2 \cdot \tau_p \cdot (1 - e^{-T/\tau_p}) \quad \text{Eq.2.31}$$

According to diagram D of *Figure 8* in the work of Krassowska and Filev (2007), the total area of pores ( $K \cdot \pi \cdot r_p^2$ ) as a fraction of the cell surface



( $A_{cell}$ ) is approximately rather constant, with a value of about  $7 \cdot 10^{-4}$  at field strength above 400 V/cm.<sup>55</sup> This is in agreement with the results of an experimental study on the outcome of electro-enhanced chemotherapy, which suggested that the uptake ratio depends mostly on the pulse length and number of applied pulses.<sup>58</sup>

$$total\ pore\ area: K \cdot \pi \cdot r_p^2 = A_{cell} \cdot 7 \cdot 10^{-4} \tag{Eq.2.32}$$

$$m_{in} = (D/d_M) \cdot C_{ex} \cdot A_{cell} \cdot \tau_p \cdot 7 \cdot 10^{-4} \cdot (1 - e^{-T/\tau_p})$$

Figure 2-13 displays the diffusion coefficients set against the molecular weight for compounds in the range of 135 and 68000 fitted to Eq. 2.33.<sup>59,60</sup>

$$D = 1.05 \cdot 10^{-8} [M_{W.}]^{-0.484} \tag{Eq. 2.33}$$

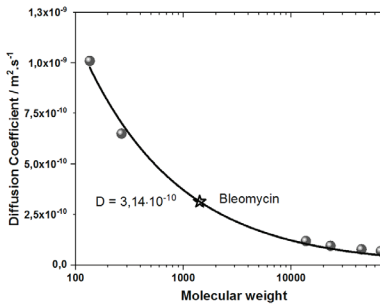


Figure 2-13  
Variation of the diffusion coefficients with the molecular weight

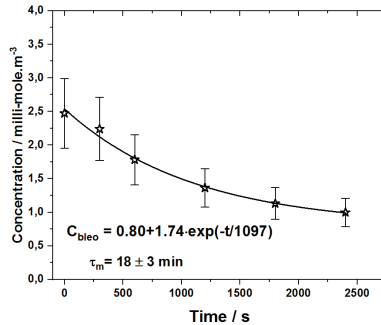


Figure 2-14  
Average of plasma concentration of Bleomycin after intravenous bolus injection of a mean dose of 26000 IU Bleomycin in 24 patients older than 65.<sup>61</sup>

With a molecular weight of 1415.5 for Bleomycin in Eq. 2.33, we see a value of  $D = 3.14 \cdot 10^{-10} \text{ m}^2 \cdot \text{s}^{-1}$  for this drug. The average radius for a tumour cell is considered to be about  $50 \mu\text{m}$ .<sup>55</sup> Thus, the area ( $A=4\pi r^2$ ) of the tumour cell is about  $3.14 \cdot 10^{-8} \text{ m}^2$ . The thickness of the cell membrane  $d_M$  is considered to be  $7 \text{ nm}$ .<sup>62</sup>

**Intravenous administration** of Bleomycin is recommended by ESOPE as a dose of 15000 IU per  $\text{m}^2$  body surface, 15 000 IU (International Units) = 15 USP units = 1mg. Administration of 15 mg of Bleomycin thus corresponds to about 10 micromole ( $1.06 \cdot 10^{-5}$  mole). Eq. 2.34 for the excretion of Bleomycin is estimated using data from a clinical study of intravenous bolus injections of a mean dose of 26000 IU of Bleomycin.<sup>61</sup>

Figure 2-14 shows the average of Bleomycin plasma concentration after an intravenous bolus injection of a mean dose of 26000 IU of Bleomycin in 24 patients older than 65 a.<sup>58</sup> The elimination curve of Bleomycin plasma concentration values converted to milli-mole per m<sup>3</sup> presented in Figure 2-14 fitted to an exponential decay gives us the following equation:

$$C_{Bleo} = 0.80 + 1.74 \cdot e^{-t/1097} \text{ [millimole} \cdot \text{m}^{-3} \text{]} \quad \text{Eq.2.34}$$

The mean elimination time is 1097 s, which corresponds to  $\tau_m = 18 \pm 3$  min and the half-time  $\tau_{1/2} = 12.5 \pm 2$  min. About 8 minutes after the bolus injection of Bleomycin, the electro pulse treatment is performed. At this time, the Bleomycin plasma concentration is about  $2 \cdot 10^{-3}$  mole.m<sup>-3</sup> and, after about  $T = 20$  s, the total uptake of Bleomycin in the cell became  $1 \cdot 10^{-14}$  mole per cell according to Eq.2.35. Considering that the Avogadro's Constant is  $6.022 \cdot 10^{23}$  molecules.mole<sup>-1</sup>, the Bleomycin uptake is equivalent to  $6 \cdot 10^9$  molecules per cell.

$$m_{in} = (3.14 \cdot 10^{-10} / 7 \cdot 10^{-9}) \cdot 2 \cdot 10^{-3} \cdot (3.14 \cdot 10^{-8}) \cdot 5 \cdot (7 \cdot 10^{-4}) \quad \text{Eq. 2.35}$$

$$m_{in} = 1 \cdot 10^{-14} \text{ (mole per cell)}$$

# CHAPTER III

## ELECTRO-DOSIMETRY

### 3.1 INTRODUCTION

External electric fields applied to biological materials interact directly with free electric charges such as electrons and ions, as well as on ionic groups in larger molecules. They also interact with dipoles such as water, and induce dipoles in molecules with polarizable groups. The cell membranes seem to be the critical target for interaction, causing intramolecular transitions and intermolecular processes that lead to structural reorganization of the cell membranes.

Applying high voltage pulses to cells in cultures or in tissue causes various degrees of structural reorganisations in the cell membranes, which might end with a dielectric collapse or breakdown. This condition is either called “*electroporation*” or “*electro-permeabilization*”, and can be either reversible or irreversible depending on the characteristics of the applied voltage pulses.<sup>5</sup>

In such a transient state, the cell membrane becomes permeable to compounds that generally do not pass this barrier into the cytoplasm of the cell. Direct transfer of DNA plasmids, and other nucleic acids (such as RNA), proteins, and other molecules into cells and microorganisms use that condition. Another possibility is that neighbouring cells with membranes in a transient state might fuse their membranes and form a new giant cell. These properties of membranes in a transient state have led to electrical field pulse techniques that are gaining increasing importance in cellular and molecular biology, in gene technology, and in various medical therapeutic procedures.<sup>24,63</sup>

### 3.2 MODELLING OF THE IMPEDANCE OF TISSUE

#### 3.2.1 MODEL OF THE CELL MEMBRANE

Figure 3-1 shows a simple model of the cell membrane, where  $R_m$  is the resistivity and  $C_m$  is the capacitance of the cell membrane.

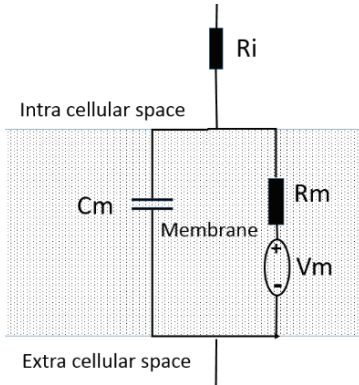


Figure 3-1

An equivalent circuit of a cell membrane  $R_m$  is the resistivity and  $C_m$  is the capacitance of the cell membrane.

$V_m$  is the voltage created by the ions  $Na^+$   $K^+$  and  $Cl^-$  covering the surface of the membrane.

An externally applied voltage  $dV$  during the time  $dt$  over the membrane “ $m$ ” induces a charge  $dQ = C_m \cdot dV$  in the capacitor that creates the current

$$i_m = dQ/dt = C_m \cdot dV/dt = (V - V_m)/R \quad \text{Eq.3.1}$$

Thus,  $dV/dt = (V - V_m)/R_m C_m$ , which is a first order kinetic equation with the rate constant  $1/R_m C_m$  or the time constant  $\tau_m = R_m C_m$ . The impedance of the cell membrane  $Z_m$  is derived by the parallel resistance  $Z_r = R_m$  and capacitance  $Z_c = -j/\omega \cdot C_m$ , where  $j = \sqrt{-1}$  is the imaginary unit,  $\omega = 2\pi \cdot f$ , and  $f$  is the frequency in Hz.

$$\frac{1}{Z_m} = \frac{1}{R_m} + \frac{1}{Z_c} = \frac{1}{R_m} + j \cdot \omega \cdot C_m = G_m + j \cdot \omega \cdot C_m = Y; \quad \text{Eq.3.2}$$

where  $G$  is the conductance and  $Y$  is called the admittance:

$$\begin{aligned} Z_m &= \frac{R_m}{1 + j \cdot \omega \cdot C_m \cdot R_m} = \frac{R_m \cdot (1 - j \cdot \omega \cdot C_m \cdot R_m)}{(1 + j \cdot \omega \cdot C_m \cdot R_m) \cdot (1 - j \cdot \omega \cdot C_m \cdot R_m)} \\ &= \frac{R_m}{1 + \omega^2 \cdot C_m^2 \cdot R_m^2} - \frac{j \cdot \omega \cdot C_m \cdot R_m^2}{1 + \omega^2 \cdot C_m^2 \cdot R_m^2} \end{aligned} \quad \text{Eq.3.3}$$

$$Z_m = Re[Z_m] + j \cdot Im[Z_m] \quad \text{Eq.3.4}$$

The resistance is the real part of the membrane impedance:

$$Re[Z_m] = \frac{R_m}{1 + \omega^2 \cdot C_m^2 \cdot R_m^2} \quad \text{Eq.3.5}$$

The reactance is the imaginary part of the membrane impedance:

$$Im[Z_m] = - \frac{\omega \cdot C_m \cdot R_m^2}{1 + \omega^2 \cdot C_m^2 \cdot R_m^2} \quad \text{Eq.3.6}$$

The modulus or absolute value of the membrane impedance is  $|Z_m| = \sqrt{Z_m \cdot Z_m^*}$ , where  $Z_m^*$  is the complex conjugate ( $j$  replaced with  $-j$ ) of the membrane impedance.

$$Z_m = Re[Z_m] + j \cdot Im ;$$

$$|Z_m| = \sqrt{Re[Z_m]^2 + Im[Z_m]^2} ;$$

$$|Z_m| = \frac{R_m \cdot \sqrt{1 + \omega^2 \cdot C_m^2 \cdot R_m^2}}{1 + \omega^2 \cdot C_m^2 \cdot R_m^2} ;$$
Eq.3.7

The characteristic time constant of the membrane is  $\tau_m = R_m \cdot C_m$ , and thus the characteristic frequency  $f_c = 1/\tau_m = 1/ R_m \cdot C_m$ . The time-constant  $\tau_m$  is in the order of 1-10ms for a typical biological membrane, and thus the characteristic frequency is in the order of 0.1-1 kHz.

The equation for the impedance  $Z_m$  in terms of the time-constant  $\tau_m$ :

$$Z_m = \frac{R_m}{1 + j \cdot \omega \cdot \tau_m} = \frac{R_m}{1 + \omega^2 \cdot \tau_m^2} - \frac{j \cdot \omega \cdot \tau_m \cdot R_m}{1 + \omega^2 \cdot \tau_m^2} \quad \text{and}$$

$$|Z_m| = \frac{R_m \cdot \sqrt{1 + \omega^2 \cdot \tau_m^2}}{1 + \omega^2 \cdot \tau_m^2}$$
Eq.3.8

At low frequency  $f \approx 0$ ,  $Z_m = R_m$ , and at very high-frequency  $f \rightarrow \infty$   $Z_m \rightarrow 0$ , the admittance  $Y$  is defined in Eq. 3.9:

$$Y = G + j \cdot \omega \cdot C \quad \text{where } G = \frac{A}{d} \cdot \sigma \quad \text{and } C = \frac{A}{d} \cdot \varepsilon$$
Eq.3.9

Where  $G$  is the conductance ( $\Omega^{-1}$ );  $\sigma$  (S) is the conductivity;  $C$  (F) is the capacitance; and  $\varepsilon$  is the permittivity of a membrane with thickness  $d$  (m) between two plate electrodes of cross-section  $A$  ( $m^2$ ). The capacitance of a patch of a typical biological membrane is about  $1 \mu F/cm^2$  ( $10 \text{ mF}/m^2$ ).

### 3.2.2 MODEL OF THE CELL

Figure 3-2 displays the frequency dependence of cell resistance ( $Re[Z_m]$ ) derived from the equations for the impedance of the cell  $Z_c = R_i + Z_m$ , where  $Z_m$  is the impedance of the membrane. These equations for the calculation of the Nyquist Plot are shown in Figure 3-3.

$$Z_m = \frac{R_m}{1 + j \cdot \omega \cdot \tau_m} = \frac{R_m}{1 + \omega^2 \cdot \tau_m^2} - \frac{j \cdot \omega \cdot \tau_m \cdot R_m}{1 + \omega^2 \cdot \tau_m^2}$$
Eq.3.10

$$Z_c = R_i + \frac{R_m}{1 + \omega^2 \cdot \tau_m^2} - \frac{j \cdot \omega \cdot \tau_m \cdot R_m}{1 + \omega^2 \cdot \tau_m^2} = \frac{R_i + R_m + \omega^2 \cdot \tau_m^2 \cdot R_i}{1 + \omega^2 \cdot \tau_m^2} - \frac{j \cdot \omega \cdot \tau_m \cdot R_m}{1 + \omega^2 \cdot \tau_m^2}$$
Eq.3.11

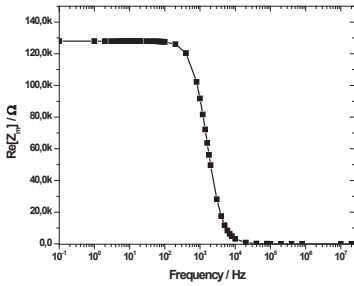


Figure 3-2  
 Frequency dependence of cell resistance =  $Re[Z_m]$ ,  $C_m=7.81 \cdot 10^{-10}$  F;  $\tau_m = 10^{-4}$  s;  $R_m = 128k\Omega$ ;  $R_i = 300 \Omega$

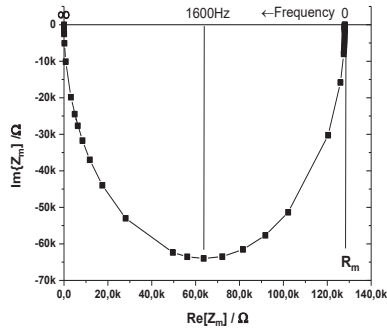


Figure 3-3  
 Nyquist Plot of the reactance =  $Im[Z_m]$  versus resistance of the cell with  $R_i = 300 \Omega$ ;  $C_m=7.81 \cdot 10^{-10}$  F;  $\tau_m = 10^{-4}$  s;  $R_m = 128k\Omega$

At low frequency,  $f \approx 0$   $Z_c = R_m + R_i$ , and, at very high-frequency,  $f \rightarrow \infty$   $Z_c \rightarrow R_i$ .

### 3.2.3 IMPEDANCE MODEL OF TISSUE

Figure 3-4 shows a simple impedance model of intact tissue-assuming cells surrounded by a cell membrane of infinite high resistance and a capacitance of  $C_m$ . The interstitial fluid of the cells has a resistance of  $R_i$ . An extracellular fluid of resistance  $R_x$  fills the space between separate cells in the tissue.

Exposure of tissue to pulsed electric fields changes the conductivity of the cell membrane. This process is often called electroporation because one believes that the membrane is perforated and, through the ions, moves freely through the pores. The intact cell membrane has a very high resistance that decreases considerably after exposure to the pulsed electric field.

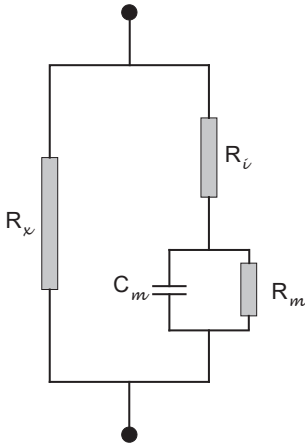


Figure 3-4  
The equivalent circuit of tissue where \$R\_x\$ is the resistivity of the extracellular fluid, \$R\_i\$ is the resistivity of intracellular fluid, \$R\_m\$ is the resistivity of the cell membrane, and \$C\_m\$ is the capacitance of the cell membrane. The impedance of the cell is \$Z\_c = R\_i + Z\_m\$

$$\frac{1}{z_m} = \frac{1}{R_m} + j \cdot \omega \cdot C_m \quad \omega = 2\pi \cdot f \tag{Eq.3.12}$$

$$|Z_m| = \frac{1}{\sqrt{\left(\frac{1}{R_m}\right)^2 + (\omega \cdot C_m)^2}} = \frac{R_m}{\sqrt{1 + (\omega \cdot R_m C_m)^2}} \tag{Eq.3.13}$$

$$|Z_m| = \frac{R_m}{\sqrt{1 + (\omega \cdot \tau_m)^2}} \tag{Eq.3.14}$$

The impedance of the whole tissue derives from the expression for adding parallel circuits of impedance:

$$\frac{1}{Z_{tis}} = \frac{1}{R_x} + \frac{1}{Z_c} = \frac{1}{R_x} + \frac{1}{R_i + Z_m} = \frac{R_i + Z_m + R_x}{R_x \cdot (R_i + Z_m)} \tag{Eq.3.15}$$

$$Z_{tis} = \frac{R_x \cdot (R_i + Z_m)}{R_i + Z_m + R_x} = \frac{R_x \cdot Z_c}{Z_c + R_x} = \frac{R_x \cdot (Z_c^{RE} + j \cdot Z_c^{IM})}{(Z_c^{RE} + j \cdot Z_c^{IM}) + R_x} \tag{Eq.3.16a}$$

$$= \frac{R_x \cdot (Z_c^{RE} + j \cdot Z_c^{IM})}{(Z_c^{RE} + R_x) + j \cdot Z_c^{IM}}$$

$$Z_{tis} = \frac{R_x \cdot (Z_c^{RE} + j \cdot Z_c^{IM}) \cdot [(Z_c^{RE} + R_x) - j \cdot Z_c^{IM}]}{[(Z_c^{RE} + R_x) + j \cdot Z_c^{IM}] \cdot [(Z_c^{RE} + R_x) - j \cdot Z_c^{IM}]} = \tag{Eq.3.16b}$$

$$R_x \cdot \frac{[(Z_c^{RE} + R_x) \cdot Z_c^{RE} + (Z_c^{IM})^2 - j \cdot Z_c^{IM} Z_c^{RE} + (Z_c^{RE} + R_x) \cdot j \cdot Z_c^{IM}]}{[(Z_c^{RE} + R_x)^2 + (Z_c^{IM})^2]}$$

$$Z_{tis} = \frac{R_x \cdot [(Z_c^{RE} + R_x) \cdot Z_c^{RE} + (Z_c^{IM})^2]}{[(Z_c^{RE} + R_x)^2 + (Z_c^{IM})^2]} \tag{Eq.3.16c}$$

$$+j \cdot \frac{R_x \cdot [(Z_c^{RE} + R_x) \cdot Z_c^{IM} - Z_c^{IM} \cdot Z_c^{RE}]}{[(Z_c^{RE} + R_x)^2 + (Z_c^{IM})^2]}$$

At low frequency,  $f \approx 0$   $Z_c^{RE} = R_m + R_i$ ,  $Z_c^{IM} = 0$ , and since  $R_m \gg R_i$  and  $R_x$ :

$$Z_c^{RE}(0) = \frac{R_x \cdot (R_m + R_i)}{R_m + R_i + R_x} = R_x \tag{Eq.3.17}$$

and at very high-frequency,  $f \rightarrow \infty$   $Z_c^{RE} \rightarrow R_i$   $Z_c^{IM} \rightarrow 0$ , thus:

$$Z_c^{RE}(\infty) = \frac{R_x \cdot R_i}{R_i + R_x} \tag{Eq. 3.18}$$

The following equation (3.19) can thus estimate the resistivity of the intracellular fluid  $R_i$  in intact tissue:

$$R_i = \frac{Z_c^{RE}(\infty) \cdot R_x}{R_x - Z_c^{RE}(\infty)} \tag{Eq. 3.19}$$

The effect of the application of pulsed electric fields is assumed to permeabilize the cell membrane which decreases the impedance mainly at a frequency region below 10 kHz.

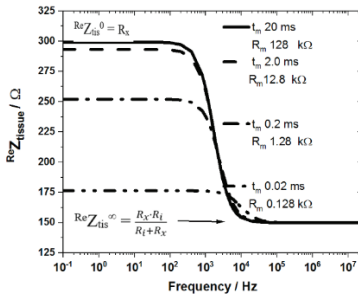


Figure 3-5  
Frequency dependence of tissue resistance =  $\text{Re}[Z_{\text{tissue}}]$ ;  $\tau_m = 0.02$ - $20\text{ms}$ ;  $R_m = 128 - 0.128 \text{ k}\Omega$ ;  $R_i = R_x = 300 \Omega$ .

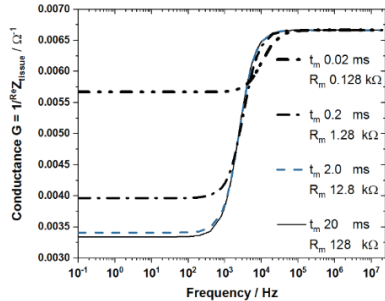


Figure 3-6  
Frequency dependence of tissue conductance  $G = 1/\text{Re}[Z_{\text{tissue}}]$ ;  $\tau_m = 0.02$ - $20\text{ms}$ ;  $R_m = 128 - 0.128 \text{ k}\Omega$ ;  $R_i = R_x = 300 \Omega$ .



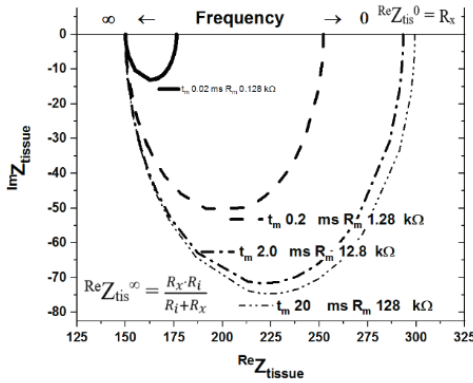


Figure 3-7  
Nyquist Plot of the reactance =  $Im[Z_m]$  versus resistance of tissue model with  $\tau_m = 0.20\text{-}20\text{ ms}$ ;  $R_m = 128 - 0.128\text{ k}\Omega$ ;  $R_i = R_x = 300\ \Omega$ .

Complex parameters express the admittance  $Y$  with a capacitor, the dielectric constant of which ( $\epsilon$ ) represents its ability to store electrical energy.

$$Y^* = j \cdot \omega \cdot C^* = j \cdot \omega \frac{A}{d} \cdot \epsilon^* = j \cdot \omega \frac{A}{d} (\epsilon - j \cdot \epsilon) = \text{Eq.3.20}$$

$$= j \cdot \frac{A}{d} (\epsilon \cdot \omega - j \cdot \omega \cdot \epsilon) = G + j \cdot \omega \cdot C$$

Thus, the conductance is expressed as:

$$G = \frac{A}{d} \cdot \sigma \equiv \frac{A}{d} \cdot \omega \cdot \epsilon'' \text{ and therefore } \epsilon'' = \frac{\sigma}{\omega}$$

$$\epsilon_r'' = \frac{\epsilon''}{\epsilon_0} = \frac{\sigma}{\epsilon_0 \cdot \omega};$$

and the relative permittivity:

The loss angle  $\delta$  of a capacitor is defined so that the ideal capacitor with zero losses has a zero loss angle, which means that  $\delta = 90^\circ - \theta$ , where  $\theta$  is the recorded phase angle. Thus,  $\tan \delta = 1/\tan \theta$ . The *loss tangent*,  $\tan \delta$ , is also called the *dissipation factor*, and is equivalent to the energy loss per cycle divided by the energy stored per cycle (RMS or peak value).

The impedance of the equivalent circuit is  $Z = |Z| \cdot \cos \theta + j \cdot |Z| \cdot \sin \theta$ , and  $\tan \theta = \frac{Im[Z]}{Re[Z]}$ .

The following equation gives the loss tangent for a cell membrane

$$\tan \delta = 1/\tan \theta = \frac{Re[Z]}{Im[Z]} = -1/\omega \cdot C_m \cdot R_m = 1/\omega \cdot \tau_m \text{ Eq.3.21}$$

The power loss in the circuit only takes place in the resistive part  $Re[Z]$  if the capacitive part is an ideal capacitor. The frequency characteristic depends on the power loss of the circuit. With the constant amplitude

voltage  $U$ , the power loss moves from zero levels at very low frequencies to a defined value  $U^2/R$  at high frequencies. With a constant amplitude current, the power level moves from a constant value at very low frequencies through a maximum at the frequency determined by the time constant  $\tau = RC$  and to zero at high frequency.

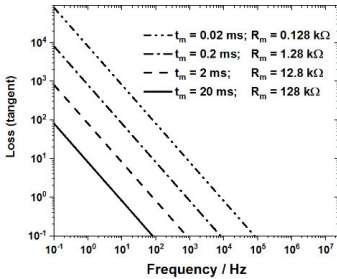


Figure 3-8  
Loss tangent for the cell membrane  
 $\tau_m = 0.02\text{-}20\text{ms}$ ;  $R_m = 128 - 0.128 \text{ k}\Omega$ .

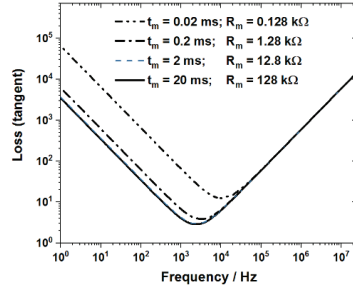


Figure 3-9  
Loss tangent  $\tan \delta$  as a function of  
frequency of the tissue model with  $R_m$   
 $= 128 - 0.128\text{k}\Omega$ ;  $R_i=R_x= 300\Omega$ ;

In Figure 3-8, the values of  $\tan \theta = \frac{Im[Z]}{Re[Z]}$  multiplied by 1000 of the tissue model of Figure 3-9, with  $\tau_m = R_m \cdot C_m$  varied from 0.02-20ms and  $R_m$ , varied from 128 to 0.128k $\Omega$  to simulate the effect of electroporation. Figure 3-9 shows that the minimum value of  $\tan\theta$  decreases and shifts towards higher frequencies by decreasing the value of  $R_m$ . The ratio of the loss-tangent at a specific frequency before and after exposure of the tissue to pulsed electric fields applies as a dosimetry quantity. This parameter is called the “loss factor” and is evaluated as shown in Eq.3.22. It depends on the power of the exposure that controls the process of electroporation.

$$Loss\ Factor = \left( \frac{\tan \theta_{after}}{\tan \theta_{before}} \right) = \left| \frac{\tan \delta_{before}}{\tan \delta_{after}} \right| \quad Eq.3.22$$

The loss factor measured at about 1 kHz to record the effect of exposure to a pulsed electric field is 1 if there is no change in the phase angle after pulse exposure. In case of extreme powerful exposure, the value of the recorded loss factor of the exposed object tends to approach zero. Therefore, this results in another quantity, the “loss change index” (LCI), which is defined as 1- loss factor and shown in the following Eq. 3.23.

$$LCI = \left( 1 - \frac{\tan \theta_{after}}{\tan \theta_{before}} \right) \quad Eq.3.23$$

By this definition, the loss change index is 0 if there is no change in the phase angle after pulse exposure, and is equal to 1 when the phase angle after exposure approaches 0, meaning that the loss tangent becomes infinite.

### 3.3 EVALUATION OF MODEL PARAMETERS USING IMPEDANCE DATA

Direct electrical currents (DC) and low-frequency currents are limited to the extracellular space. With the increasing frequency of the alternating current, the impedance of the cell membrane decreases, and the current travels straight through the cells, as demonstrated in Fig. 3-10. Electrical impedance readings over a frequency range then allow the separation of extracellular space and the membrane.

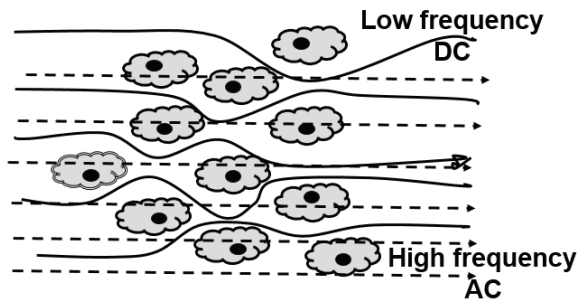


Figure 3-10

Electrical DC and low-frequency current travel in the extracellular space between the cells (represented by the solid line), while high-frequency AC-current (represented by the dashed line) passes the cell membrane and travels straight through the cells.

Electro-permeabilization is a membrane-associated process which affects the membrane resistance to direct electrical currents. From experiences of electro-permeabilization, the situation *in vivo* appears to be more complex than shown by the model of the single cell membrane, which resembles an ultra-thin capacitor of high resistance that envelops the intracellular fluids, as shown in Figure 3-4 in the modelling section.

### 3.3.1 IMPEDANCE MEASUREMENTS

In Figure 3-11, we can see the results from an experiment with impedance measurements in the thigh of a rat both before and 4 minutes after electro-pulse treatment with 8 exponential pulses of 1200 V/cm with a time-constant of 1ms. To simulate the drug administration, a volume of 0.2ml of saline was administered intramuscularly into the target area.

Figure 3-12 shows the impedance difference of measurements in the frequency interval 15 - 200 000 Hz in the thigh of a rat before and 4 minutes after electro-pulse treatment with eight exponential pulses of various field strengths (V/cm) with a time constant of 1ms.

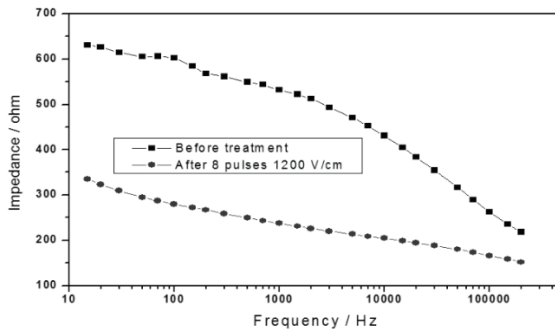


Figure 3-11

Results from an experiment with impedance measurements in the thigh of a rat both before and 4 minutes after electroporation treatment with 8 exponential pulses of initial amplitude of 1200V/cm with a time-constant of 1ms. Saline (0.2ml) was injected intramuscularly 4 minutes before the first measurement.

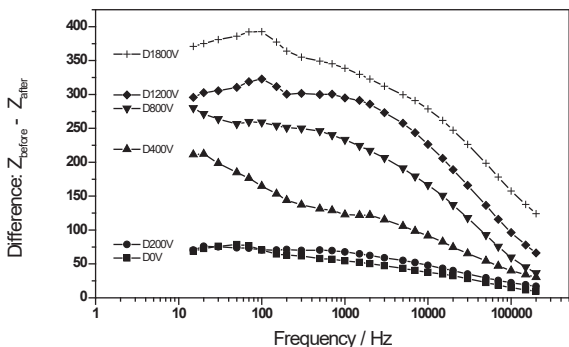


Figure 3-12

The difference of impedance measurements in the frequency interval 15Hz – 200kHz in the thigh of a rat before and 4 minutes after electro-pulse treatment with 8 exponential pulses of various initial amplitude D(V) with a time constant of 1ms. Saline (0.2 ml) was injected intramuscular 4 minutes before the first measurement.

Figure 3-13a displays the conductance  $G$  ( $\Omega^{-1}$ ) at various frequencies before (0) and after applying 2, 4, 8, 12, and 20 exponential pulses of initial field strength 1 200 V/cm, and  $\tau = 1.0\text{ms}$  to the muscles of rats. The corresponding conductance ratio  $G_{\text{after}}/G_{\text{before}}$  is displayed in Figure 3-13b.

As seen in Figure 3-13b, the conductance ratio  $G_{\text{after}}/G_{\text{before}}$  shows a maximum in the frequency range 1 - 50 kHz. At higher frequencies, however, the membrane resistance is short-circuited, and the electric field lines pass more uniformly through the tissue structure, and less change in the conductivity caused by the applied pulses occurs.

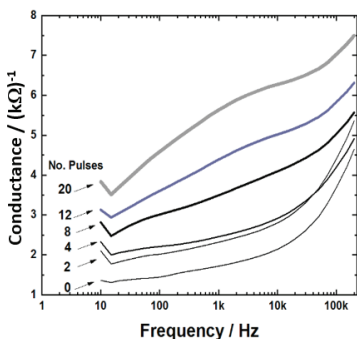


Figure 3-13a

Conductance  $G$  after 0, 2, 4, 8, 12, and 20 exponential pulses of initial field strength 1200 V/cm, and  $\tau = 1.0\text{ms}$ .

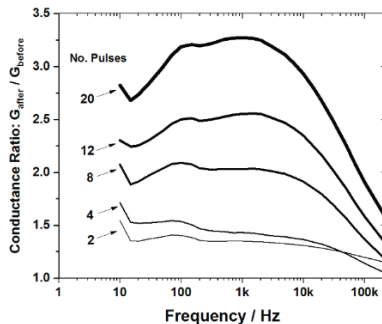


Figure 3-13b

Conductance ratio,  $G_{\text{after}} / G_{\text{before}}$  for 2, 4, 8, 12 and 20 exponential pulses of initial field strength 1200 V/cm,  $\tau = 1.0\text{ms}$ .

At low frequency  $f \approx 0$ , the following equation expresses the low frequency impedance  $Z_{tis}^{RE}(LF)$  of the tissue:

$$Z_c^{RE} = R_m + R_i, \quad Z_c^{IM} = 0 \quad \text{thus} \quad \lim_{f \rightarrow 0} Z_{tis}^{RE} = \frac{R_x \cdot (R_m + R_i)}{R_m + R_i + R_x} = R_x = Z_{tis}^{RE}(LF) \quad \text{Eq.3.24}$$

At high frequency  $f \rightarrow \infty$ , the following equation expresses the high frequency impedance  $Z_{tis}^{RE}(HF)$  of the tissue:

$$Z_c^{RE} \rightarrow R_i, \quad Z_c^{IM} \rightarrow 0 \quad \text{thus} \quad \lim_{f \rightarrow \infty} Z_{tis}^{RE} = \frac{R_x \cdot R_i}{R_i + R_x} = Z_{tis}^{RE}(HF) \quad \text{Eq.3.25}$$

The resistivity of the intracellular fluid  $R_i$  in intact tissue can thus be estimated by the equation:

$$R_i = \frac{Z_{tis}^{RE}(HF) \cdot R_x}{R_x - Z_{tis}^{RE}(HF)} \quad \text{Eq.3.26}$$

By assuming  $R_i \approx R_x = R$ ;  $Z_{tis}^{RE}(HF) = R/2$ ; and

$$Z_{tis}^{RE}(LF) = \frac{R \cdot (R_m + R)}{R_m + 2R} \approx R; \quad \text{Eq.3.27}$$

### 3.3.2 RESISTIVITY CHANGE INDEX, RCI

Equation 3.28 defines the resistivity change index (RCI) as the relative decrease in resistivity after electroporation or the relative increase in conductance  $G = 1/R$ ,  $RCI=0$ , if there is no change (i.e.  $R_{\text{after}}=R_{\text{before}}$ ).

$$RCI = \left( 1 - \frac{R_{\text{after}}}{R_{\text{before}}} \right) = \left( 1 - \frac{G_{\text{before}}}{G_{\text{after}}} \right) \quad \text{Eq.3.28}$$

where

$R_{\text{before}}$  is the resistivity ( $\Omega$ ) measured before the first pulse.

$R_{\text{after}}$  is the resistivity after electroporation with  $N_p$  pulses.

If no change occurs,  $RCI = 0$ . If substantial changes occur,  $RCI \rightarrow 1$ .

### 3.3.3 LOSS TANGENT AND LOSS CHANGE INDEX

Figures 3-14a and 3-14b show the loss tangent recorded in rat muscle tissue before and after applying 0, 1, 4, and 8 rectangular pulses of 1000 V amplitude and 0.1ms pulse-length, and Figures 3-15a and 3-15b display the *loss change index* calculated according to Eq. 3.23.

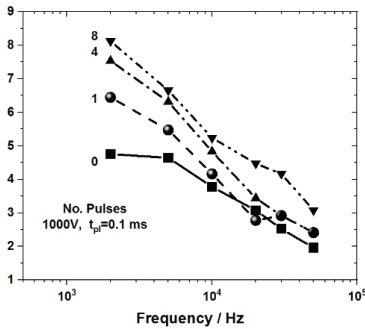


Figure 3-14a  
Loss tangent after 0, 1, 4, and 8 rectangular pulses of  $E=1000$  V/cm,  $PL=0.1$ ms,

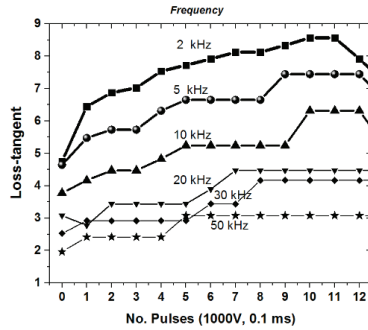


Figure 3-14b  
Loss tangent recorded at various frequencies for various numbers of rectangular pulses of  $E=1000$  V/cm,  $PL=0.1$ ms.

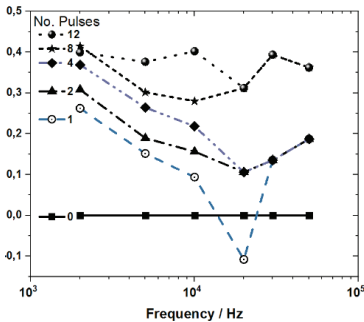


Figure 3-15a  
Loss change index after 0, 1, 3, 4, 8, and 12 rectangular pulses of  $E=1000$  V/cm,  $PL=0.1$ ms.

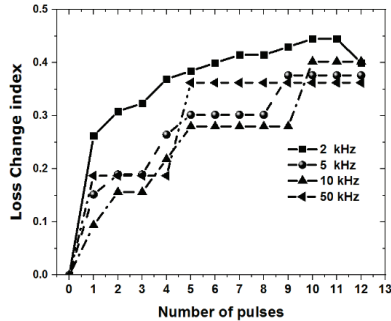


Figure 3-15b  
Loss change index recorded at various frequencies for various numbers of rectangular pulses of  $E=1000$  V/cm,  $PL=0.1$ ms.

### 3.3.4 CONDUCTANCE RELAXATION

Figure 3-16 shows the ratio of conductance after each pulse against the conductance before pulse treatment. The conductance ratio  $R_G^N = G_N/G_0$  steadily increases after each applied pulse of 1000 V/cm and 0.1ms pulse length. After the last pulse,  $N=12$ , the conductance ratio  $R_G^{12} = R_G^{end}$  begins to decrease due to the recovery of the permeabilized membrane. However, only a fraction of the conductance ratio  $R_G^{end}$  is reversible, and after some

time the conductance ratio reaches a plateau value indicating the conductance ratio of irreversible permeabilization  $R_G^{end}(irr)$ .

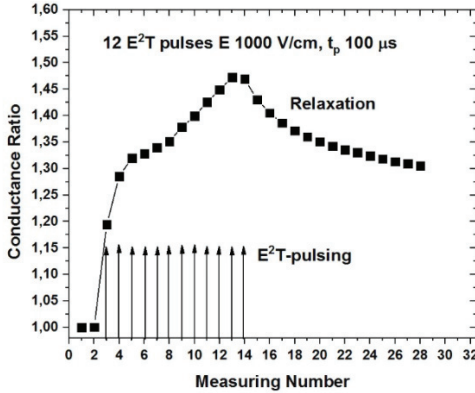


Figure 3-16  
Conductance ratio  $G_{afterN}/G_0$  recorded at 2 kHz before, during and after 12 consecutive EP pulses of 1000 V/cm amplitude and 100  $\mu$ s pulse length.

The relaxation of the conductance ratio at the end of electro-pulsing  $R_G^{end}$  follows a first order differential equation:

$$\frac{dR_G^{end}}{dt} = -k_{relax} \cdot R_G^{end} \tag{Eq.3.29}$$

Where

- $k_{relax}$  is the rate constant of the conductance relaxation
- $R_G^{end}$  is the conductance ratio at the end of electro-pulsing
- $R_G^{end}(irr)$  is the conductance left after its relaxation

$$R_G^{end}(t) = R_G^{end}(irr) + \{R_G^{end}(0) - R_G^{end}(irr)\} \cdot e^{-k_{relax} \cdot t} \tag{Eq.3.30}$$

- The fraction of reversible electro permeabilization  $f_{rev}$  is equal to  $\{R_G^{end}(0) - R_G^{end}(irr)\}/R_G^{end}(0)$ , and;
- The fraction of irreversible electro-permeabilization  $f_{irr} = (1 - f_{rev})$ .

The data displayed in Figure 3-16 yield the following values for  $f_{rev}$  and  $f_{irr}$ :

- $f_{rev} = (1.455 - 1.30) / 1.455 = 0.107$ , and;
- $f_{irr} = 0.893$ .



### 3.3.5 CONDUCTANCE RELAXATION AFTER EACH PULSE

Experiments performed with 12 DC-pulses of 100 V amplitude and 20ms pulse length delivered with 167 ms intervals were conducted through electrodes of 1mm diameter, and inserted in the thigh rat muscle at a distance of 8mm. The upper diagram in Figure 3-17 presents the ratio  $R_G^N = G_N / \overline{G_0}$  of the recorded conductance values  $G_N$  relative to the average value  $\overline{G_0}$ , before pulsing.

The second diagram in Figure 3-17, on the other hand, shows the consecutive difference  $R_G^N - R_G^{N-1}$  of the progressive conductance values. The conductance ratio increases most rapidly after the first pulse, before gradually increasing more slowly.

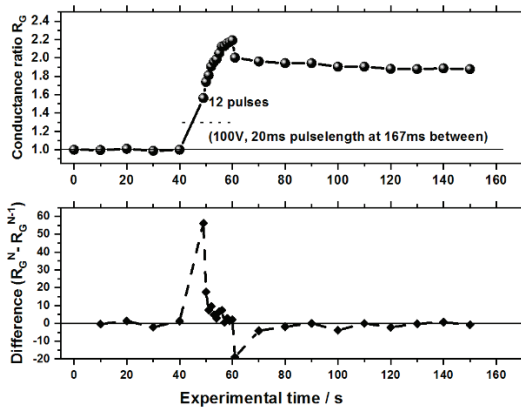


Figure 3-17

The first diagram above shows the conductance value relative to the average before pulsing, after each of the 12 pulses with 100 V amplitude and 20ms pulse-length, and with 10 measurements conducted after the last pulse. The second diagram shows the consecutive difference of the conductance  $R_G$ .

Figure 3-18 shows the results of another experiment exposing rats to 6 DC pulses of 100 V amplitude and 20ms pulse length delivered with 167ms intervals with four measurements of conductance performed before the first EP pulse and at 50ms after each next EP pulse.

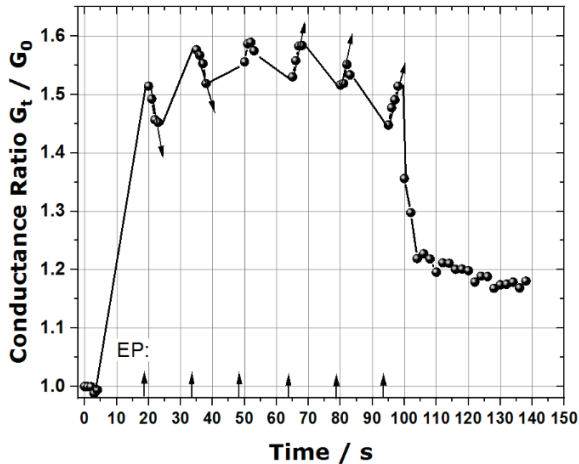


Figure 3-18

The conductance relative to the first measured value before any treatment with pulses of 100 V amplitude and 20ms pulse-length. The arrows at the bottom indicate the execution of the electro-pulses (EP). Four conductance measurements of 28ms are performed before the first EP pulse and at 50ms after each next EP pulse.

The first measuring pulses indicate a slight conductance increase probably due to primary electrode polarization processes. The first electro-pulse (EP) causes a 35% increase in conductance, and the following conductance measurements indicate a relaxation of the opened pores that cause a decrease of the conductance. The next EP pulse just compensates for the relaxation. The 4<sup>th</sup> and following pulses, however, cause an increasing conductivity, probably due to tissue destruction causing swelling and disruption of cells. After the last EP pulse, the conductance relaxes in two exponential steps to a level of about 1.18, that is the level due to non-reversible electroporation.

### 3.4 ELECTRICAL CONDUCTIVITY OF TISSUE

#### HEALTHY TISSUE

The data on the electrical conductivity of human tissues used in electro-dosimetry are drawn from both in vitro and ex vivo measurements. In vivo tissues may differ from in vitro and ex vivo states due to the various degrees of blood perfusion in living organs.<sup>64,65,66</sup> Recent studies with magnetic resonance imaging (MRI) combined with electrical impedance tomography

provide information about the *in vivo* conductivity of human tissues at DC or below the 1 kHz frequency range.<sup>64</sup>

Andreuccetti and Fossi (2000) developed a client-server approach for determining the dielectric properties of human body tissues in the frequency range from 10 Hz to 100 GHz using the parametric model and the parameter values previously developed by Gabriel and colleagues (1996).<sup>67,66,68,69</sup>

The webpage <http://www.dtic.mil/dtic/tr/fulltext/u2/a305826.pdf> recalls the definitions and underlying theory of the dielectric properties of biological tissues. Mathematical and computational codes and various online and offline applications are presented, based on Gabriel's parametric model.<sup>67,66,68,69</sup>

The server program (found on <http://niremf.ifac.cnr.it/tissprop/htmlclie/htmlclie.php>) runs in the background on a central system and is responsible for the management of the parameter database (14 parameters for each defined tissue) and the calculation of the dielectric properties of requested tissues at requested frequencies. These properties comprise relative permittivity, electrical conductivity, and a few significant derived quantities, such as the loss tangent, the wavelength, the penetration, and skin depth.

The user executes the client program using a remote system, connected to the server by a local or a wide area network supporting the TCP/IP protocol. The client program implements the user interface and translates user requests into commands for the server. The program also deals with the reception and display of the requested data.

The main advantage of the client/server approach consists in the centralized management of the tissue parameters, allowing new tissues to be defined and changing parameter values, without having to redistribute the software to the users. The users, on their side, also get rid of the need to implement the code for the calculation of the dielectric properties from the parameter values.<sup>1</sup>

Figure 3-19 shows relative permittivity in the frequency region 1 Hz – 1 GHz for muscle tissue derived from the ITIS database. Figures 3-20 shows the conductivity in Siemens per m ( $S \cdot m^{-1}$ ) in the frequency region 1 Hz – 1 GHz for muscle tissue derived from the ITIS database.

---

<sup>1</sup> (Internet document;

URL: <http://www.dtic.mil/dtic/tr/fulltext/u2/a305826.pdf> (authorized mirror at <http://niremf.ifac.cnr.it/docs/dielectric/home.html>). See Appendix C, for the modelling of the data (authorized mirror here).<sup>70,71,65,68,69,67,72</sup>

Documents available online at the address:

<http://niremf.ifac.cnr.it/tissprop/document/tissprop.pdf>

The Foundation for Research on Information Technologies in Society (ITIS) database for the dielectric properties of various human tissues can be reached at the web address: <https://www.itis.ethz.ch/virtual-population/tissue-properties/database/dielectric-properties/>

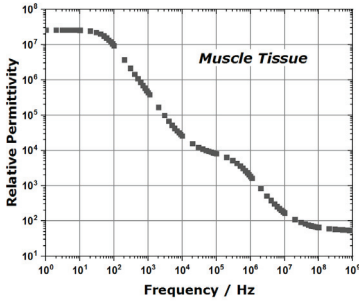


Figure 3-19  
Relative permittivity of muscle tissue in the frequency region of 1 Hz – 1 GHz (Log<sub>10</sub>/Log<sub>10</sub>–scale)

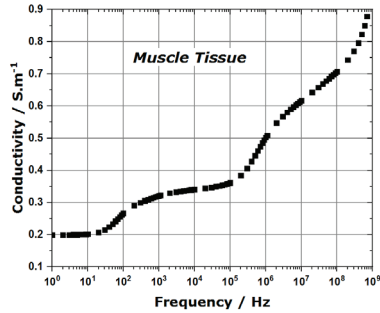


Figure 3-20  
Conductivity of muscle tissue in the frequency range of 1 Hz – 1 GHz (Log<sub>10</sub> x/ Lin y–scale)

### TUMOUR TISSUE

Figure 3-21 displays the conductivity (S/m) for muscle tissue derived from the ITIS database, and the corresponding tumour tissue derived from actual ratios presented in *Table 1* of Haemmerich et al. (2009) (represented by the black dots) and Eq. 2.18 (represented by solid line).<sup>43</sup>

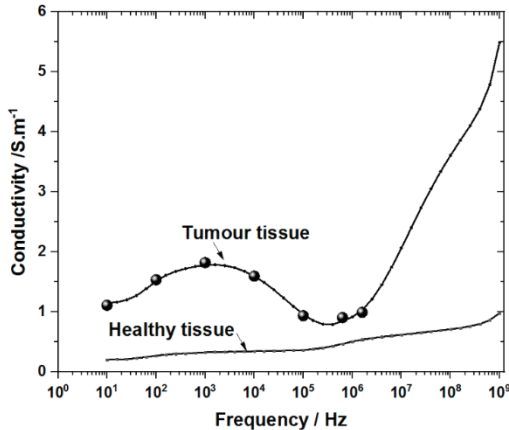


Figure 3-21  
The conductivity (S/m) for healthy tissue derived from the ITIS database and tumour tissue taken from actual ratios presented in *Table 1* of Haemmerich et al. (2009) (represented by the black dots) and Eq. 2.18 (represented by the solid line).

### 3.5 E-FIELD, CURRENT, AND POWER DISTRIBUTION IN TISSUE

#### 3.5.1 DISTRIBUTION OF FIELD STRENGTH AND CURRENT DENSITY

Figure 3-22 shows an estimation of the electric field-strength profile between two needle electrodes in tissues of various conductivities (0.1, 0.15, 0.2, 0.25, and 0.3 S/m) separated by 8mm with an applied voltage of 1000 V. The overall field-strength average is  $870 \pm 470$  V/cm; and the average between electrodes is  $905 \pm 480$  V/cm. Although the average is close to the nominal value of applied voltage divided by electrode distance, the field inhomogeneity is enormous. The E-profile and averages do not depend on the variation in tissue conductivity.<sup>73</sup> Eq. 3.31 estimates the current density  $J$  ( $A/cm^2$ ), where the cross-section *area* of current between the needle electrodes is estimated to be  $1cm^2$ .

$$J = \sigma \cdot E / \text{area} \tag{Eq.3.31}$$

The distribution of the corresponding electric current density J-profiles, however, varies a lot with tissue conductivity, as shown in Figure 3-23.

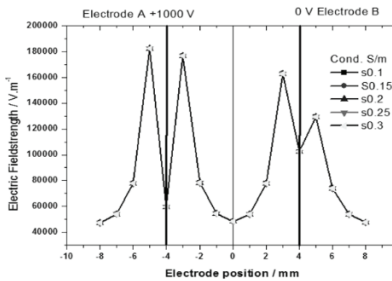


Figure 3-22  
Electric field-strength (E-profile) at an applied voltage of 1000 V over 8 mm electrode spacing. Overall average,  $E=870 \pm 470$  V/cm; average between electrodes,  $E=905 \pm 480$  V/cm

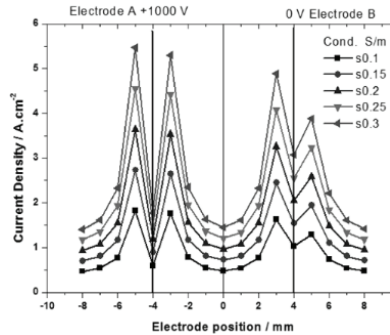


Figure 3-23  
Electric current density distribution at an applied voltage of 1000 V over 8 mm electrode spacing in tissues with various conductivities of 0.1; 0.14; 0.20; 0.25; 0.30 S/m .

Figure 3-24 displays the average current density ( $A/cm^2$ ) in tissues with various conductivities at 1000V between electrodes at a distance of 8mm apart. By experience, the recorded current between 2 needle electrodes in

tissue correlates well with the corresponding modelled current density ( $A/cm^2$ ).

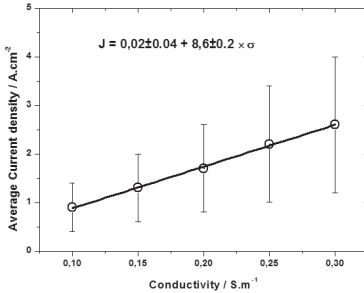


Figure 3-24  
Average current density ( $A/cm^2$ ) in tissues with various conductivities at 1000V between electrodes at a distance of 8 mm.

### 3.5.2 SPECIFIC ABSORBED ENERGY AND TEMPERATURE INCREASE

The following expression predicts the specifically absorbed energy  $sW$  in an electro-pulse treatment

$$sW = \frac{\sigma \cdot E^2}{\rho} \cdot t_p \cdot N \quad [J.kg^{-1}] \quad \text{Eq.3.32}$$

where

$\sigma$  is the tissue conductivity for the tissue [S/m];

$E$  is the electric field strength [V/m];

$t_p$  is the pulse length [s];

$N$  is the number of applied pulses;

$\rho$  is the density of tissue (muscle 1060  $kg.m^{-3}$ ).

$$\sigma_{tafter} = \sigma_{before} \cdot R_{before} / R_{after} \quad \text{Eq.3.33}$$

Equation 3.33 predicts the conductivity  $\sigma_{tafter}$  of the tissue after electro-pulse treatment with two needle electrodes separated by 8 mm<sup>73</sup>.

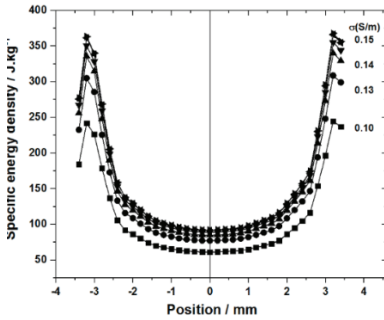


Figure 3-25  
The specific absorbed energy profiles in tissues at various conductivity values achieved after each of 6 consecutive electroporation pulses of 1000 V and 100 μs pulse length<sup>73</sup>.

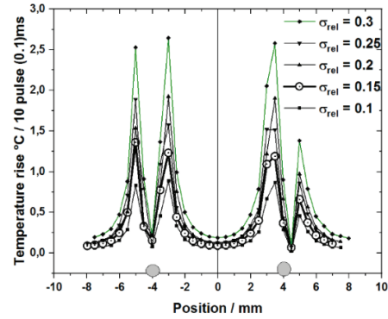


Figure 3-26  
Temperature rise at different values of relative conductivity after 10 pulses (0.1ms) 1000V<sup>73</sup>

The thermal effect of absorbed power is heat generation through the relation:

$$sW = c \cdot \Delta T \tag{Eq.3.34}$$

where

- sW = the specific absorbed energy [J.kg<sup>-1</sup>];
- c = the heat capacity 3421 ± 460 [J.kg<sup>-1</sup>.°C<sup>-1</sup>];
- ΔT = the change in temperature [°C].

The value of the heat capacity of muscle tissues is 3421 ± 460 [J.kg<sup>-1</sup>.°C<sup>-1</sup>].<sup>74</sup> The temperature rises in the tissue after 10 electric 0.1ms pulses of 1000V are applied, which has been estimated using the same FEM model assuming no loss of absorbed energy (the maximum attainable temperature). At the 0.15 S/m corresponding to muscle tissue, the temperature rise does not exceed 1°C. Thus, no thermal effect is expected. In tissues with a higher conductivity of 0.3 S/m, the maximum temperature increase around the electrodes is about 2.5°C. Thus, the electroporation procedure does not induce any hyper-thermic effects.

### 3.5.3 CHARGE DISPLACEMENT OR CHARGE DEPOSITION

The electro-permeabilization efficiency *in vitro* depends on the applied pulse energy  $W \sim E^2$  (where E is the applied field strength), while the

electro-permeabilization efficiency *in vivo* seems to depend more on the charge displacement which is equivalent to the charge density.<sup>73</sup>

$$\text{Charge density } Q = J \cdot t_p \cdot N = \sigma \cdot E \cdot t_p \cdot N; [\text{As.m}^{-2}] \quad \text{Eq. 3.35}$$

where

- $\sigma$  = conductivity [ $\text{S.m}^{-1}$ ];
- $J$  = current density [ $\text{A.m}^{-2}$ ];
- $E$  = field strength [ $\text{V.m}^{-1}$ ];
- $t_p$  = pulse length [s];
- $N$  = number of pulses.

Figure 3-27 displays the result of an FEM simulation of charge density. The value of the charge density between the two needle electrodes approaches about  $1.3 \text{ As/m}^2 = 1.4 \cdot 10^{-4} = \text{As/cm}^2 = 0.14 \text{ mAs/cm}^2$

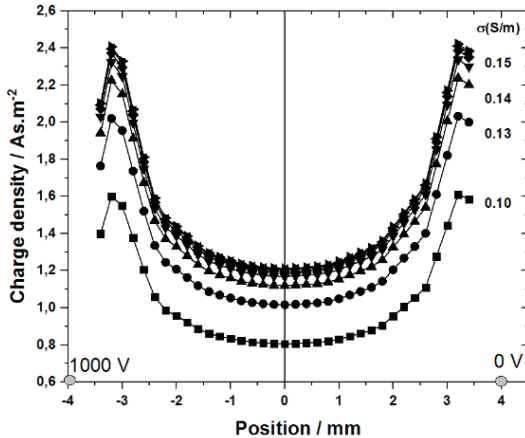


Figure 3-27

The charge density ( $\text{As.m}^{-2}$ ) profiles in tissues at various conductivity values achieved after each of 6 consecutive electroporation pulses of 1000 V and 100  $\mu\text{s}$  pulse length on two needle electrodes separated by 8 mm were conducted.<sup>73</sup>

### 3.6 MODELLING THE U,E,J, W DISTRIBUTIONS FOR SUCCEEDING PULSES

#### 3.6.1 POTENTIAL DISTRIBUTION U

Figure 3-28 show the potential  $U$ (volt) profile between two needle electrodes with a diameter of 1mm inserted into muscle tissue with conductivity 0.20 S/m. The electrodes of steel with a conductivity of  $6.2 \cdot 10^6$



S/m were separated 8 mm with an applied voltage of 1000 V at the left electrode and 0 V at the right.

At the 2<sup>nd</sup> pulse the conductivity is set to 1 S/m in a region of 3 mm outer diameter around the electrode while the rest of tissue has a conductivity of 0.2 S/m. Figure 3-29 displays the centre x-distribution of scalar electric potential  $U$ , with an applied voltage of 1000 V over two electrodes of 1 mm diameter and 8 mm electrode spacing. the conductivity is set to 1S/m in a region of 3mm outer diameter around the electrode while the rest of tissue has a conductivity of 0.2 S/m.<sup>75</sup>

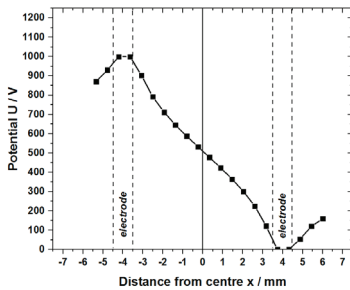


Figure 3-28  
Distribution of Electric field strength  $E$  and scalar electric potential  $U$ , at the primary pulse with an applied voltage of 1000V over two electrodes of 0.7mm diam., and 8mm electrode spacing.

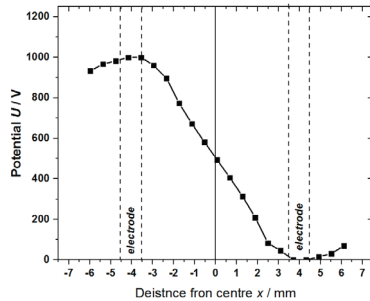


Figure 3-29  
Centre x-distribution of scalar electric potential  $U$ , at the 2<sup>nd</sup> pulse with an applied voltage of 1000V over two electrodes of 1 mm diameter and 8 mm electrode spacing. The conductivity is set to 1S/m in a region of 3mm outer diameter around the electrode while the rest of tissue has a conductivity of 0.2S/m.

### 3.6.2 ELECTRIC FIELD-STRENGTH DISTRIBUTION E

The upper figure 3-30 shows the distribution of Electric field-strength  $E$ , modelled between two needle electrodes with a diameter of 1 mm inserted into muscle tissue with conductivity 0.20 S/m. The electrodes of steel with a conductivity of  $6.2 \cdot 10^6$  S/m were separated 8 mm with an applied voltage of 1000 V at the left electrode and 0V at the right.

The lower figure 3-30 displays the profile of electric field-strength distribution along a horizontal line through the electrodes. The average electric field in the region of  $\pm 2$  mm from the centre estimated by modelling with various tissue conductivities shown in Figure 3-5 is about 1050 V/cm

independent of conductivity.

The upper figure 3-31 shows the distribution of electric field strength  $E$  at the 2<sup>nd</sup> pulse with an applied voltage of 1000 V over two electrodes of 1 mm diameter and 8 mm electrode spacing. The conductivity is set to 1 S/m in a region of 3 mm outer diameter around the electrode while the rest of tissue has a conductivity of 0.2 S/m.

The lower figure 3-31 displays the profile of the electric field strength  $E$  along the centre  $x$ -axis, with an applied voltage of 1000 V over two electrodes of 1 mm diam., and 8 mm electrode spacing. The conductivity in region of 3 mm diameter around the electrode is increased to 1 S/m due to the effect of the first pulse, while the rest of tissue has a conductivity of 0.2 S/m. The average field strength along a horizontal line in the region  $\pm 2$  mm between the electrodes is about 1750 V/cm, compared to 1150 V/cm in the first pulse.

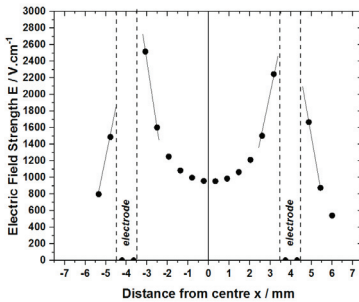
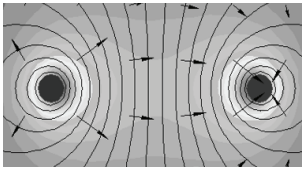


Figure 3-30  
Distribution of electric field strength  $E$ , at the primary pulse with an applied voltage of 1000 V over two electrodes of 1mm diam. and 8 mm electrode spacing in muscle tissue with conductivity 0.2 S/m.

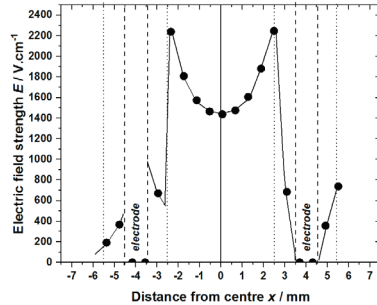
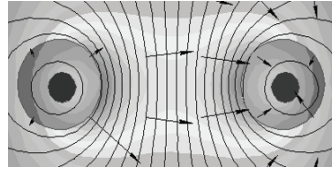


Figure 3-31  
Distribution of electric field strength  $E$ , at the 2<sup>nd</sup> pulse with an applied voltage of 1000 V over two electrodes of 1mm diameter and 8 mm electrode spacing. The conductivity is set to 1 S/m in a region of 3 mm outer diameter around the electrode while the rest of tissue has a conductivity of 0.2 S/m.

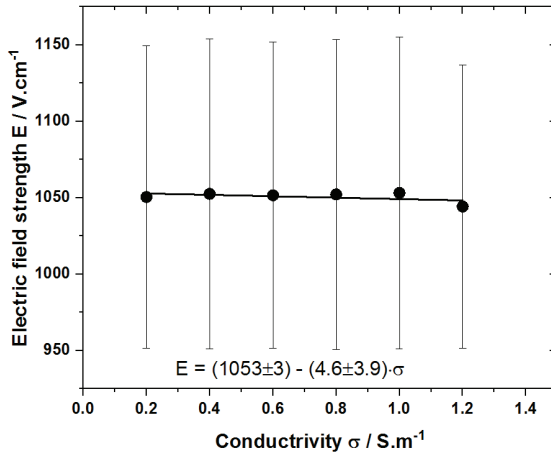


Figure 3-32  
 The average Field strength at the primary pulse in tissue of various conductivity in the central region of  $\pm 2$  mm between two electrodes of 1mm diam., and 8mm electrode spacing with an applied voltage between the electrodes of 1000V.

### 3.6.3 CURRENT DENSITY DISTRIBUTION J OF THE PRIMARY PULSE

Figure 3-33 shows the average electric current density in the region of  $\pm 2$ mm from the centre estimated by modelling with various tissue conductivities  $\sigma$ , increase linearly with conductivity. The current density expressed in  $A.cm^{-2}$  corresponds approximately to the recorded current between the electrodes.

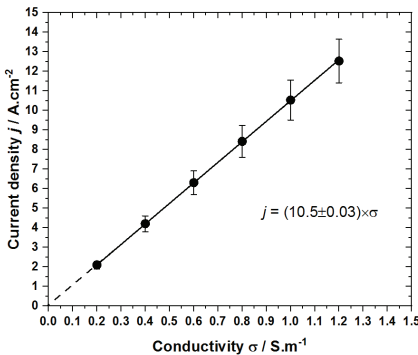


Figure 3-33  
 The average current density  $j$  in tissue of various conductivities in the region of  $\pm 2$ mm between two electrodes of 1 mm diameter, and 8 mm electrode spacing at an applied voltage between the electrodes of 1000 V.

$$I \approx 10 \cdot \sigma$$

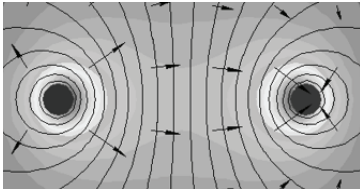


Figure 3-34  
Distribution of current density  $j$  with an applied voltage of 1000 V over two electrodes of 1mm diam. and 8mm electrode spacing in muscle tissue with conductivity 0.20S/m. The average current distribution in the region  $\pm 2$ mm between the electrodes is about 2A.cm<sup>-2</sup>.

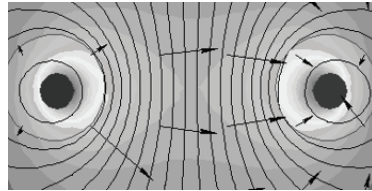


Figure 3-35  
Distribution of electric current distribution  $j$  at the 2<sup>nd</sup> pulse with an applied voltage of 1000V over two electrodes of 1mm diameter and 8mm electrode spacing. The conductivity is set to 1S/m in a region of 3 mm outer diameter around the electrode while the rest of tissue has a conductivity of 0.2S/m. The average current density in the region  $\pm 2$  mm between the electrodes is about 3.5A.cm<sup>-2</sup>

Figure 3-34 shows the distribution of electric current density  $j$  modelled between two needle electrodes with a diameter of 1 mm inserted in muscle tissue with conductivity 0.20S/m. The electrodes of steel with a conductivity of  $6.2 \cdot 10^6$  S/m were separated 8mm with an applied voltage of 1000 V at the left electrode and 0V at the right.

Figure 3-35 shows the distribution of electric current distribution  $j$  at the 2<sup>nd</sup> pulse with an applied voltage of 1000 V over two electrodes of 1 mm diameter and 8 mm electrode spacing. The conductivity is set to 1 S/m in a region of 3 mm outer diameter around the electrode while the rest of tissue has a conductivity of 0.2 S/m. The average is about 3.5 A.cm<sup>-2</sup>, compared to 2 A.cm<sup>-2</sup> in the first pulse. Thus in order to keep the current density at the level of the first pulse the applied voltage amplitude of the second pulse should be reduced.

### 3.6.4 DISTRIBUTION OF ABSORBED POWER DENSITY $P$ OF THE PRIMARY PULSE

Figure 3-36 shows the absorbed power density  $P_v$  (W/m<sup>3</sup>) between two needle electrodes with a diameter of 1 mm inserted into muscle tissue with conductivity 0.20 S/m. The electrodes of steel with a conductivity of  $6.2 \cdot 10^6$

S/m were separated 8 mm with an applied voltage of 1000 V at the left electrode and 0 V at the right.

The average absorbed power density along a horizontal line in the region  $\pm 2$  mm between the electrodes is about  $2.22 \cdot 10^9 \text{ W} \cdot \text{m}^{-3}$ , which corresponds to  $2.22 \cdot 10^6 \text{ W/kg}$ .

For a 100  $\mu\text{s}$  long pulse of 1000 V/cm amplitude the absorbed energy density is  $2.22 \cdot 10^2 \text{ J/kg} = 0.22 \text{ J/g} = 0.22 \text{ Mir}^*$ .

*\*) The unit for absorbed dose in radiation therapy is named “gray”, ( $1 \text{ Gy} = 1 \text{ J/kg}$ ) to honour Louis Harold Gray.*

*The unit for absorbed dose in electro chemo therapy is here suggested to be named “mir”, ( $1 \text{ Mr} = 1 \text{ J/g}$ ), to honour Lluís M Mir for his great contributions to the field of electrochemotherapy.*

Figure 3-37 shows the distribution of **absorbed power density**  $P_v$  distribution at the 2<sup>nd</sup> pulse with an applied voltage of 1000 V over two electrodes of 1 mm diameter and 8 mm electrode spacing. The conductivity is set to 1 S/m in a region of 3 mm outer diameter around the electrode while the rest of tissue has a conductivity of 0.2 S/m.

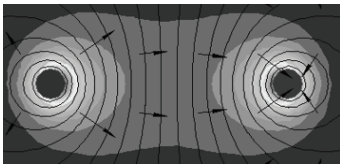


Figure 3-36  
Distribution of absorbed power density  $P_v \text{ W/m}^3$  with an applied voltage of 1000 V over two electrodes of 1mm diam. and 8mm electrode spacing in muscle tissue with conductivity 0.20S/m.

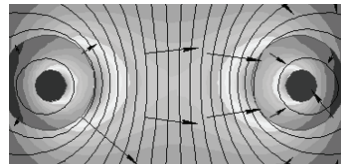


Figure 3-37  
Distribution of absorbed power density  $P_v$  distribution at the 2<sup>nd</sup> pulse with an applied voltage of 1000V over two electrodes of 1mm diam. and 8 mm electrode spacing and a region of 3 mm diameter around the electrode with the conductivity of 1S/m while the rest of tissue has a conductivity of 0.2S/m.

At the second pulse the average **absorbed power density** in the region  $\pm 2$  mm between the electrodes is about 0.63 J/g compared to 0.22 J/g at the first pulse.

### 3.6.5 SPECIFIC ABSORBED ENERGY AND TEMPERATURE INCREASE

The specific absorbed energy SAE is calculated from the following expression

$$SAE = \frac{\sigma \cdot E^2}{\rho} \cdot t_p \cdot N \text{ [J.kg}^{-1}\text{]} \quad \text{Eq. 3.36}$$

where

$\sigma$  is the tissue conductivity for the tissue [S/m]  
 $E$  is the electric field strength [V/m]  
 $t_p$  is the pulse length [s]  
 $N$  is the number of applied pulses  
 $\rho$  is the density of tissue (muscle 1060) kg.m<sup>-3</sup>

The following equation predicts the conductivity of the tissue after electroporation

$$\sigma_{after} = \sigma_{before} \cdot R_{before}/R_{after} \quad \text{Eq. 3.37}$$

The average specific absorbed energy in tissue of various conductivity of a single 100  $\mu$ s long pulse of 1000 V amplitude varies with the conductivity in the region of  $\pm 2$  mm between two electrodes of 1 mm diam., and 8 mm electrode spacing of the medium as equation Eq. 3.38.

$$\begin{aligned} SAE &= (1.11 \pm 0.006) \times \sigma; \text{ [J/g]} \\ \text{R-Square (COD)} &= 0.9998 \end{aligned} \quad \text{Eq. 3.38}$$

The value for the heat capacity of muscle issues is  $3421 \pm 460$  [J.kg<sup>-1</sup>.°C<sup>-1</sup>].<sup>74</sup> The temperature rise in the tissue after in tissue of various conductivity of a single 100  $\mu$ s long pulse of 1000 V amplitude varies with the conductivity in the region of  $\pm 2$  mm between two electrodes of 1 mm diam., and 8 mm electrode spacing of the medium is given in the equation:

$$\Delta T = (0.33 \pm 0.05) \times \sigma; \text{ [}^\circ\text{C]} \quad \text{Eq. 3.39}$$

Thus the electro pulse therapy procedure does not do not induce any significant hyper-thermic effects.

### 3.6.6 DISCUSSIONS

The extensively increase of the electric-field in the centre of the target volume could be avoided by decreasing the amplitude of the second and following pulses in the pulse train. Figure 3-38 shows an example of a pulse sequence with exponentially decreasing pulse amplitude with a time constant of 1 ms. A pulse sequence with exponentially decreasing pulse amplitude an excellent therapy efficiency of adenocarcinoma implanted in rat liver with a high degree of immune response, resulting in anti-metastatic effect.<sup>76</sup>

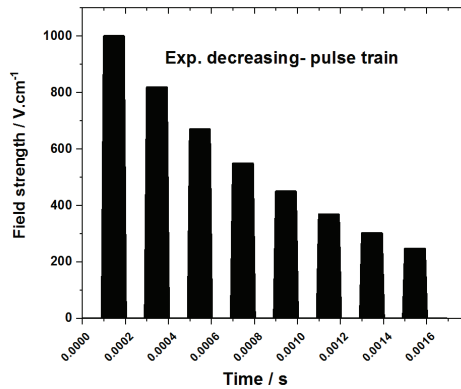


Figure 3-38  
Pulse train of Exponentially decreasing E-field that could preferentially apply to Electro-pulse therapy.

## CHAPTER IV

# GAMMA CAMERA STUDIES OF ELECTRO-PULSE ENHANCED DRUG UPTAKE

### 4.1 GAMMA CAMERA STUDIES OF BLEOMYCIN UPTAKE

Per Engström (1998) in his thesis work studied the uptake and retention of intravenously administered Bleomycin labelled with radioactive Indium-111. After treatment with electric pulses, gamma camera measurements verified the distribution of  $^{111}\text{In}$ -Bleomycin in Fischer 344 rats with subcutaneously implanted N32 glioma tumours.<sup>77,78,79,80</sup>

Figure 4-1 shows a gamma-camera image taken 2 days after intravenous administration of  $^{111}\text{In}$ -Bleomycin in non-treated rats. There is no uptake in the area of the implanted tumour, while a high accumulation of  $^{111}\text{In}$  appears in the kidneys.<sup>79,78</sup>

Figure 4-2 shows the gamma camera images of  $^{111}\text{In}$ -Bleomycin accumulation 3 days after electro-pulse treatment.  $^{111}\text{In}$ -Bleomycin gradually disappears from circulation, while it stays in the electro-pulse treated tumour and the kidneys for several days.<sup>80</sup>

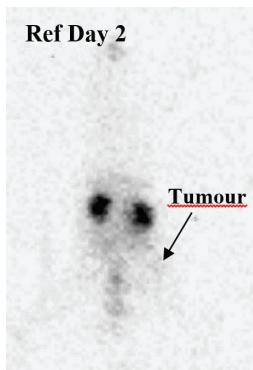


Figure 4-1  
Gamma camera image of a non-treated rat 2 days after intravenous administration of  $^{111}\text{In}$ -Bleomycin, showing uptake in the kidneys while no accumulation appears in the area of the transplanted tumour.<sup>80</sup>



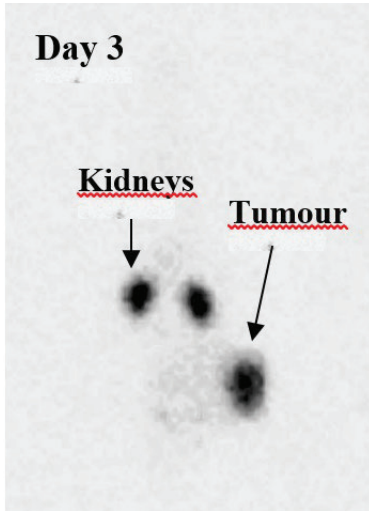


Figure 4-2  
Gamma camera image showing  $^{111}\text{In}$ -Bleomycin accumulation 3 days after electro-pulse treatment of a tumour.<sup>80</sup>

## 4.2 ELECTRO-ENHANCED UPTAKE OF $^{99\text{m}}\text{Tc}$ -DTPA

### 4.2.1 UPTAKE MEASUREMENTS OF $^{99\text{m}}\text{Tc}$ -DTPA

$^{99\text{m}}\text{Tc}$ -DTPA (diethylene-triamine-penta-acetic acid) is a common, clinically used radiopharmaceutical which shows several pharmacokinetic similarities with Bleomycin.<sup>81</sup> Intramuscular injection (i.m.) of 150MBq  $^{99\text{m}}\text{Tc}$ -DTPA in several fractions of 50  $\mu\text{l}$  each, at 1-minute intervals in the shoulder of a rat, created a depot of  $^{99\text{m}}\text{Tc}$ -DTPA for gradual uptake in the circulation in order to explore the enhanced uptake with a gamma camera after electric pulse treatment.<sup>56,58</sup>

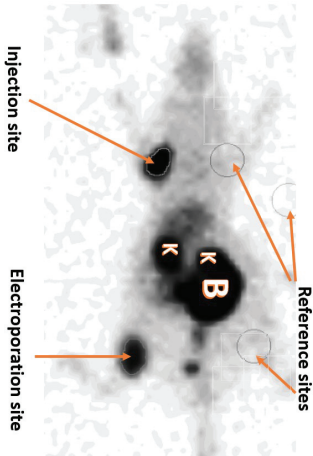


Figure 4-3  
GK-image 6 hours after electro-pulse treatment of a rat with 12 pulses of 800 V/cm and 0.25 ms. K= kidney, B= bladder.

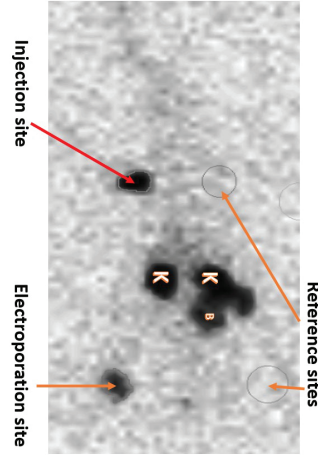


Figure 4-4  
GK-image 24 hours after electro-pulse treatment of the same animal as in Fig 4-3. K= kidney, B= bladder.

Figure 4-3 shows a typical gamma camera (GK) image of the distribution of radioactivity at 6 and 24 hours after electro-poration in the thigh muscle of a rat. The administration site on the shoulder appears as a dark spot, and the uptake in the electric pulse-treated region on the thigh shows as a dark spot. The corresponding areas at the untreated opposite sides of the rat represent the reference area for extracellular activity. Kidney (K) and bladder (B), showing urine activity, are visualized as dark areas in the image.

In the evaluation of the activity uptake, a line profile in the gamma camera images crosses the treated region within the “full width at half maximum” (FWHM). This measure defined the diameter of the circular region of interest (ROI) used for the evaluation of the drug uptake-ratio.

During the year 2000, the author performed a gamma camera imaging study of how 2, 4, 6 or 12 applied electric pulses of different field-strengths (600; 800; 1000; 1200: V/cm and pulse length 100 or 500  $\mu$ s) influence the uptake of the radiolabelled pharmaceutical  $^{99m}\text{Tc}$ -DTPA in rat muscular tissue. Figure 4-3 shows a typical gamma-camera image six hours after electro-pulse treatment in the thigh muscle of a rat, and Figure 4-4 the corresponding image after 24 hours.

Table 4-1 displays the results for each rat: the applied field strength (V/cm); pulse-length ( $\mu$ s); number of applied pulses N; and the uptake-ratio

of  $^{99m}\text{Tc}$ -DTPA in the target region after six hours (UR<sub>6h</sub>) and after 24 hours (UR<sub>24h</sub>) respectively.

**Table 4-1**

Applied field strength (V/cm), pulse-length ( $\mu\text{s}$ ), number of applied pulses N, and the uptake-ratios of  $^{99}\text{Tc}^m$ -DTPA in the target region after six hours (UR<sub>6h</sub>) and 24 hours (UR<sub>24h</sub>).

E (V/cm)	t ( $\mu\text{s}$ )	N	TcUR 6h	TcUR 24h
800	500	8	8.27	3.57
800	500	8	5.87	4.04
800	500	8	6.45	4.08
225	500	8	1.74	
225	500	8	1.01	
225	500	8	1.14	
400	500	8	1.47	2.43
400	500	8	3.25	4.05
400	500	8	5.36	2.79
1200	500	8	9.07	6.13
1200	500	8	9.01	3.14
1200	500	8	8.45	4.97
1800	500	8	10.12	
1800	500	8	7.82	
400	500	8	6.61	
1500	500	8	7.25	4.88
800	500	8	4.85	3.69
Table continued				
800	500	8	5.38	3.83
800	500	8	6.46	2.72
1500	500	8	7.76	6.32
1500	500	8	7.85	6.14
1200	500	8	9.01	9.07
1200	500	8	5.81	4.7
1200	500	8	5.53	4.22
1200	500	6	8.92	7.15
1200	500	6	4.41	2.79
1200	500	6	7.73	4.12
1200	500	10	8.66	8.01
1200	500	10	7.64	6.48
1200	500	10	11.4	5.82
1200	500	12	12.84	14.17
1200	500	12	11.23	5.61
1200	500	12	7.59	8.05
1200	500	4	10.35	8.36
1200	500	4	7.57	8.93
1200	500	2	3.34	3.22

1200	500	2	2.29	1.53
1200	500	2	2.92	2.52
1000	500	12	10.72	18.13
1000	500	12	14.52	6.74
1000	500	12	10.14	13.05
800	500	12	13.31	12.11
800	500	12	11.2	9.32
800	500	12	10.25	9.3
600	500	12	9.21	7.13
600	500	12	5.76	5.88
800	250	12	12.93	17.23
800	250	12	11.1	18.9
800	250	12	12.28	21.78
1200	500	4	13.49	14.81
1200	500	4	7.59	17.49
1200	500	4	6.18	3.02
1000	100	6	1.45	1.61
1000	100	6	3.58	4.44
1000	100	6	3.26	11.59
1000	100	12	9.72	5.77
1000	100	12	10.63	12.84
1000	100	12	6.66	11.99

Statistical analysis of the data applies multivariate data processing methods, such as principal component analysis (PCA).

Modelling of the data uses the method of projection to latent structures (PLS), also called partial least square regression (PLSR). Herman Wold introduced the practice of this method,<sup>82</sup> and his son, Svante Wold, a chemist (and in 1963, my comrade in military service), developed its application for chemometrics.<sup>83</sup> According to him, the projection to latent structures should be the correct name of the technique.<sup>84,85</sup> These methods are nowadays commonly used in chemometrics, bio-pharmacology and related areas.

Table 4-2 shows the correlation matrix of the uptake ratios with field-strength  $E(V/cm)$ , pulse-length  $PL(ms)$ , and the number of pulses:

**Table 4-2**  
Correlation matrix with E, PL and N as descriptor variables,  
and with UR<sub>6h</sub>, and UR<sub>24h</sub> as depending variables.

Variables	E V/cm	PL ms	N pulses	UR6h	UR24h
E V/cm	<b>1.000</b>	0.305	-0.591	-0.252	-0.356
PL ms	0.305	<b>1.000</b>	-0.163	0.172	-0.197
N pulses	-0.591	0.163	<b>1.000</b>	0.616	0.434
UR <sub>6h</sub>	-0.252	0.172	0.616	<b>1.000</b>	0.612
UR <sub>24h</sub>	-0.356	-0.197	0.434	0.612	<b>1.000</b>

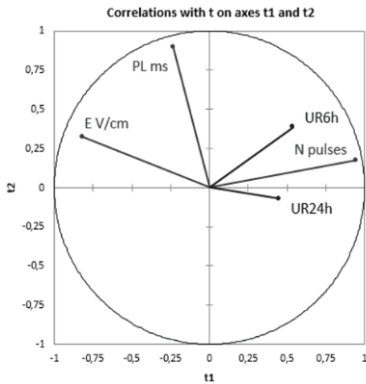


Figure 4-5

The plot of the correlation of variables with the t1 and t2 components of PLS modelling.

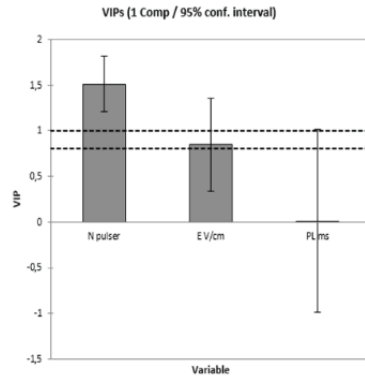


Figure 4-6

The *variable importance of projections* (VIP) of the experimental variables used in the modelling of the projection of latent variables.

Figure 4-5 displays the PLS score values  $t_2$  as plotted against the values  $t_1$  for all variables. The uptake ratios show a strong correlation with the number of pulses, but are independent of pulse-length, and inversely correlated to the applied pulse length. Figure 4-6 also shows that the number of pulses is the most important variable of projection to latent structures (VIP), followed by the field strength

Table 4-3 shows the parameters of the PLS model equations (Eq. 4.1 and Eq. 4.2) which predict the value of the uptake-ratios at 6 and 24 hours respectively. It is interesting that the parameter for the applied field strength is negative at both the 6 and 24-hour uptake-ratio, which indicates the benefit of decreasing field-strength in clinical applications.

Figures 4-7 and 4-8 display the linear relationships of the uptake ratios predicted according to the PLS modelling equations as opposed to the measured values.

**Table 4-3**  
PLS Model parameters of UR

Variable	UR <sub>6h</sub>	UR <sub>24h</sub>
Intercept	1.709	12.342
E V/cm	$-1.32 \cdot 10^{-3}$	$-5.87 \cdot 10^{-3}$
PL $\mu$ s	$7.67 \cdot 10^{-3}$	$-2.01 \cdot 10^{-3}$
N pulses	0.571	0.409
R <sup>2</sup>	0.44	0.21

**Equations of the model:**

$$UR_{6h} = 1.709 - 1.32 \cdot 10^{-3} \times E + 7.67 \cdot 10^{-3} \times PL + 0.571 \times N \quad \text{Eq. 4.1}$$

$$UR_{24h} = 12.342 - 5.87 \cdot 10^{-3} \times E - 2.01 \cdot 10^{-3} \times PL + 0.409 \times N \quad \text{Eq. 4.2}$$

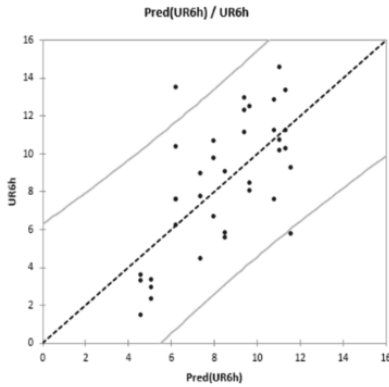


Figure 4-7  
The regression between the experimental and predicted uptake ratios 6 hours after EP

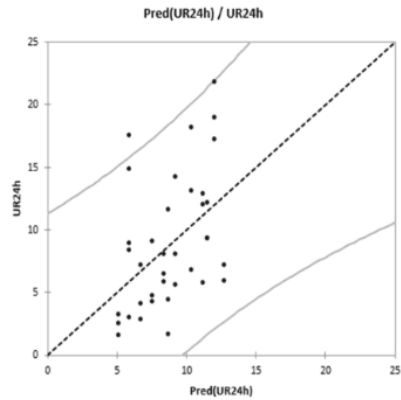


Figure 4-8  
The regression between the experimental and predicted uptake ratios 24 hours after EP

### 4.2.2. EXPLORATION OF CONDUCTIVITY CHANGE AND LOSS CHANGE INDEX

**Conductance and phase angle  $\theta$  measurements** were performed at 2 and 20kHz in Fischer 344 rats with two needle electrodes separated by 8mm inserted in the right posterior thigh muscle before and after applying the EP treatment pulse. The first two measurements established the reference level  $R_{\text{before}}$  and  $\tan(\theta_{\text{before}})$ , before the measurements were performed between each  $N_p$  consecutive pulse ( $N_p = 2, 4, 6, 10, 12$ ) of field strength amplitude  $E = 600, 800, 1000, 1200$  V/cm, and pulse-length 100, 250, 500  $\mu\text{s}$  applied at 1s intervals. To study the relaxation of the electroporation, the conductance measurements were continued 15 times after the last pulse in 1s intervals.

Table 4-4 shows the model parameters of PLS modelling the resistivity change index (Eq. 3.28), and the loss change index (Eq. 3.23) recorded at 2 and 20kHz as dependent variables, and with field strength amplitude  $E$ , pulse length PL and number of pulses  $N_p$  as descriptor variables.

**Table 4-4**  
Model parameters of PLS modelling RCI and LCI.

Variable	RCI <sub>2kHz</sub>	RCI <sub>20kHz</sub>	LCI <sub>2kHz</sub>	LCI <sub>20kHz</sub>
Intercept	-0.226	-0.288	0.114	-0.280
E V/cm	$3.76 \cdot 10^{-4}$	$3.85 \cdot 10^{-4}$	$1.20 \cdot 10^{-4}$	$2.65 \cdot 10^{-4}$
PL $\mu\text{s}$	$2.75 \cdot 10^{-4}$	$2.57 \cdot 10^{-4}$	$2.49 \cdot 10^{-4}$	$3.03 \cdot 10^{-4}$
$N$ pulses	0.024	0.023	0.012	0.034
$R^2$	0.453	0.392	0.491	0.723

Correlation of the first and second principal latent component of the various variables shown in Figure 4-9 indicates that the resistivity and phase variables are closely correlated to the pulse length and number of applied pulses. The field-strength, however, indicates a negative correlation to the number of pulses, and has no relationship with the other parameters.

Figure 4-10 also shows that “the number of pulses” is the variable of most importance to the projection of latent structures (VIP), followed by the pulse length. However, the field strength seems to be of less importance.

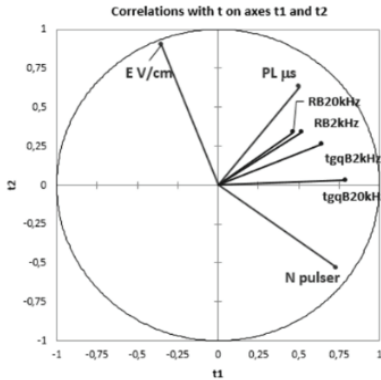


Figure 4-9  
The correlation plot of the first and second principal latent components of the various variables.

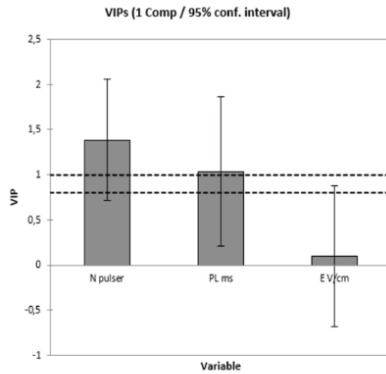


Figure 4-10  
Variable importance in the 1<sup>st</sup> projection (VIP) with the largest variance.

The best fitting to the PLS model was found for LCI recorded at 20 kHz, for which the following equations of the PLS model were achieved:

#### Loss Change Index LCI<sub>20 kHz</sub>:

$$\text{LCI}_{20\text{kHz}} = -0.280 + 0.034 \times N + 3.03 \cdot 10^{-4} \times \text{PL} + 2.65 \cdot 10^{-4} \times E \quad \text{Eq. 4.3}$$

Table 4-5 shows the current density  $J \text{ A/cm}^2$  (Eq. 3.3) estimated by Eq. 3.31 and specific absorbed energy  $W$  calculated from the Eq. 3.32 from the values of  $E$ ,  $PL$ , and  $N$  from a series of rat experiments.



**Table 4-5**

The current density  $J \text{ A.cm}^{-2}$  and specific absorbed energy  $W \text{ J.kg}^{-1}$  with E, PL, and N as predictor variables.

Rat ID	E V/cm	PL $\mu\text{s}$	N pulses	$J \text{ A.cm}^{-2}$	$W \text{ J.kg}^{-1}$
1	1200	500	2	14.47	3276
2	1200	500	2	16.17	3660
3	1200	500	2	15.32	3547
4	1200	500	4	15.50	7018
5	1200	500	4	25.00	11321
6	1200	500	4	20.69	9370
7	1200	500	4	16.89	7647
8	1200	500	4	17.07	7732
9	1200	500	4	29.38	13306
10	1200	500	10	15.67	17735
11	1200	500	10	18.95	21448
12	1200	500	10	23.29	26364
13	1200	500	12	32.19	43725
14	1200	500	12	37.57	51039
16	1000	100	6	2.74	1549
17	1000	100	6	2.22	1256
18	1000	100	6	2.34	1326
19	1000	100	12	2.32	2632
20	1000	100	12	2.63	2983
21	1000	100	12	3.12	3529
22	1000	500	12	3.34	21165
23	1000	500	12	3.82	15574
24	1000	500	12	3.16	17881
25	800	500	12	2.15	9754
26	800	500	12	2.28	10303
28	800	250	12	1.91	4327
29	800	250	12	3.11	7034
30	800	250	12	2.66	6029
31	600	500	12	1.64	5580
32	600	500	12	1.44	4899
15 <i>outlayer</i>	1200	500	12	258.15	45482

Figure 4-11 displays the correlation of  $t_1$  and  $t_2$  PLS modelling scores with  $J$  and  $W$  acting as dependent variables and field strength amplitude  $E$ , pulse length  $PL$  and number of pulses  $N_p$  as descriptor variables. The plot in Figure 4-11 indicates that the current density  $J$  and specific absorbed energy  $W$  correlate to the applied field-strength  $E$  and pulse length. Figure 4-12 shows the applied field-strength to be the most *important variable in the projection* (VIP) followed by pulse-length. The number of pulses seems to be less critical.

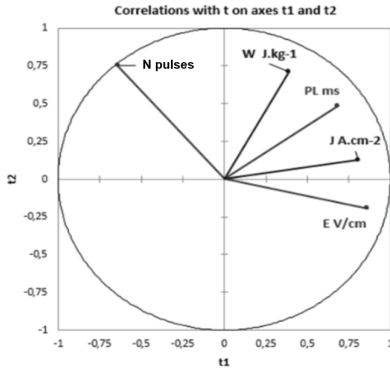


Figure 4-11

A correlation plot of the first and second principal latent components of the various variables

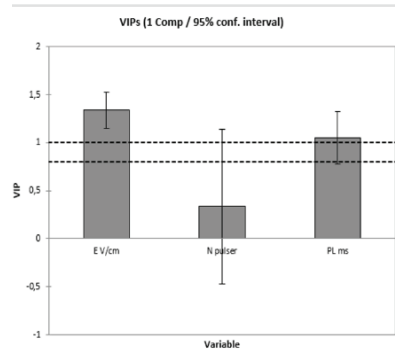


Figure 4-12

Variable importance in the 1<sup>st</sup> projection (VIP) with the most substantial variance

With current density  $J$  and specific absorbed energy  $W$ , as dependent variables, and applied field strength, pulse length and number of pulses as descriptor variables, a PLSR modelling resulted in the following model equations:

$$J [\text{A.cm}^{-2}] = -45.2 + 0.043 \times E + 0.022 \times PL + 0.398 \times N \quad \text{Eq.4.4}$$

$$W [\text{J.kg}^{-1}] = -71791 + 47.9 \times E + 28.6 \times PL + 2616 \times N \quad \text{Eq. 4.5}$$

### 4.2.3 EXPLORATION OF CONDUCTIVITY RELAXATION

After the applied electro-permeabilization pulse, the conductivity started to decrease and approach a plateau value. The fraction of the plateau value relative to the conductivity recorded after the last pulse is a measure of the fraction of reversible electropermeabilized cells. This value is of importance for the long-term transfer of exogenous substances to the cell and outflow of immunogenic material from the cell. Figure 4-13 displays the results of PLS modelling, with the fraction of reversible relaxation  $F_{\text{rev}}$  evaluated by Eq. 3.30 using the relaxation curves and the mean relaxation time  $T$  for each rat fitted to a single exponential decay as dependent variables and field strength amplitude  $E$ , pulse length  $PL$  and number of pulses  $N_p$  as descriptor variables.

The plot in Figure 4-13 indicates that a fraction of reversible relaxation  $F_{rev}$  correlates positively to the applied field-strength  $E$  and negatively to the number of applied pulses. Figure 4-14 shows the applied field-strength to be the most important variable in the projection (VIP), followed by the number of pulses. The pulse length seems to be less critical.

The PLS model parameters given in Table 4-6 show a negative relationship to the applied field strength and pulse length, while the fraction of reversible relaxation  $F_{rev}$  shows a positive relationship.

$$T [s^{-1}] = 6.056 - 1.82 \cdot 10^{-3} \times E - 1.18 \cdot 10^{-3} \times PL + 0.065 \times N; \quad \text{Eq. 4.6}$$

$$R^2 = 0.30$$

$$F_{rev} = -0.257 + 5.07 \cdot 10^{-4} \times E + 3.28 \cdot 10^{-4} \times PL - 0.018 \times N; \quad \text{Eq. 4.7}$$

$$R^2 = 0.73$$

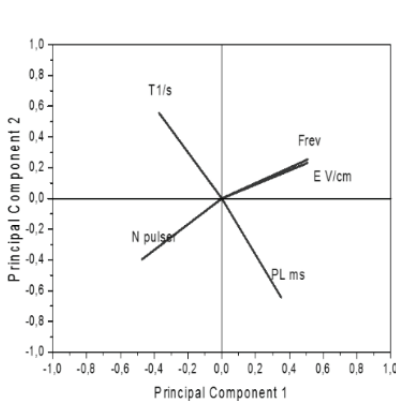


Figure 4-13

A correlation plot of the first and second principal latent components of the various variables

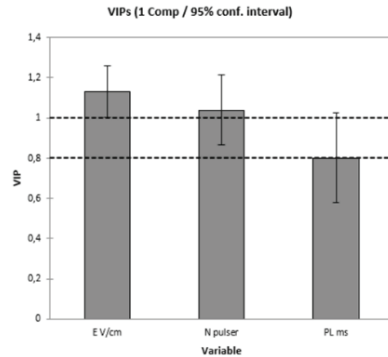


Figure 4-14

Variable importance in the projection (VIP) of the variables with the most substantial variance

### 4.3 CONCLUSION

The parameters with the most regression to the drug uptake ratio 6 and 24 hours after electroporation are  $LCI_{20kHz}$ ;  $LCI_{2kHz}$ ;  $W J \cdot kg^{-1}$ ; and  $RCI_{2kHz}$ .<sup>56,58</sup> Thus, the most optimal scenario to predict the outcome of the electro-chemotherapy session (i.e., to achieve the highest uptake ratio of Bleomycin) would be to use  $LCI_{20kHz}$  and  $LCI_{2kHz}$  as descriptors beside the parameters  $E$ ,  $PL$  and  $N$ . Figure 4-15 displays the variable importance in the projection (VIP): of PLS modelling with all descriptor variables. Figure 4-16 displays the variable importance in the projection (VIP) of PLS modelling with only  $LCI$  and the number of pulses as descriptor variables.

PLS modelling with all five descriptor variables (LCI<sub>20kHz</sub>;LCI<sub>2kHz</sub>, E kV/cm, PL ms, and N) resulted in the following equation with the coefficients summarized in Table 4-6:

$$UR_{6h} = 2.22 - 1.85 \times E - 0.22 \times PL + 0.22 \times N + 9.38 \times LCI_{2kHz} + 6.32 \times LCI_{20kHz} \quad \text{Eq.4.8}$$

$$UR_{24h} = 3.37 - 1.61 \times E - 0.19 \times PL + 0.19 \times N + 8.13 \times LCI_{2kHz} + 5.48 \times LCI_{20kHz} \quad \text{Eq.4.9}$$

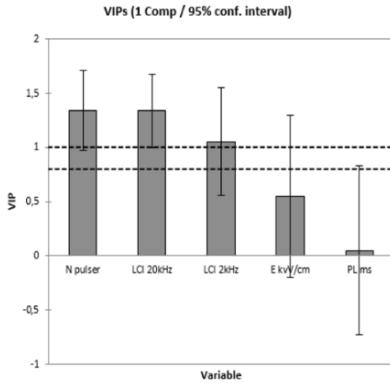


Figure 4-15  
Variable importance in the projection (VIP) of all descriptor variables

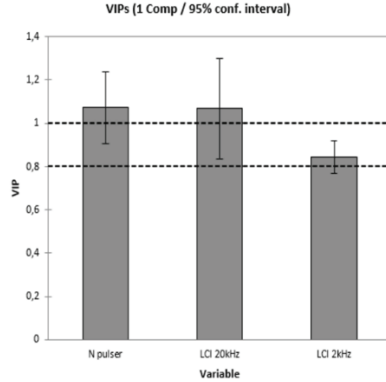


Figure 4-16  
Variable importance in the projection (VIP) of LCI and number of pulses as the descriptors

Surprisingly the coefficient for the E-field becomes negative, which means that the uptake decrease by increasing the field strength. It also indicates that the large inhomogeneity of the field is of less importance.

**Table 4-6**  
Model parameters of PLS modelling uptake ratio

Variable	UR <sub>6h</sub>	UR <sub>24h</sub>
Intercept	2.22	3.37
E kV/cm	-1.85	-1.61
PL ms	-0.22	-0.19
N pulses	0.22	0.19
LCI <sub>2kHz</sub>	9.38	8.13
LCI <sub>20kHz</sub>	6.32	5.48
R <sup>2</sup>	0.46	0.16

Table 4-7 displays the modelling results achieved through PLS modelling by omitting the E-field and pulse length as descriptor variables.

**Table 4-7**  
Model parameters of PLS modelling

Variable	UR <sub>6h</sub>	UR <sub>24h</sub>
Intercept	-0.51	-1.46
N pulses	0.24	0.20
LCI <sub>2kHz</sub>	10.17	8.34
LCI <sub>20kHz</sub>	6.82	5.60
R <sup>2</sup>	0.47	0.14

$$UR_{6h} = -0.51 + 0.24 \times N + 10.17 \times LCI_{2kHz} + 6.82 \times LCI_{20kHz} \quad \text{Eq.4.10}$$

$$UR_{24h} = -1.46 + 0.20 \times N + 9.34 \times LCI_{2kHz} + 5.60 \times LCI_{20kHz} \quad \text{Eq.4.11}$$

## CHAPTER V

# PRECLINICAL STUDIES OF ELECTRO-PULSE ENHANCED THERAPY

### 5.1 PRECLINICAL *EpEChT* STUDIES WITH BLEOMYCIN

#### 5.1.1 INTRODUCTION

Okino and Mohri reported the first preclinical study using the electroporation effect for enhanced transport of the anticancer drug Bleomycin across the cell membrane in 1987.<sup>26,27</sup> The first clinical trial using Bleomycin and electric pulse treatment (known as “electro-chemotherapy” (ECT)) was performed on head and neck tumours by Mir and colleagues in France in 1991.<sup>86,87,88,89</sup> Following clinical trials, this method has, as of 2018, been used to treat more than 1500 patients with either malignant melanoma, Kaposi’s sarcoma, breast cancer, squamous cell carcinoma and basal cell carcinoma. The clinical results reviewed and analysed in the following chapter are very challenging. These results of extensive preclinical studies indicate enhanced therapeutic effects as a consequence of combining pulsed electric field treatment with chemotherapy, immunotherapy, and radiation therapy regimes.

Electro-pulse-enhanced chemotherapy (*EpEChT*) investigations use many different tumour models in mainly small mammals such as rats and mice. Because of their accessibility and practicality, coetaneous and subcutaneous malignancies constitute the major part of these studies. The pulse-enhanced protocols used clinically initially were derived from *in vitro* studies. Most of these studies use square wave pulses or exponentially decaying pulses.<sup>78,90,91</sup>

The amplitudes of the applied electric fields vary from 800 to 1500 V/cm. The pulse length used in square wave protocols is usually about 0.1ms, and in exponential pulse protocols, the mean decay time is about 1ms. The number of pulses applied is typically between 6 and 12.

Transmembrane breakdown of cells *in vivo*, as well as *in vitro*, occurs only when the external field exceeds a specific threshold value. This

threshold, however, is more difficult to define *in vivo* than *in vitro*. Drug and gene delivery by *in vivo* electro-permeabilization of muscle cells occurs at a field strength of 100-200V/cm and pulse lengths of 20-100ms.<sup>92,93,31</sup> The electro-permeabilization efficiency also depends on the size of cells and the dielectric properties of the tissue. One remarkable observation from all the animal studies of electro-pulse enhanced chemotherapy is the overall favourable treatment efficiency, regardless of the tumour model.

Electro-pulse -enhanced chemotherapy has been performed on the following tumour models:

- mammary tumours,<sup>94</sup>
- melanoma,<sup>95,30,96</sup>
- hepatic tumours from colorectal cancer,<sup>37,76</sup>
- hepatomas,<sup>36</sup>
- subcutaneous and orthotopic pancreatic adenocarcinoma.<sup>38</sup>
- soft tissue sarcomas,<sup>33,97,98</sup>
- bladder cancer,<sup>99,100</sup>
- subcutaneous and intracerebral gliomas,<sup>78,34</sup>

Electropermeabilization has also been employed to enhance the intratumoural uptake of Boron-compounds in Boron neutron capture therapy of malignant gliomas.<sup>101</sup>

Electro-pulse-enhanced chemotherapy has hitherto mainly been used as single-treatment cancer therapy. However, treatments performed once a week on three occasions on mice with B16 melanoma, a tumour with a very high recurrence rate, markedly improved the response rate and increased the survival time, although the cure rate was low.<sup>102,103</sup>

### **5.1.2 ELECTRO-PULSE ENHANCED TREATMENT OF RAT GLIOMA**

The first intracerebral electro-pulse-enhanced chemotherapy was performed in 7 rats with RG2 glioma cells inoculated in the brain and electric pulses delivered through two acupuncture needles inserted 5mm into the parenchyma on each side of a tumour.<sup>34</sup> Bleomycin was administered intravenously before electric pulse delivery. Two complete remissions were recorded and a significantly prolonged survival time of 200% was achieved for the seven treated animals compared to all other groups.

Bleomycin reaches, and to some extent accumulates in, glioma and meningioma after intravenous injection, via the disrupted blood-brain barrier.<sup>104,105,106,107,108</sup> A study of intracerebral electro-pulse chemotherapy treatment performed with radioactive <sup>111</sup>In-labelled Bleomycin resulted in several cases of complete remission of N32 tumours.<sup>79</sup>

### 5.1.3 ELECTRO-PULSE ENHANCED TREATMENT OF RAT LIVER TUMOURS

Since 1997, four studies have reported on electro-pulse-enhanced chemotherapy of tumours treated in the liver, of which two have been colorectal cancer.<sup>37,36,109,110</sup> The treatment protocol and outcome of these studies are summarised in Table 5-1 and compared to the one described in 2001 by Engström and collaborators.<sup>76</sup> In all studies, except one, Bleomycin was applied intralesionally to a tumour.<sup>110</sup> Generally, the studies used low doses of Bleomycin in combination with electro-pulse treatment. A high dose, one-tenth of the LD50, did not improve the treatment outcome, probably due to a suppressed immune system caused by the high Bleomycin dose.<sup>109</sup>

**Table 5-1**  
Summary of treatment protocols and outcome for electro-pulse-enhanced chemotherapy performed on liver tumours.

Tumour (animal)	Volume at treatment mm <sup>3</sup>	E V/cm	Pulse parameters	
			t (ms)	N
Hepatoma (rat)	220	1000	0.1	6
Colon (rat)	24	1300	0.1	6
Papilloma (rabbit)	380	850	0.1	?
Colon (mouse)	visible	1000	0.1	8
Colon (rat)	300	1300	1.0 Exp.	8+8



**Table 5-1** (continued)

Study	Dose (BLM) mg/kg	Response Cure rate	CR rate
Jaroszeski, 1997 <sup>36</sup>	1.7 (i.t)	ND	69%
Chazal, 1998 <sup>37 34</sup>	2.25 (i.t)	22 %	
Ramirez, 1998 <sup>110</sup> .		30 %	
Kuriyama, 1999 <sup>109</sup>	0.5-1.0 (i.v.)	0 %	
Engstrom, 2001. <sup>76</sup>	23 (i.t)	92 %	

The study by Engström *et al.* (2001) reports better treatment results than the others.<sup>76</sup> The protocol used differs from the others in terms of the pulse duration and the number of pulses. Exponential pulses of 1.0ms time constant were applied, which have shown to result in higher drug uptake in tissue compared to 0.1ms square pulses.<sup>90</sup> The square wave pulses are less damaging to the healthy tissue surrounding the tumour, but may not always be as effective in tumour treatment. No increase in the alanine-aminotransferase level appeared, and an overall gain in weight supports the view that the treatment trauma was mild. At 40 days after treatment, the tumours were almost wholly eradicated with only minor fibrous tissue remnants.

## 5.2 PRECLINICAL STUDIES OF CISPLATIN CHEMOTHERAPY

A study of cell survival *in vitro* was performed to determine whether electroporation may increase the absorption of various anticancer drugs, and thereby increase their toxicity to human colorectal cancer cells.<sup>111</sup> The 50% survival level of cancer cells decreased by 100-1000 times after treatment with Bleomycin and electroporation, but only by 2-5 times when using 5-fluorouracil, and not at all with Cisplatin. Cancer cells transplanted subcutaneously onto nude mice and treated with a combined treatment of Bleomycin and electroporation, caused, after 3 weeks, reduced tumour size<sup>111</sup> Another study was performed to determine whether electroporation may increase the absorption of various anticancer drugs and thereby increase their toxicity to gastrointestinal cancer cells. The 50% survival level of the cancer cells decreased by a factor of 10000 after treatment with

Bleomycin and electroporation, but only with a factor of 10 when using Cisplatin or 5-fluorouracil. Cancer cells transplanted subcutaneously onto nude mice and treated with a combined treatment of Bleomycin and electroporation, caused, after 3 weeks, reduced tumour size.<sup>112</sup>

In vitro electroporation treatment increases the cytotoxicity of Cisplatin in human ovarian cancer and also in its resistant sub-clone.<sup>113</sup> In another study of mice treated with electroporation in 3 groups, only intra-tumoural (i.t.) administration of Cisplatin, and a combination of electroporation and i.t. Cisplatin, resulted in any improvement. Treatment performed with only i.t. Cisplatin resulted in up to 20 days' delay in tumour growth, but a combined treatment of electroporation and i.t. Cisplatin resulted in two times more tumour control.<sup>114</sup>

In addition to Cisplatin (CDDP), there is another platinum-based chemotherapeutic: Oxaliplatin (OXA). A study comparing the effect of these compounds in combination with electroporation showed that CDDP was nearly twice as effective as OXA. The study also showed that electro-pulse-enhanced chemotherapy with platinum-based chemotherapeutics increases lymphocyte infiltration in the tumour.<sup>115</sup>

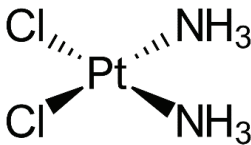


Figure 5-1  
Cisplatin (CDDP)

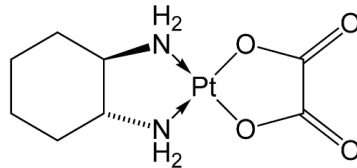


Figure 5-2  
Oxaliplatin (OXA)

### 5.3 *EpEChT* AND CYCLOPHOSPHAMIDE (CTX)?

Cyclophosphamide has been found to induce beneficial immunomodulatory effects on adaptive immunotherapy. The suggested mechanisms involved in the creation of this immunologic effect were the following events:<sup>116</sup>

- Elimination of T regulatory cells (CD4<sup>+</sup>, and CD25<sup>+</sup> T cells) in naive and tumour-bearing hosts;
- Induction of T cell growth factors, such as type I interferons (IFNs);
- Enhanced grafting of acquired transferred, tumour-killing effector T cells (CTL).

Thus, cyclophosphamide preconditioning of recipient hosts (for donor T cells) might be used to enhance immunity in naïve hosts.

Since cyclophosphamide has been found to induce beneficial immunomodulatory effects in immunotherapy, electro-enhanced chemotherapy using cyclophosphamide in combination with Bleomycin would be an effective tumour treatment modality as well. A recent *in vitro* study showed that electro-pulse-enhanced chemotherapy using cyclophosphamide (CTX) has a similar anti-tumoural effect to Bleomycin.<sup>117</sup>

The combination of electro-enhanced gene-therapy with Vasostatin-gene and cyclophosphamide administration was found to inhibit tumour growth, and resulted in extended survival in mice with melanoma tumours.<sup>118</sup>

## 5.4 ELECTRO-PULSE ENHANCED IMMUNO THERAPY

### 5.4.1 IMMUNE RESPONSE OF *EpEChT*

Immunogenic Fibrosarcoma treated with electro-pulse enhanced chemotherapy using Bleomycin in immunocompetent syngeneic mice and immune-deficient (nude) mice, resulted in only a temporary delay in tumour growth.<sup>103</sup> Further studies showed that the host's immune system activates after tumour treatment with electro-permeabilization.<sup>119</sup> Mir and colleagues achieved a systemic, anti-metastatic immune response by delivering histoincompatible cells secreting interleukin-2 (IL-2) in combination with electro-pulse enhanced chemotherapy to 3LL-Lewis lung carcinoma in mice.<sup>120</sup> In another study, a stimulated immune response, through increased monocyte and T-lymphocyte activity, was found by using Cisplatin instead of Bleomycin.<sup>121</sup>

Genetically engineered IL-2-secreting cells injected intratumourally or in peri-tumoural oedema after electro pulse enhanced chemotherapy of VX2 tumours transplanted into rabbit liver increased the cure rate from 30% to 40%. More importantly, treatment resulted in a clear anti-metastatic effect on tumour spread in the liver and lungs, which led to cures also of the untreated contralaterally implanted tumours. This systemic antitumor effect also resulted in immunity with complete protection against further tumour cell inoculation.<sup>122</sup>

The results of treatment of liver tumours also imply that electro-pulse enhanced chemotherapy stimulates a response in the host's immune system against the tumour.<sup>76</sup> Two weeks after electro-pulse-enhanced chemotherapy of colorectal tumours in the liver, with exponential decaying pulses of 1.0ms time constant and Bleomycin, macrophages, T-lymphocytes were found in

excised stained viable tumours.<sup>76</sup> The results showed overall low levels of CD4 positive lymphocytes and ED2 positive macrophages. The most significant amounts of CD8 positive lymphocytes were found in a viable tumour treated with electro-pulse enhanced chemotherapy with Bleomycin, and the lowest amounts in tumours treated with Bleomycin only. The most substantial amounts of ED1 positive macrophages were found in tumours treated with electrical pulses only and combined with Bleomycin. The electro-pulse chemotherapy treatment also seemed to have anti-metastatic effects. Intra-abdominal metastases developed, however, after surgical excision of the tumour-bearing lobe. At 14 days after electro-pulse enhanced chemotherapy treatment, none out of 13 treated animals showed signs of tumour spread. These results strongly suggest that electro-pulse-enhanced chemotherapy stimulates activation of the host's immune system against a tumour and prevents metastases development.<sup>76</sup>

Calvet and collaborators showed in 2014 that the injection of CT26 murine colon cancer cells, in vitro treated with *EpEChT*, elicits an antitumor immune response that prevents the growth of a subsequent administration of viable cancer cells. The treatment caused complete regressions in immunocompetent animals but not in immune-deficient ones, which supports the role of immunity in allowing for a beneficial outcome of electro-pulse-enhanced cancer therapy.<sup>123,124</sup>

#### 5.4.2 ELECTRO-PULSE THERAPY WITH IL-18 AND IFN $\gamma$ SECRETING CELLS

The brain tumour models used in electro-pulse-enhanced immunotherapy treatment are two strains of rat brain glioma: N32 and N29 were chemically induced (ethyl-N-nitrosourea) and developed at the Department of Tumour Immunology of Lund University, Sweden. These tumours are only weakly immunogenic and grew intra-cerebrally, subcutaneously and in vitro.<sup>125</sup> In the present study, the tumours were created by subcutaneously injecting 100 000 tumour cells into the thigh of the rats' hind legs. After 4 weeks, a solid tumour developed with a diameter of 1 to 1.5 cm, and the animals were then treated.

In an attempt to achieve immunoreactions against implanted brain tumours, rats with N29 glioma tumours were treated with electric pulses followed by injections of IL-18 and IFN- $\gamma$  secreting cells.<sup>126</sup>

Tumours were inoculated subcutaneously on both thighs of female Fischer-344 syngeneic rats. The left tumour was treated once with 16 pulses of 1400 V/cm with durations of 1.0ms (time constant), without anticancer drugs given at any time. The following day, and then once a week for three

weeks, the animals were given intraperitoneal injections of irradiated, modified N29 tumour cells, secreting either interleukin-18 (IL-18) or interferon-gamma (IFN- $\gamma$ ).

No effect in contralateral tumour growth appeared in animals given no treatment, or treatment with only electric pulses, with only IFN- $\gamma$  secreting cells and with only IL-18 secreting cells. Having said this, an inhibited growth rate of contralateral tumours appeared in animals given electric pulse treatment followed by intraperitoneal injections of IL-18 secreting cells. This treatment resulted in prolonged survival (the time for a contralateral tumour to reach the predetermined limit volume) of 50%.

These results show that the systemic response of the host's immune system can be achieved against a tumour using *syngeneic* tumour cells. This is an essential step towards the development of electro-pulse-enhanced immunotherapy for an effective tumour treatment modality.<sup>126</sup>

### 5.4.3 EpEIT WITH DAC-TREATED IL-18 AND IFN $\gamma$ SECRETING CELLS

The DNA de-methylating agent 5-aza-2-deoxycytidine (DAC) is a cytosine analogue that covalently binds to DNA methyl-transferase and inhibits its activity in causing de-methylation. The gene expressions which may be silenced by the hypermethylation of their promoters are re-activated by DAC. Expressions of HLA class I are significantly increased in DAC-treated glioma cells when compared to those of untreated cells, which makes DAC a potent immune stimulator.

These findings provide the basis to consider the use of 5-aza-2-deoxycytidine (DAC) treatment of IFN- $\gamma$  transfected tumour cells aiming for immune therapy. The study was performed in Fischer 344 rats with N29 glioma tumours subcutaneously implanted on both flanks to study the immunoreactions against implanted brain tumours. After treatment of a contralateral tumour with pulsed electric fields (PEF), injections of IL-18 or IFN- $\gamma$  secreting cells followed. The following day, and once a week for three weeks, the animals received intraperitoneal injections of radiation sterilized, gene-modified N29 tumour cells, secreting either interleukin-18 (IL-18) or interferon- (IFN- $\gamma$ ).

In one group of animals, IFN- $\gamma$  transfected cells treated with DAC were used for immunization. The size of the tumours on the flank was measured daily to evaluate the tumour growth-rate (TGR) regarding the specific therapeutic effect (STE), which is the difference in tumour growth-rate between the control and exposed tumours, divided by the tumour growth rate of the controls. The therapeutic enhancement ratio (TER) expresses the

quantitative estimate of the sensitisation effect of the combination of pulsed electric fields and radiation therapy. TER is the ratio of the STE of the experimental combination of pulsed electric fields (PEF), and immunization and STE of the hypothetical independent combination of the two agents.<sup>127</sup>

Treatment with only PEF in 32 animals resulted in a specific therapeutic effect of  $20 \pm 6$  %. The effect on the contralateral non-targeted tumour was negligible ( $0 \pm 4$  %).

Immunization with  $\text{IFN}\gamma$  secreting cells in 27 animals showed a slightly increased growth-rate of both the left and right tumours. This adverse effect is probably due to strong immune-suppression caused by the heavy tumour burden. However, immunization with DAC treated  $\text{IFN}\gamma$  secreting cells ( $\text{IFN}\xi$ ) in 12 animals showed decreased growth-rates on both the left (10%) and right (5%) tumours. Thus, the DAC treatment had induced such a strong antigen expression that the immune response was partly able to overcome the immune-suppression.

For the combination of  $\text{PEF} + \text{IFN}\gamma$ , there was no therapeutic enhancement, but in the combination of PEF and  $\text{IFN}\gamma$  secreting cells grown in a 5-Azacytidine medium ( $\text{IFN}\zeta$ ), the therapeutic enhancement factor was about 2 on both sides. However, for the combination of PEF + immunization with DAC-treated  $\text{IFN}\gamma$  secreting cells ( $\text{IFN}\xi$ ), there was a sizeable therapeutic enhancement in the combination of PEF and  $\text{IFN}\xi$  (50%), and on a non-targeted tumour there was an effect of about 20%.

Thus for the combination of PEF +  $\text{IFN}\gamma$ , there was no therapeutic enhancement, but in the combination of PEF and  $\text{IFN}\gamma$  secreting cells grown in a 5-Azacytidine medium ( $\text{IFN}\zeta$ ), the therapeutic enhancement factor was about 2 on both sides of the tumours.

## 5.5 ELECTRO-PULSE ENHANCED RADIATION THERAPY “*EpERT*”

### 5.5.1 *EpERT* TREATMENT OF FIBROBLAST CELLS

The remarkable effective killing of V-79 fibroblast cells appeared after combined exposure with 2Gy radiation (RAD) and exponentially shaped, pulsed electric fields with an amplitude of 1600V/cm and a time constant of  $\tau = 1$  ms at 1Hz repetition (PEF).<sup>128,77,129,130</sup>

Radiation therapy alone is known to have a limited therapeutic effect on brain tumours, but the combination of ionizing radiation exposure with high voltage pulses was never studied before. Encouraged by the results from V-79, we carried out the combined treatment  $\text{PEF} + \text{RAD}$  on a rat brain tumour

model. In the study of tumours created by subcutaneously injecting 100 000 N29 brain tumour cells onto the thigh of the rat's hind leg, after 4 weeks, a solid tumour developed with a diameter of one to 1.5 cm. The animals were then treated.

The Fischer rats with N32 tumours grown on their flanks received four daily combined treatments with RAD+PEF and the reversed PEF+RAD. The tumour response was evaluated by observing the change of tumour volume measured as an ellipsoid (as is shown in Figures 5-3 and 5-4).

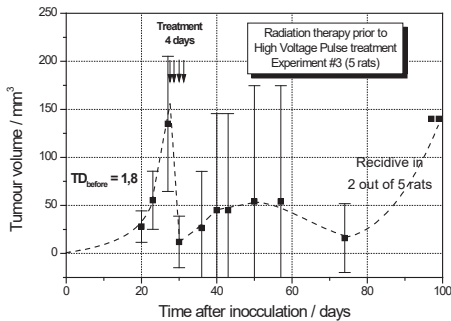


Figure 5-3

Average effect in five rats of combined treatment first with  $^{60}\text{Co}$ -radiation 5 Gy and then with 16 high voltage pulses (1300V/cm.  $\tau=1\text{ms}$ ), over 4 consecutive days

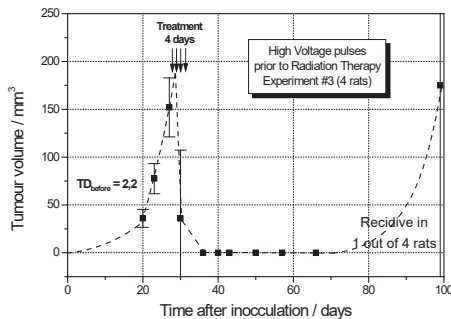


Figure 5-4

Average effect in four rats of combined treatment first with 16 high voltage pulses (1300 V/cm.  $\tau=1\text{ms}$ ) and then with  $^{60}\text{Co}$ -gamma radiation 5Gy, over 4 progressive days

### 5.5.2 *EpERT* OF SUBCUTANEOUS IMPLANTED N29 TUMOURS IN FISCHER RATS

Another experiment arranged Fischer rats with subcutaneous implanted N29 tumours into five groups. One group of 8 rats were controls (Ctrl) and received no treatment. A treatment group (RAD) with 5 rats received radiation (4×6 Gy), and a treatment group PEF with 4 rats received pulsed electric fields (4×8 pulses of 1400 V/cm). The groups of combined treatment (PEF+RAD) with 9 rats received pulsed electric treatment combined with a total absorbed radiation dose of 20Gy, given in four daily fractions of 5Gy each.

Animals (single-treated and controls) put to death when a tumour had reached a size of 5 cm<sup>3</sup>. Table 5-2 shows the averages of the time until this event as “survival time” for the various groups. There was a significant difference (p<0.05) in survival time between the combined treatment and the control groups. Fisher's exact probability test of 2×2 contingency tables was used to calculate p-values of significant differences. The number of cures was significantly larger for the EP+RT group compared to the control group (p=0.009) and the RAD group (p=0.03). There were no significant differences in the number of cures for PEF as opposed to controls or PEF vs. RAD.

Results from combined treatment with <sup>60</sup>Co-gamma radiation therapy (RAD) and pulsed electric field therapy (PEF) show the average time when a tumour had reached a size of 5cm<sup>3</sup>:

- > 94 days when treated first with RAD then PEF
- >100 days when treated first with PEF then RAD

**Table 5-2**

Treatment data, a summary of results and statistics

<i>Treatment</i>	<i>Survival (days) excl. cures</i>	<i>TGD (%) of non-cured</i>	<i>N</i>	<i>Number of cures (CR&gt;80) d Post treatm.</i>	<i>Fisher's exact probability test</i>
Control	41.5 ± 1.1	0	8	0	
RAD	50 ± 1.1	21	5	0	NS (vs.Ctrl.)
PEF	70 ± 14.6	69	4	1	NS (vsCtrl.)
PEF+RAD	98.3 ± 0.7	137	9	6	P<0.01 (vs.Ctrl.) p<0.05 (vs.RAD)



All treated animals showed an initial partial or complete tumour remission within a few days after the end of the 4-day treatment for the combination radiation RAD (4×5Gy) and then PEF (4×1300V/cm). Three out of the 11 treated animals had complete remission lasting more than 100 days. For the combination (4×PEF1300V/cm) and then radiation (4×5Gy), 3 out of the 4 treated animals had complete remission >100 days. The outcome of this preliminary study of combining pulsed electric field and radiation therapy suggests an astonishingly effective therapeutic response.<sup>131,77,132,80</sup>

### 5.5.3 T-LYMPHOCYTE INFILTRATION IN TUMOURS

Infiltration of T-cells CD4<sup>+</sup> and CD8<sup>+</sup> was studied in subcutaneous implanted N29 tumours after various types of treatments.<sup>78,90</sup> The tumours were excised after treatment and embedded in paraffin. The scanned images shown in Figure 5-5 and 5-6 below are microscopic slides scanned in a CCD scanner, and the degree of staining evaluated by Image processing (Image Pro 5).

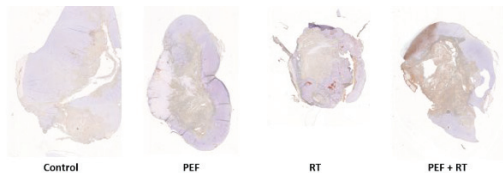


Figure 5-5 CD4<sup>+</sup> infiltration in tumours of various treatment: Controls, pulsed electric fields PEF (1400 V/cm), radiation therapy RT (4x5 Gy) and the combination PEF+RT (*EpERT*)

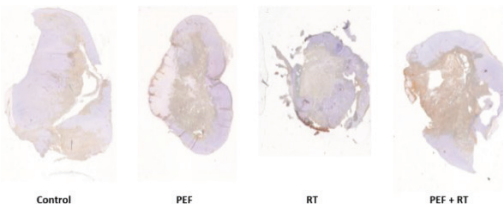


Figure 5-6 CD8<sup>+</sup> infiltration in tumours of various treatment: Controls, pulsed electric fields PEF (1400 V/cm), radiation therapy RT (4x5 Gy) and the combination PEF+RT (*EpERT*)

Figures 5-7 and 5-8 show the average results of the area of a tumour stained for CD4<sup>+</sup> CD8<sup>+</sup> respectively after a number of different treatments for each group.

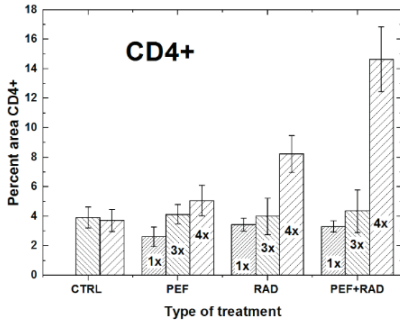


Figure 5-7

Percent area of tumours stained for CD4+ after a number of different treatments: Controls (CTRL), pulsed electric fields (PEF 1, 2, and 4x 8 pulses of 1400 V/cm), radiation therapy (RAD 1, 3 and 4x5 Gy), and a combination (PEF+RAD 1, 3, and 4 times of each).

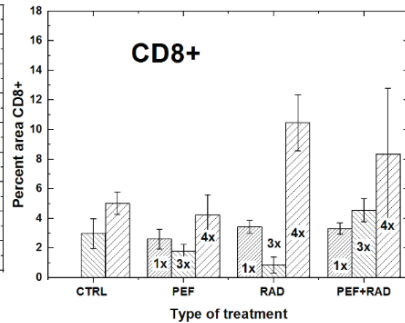


Figure 5-8

Percent area of tumours stained for CD4+ after a number of different treatments. Controls, pulsed electric fields PEF (1, 2, and 4x 8 pulses of 1400 V/cm), radiation therapy RT (1, 3, and 4x5 Gy) and the combination PEF+RT,

By using the presented system for treating tumoural diseases (cancer) with a combination of ionizing radiation and pulsed electric fields, a new regime of radiation fractionation is possible. A short intensive treatment using high radiation dose fractions combined with pulsed electric fields followed by a longer resting interval allows the patient's own immune system to be effectual. The intensity of the following therapy session may depend on the outcome of the previous treatments. Recurrent tumours already given full dose with conventional therapy could receive further radiation fractions up to a total absorbed dose of less than 15Gy combined with pulsed electric fields. It is thus worthwhile to further explore this combined type of treatment to improve the therapy of resistant tumours. It might be of particular interest to apply high voltage impulses combined with brachytherapy where the radioactive source (i.e., Iridium-192) can serve as an electrode.<sup>133</sup>

## 5.6 *EpEChT* COMBINED WITH RADIATION THERAPY

### 5.6.1 EAT TUMOURS IN MICE WITH CISPLATIN AND RT

Sersa and colleagues studied the combined modality of electro-pulse enhanced chemotherapy with Cisplatin and radiation using subcutaneous

Ehrlich ascites tumours (EATs) in CBA mice.<sup>134,135</sup> The mice were treated either with Cisplatin (CDDP), electric pulses (EP), or ionizing radiation (RT), as well as combinations thereof. Table 5-3 shows the results of the combined treatments recorded 100 days after treatment. These results show that delivery of Cisplatin into the cells through electroporation of tumours increases the radio-sensitizing effect of Cisplatin. However, the effect may also be due to the radiation reduced immunosuppression through a tumour which enhances the effect of electro-pulse chemotherapy.

**Table 5-3**  
The published results by Sersa et al. (2000).<sup>135</sup>

<b>Treatment</b>	<b>Complete remissions / %</b>
Control	0
CDDP 4 mg/kgBW	0
EP (8x1300 V/cm. 0.1ms)*	0
EP+CDDP	12
RT (15 Gy)^	37
EP*+RT^	54
RT^+CDDP	73
EP*+CDDP+RT^	92

### 5.6.2 TREATMENT OF LPB SARCOMA IN MICE WITH CISPLATIN *EpEChT* and RT

In a study in 2003, Kranjc and colleagues treated LPB murine sarcoma cells and tumours in mice either with Cisplatin, electroporation or ionizing radiation, as well as combinations of these. In vitro response was determined by colony forming assay, while in vivo treatment effectiveness was determined by the values of the 50% tumour control dose (TCD<sub>50</sub>).

They found that exposure of cells in vitro to a combination of Cisplatin and electroporation increased and prolonged accumulation of Cisplatin and reduced tumour perfusion. Combined with ionizing radiation, the effectiveness of the treatment is significantly enhanced by 60%, compared to the irradiated tumours, and 40% compared to tumours treated with Cisplatin and irradiation.<sup>136</sup>

### 5.6.3 TREATMENT OF LPB SARCOMA IN MICE WITH *EpEChT* BLEOMYCIN, and RT

In a study in 1995, Okunieff et al. investigated the effect of Bleomycin *EpEChT* combined with radiation therapy (RT) on subcutaneous Murine

sarcoma LPB tumours in C57Bl/6 mice.<sup>137</sup> Three minutes after intravenous injection of BLM (injection volume 150 $\mu$ l), 8 electric pulses of 1300 V/cm with 0.1ms duration at 1 Hz were applied to the tumours using plate electrodes placed on the skin overlying the tumour.

**Table 5-4**

The values of the 50% tumour control dose (TCD<sub>50</sub>) and the relative tumour control (RTC) versus radiotherapy RT only for various combinations of treatment.<sup>137</sup>

Treatment	TCD <sub>50</sub>	SD	RTC
RT	23.1	0.3	1.0
<i>EpE</i> +RT	22.1	0.3	1.0
Bleo+RT	22.8	0.3	1.0
<i>EpEBleo</i> +RT	12.4	0.3	1.9

They used the TCD<sub>50</sub> value (i.e., the dose that decreases the treated tumour to half its size) as a measure of the therapeutic effect.<sup>137</sup> Table 5-4 shows the values of the 50% tumour control dose (TCD<sub>50</sub>) for various combinations of treatment and the relative tumour control (RTC) versus radiotherapy RT only.

Neither treatment of animals with radiation alone (RT) nor the application of electric pulses or Bleomycin to the tumours before irradiation (*EpE*+RT and Bleo+RT) of tumours had any effect on the 50% TCD value (TCD<sub>50</sub>) (Table 5-4). However, the application of electric pulses with Bleomycin combined with radiation therapy (*EpEBleo*+RT) decreased the TCD<sub>50</sub> value of tumours by a factor of 1.9 compared to any other treatment. Hence it is evident that radiation therapy of tumours significantly contributed to the therapeutic effect of Bleomycin *EpECT*.<sup>138</sup>

In a 2009 study, Kranjc et al. evaluated the interaction between electro-chemotherapy using Bleomycin and single-dose or fractionated radiation in two murine tumour models with different histology.<sup>139</sup> They found that electro-pulse chemotherapy before radiotherapy of the tumours potentiated the response to a single fraction ionizing radiation of 10Gy or five daily fractions of 2Gy.

Figure 5-9 shows the results of the data for the radiosensitive sarcoma SA-1 extracted from *Figure 2A* of Kranjc's 2009 publication and normalized to 100% at the beginning of treatment fitted to Boltzmann's logistic functions.<sup>138</sup>

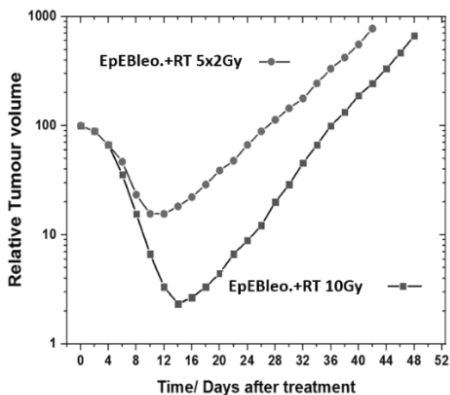


Figure 5-9  
The tumour growth curves after treatment with Bleomycin *EpEChT* combined with radiation therapy in a single fraction of 10Gy or five daily fractions of 2Gy.<sup>138</sup>

Figure 5-10a shows the decrease of tumour volume during the first 15 days after treatment with Bleomycin *EpEChT*, and a single fraction radiation RT10Gy, and Figure 5-11a offers the corresponding curve after *EpEChT*, and five fractions of radiation RT5x2Gy.<sup>139</sup>

Figure 5-10b shows the increase of tumour volume during the regrowth period, starting at 15 days after Bleomycin *EpEChT*, and a single fraction radiation and Figure 5-11b shows corresponding curve after *EpEChT* and five fractions of radiation +RT5x2Gy.<sup>139</sup>

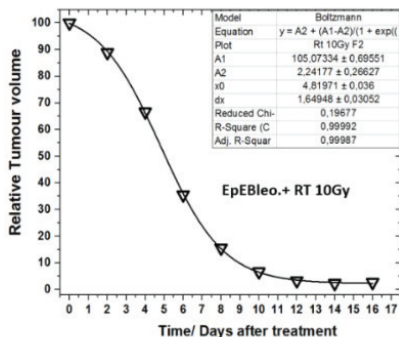


Figure 5-10a  
The decrease of tumour volume in the first 15 days after treatment with Bleomycin *EpEChT*+RT10Gy, and the data fitted to the Boltzmann sigmoid equation.

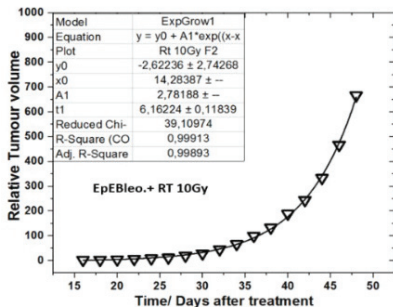


Figure 5-10b  
The increase of tumour volume during the regrowth from 15 days after Bleomycin *EpEChT*+RT10Gy treatment, and the data fitted to an exponential growth equation.

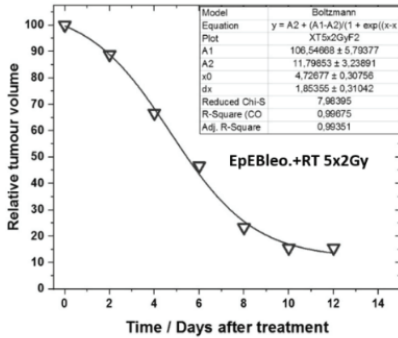


Figure 5-11a  
The decrease of tumour volume in the first 15 days after treatment with Bleomycin *EpEChT* + RT5x2Gy, and the data fitted to the Boltzmann sigmoid equation

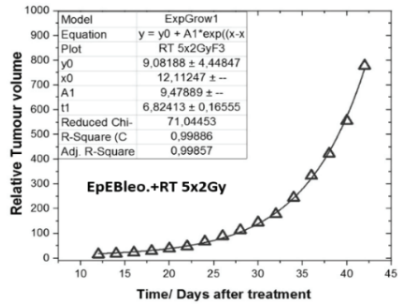


Figure 5-11b  
The increase of tumour volume during the regrowth from 15 days after Bleomycin *EpEChT*+RT5x2Gy treatment, and the data fitted to an exponential growth equation

The minimum tumour volume after 14 days is about 2% for single fraction radiotherapy and about 15% after 12 days for fractionated radiation therapy. In both cases, however, there is a tumour regrowth with about 15% per day.

The mechanism behind the effect of the combination of *EpECT* ad RT is probably similar to the enhancement of the effect of tumour vaccine by a single fraction of RT.<sup>140,141,142,143</sup> The creation of a bolus of dead tumour cells as a result of the *EpEChT* treatment is similar to the administration of a bolus of dead tumour cells, which activates the tumour suppression through an accumulation of myeloid-derived suppressor cells (MDSC) in the tumour microenvironment. A single fraction of ionizing radiation of about 8 Gy deactivates the immune-suppressive effect during the following 10-14 days. If there are surviving tumour cells present after the treatment, the tumour starts growing again. Thus, several repeated treatment regimens are required to achieve a complete cure.

The results of the combination of *EpEChT* and radiation therapy suggest a therapy regime with repeated treatments of *EpEChT*+RT once a week until a complete cure appears. The absorbed dose and number of treatment procedures required might vary with the histology of a tumour and from patient to patient. Thus, the oncology community should urgently start clinical trials to standardize the treatment parameters for the combination of electro-pulse enhanced chemotherapy and radiation therapy.

## 5.7 PRECLINICAL STUDIES OF ELECTRO-ENHANCED THERAPEUTIC EFFICIENCY OF OTHER DRUGS

### 5.7.1 ELECTRO-ENHANCED THERAPEUTIC EFFECTS OF CALCIUM

Calcium is essential for plant cells, as well as for mammalian cells. However, an overload of intracellular calcium-ions is toxic already at small concentrations deviating from normal conditions.<sup>144,145</sup>

In 1995, weed control experiments were performed with seeds of *Sinapsis Alba* as a model to investigate the effect of high voltage pulses at various calcium concentrations.<sup>146,147</sup>

The seeds of *Sinapsis Alba* were first steeped in ordinary tap water during 40 minutes and then placed in solutions of different calcium concentrations (0.05, 3, 10 and 50mM). After treatment with pulsed electric fields of various field-strengths ranging from 500 to 3000 V/cm, the seeds were set to grow in a climate controlled environment to examine their survival. A control group was established with seeds treated in the same way as above, but without electric field exposure. After treatment, the seeds were placed on wet filter paper in petri-dishes, and set to grow during 7 days for evaluation with the sprout length (SL) as a measure of survival.

Figure 5-12 shows the survival fraction (SF = SL(EP-exposed)/SL(control)) for seeds of *Sinapsis Alba* steeped with various Ca-concentrations and then treated with 20 exponential pulses (1ms time-constant) at various electrical field-strengths. Figure 5-13 displays the survival fraction for seeds of *Sinapsis Alba*, steeped with various concentrations of calcium ions and then treated with 20 exponential pulses (1ms time-constant) at 1000V/cm.

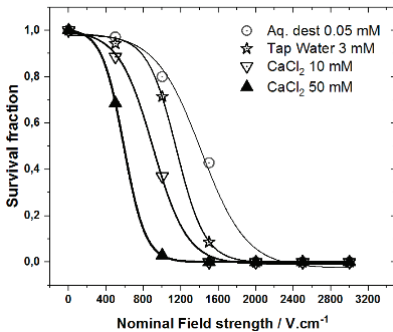


Figure 5-12  
Survival curves for seeds of *Sinapsis Alba* steeped with various Ca-concentrations and then treated with 20 exponential pulses (1ms time-constant) at various electrical field-strengths.

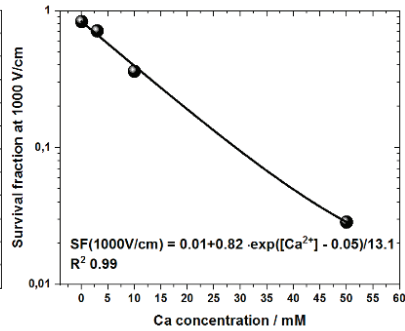


Figure 5-13  
Survival fraction for seeds of *Sinapsis Alba* steeped with various Ca-concentrations and then treated with 20 exponential pulses (1ms time-constant) at 1000V/cm.

These results clearly show the enhanced seed killing effect of increased Ca-concentration in the electro pulse medium. The effect is believed to depend on a decreased threshold membrane potential for dielectric breakdown. A study exploring how electric field pulses can induce apoptosis recorded that divalent ions in the medium apoptosis occurred at much lower (about 10 times) concentrations than monovalent ions.<sup>148</sup>

In 2014, Frandsen et al. confirmed the Ca-effect in three different cell lines (DC-3F), and transformed Chinese hamster lung fibroblast; K-562, human leukaemia; and murine Lewis Lung Carcinoma. With the aim to apply this finding in electro-enhanced cancer therapy they clinically investigated the effects of electrical pulsing parameters and calcium as further reviewed in the next chapter.<sup>149,150,151</sup>

### 5.7.2 ELECTRO ENHANCED THERAPEUTIC EFFICIENCY OF MITOMYCIN C

Human pancreatic tumours (Pan-4-JCK) were implanted onto nude mice treated with Bleomycin, Mitomycin C or Carboplatin as single agents in electro-pulse chemotherapy. The therapeutic effect on tumour growth monitored for 89 days was in the order Bleomycin >> Mitomycin C > Carboplatin.<sup>152</sup>



Mitomycin C electro-pulse treatment of a T24 bladder cancer cell line enhanced the cytotoxicity by about 30%, which supports the use of this combination in the treatment of bladder cancer.<sup>153</sup> Further in vivo studies revealed a tumour response rate of 100% for electro-pulse treatment in combination with Mitomycin C with significant tumour volume reduction.<sup>154</sup>

# CHAPTER VI

## CLINICAL STUDIES OF ELECTRO-PULSE- ENHANCED CHEMOTHERAPY

### 6.1.1 INTRODUCTION

In the early 1990<sup>th</sup> Belehraddek and collaborators performed an initial clinical trial with Bleomycin, followed by 4 or 8 electric pulses of 1.3 kV per cm electrode distance, and 0.1ms in duration, resulted in an apparent antitumor effect, reaching 72% of objective responses OR, with 57% of complete response CR.<sup>155,94</sup> The first Phase I-II clinical trial of electro-chemo-therapy performed in 8 patients with 40 nodules of head and neck squamous cell carcinomas, previously irradiated and surgically treated without cure and with tumours resistant to conventional chemotherapy. The patients were given Electro-pulse enhanced chemotherapy with an intravenous bolus of 10 mg/m<sup>2</sup>BSA.<sup>156</sup>

Another clinical study was performed in a group of 34 patients, to determine whether the dose of intra-lesional administered Bleomycin based on tumour volume in combination with electric pulses could improve the treatment result. The Figures 6-1a and 6-1b display the dose of Bleomycin versus tumour volume.<sup>32</sup>

In Figure 6-1 the dotted line is the graph of the fitted “*Dose response equation*” (Eq. 6.1).

$$\text{Dose} = A1 + (A2-A1)/[1 + 10^{(\text{LOGx0-TV}) \cdot p}] \quad \text{Eq.6.1}$$

R-Square(COD)=0.98

where:

A1 = bottom asymptote =-4123;  
 A2 = top asymptote =4147,  
 LOGx0 = centre =-574,  
 TV = Tumour Volume,  
 P = hill slope =2.15·10<sup>-4</sup>,

Figure 6-2 displays the Bleomycin data in USP units fitted to a 2<sup>nd</sup> degree polynomial of the logarithm of tumour volumes (TV) between 100 - 5000 mm<sup>3</sup> Eq. 6.2.

$$\text{Bleo (USP units)} = 5.55 - 4.74 \cdot \log_{10}(\text{TV}) + 1.147 \cdot (\log_{10}(\text{TV}))^2; \quad \text{Eq.6.2}$$

R-Square(COD) = 0.98.

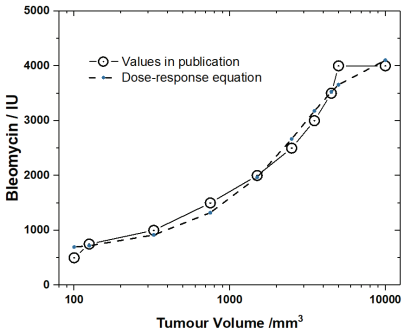


Figure 6-1  
The open circles are data extracted from the publication<sup>32</sup>, and the dashed line is the graph of the fitted equation..

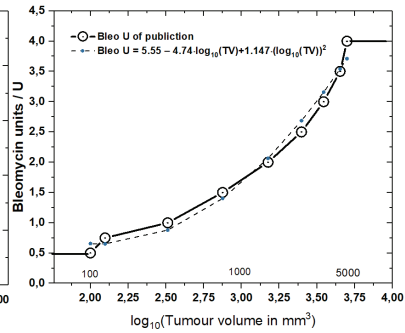


Figure 6-2  
The open circles are data extracted from the publication<sup>32</sup>, and the dotted line is the graph of the fitted equation.

At 10 minutes after the Bleomycin administration six to eight electric pulses of 1.3 kV amplitude per cm electrode distance and 0.1 ms in duration delivered, and within 12 weeks complete responses observed in 91% of the treated nodules.<sup>32</sup>

From January 1995 to August 1996, a clinical study with electro-enhanced chemotherapy enrolled 29 male and five female patients (mean age, 62.2 years) with BCC, advanced melanoma metastatic to local or distant soft tissue and skin sites, squamous-cell carcinoma (SCC), or Kaposi's sarcoma.<sup>157</sup>

1998, Mir et al. summarized the results of independent clinical trials, performed by five cancer.<sup>31</sup> In those trials, a total of 291 cutaneous or subcutaneous tumours of basal cell carcinoma (32), malignant melanoma (142), adenocarcinoma (30) and head and neck squamous cell carcinoma (87) treated in 50 patients. Complete response appeared in 56% of the treated tumours, and partial response in 29% of all tumours treated.

A phase II prospective clinical trial took place during 1998-1999, that involved two patients with nine nodules of basal cell carcinomas, two patients with 13 metastases of melanoma, two patients with two nodules of

squamous-cell carcinomas (SCC), and two patients with 14 skin metastases from breast cancer. Intra-lesional Bleomycin administered according to Figure 6-1, and 10min after Bleomycin injection, electric pulses at a field strength of 1300V/cm and pulse-length of 100 $\mu$ s were delivered at a frequency of 1Hz. The mean follow-up was 8.6 months, with overall objective responses of 98%, complete or partial responses of 49%, and stable disease (i.e., no response) in 2%. In the two patients with basal cell carcinoma, a 78 % complete response was achieved.<sup>158</sup>

A review of electro-enhanced chemotherapy with Bleomycin in clinical studies involving 96 patients with altogether 411 malignant tumours reported a wide spread of the fraction of complete remissions between 9-100 % depending on the technique used in the treatment. The results indicate that the treatment, for the most part, is palliative, while curative in the patients with basal cell carcinoma and solitary tumours without metastases.<sup>159</sup>

From the 1<sup>st</sup> of January 2003 to the 31<sup>st</sup> of December 2005 a European project “*European Standard Operating Procedures of Electro-chemotherapy*” (ESOPE), was launched with the aim of prepare standard operating procedures (SOP) for electro-enhanced chemotherapy. The project based on the electro-pulse enhanced chemotherapy activities of four European cancer clinics.

The final ESOPE recommendations are summarized in a number of publications in *European Journal of Cancer*, EJC Supplements 4 (2006).<sup>160,161,162,163,164,165,166,167,168</sup>

An updated standard operating procedure for electrochemotherapy of cutaneous tumours and skin metastases was recently released.<sup>169</sup> This updated ESOPE considers recommendations for indications and treatment choices for electro-enhanced chemotherapy, and information about pre-treatment, evaluation, and patient follow-up.<sup>169</sup>

### **Anaesthesia**

Consider local anaesthesia if tumour count  $\leq 7$  and size  $\leq 3$ cm

Consider general anaesthesia if tumour count  $> 7$  and size  $> 3$ cm.<sup>169</sup>

### **An intravenous administration**

ESOPE recommends intravenous administration of Bleomycin to a dose of 15000 IU per m<sup>2</sup> body surface, 15 000 IU (International units) = 15 USP units = 15 mg.

### **An intra-tumoural administration**

Bleomycin at a concentration of 1000 IU/ml is recommended by ESOPE to a dose depending on tumour volume according to the following rules:<sup>165, 169</sup>The injection volume depends on the size of the tumour nodules =  $TV \text{ cm}^3$ ,

Injection volume (ml) = Bleo i.t. dose (IU) / 1000 (IU/ml)

For tumour  $> 1 \text{ cm}^3$  250 IU/cm<sup>3</sup>, Bleo i.t. Dose =  $250 \times TV$  [IU]

For tumour  $1 - 0.5 \text{ cm}^3$  500 IU/cm<sup>3</sup>, Bleo i.t. Dose =  $500 \times TV$  [IU]

For tumour  $< 0.5 \text{ cm}^3$  1000 IU/cm<sup>3</sup>. Bleo i.t. Dose =  $1000 \times TV$  [IU]

### **Parameters for electric pulse treatment with the type of electrodes:**

**Electric pulses** should be applied to the tumour nodules in a time window between 8 and 28 min after the intravenous injection of Bleomycin, or as soon as possible within 2 min after its intra-tumoural injection.

#### **Plate electrodes.**

8 electric pulses of 1.3 kV amplitude per cm electrode distance and 0.1ms in duration, delivered at either 1Hz or 5 kHz repetition frequency;

#### **Four needle electrodes placed in parallel rows.**

8 electric pulses of 1 kV amplitude per cm electrode row distance and 0.1ms in duration, delivered at either 1Hz or 5 kHz repetition frequency;

#### **Seven needle electrodes which are hexagonally centred.**

96 electric pulses (eight pulses per pair of needles) of 1 kV amplitude per cm electrode distance and 0.1 ms in duration, delivered at either 1Hz or 5 kHz repetition frequency.<sup>162</sup>

To further improve the treatment results of electro-enhanced chemotherapy particularly of larger tumours, the present author suggests a new dimension of intra-tumour administration of Bleomycin:

Instead of a decreasing concentration with tumour volume as is recommended by ESOPE, the Bleomycin concentration could be the same for all tumoural volumes. The concentration of Bleomycin suggested is 500 IU per cm<sup>3</sup> of tumoural volume. A maximum dose limit of 40 000 IU that corresponds to a tumour volume of 80 cm<sup>3</sup>, and 10% of the maximal allowed

i.v. Bleomycin dose, avoid too high doses. In order to avoid injection of too high volumes the concentration of the Bleomycin preparation for tumours larger than  $5\text{cm}^3$  could increase.

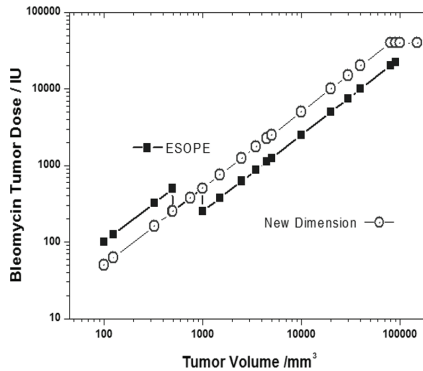


Figure 6-3

Bleomycin Dose (IU) in tumours of various volume ( $\text{mm}^3$ ) at intra-tumoural administration according to the ESOPE recommendations,<sup>165</sup> and according to a constant Bleomycin concentration of  $500\text{ IU/cm}^3$  in a tumour up to a dose-limit of  $40,000\text{ IU}$ .

In recent years several authors have reviewed the clinical results of Electro Enhanced Chemotherapy:

- Electro-enhanced chemotherapy for primary skin cancer and skin metastasis related to other malignancies<sup>170</sup>.
- Utility of electro- enhanced chemotherapy in melanoma treatment<sup>171</sup>.
- Antitumor effectiveness of electro- enhanced chemotherapy: A systematic review and meta-analysis<sup>172</sup>.
- Electro- enhanced chemotherapy in Breast Cancer: A review of references<sup>173</sup>.
- Treatments of advanced basal cell carcinoma: a review of the literature<sup>174</sup>.
- Treatment efficacy with electro-enhanced chemotherapy: A multi-institutional prospective observational study on 376 patients with superficial tumours<sup>175</sup>.
- Basal cell carcinoma: 10-year experience with electro-pulse enhanced chemotherapy<sup>176</sup>.
- Electro-pulse enhanced chemotherapy in Breast Cancer - Discussion of the method and literature review<sup>177</sup>.

The treatment results are in most publications reported regarding the following quantities where the fractional response

$$f = (\text{No. cases with the actual response} / \text{Total No. Cases})$$

CR = Complete response;  $f_{\text{CR}}$  = fractional complete response;  
 PR = partial response;  $f_{\text{PR}}$  = fractional partial response;  
 SD = stable disease;  $f_{\text{SD}}$  = fractional stable disease;  
 PD = progressive disease;  $f_{\text{PD}}$  = fractional progressive disease;  
 OR = objective response;  $f_{\text{OR}}$  = fractional objective response

Usually, the sum of complete and partial responses called an Objective Response (OR = CR + PR) is used as a general quantity for the response of the treatment in question without considering the responses of stable and progressive disease. This quantity, however, does not take into account the number of cases of progressive disease PR.

To create a quantity that estimate the response taking all four response quantities into account a quantity named “*fractional weighted response,*”  $f_{\text{WR}}$ , was previously defined as follows<sup>178</sup> :

$$\text{WR}_3 = (3 \cdot f_{\text{CR}} + 1 \cdot f_{\text{PR}} + 0 \cdot f_{\text{SD}} - 3 \cdot f_{\text{PD}}) / 3; \quad \text{Eq. 6.3}$$

Here introduces a second attempt of defining a weighted response  $\text{WR}_4$  which include all four response parameters, i.e., also the stable disease with weights according to the following equation 6.4 below.

$$\text{WR}_4 = (4 \cdot f_{\text{CR}} + 2 \cdot f_{\text{PR}} + 1 \cdot f_{\text{SD}} - 4 \cdot f_{\text{PD}}) / 4; \quad \text{Eq. 6.4}$$

The following sections summarize the published responses of clinical electro-pulse enhanced chemotherapy for each specific type of a tumour and estimate the fractional weighting response  $\text{WR}_4$  from the data extracted from each published report. The results are presented for each specific treatment device used for the treatment.

### 6.1.2. MALIGNANT MELANOMA

In 1996 Heller et al. initiated the first clinical study to determine if electro-pulse enhanced chemotherapy would be effective against specific primary and metastatic malignant melanoma.<sup>179</sup> The study enrolled a group of three patients with malignant melanoma. The objective response of electro-pulse enhanced chemotherapy (*EpEChT*) treatment of 11 tumours in the study was 47%, with 3 complete remissions (CR 25%), and 2 partial

remissions (PR 22%). The number of tumours with no response was 5 (42%).

Results were encouraging enough to continue the studies in another five patients with 35 metastases of malignant melanoma.<sup>179</sup> The objective responses of *EpEChT* treatment of these patients with intra-lesional Bleomycin-sulphate in 23 nodules were 95%, with 78% complete remissions (CR) and 17%, partial remissions (PR), while the fraction of *EpEChT* treated tumours with no response was 5%. In 9 nodules that received Bleomycin-sulphate only, and in 3 nodules that receive electric pulses only, there was no response observed. This study clearly showed antitumor effects of *EpECT* in metastatic melanoma. Although it not achieved a 100 % cure, it may be an effective alternative to palliative surgery or irradiation in these patients.<sup>180</sup>

Five cancer centres have performed an independent clinical trial with 20 malignant melanoma patients with 142 nodules treated with electro-pulse enhanced chemotherapy, and the objective responses of treatment the metastatic malignant melanoma nodules is estimate to be 95%.<sup>181</sup> In 57 % of the treated tumours, the tumour rapidly disappeared within 1-2 weeks after treatment which resulted in a complete response, and no regrowth of these nodules observed. The observed partial response was 38 %, and 3.5 % showed stable disease. In two cases, however, progress of the disease was observed.<sup>31</sup>

Bleomycin 10 mg/m<sup>2</sup>BSA administered intravenously in eight patients with cutaneous metastases in malignant melanoma enrolled in another clinical study in France. Four patients received 4 pulses per nodule at an amplitude of 1000V per cm of electrode distance, and another four patients received 8 pulses at 1300V per cm of electrode distance. The result of the 1000V/cm exposure group, with an average tumour size of 6 mm, was 14% complete remissions and 86% partial remissions. In the group of 1300 V/cm, with average tumour size of 15 mm, there was 8 % complete remissions and 84% partial remissions, while 8% experienced stable disease.<sup>182</sup>

Bleomycin *EpEChT* of a patient with haemorrhaging malignant melanoma skin metastases in Denmark led to an effective and immediate relief of symptoms. Treatment of the 9 skin metastases, of which seven were ulcerated developed crusts, and the lesions healed in a matter of weeks. Thus Bleomycin electro-pulse enhanced chemotherapy could be considered for the palliation of haemorrhaging metastases as it is an efficient and tolerable treatment.<sup>183,184</sup>

From November 1998 through to November 1999, 15 patients with 38 skin lesions participated in phase II prospective clinical trial. There were 2



patients with 13 nodules of malignant melanoma (MM) treated with intra-lesional Bleomycin plus electric pulses at a field strength of 1300 V/cm and 100  $\mu$ s pulse-length delivered 10 min after Bleomycin injection at a frequency of 1 Hz. After a follow-up of about 9 months there was 84.5 % objective response, with 23% complete response, 61.5 % partial response and 15.3 % stable disease.<sup>158</sup>

Nineteen patients with metastatic melanoma were enrolled in a phase two, randomized, open-label study comparing intra-lesional Bleomycin + EPT, and intra-lesional Bleomycin alone. Of 18 study lesions, 13 (72%) showed a complete response, one (5%) showed a partial response, three (18%) showed no change and one (5%) showed disease progression over a period of more than 12 weeks.<sup>185,186</sup>

A case of electro-pulse enhanced chemotherapy with Bleomycin, of multiple small unresectable cutaneous melanoma metastases on the thigh of a 59-year-old woman, resulted after 4 treatment sessions in a complete response of 224 treated melanoma nodules.<sup>187</sup>

In a study of treatment of subcutaneous melanoma metastases with electro-chemotherapy, seven patients with 81 cutaneous were treated under general anaesthesia using intravenous Bleomycin injection. After 218 days' follow-up, the objective response was 68%, with 25% complete response and 43% partial response. No response appeared in 26% of the patients, and 6% experienced progressive disease.<sup>188</sup>

In the following case series, the clinical effectiveness of *EpEChT* was studied as an alternative palliative treatment option for unresectable metastatic lesions of malignant melanoma with a systematic review of reported outcomes. Nine patients with 158 cutaneous and subcutaneous metastases, were treated with ECT under general anaesthesia using intravenous Bleomycin injection. After a follow-up time of 195 days, the fraction of complete response was 23%, and partial response was 39%. No response recorded in 30% and 8% of the cases experienced progressive disease.<sup>189</sup>

In a retrospective study, clinical features, treatment response, and side effects evaluated in 56 patients treated with electro-pulse enhanced chemotherapy at 6 German dermatology departments. The mean age of the patient cohort (14 men, 42 women) was 69.3 years. The fraction of complete response was 20%, partial response was 30%, and no response recorded in 20% of cases. The objective response was 50%, but as much as 30% of the cases experienced progressive disease.<sup>190</sup>

Thirteen cancer centres participated in the “*International Network for Sharing Practices on Electro-pulse enhanced chemotherapy with intra-tumoural or intravenous injection of Bleomycin under local or general*

*anaesthesia,*” studied in total, 151 patients with metastatic melanoma. The study included 114 who had follow-up data of 60 days or more. Treatment of these patients with 394 lesions for 60 days resulted in an objective response of 78%, with 58% complete response, and 20% partial response. A follow-up of the 114 evaluable patients after more than 60 days, resulted in an objective response of 74%, with 48% complete response, and 26% partial response. Stable disease observed in 23% of the patients, and 3% experienced disease progression.<sup>191</sup>

Table 6-1 shows the data of the response of Electro-pulse enhanced chemotherapy treatments of Malignant Melanoma nodules of various sizes reported in 2017 by Kunte et al.<sup>191</sup>

**Table 6-1**  
Response of Electro-pulse enhanced chemotherapy treatments of Malignant Melanoma nodules of various sizes.<sup>191</sup>

Tumour Volume	f <sub>CR</sub>	f <sub>PR</sub>	f <sub>SD</sub>	f <sub>PD</sub>	OR	WR <sub>3</sub>	WR <sub>4</sub>
5	0.68	0.11	0.21	0.00	0.79	0.72	0.79
8	0.64	0.15	0.21	0.00	0.79	0.69	0.77
16.5	0.56	0.18	0.25	0.01	0.74	0.61	0.70
25.5	0.34	0.44	0.20	0.02	0.78	0.47	0.59
30	0.38	0.38	0.21	0.03	0.76	0.48	0.59

There seems to be no variation in the objective response due to the size of the lesion, while as seen in Figure 6-4 the weighted responses WR<sub>3</sub> and WR<sub>4</sub> seem to follow a “dose-response functional relation with the size of the lesion (LS).

The decrease the weighted response is mainly due to the increase of progressive disease for patients with nodules of larger size.

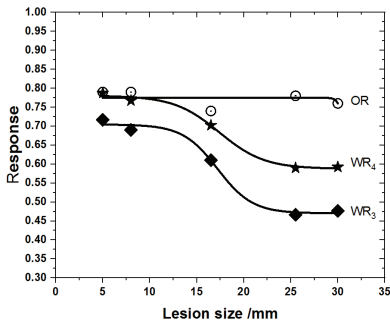


Figure 6-4  
Objective response OR and Weighted responses WR<sub>3</sub> and WR<sub>4</sub> of Electro-pulse enhanced chemotherapy treatments of Malignant Melanoma nodules of various sizes. The data of Table 6-1<sup>191</sup> are fitted to dose response equation.

### Summary of Malignant Melanoma

Table 6-2 shows a summary of the results of treatment Malignant Melanoma with electro enhanced chemotherapy reviewed in this section.

**Table 6-2**  
Responses of Malignant Melanoma treatment with Electro Enhanced  
Chemotherapy using various devices.

Device Author <sup>Reference</sup>	No. Pat	No. Tum	f <sub>CR</sub>	f <sub>PR</sub>	f <sub>SD</sub>	f <sub>PD</sub>	OR
<b>BTX (USA)</b>							
<b>Medpulser</b>							
Heller,1996 <sup>179</sup>	5	23	0.78	0.17	0.05	0.00	0.95
Glass,1996 <sup>180</sup>	3	18	0.25	0.22	0.42	0.00	0.47
Byrne,2005 <sup>186</sup>	19	18	0.72	0.05	0.18	0.05	0.77
<b>HM (Mexico)</b>							
Rodriguez- Cuevas, 2001 <sup>158</sup>	2	13	0.23	0.62	0.15	0	0.85
<b>Juan (France)</b>							
Mir,1998 <sup>31</sup>	20	142	0.57	0.38	0.04	0.01	0.95
Mir,1998 <sup>31</sup>	20	142	0.53	0.39	0.08	0.01	0.92
Rols,2000 <sup>182</sup>	4	51	0.08	0.84	0.08	0	0.92
<b>Cliniporator</b>							
<b>IGEA(Italy)</b>							
Gehl,2000 <sup>183</sup>	1	9	1.00	0.00	0.00	0.00	1.00
Snoj,2007 <sup>187</sup>	1	224	1.00	0.00	0.00	0.00	1.00
Kis,2010 <sup>188</sup>	7	81	0.25	0.43	0.26	0.06	0.68
Kis,2011 <sup>189</sup>	9	158	0.23	0.39	0.30	0.08	0.62
Kreuter,2015 <sup>190</sup>	20	20	0.20	0.30	0.20	0.30	0.50
Kunte,2017 <sup>191</sup> .	151	506	0.58	0.20	0.20	0.02	0.78
Kunte,2017 <sup>191</sup> .	114	394	0.48	0.26	0.23	0.03	0.74
Sum/Average	376	1799	0.49	0.30	0.16	0.04	0.80
/SD		14	0.29	0.23	0.12	0.08	0.17
/SE			0.08	0.06	0.03	0.02	0.05

**Table 6-3**

The objective responses and all weighted response of treating malignant Melanoma, with different devices

Device	OR	SD	WR <sub>3</sub>	SD	WR <sub>4</sub>	SD
Medpulsar	0.73	0.14	0.62	0.15	0.69	0.12
HM, Mexico	0.85		0.44		0.58	
Juan(France)	0.3	0.01	0.56	0.10	0.67	0.08
Cliniporator	0.76	0.07	0.54	0.14	0.62	0.12
All Average	0.80	0.05	0.55	0.07	0.64	0.06

Figure 6-5 shows the objective responses OR and weighted responses WR<sub>4</sub> of treatment Melanoma with various devices. The overall average is shown at the top of the figure.

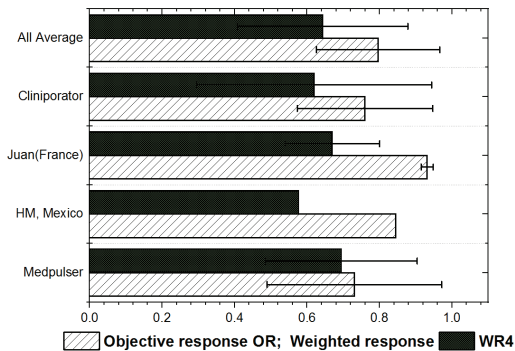


Figure 6-5

The objective response OR and weighted response of treatment Melanoma with various devices. The overall average is shown at the top of the figure.

### 6.1.3. SQUAMOUS CELL CARCINOMA

The first clinical trial of electro-pulse enhanced chemotherapy was on 8 patients with 42 nodules of head and neck squamous cell carcinoma.<sup>28</sup> There were 55% complete remissions and 14% partial remissions. Thus the objective response was 69%, and in 31 % there was no response.<sup>28,156</sup>

A phase I clinical trial performed with patients with head and neck squamous cell carcinoma (HNSCC) permeation nodules, treated with electro-pulse enhanced chemotherapy after intravenous injection of 10-15mg Bleomycin per m<sup>2</sup>BSA. Of the ten evaluable patients, there were 11% with complete remissions and 11% with partial remissions. In 56% there was no response, and 22% experienced progressed disease.<sup>192,193</sup>

In one study of electro-pulse enhanced chemotherapy of cutaneous and subcutaneous tumours using intra-lesional Bleomycin, a single SCC a tumour achieved a partial remission.<sup>32</sup>

Independent clinical trials of electro-pulse enhanced chemotherapy performed by five cancer centres involved 17 patients with a total of 87 head and neck nodules of Squamous Cell Carcinoma, and resulted in complete responses appeared in 43 % and partial response in 19% which give an objective response of 62%.<sup>31</sup>

Electro-pulse enhanced chemotherapy with an intra-tumoural injection of Bleomycin of one patient with a single nodule of squamous cell carcinoma resulted in partial response.<sup>194</sup>

A phase II prospective clinical trial took place during 1998-1999 that involved two patients with 2 nodules of squamous-cell carcinomas (SCC). Intra-lesional Bleomycin administered according to Figure 6-1, and 10min after Bleomycin injection, electric pulses at a field strength of 1300 V/cm and pulse-length of 0.1ms were delivered at a frequency of 1Hz. The pulse generator and the needle array electrodes were especially designed and constructed by the Biomedical Engineering Department at *Instituto Mexicano del Seguro Social (IMSS), Mexico City, Mexico*. After a follow-up of about 9 months, there appeared no complete response and 100% partial response.<sup>158</sup>

Another study within the framework of a European clinical trial of electro-chemotherapy included 12 patients with oral squamous cell carcinoma. After treatment, ten patients were free of a tumour, and 2 patients had signs of SCC left, while one patient died due to neck metastasis. Thus the objective response was 100%, with 83% complete remissions and 17 % partial remission, while there was 8% progressive disease.<sup>195</sup>

A different clinical study looked at the effect of electric pulse's duration and number in a sequence for electro-pulse enhanced chemotherapy of

patients with spindle-squamous cell carcinoma, One group exposed to 16 biphasic pulses of 25+25 $\mu$ s duration, which resulted in 71.4% complete remissions and 28.6% progressive disease, while another group exposed to 50+50 $\mu$ s biphasic pulses resulting in 78.6% complete remissions and 21.4 % progressive disease.<sup>196</sup>

Within a multicentre, single-arm Phase II study of electro-chemotherapy treatment, 54 patients were included with 69 squamous-cell carcinoma tumours of the head and neck. The treatment resulted in an objective response of 57%, with 25% complete remissions, 32 % partial remission, while 43% experienced no response. Eight patients were treated with Bleomycin alone with no clinical response and progressive disease. Thus electro-pulse enhanced chemotherapy with Bleomycin had a significant ( $p < 0.001$ ) clinical response compared to Bleomycin alone.<sup>197</sup>

A clinical trial to determine the safety and effectiveness of Bleomycin electro-pulse enhanced chemotherapy was performed in two patients with 17 tumours in the head and neck. Complete remissions appeared in 82.4 %, and partial remissions in 17.6 % of the treated tumours.<sup>198</sup>

From 2004 to 2006, a total of 26 patients with oral squamous-cell carcinoma (OSCC) were treated with electro-pulse enhanced chemotherapy according to the ESOP protocol. After 6-23 months of follow up, there was an objective response of 88% with 85% complete remissions and 4% partial remissions, while 12% experienced progressed disease. Most patients experienced pain as a complication which required high-dose pain medication for up to eight weeks.<sup>199</sup>

A study was performed between August 2003 and June 2005, in thirty patients with 111 nodules of various types treated with electro-pulse enhanced chemotherapy at the Mercy University Hospital, Cork. In five patients with 5 nodules of squamous-cell carcinoma, there was an objective response of 67 %, with 33% complete remissions. In 2 patients with 3 nodules < 3 cm, the objective response was 22 % with 11 % complete remissions.<sup>200</sup>

In a report of the clinical outcome from a single institution's experience with 52 patients, one case of squamous-cell carcinoma with 31 nodules > 30mm was involved. The authors, however, did not specify the treatment results quantitatively.<sup>201</sup>

In a clinical study of 15 patients with Head and Neck Cancers were nine cases of squamous-cell carcinoma involved. The authors, however, did not specify the treatment results of those cases quantitatively.<sup>202</sup>

In a clinical study, 6 patients with skin cancer of the head and neck were treated using electroporation therapy with intra-tumorally injected Bleomycin. After 4 weeks follow up the single patient with SCC of the

external meatus of the auditory canal, experienced persistent SCC with no response to a second treatment.<sup>203</sup>

A clinical study of primary T1 and T2 oral tongue cancer, included 15 patients of whom 14 had squamous cellular carcinoma. The objective response was 71.4% complete remissions while 38.6% experienced progress disease.<sup>204</sup>

A clinical electro-pulse enhanced chemotherapy phase II study took place as a collaboration between two centres, one in Denmark and the other in the UK. The study included fifty-two patients with cutaneous metastases of any histology of whom there were 3 with squamous-cell carcinoma. The authors, however, did not specify the treatment results of those cases.<sup>205,206</sup>

A case of an 80-year-old male with multiple erythematous nodules at the right *fronto-parieto-occipital* region was treated with electro-pulse enhanced chemotherapy with Bleomycin 15 mg/m<sup>2</sup> i.v., by using the Cliniporator™ device (IGEA Ltd.). At week 2 after treatment, there was a complete response. At week 8, however, a relapse occurred and a second *EpEChT* treatment performed. New complete regression appeared, but the patient died 3 months later of a systemic progression.<sup>207</sup>

In Greece, five medical centres performed electro-pulse enhanced chemotherapy according to the ESOPE protocol in 52 patients with a variety of tumours. Fourteen patients with Head and Neck tumours (very likely SCC) showed an objective response to the treatment of 93% with 64% complete remissions and 29% partial remission, while 7% experienced stable disease.<sup>208</sup>

From April 2009 to January 2011, a clinical study of electro-pulse enhanced chemotherapy was performed with a total of 15 patients with head and neck cancers, of whom 13 with squamous-cell carcinoma. After a follow-up in early 2012, the treatment 28 nodules resulted in an 86% objective response with 50% complete remissions and 36% partial remissions. Stable disease occurred in 4%, and 11% experience progressive disease.<sup>209</sup>

A clinical study focused on the role of electro-pulse enhanced chemotherapy in the treatment of 25 patients with head and neck cutaneous and subcutaneous cancers, of whom 13 had squamous-cell carcinoma. Treatments were performed using i.v. Bleomycin and the ESOPE protocol and after about 22 months, the treatment result was 100% objective responses, with 62% complete remissions, and 38% partial remissions.<sup>210</sup>

A preliminary study of electro-pulse enhanced chemotherapy of head and neck cancer in 8 elderly patients with 28 nodules of squamous-cell carcinoma, resulted in 50% complete remissions and 30% partial remissions.<sup>211</sup>

A meta-analysis was conducted to investigate the differences in the effectiveness of ECT concerning tumour type, drug, and route of administration. The overall objective response of electro-pulse enhanced chemotherapy treatment across all studies included in the analysis was estimated to 84.1%. The analysis, however, did not consider the progress of disease after treatment.<sup>172</sup>

A man affected by an ulcerated SCC and extensive metastasis was treated with electro-pulse enhanced chemotherapy with excellent clinical results, although all other treatment approaches rejected.<sup>212</sup>

A clinical study of Electro-pulse enhanced chemotherapy for cutaneous and subcutaneous metastasis was performed in 39 patients, of whom 3 were squamous-cell carcinoma. The authors, however, did not specify the treatment results of the SCC cases.<sup>213</sup>

In another clinical study, eight patients with recurrent or persistent squamous cell cancer in the head and neck area were treated with electro-pulse enhanced chemotherapy. The objective treatment response was 78%, with 33.3% complete remissions and a 44.4 % partial response, while in 22.2% there was progression of the disease.<sup>214</sup>

A retrospective study of 12 patients with 24 nodules of Squamous Cell Carcinoma (SCC) of the oral cavity or oropharynx treated with Bleomycin electro-pulse enhanced chemotherapy, resulted in an objective response of 50%, with 25% complete remissions and 25% partial remission, while 46% experienced stable disease, and 6% progression of the disease.<sup>215</sup>

In a clinical electro-pulse enhanced chemotherapy study of patients with primary SCC T2 cancer of the oral cavity or oropharynx performed with intratumoural administered Bleomycin, control biopsies were carried out 2 months after treatment. Complete remission experienced in all 4 patients but complications of bleeding, osteonecrosis and a fistula occurred.<sup>216</sup> Long-term (25-57 months) follow of 18 patient with Squamous Cellular Carcinoma treated with electro-pulse enhanced chemotherapy resulted in 78% complete remissions, while 23 % experienced progress disease.<sup>217</sup>

A prospective study of electro-pulse enhanced chemotherapy according to the ESOPE protocol followed by conventional chemo-radiotherapy was conducted among four patients with squamous cell carcinoma of the oral cavity in advanced stages. After 4 weeks 75% showed a partial response, and in 25% there was stable disease.<sup>218</sup>

In a retrospective clinical study, 56 patients with the various types of tumours treated with electro-pulse enhanced chemotherapy at 6 German dermatology departments. Mean age of the patient cohort (14 men, 42 women) was 69.3 years. The “carcinoma “tumour group included 15 patients of whom five had primary squamous-cell carcinomas of the skin,



three had Merkel cell carcinomas, two had vulvar carcinomas, and five had carcinomas of the head and neck region. The objective response in this group was 20%, with 6.7% complete response and 13.3% partial response, while 80% experienced progressive response of their carcinomas.<sup>190</sup>

A clinical study involving 22 patients with squamous-cell carcinoma aimed to evaluate pain scores before and after electro-pulse enhanced chemotherapy showed that the majority of patients had no or mild pain after electro-pulse enhanced chemotherapy.<sup>219</sup>

Between 2008 and 2013, a multi-centre study with 10 clinical centres study enrolled 41 patients with squamous-cell carcinoma for electro-pulse enhanced chemotherapy with intravenous administration of Bleomycin. The objective treatment result was 85.2% with 40.7% complete remissions and 44.5% partial remissions, while 14.8% experienced stable disease.<sup>220</sup>

A three-centre prospective phase II electro-pulse enhanced chemotherapy trial involved 25 patients with 35 nodules of squamous-cell carcinoma. The objective treatment result was 80% with 52% complete remissions and 28% partial remissions, while 20 % experienced stable disease.<sup>221</sup>

A European multi-institutional prospective study of electro-pulse enhanced chemotherapy performed according to the ESOPE protocol, involved 50 patients with squamous-cell carcinoma of whom 46 were evaluable. The objective treatment result was 80.4% with 56.5% complete remissions, and 23.9 % partial remissions, while 15.2% experienced stable disease and 4.3% progress of the disease.<sup>222</sup>

A retrospective single-centre study was performed to evaluate electro-pulse enhanced chemotherapy efficacy in the treatment of locally advanced stage III cutaneous squamous-cell carcinoma in 22 patients. The treatment followed the ESOPE guidelines, and after a mean follow-up 4 weeks, the objective response (according to *Table 1*) was 77%, with 22.7% complete responses and 54.5% partial responses, while 14 % experienced no response and 9 % progression of the disease.<sup>223</sup>

The D-EECT™ protocol, with successively decreasing voltage for each pulse, was recently applied in a clinical case study in India.<sup>178</sup> The study involved 8 patients with head & neck squamous cell carcinoma, a Bleomycin dose of 15 USP units/m<sup>2</sup> was administrated intra-tumorally i.t., or intravenously i.v. The objective response was 100%, with 15% complete response and 85% partial response, and none with stable or progress disease.

Plaschke (2019), presented the *DAHANCA 32* study, that is a phase II clinical trial in 26 patients with recurrent head and neck carcinomas with no curative treatment options. Electrochemotherapy was performed according to the ESOPE protocol under general anaesthesia with no serious adverse

events occurred during treatment. The tumour response was evaluated by using CT scanning, MRI and  $^{18}\text{F}$ FDG-PET as well as biopsy results and questionnaires about, safety, toxicity, pain score, and quality-of-life. In the follow-up at week-4 follow-up of the 26 patients treated of whom 22 were evaluated resulted in 18% CR, 36% PR, 41% SD and 5% PD which gave an objective response OR of 55%. In the follow-up week-8 were 25 patients evaluated which resulted in 20% CR, 40% PR, 36% SD and 4% PD, which resulted in an objective response OR of 60%. Two responders remain without recurrence. Four events occurred post treatment: one bleeding episode, two episodes with mucosal swelling, and one patient died due to disease progression.<sup>224</sup>

**Table 6-4**

The number of cases, and clinical fractional treatment response ' $f$ -TR' at week 4, and week 8 follow-up after the treatment.<sup>224</sup>

Response	Week 4 No. cases	Week 8 No. cases	Week 4 $f$ -TR	Week 8 $f$ -TR
CR	4	5	0.18	0.20
PR	8	10	0.36	0.40
SD	9	9	0.41	0.36
PD	1	1	0.05	0.04
SUM	22	25	1.00	1,00
Not Applicable	3	0		
Tot Sum	25	25		
OR			0.54	0.60

Before treatment, and at follow-up at week4 and week 8, the tumour expanse evaluated by CT using the longest diameter of the entire tumour according to RECIST criteria version 1.1. The tumour expanse values 'TX' was evaluated by using MR expanse area  $TA$ , and by using PET standardized uptake values (SUVs).

The specific therapeutic response ( $STR_x$ ) of the treatment was estimated as the difference between the untreated "UT" and treated "T" total tumour expanse "TX", as recorded by CT, MRI or PET, divided by the expanse of untreated tumour:

$$STR_x(t) = \frac{TX^{UT} - TX^T(t)}{TX^{UT}} \quad \text{Eq. 6.5}$$

where

$x$  = expanse recorded by  $x = CT, MRI$  or  $PET$  respectively  
 $STR_x(t)$  = Specific Therapeutic Response at follow-up time  $t$   
 $TX^{UT}$  = Tumour expanse of untreated “UT” tumour as recorded by  $x$   
 $TX^T(t)$  = Tumour expanse of treated “T” tumour at follow-up time  $t$

The STR is equal to 1 when,  $TX^T = 0$  which indicate CR  
 The STR is less than 1 when,  $0 < TX^T < TX^{UT}$  which indicate PR  
 The STR is about 0 when,  $TX^T \approx TX^{UT}$  which indicate SD  
 The STR is less than 0, when,  $TX^T > TX^{UT}$  which indicate PD

### Response evaluated by CT imaging

The specific therapeutic response  $STR_{CT}(t)$ , was evaluated by using the values of CT-RECIST (cm/response) given in *Table-3* of the publication.<sup>224</sup> The Figure 6-6 shows the specific therapeutic response at week 4 after treatment  $STR_{CT}(4)$ , and the Figure 6-7 shows the specific therapeutic response at week 8 after treatment  $STR_{CT}(8)$ .

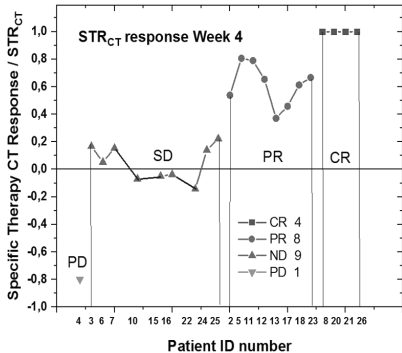


Figure 6-6  
 The Specific Therapeutic Response as recorded by CT at week 4 after treatment.

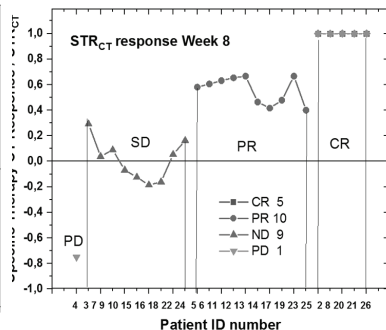


Figure 6-7  
 The Specific Therapeutic Response as recorded by CT at week 8 after treatment.

The  $STR_{CT}$  values for stable disease SD-cases are significantly different from the progressive response PR-cases ( $p = 10^{-6}$ ) which are significantly different from the complete response CR-cases. Thus CT scanning seems to be a relevant method for objective evaluating the treatment response of electro enhanced chemotherapy.

**Table 6-5**

The clinical treatment response “TR”, longest diameter “d<sup>CT</sup>” and specific therapy response “STR<sub>CT</sub>” as recorded by CT, at week 4 and week 8 follow-up.

Pat. No.	TR <sup>1)</sup>		d <sup>CT</sup>			STR <sub>CT</sub>	
	w4	w8	mm w0	mm w4	mm w8	w4	w8
2	PR	CR	3.9	1.8	0	0.54	1.00
3	SD	SD	2.4	2	1.7	0.17	0.29
4	PD	PD	2	3.6	3.5	-0.80	-0.75
5	PR	PR	3.1	0.6	1.3	0.81	0.58
6	SD	PR	3.8	3.6	1.5	0.05	0.61
7	SD	SD	5.2	4.4	5	0.15	0.04
8	CR	CR	1.7	0	0	1.00	1.00
9	SD	SD	4.5		4.1		0.09
10	SD	SD	2.9	3.1	3.1	-0.07	-0.07
11	PR	PR	1.9	0.4	0.7	0.79	0.63
12	PR	PR	2.6	0.9	0.9	0.65	0.65
13	PR	PR	2.7	1.7	0.9	0.37	0.67
14	SD	PR	2.8		1.5		0.46
15	SD	SD	4	4.2	4.5	-0.05	-0.13
16	SD	SD	2.7	2.8	3.2	-0.04	-0.19
17	PR	PR	2.4	1.3	1.4	0.46	0.42
18	PR	SD	3.1	1.2	3.6	0.61	-0.16
19	SD	PR	2.3		1.2		0.48
20	CR	CR	3	0	0	1.00	1.00
21	CR	CR	2.2	0	0	1.00	1.00
22	SD	SD	5.6	6.4	5.3	-0.14	0.05
23	PR	PR	4.8	1.6	1.6	0.67	0.67
24	SD	SD	4.3	3.7	3.6	0.14	0.16
25	SD	PR	4.5	3.5	2.7	0.22	0.40
26	CR	CR	2.4	0	0	1.00	1.00
Average						0.39	0.40
SD						0.47	0.46

<sup>1)</sup>The weights'  $w_{CR}=3$ ,  $w_{PR}=1$ ,  $w_{SD}=0$  and  $w_{PD}=-3$  are used in the numerical recording of the clinical response in *Table 2* used for PCA

**Table 6-6**

Summary of the clinical treatment response “TR”, longest diameter “d<sup>CT</sup>” and specific therapy response “STR<sub>CT</sub>” as recorded by CT, at week 4 and week 8 follow-up.

Clin. Resp	Ave. STR <sub>CT</sub>		No. w4	f-TR w4	Ave. STR <sub>CT</sub>		No. w8	f-TR w8
	Week 4	SD			w8	SD		
PD	-0.80		1	0.05	-0.75		1	0.04
SD	0.05	0.13	9	0.41	0.01	0.16	9	0.36
PR	0.61	0.15	8	0.36	0.56	0.11	10	0.40
CR	1.00	0.00	4	0.18	1.00	0.00	5	0.20
ND	-	-	3					
Ave Sum	<b>0.39</b>	0.47	22+3	1	<b>0.40</b>	0.46	25	1
WR <sub>4</sub>	<b>0.42</b>				<b>0.45</b>			

The values of weighted response WR<sub>4</sub> evaluated from the clinical response fraction values in *Table-3* are 0.42 at week 4 and 0.45 at week 8. These values correspond very well with the averages of specific treatment response STR<sub>CT</sub> evaluated with CT examination.

Figure 6-8 and Figure 6-9 shows the result of principal component analysis of the data given in *Table 2*. The three encircled groups represent the complete remissions, partial remissions and Stable disease. The figures show that the case No. 4 with progressive disease is an outsider, well separated from the others. The clinical response (TR) coincides with a specific therapeutic response STR<sub>CT</sub>, and there is no correlation with tumour expanse CT<sub>0</sub> before treatment.

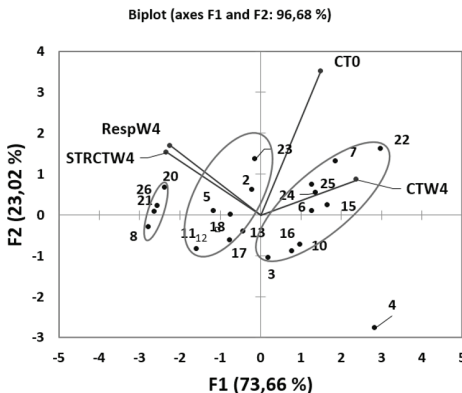


Figure 6-8  
PCA-biplot of the CT response at week 4 follow up

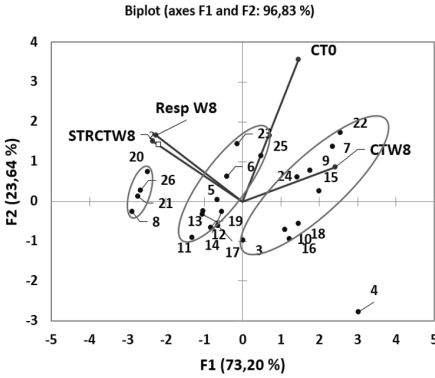


Figure 6-9  
PCA-biplot of the CT response at week 8 follow up

**Response evaluated by MR imaging**

The specific therapeutic response  $STR_{MR}(t)$  was evaluated by using the values of expanse treatment area evaluated measured on MRI from two perpendicular measurements given as “MRI (cm<sup>2</sup> response)” in Table 3 of the publication.<sup>224</sup>

The Figure 6-10 shows the specific therapeutic response  $STR_{MR}(4)$  at week 4 after treatment, and the Figure 6-11 shows the specific therapeutic response  $STR_{MR}(8)$  at week 8 after treatment.

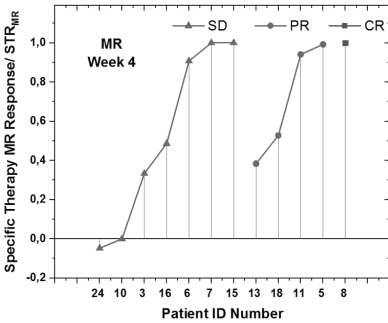


Figure 6-10  
The Specific MR Therapeutic Response at week4 after treatment

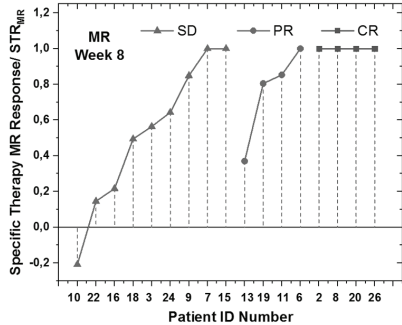


Figure 6-11  
The Specific MR Therapeutic Response at week 8 after treatment

The  $STR_{MR}$  values for stable disease SD-cases are not significantly different from partial response PR-cases ( $p=0.4$ ) which are not significantly

different ( $p=0.24$ ) from CR cases. Thus MR scanning seems not to be a relevant method for objective evaluating the treatment response of electro enhanced chemotherapy.

### Response evaluated by PET imaging

Standardized uptake values (SUVs) are used in clinical FDG-PET oncology imaging, and has a specific role in assessing patient response to cancer therapy. *Positron Emission Tomography Response Criteria in Solid Tumours* (PERCIST 1.0) were introduced in 2009 as guidelines for systematic and structured assessment of response to therapy with  $^{18}\text{F}$ -deoxyglucose (FDG) PET in patients with cancer, with suggested application in clinical trials and, potentially, in the clinical practice of PET reporting.<sup>225</sup>

In the study<sup>224</sup> the SUV<sub>peak</sub> is measured at baseline in the interior tumour using PERCIST. By week 4 and 8, SUV-peak values are evaluated by using a sphere of at least one  $\text{cm}^3$  within the treatment area. The specific therapeutic response  $STR_{PET}(t)$  was evaluated by using the values of “PET - SUV in (SU V<sub>peak</sub>/response)” given in Table 3 of the publication<sup>224</sup>. The Figure 6-12 shows the specific therapeutic response  $STR_{PET}(4)$  at week 4 after treatment, and the Figure 6-13 show the specific therapeutic response  $STR_{PET}(8)$  at week 8 after treatment.

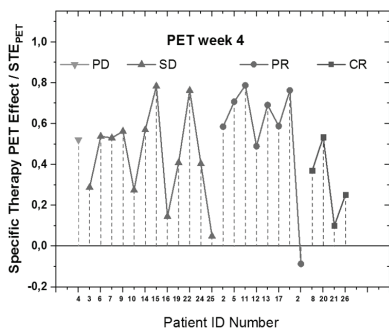


Figure 6-12  
The Specific PET-SUV Therapeutic Response at week4 after treatment

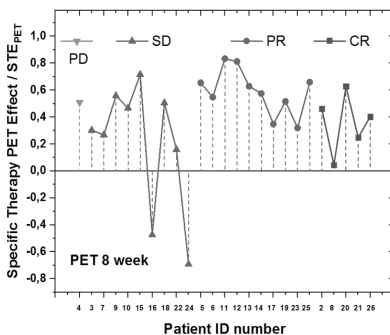


Figure 6-13  
The Specific PET-SUV Therapeutic Response at week 8 after treatment

At the week 4 follow-up the  $STR_{PET}$  values for the stable disease SD-cases are not significantly different from the progress disease PR-cases ( $p=0.32$ ) which are not significantly different ( $p=0.1$ ) from the complete response CR-cases. Thus FDG-PET scanning seems not to be a relevant method for objective evaluating the early treatment response of electro enhanced chemotherapy.

At the week 8 follow up the STR<sub>PET</sub> values for the stable disease SD-cases are significantly different from the partial response PR-cases ( $p=0.0,04$ ). Although they are not significantly different ( $p=0.08$ ) from the complete remission CR-cases. Thus FDG-PET scanning seems not to be a quite relevant method for objective evaluating the late treatment response of electro enhanced chemotherapy.

### Summary of Squamous cell carcinoma

A summary of the results of treatment Squamous Cell Carcinoma with Electro Enhanced Chemotherapy reviewed in this section is given in Table 6-7.

**Table 6-7**

Summary of the results of treatment Squamous Cell Carcinoma with Electro Enhanced Chemotherapy using various types of devices

Device Author <sup>Reference</sup>	No. Tum	No. Pat.	fCR	fPR	fSD	fPD	OR
<b>BTX(USA)</b>							
<b>Medpulsar</b>							
Heller,1998 <sup>32</sup>	1	1	0	1.00	0	0	1.00
Heller,1999 <sup>194</sup>	1	1	0	1.00	0	0	1.00
Allegretti,2001 <sup>226</sup>	12	12	0.50	0.21	0.29	0	0.71
Burian,2003 <sup>195</sup>	12	12	0.83	0.08	0	0.08	0.92
Bloom,2005 <sup>197</sup>	69	54	0.25	0.32	0.43	0.	0.57
Burian,2007 <sup>199</sup>	26	26	0.85	0.04	0	0.12	0.88
Tijink,2006 <sup>198</sup>	17	2	0.82	0.18	0.	0	1.00
Landstrom,2010 <sup>203</sup>	6	5	0.33	0.33	0.17	0.17	0.67
Landstrom,2011 <sup>204</sup>	14	14	0.71	0	0	0.29	0.71
Landstrom,2015 <sup>216</sup>	4	4	1.00	0	0.	0	1.00
Landstrom,2015 <sup>217</sup>	18	18	0.78	0	0	0.22	0.78
<b>HM Mexico</b>							
Rodriguez- Cuevas,2001 <sup>158</sup>	13	2	0.00	1.00	0	0	1.00
<b>S15 Jouan, (France)</b>							
Mir, 1991 <sup>103</sup>	42	8	0.55	0.14	0.31	0.00	0.69
Domenge,1996 <sup>193</sup>	10	7	0.11	0.11	0.56	0.22	0.22
Mir, 1998 <sup>31</sup>	77	17	0.43	0.19	0.27	0.10	0.62



<b>ESOPE, IGEA Cliniporator</b>							
Marenco,2011 <sup>207</sup>	1	1	0	0	0	1.00	0.00
Skarlatos,2011 <sup>208</sup>	14	14	0.64	0.29	0.07	0	0.93
Gargiulo,2012 <sup>210</sup>	13	13	0.62	0.38	0.00	0	1.00
Mevio,2012 <sup>209</sup>	28	12	0.50	0.36	0.04	0.11	0.86
Benevento,2013 <sup>211</sup>	8	28	0.50	0.30	0.10	0.10	0.80
Seccia, 2014 <sup>214</sup>	9	8	0.33	0.44	0.00	0.22	0.78
Campana,2014 <sup>215</sup>	24	24	0.25	0.25	0.46	0.04	0.50
Domanico, 2015 <sup>218</sup>	4	4	0.00	0.75	0.25	0.00	0.75
Kreuter,2015 <sup>190</sup>	15	15	0.07	0.13	00	0.80	0.20
Campana,2016 <sup>220</sup>	35	35	0.41	0.45	0.15	0.00	0.85
Rotunno,2016 <sup>221</sup>	35	25	0.52	0.28	0.20	0.00	0.80
Bertino2016 <sup>222</sup>	46	50	0.57	0.24	0.15	0.04	0.80
Di Monta,2017 <sup>223</sup>	22	22	0.23	0.55	0.14	0.09	0.77
Plaschke, 2017 <sup>227</sup> <3 cm	14	14	0.21	0.50	0.21	0.07	0.71
Plaschke,2017 <sup>227</sup> >3 cm	20	20	0.20	0.40	0.30	0.10	0.60
Plaschke,2017 <sup>227</sup>	34	34	0.21	0.44	0.26	0.09	0.65
Plaschke,2019 <sup>224</sup>	22	26	0.18	0.36	0.41	0.05	0.54
Plaschke,2019 <sup>224</sup>	25	26	0.20	0.40	0.36	0.04	0.60
<b>IQWave, Chemotech</b>							
Kalavathy, 2018 <sup>178</sup>	12	8	0.15	0.85	0.00	0.00	1.00
<b>Sum/Average</b>	<b>562</b>	<b>669</b>	<b>0.38</b>	<b>0.35</b>	<b>0.15</b>	<b>0.12</b>	<b>0.73</b>
<b>/SD</b>	<b>12</b>	<b>0.28</b>	<b>0.28</b>	<b>0.16</b>	<b>0.21</b>	<b>0.24</b>	<b>0.24</b>
<b>/SE</b>	<b>3</b>	<b>0.05</b>	<b>0.05</b>	<b>0.03</b>	<b>0.04</b>	<b>0.04</b>	<b>0.04</b>

### Comparison of the response of various devices

In the following Tables 6-8 to Table 6-9 the average treatment responses reported from clinical studies of squamous-cell carcinoma and breast cancers using different treatment devices are compared.

#### Squamous cell Carcinoma

- BTX Genetronix Medpulsar<sup>32,194,226,195,197,199,198,203,204,216,217</sup>
- Home Made Mexican device<sup>158</sup>
- S 15 electropulsator, Jouan, (France)<sup>103,193,31</sup>
- ESOPE, Cliniporator IGEA (Italy)<sup>207,208,210,209,211,214,215,218,190,220,221,222,223,227,224</sup>
- D-EECT, IQWave Chemotech (Sweden)<sup>178</sup>

**Table 6-8**

The average clinical responses of treating SSC with different devices

Device/Protocol	No. Pat	No. Tum	fCR	fPR	fSD	fPD
BTX Medpulsar USA	151	193	0.55	0.29	0.08	0.08
Home Made. Mexico	2	15	1.00	0	0	0
S 15 electropulsator. Jouan. (France)	32	105	0.36	0.15	0.38	0.11
Cliniporator IGEA. ESOPE	371	335	0.31	0.36	0.17	0.15
QWave Chemotech. D-EECT	8	12	0.15	0.85	0	0
Overall average	562	669	0.38	0.35	0.15	0.12

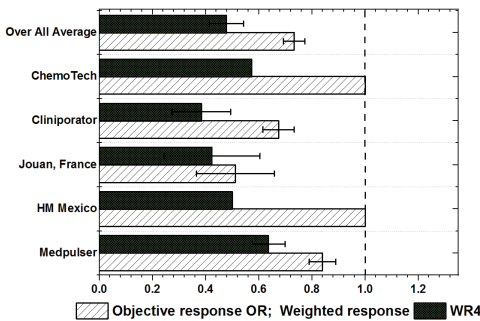


Figure 6-14  
The objective responses and weighted response WR<sub>4</sub> of treating SSC with different devices  
The overall average is shown at the top.

**Table 6-9**

The objective responses and all weighted response of treating SSC with different devices

Device/Protocol	OR	SE	WR <sub>3</sub>	SE	WR <sub>4</sub>	SE
BTX Medpulsar USA	0.84	0.05	0.57	0.08	0.64	0.06
Home Made. Mexico	1		0.33		0.50	
S15 electropulsator. Jouan. (France)	0.51	0.15	0.30	0.20	0.42	0.18
Cliniporator IGEA ESOPE	0.67	0.06	0.28	0.11	0.38	0.11
IQWave Chemotech. D-EECT	1.00	0.14	0.43		0.57	0.12
Overall average	0.73	0.04	0.38	0.06	0.48	0.06

The BTX Genetronix Medpulsar seems to deliver the best every weighted response  $WR_4=0.64$  for SCC followed by IQwave  $WR_4=0.57$ , and the Home-Made Mexican device  $WR_4=0.5$ . The ESOPE protocol with Cliniporator had the lowest response  $WR_4=0.38$ . In those judgements, the sizes of tumours treated with the different devices are not considered. However, In the next paragraph, the reports with data of tumour size will be considered.

Figure 6-15 shows the Objective response of Squamous-cell carcinoma SCC of different tumour diameter treated with various types of devices. The Medpulsar and IQwave seem both deliver 100% objective response, although the tumours treated with IQWave are twice as large. The Electroporator Jouan and Cliniporator seem both deliver an objective response of about 65%. Figure 6-15 shows the Weighted response  $WR_4$  of Squamous cell carcinoma of different tumour diameter treated with various type of devices. In treatment of large tumours (diam. $\approx$ 5cm) the IQWave-device deliver the best weighted response  $WR_4\approx 60\%$ , while with tumours of corresponding size the weighted response of Cliniporator is  $WR_4\approx 40\%$ . In treatment of small tumours (diam. $<$ 3cm) the weighted response  $WR_4$  is about 45-50% for Cliniporator, Jouan and Medpulsar.

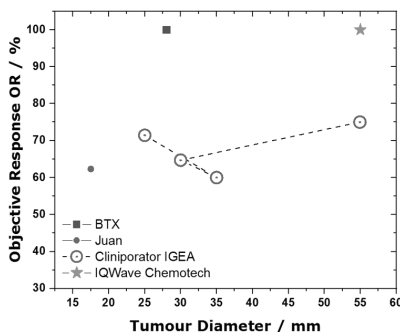


Figure 6-15  
Objective response of Squamous cell carcinoma SCC treated with different devices

BTX Genetronix Medpulsar<sup>158</sup>,  
S15 electropulsator, (Jouan, France):  
<sup>31</sup>, Cliniporator IGEA ESOPE<sup>214, 227</sup>,  
IQWave D-EECT Chemotech<sup>178</sup>.

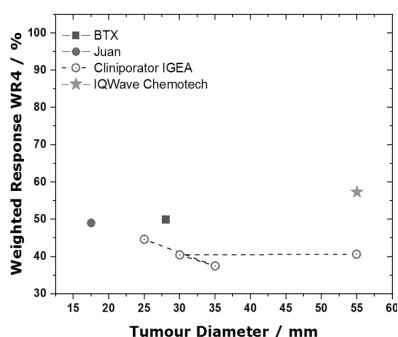


Figure 6-16  
Weighted response  $WR_4$  of Squamous cell carcinoma treated with different devices

BTX Genetronix Medpulsar<sup>158</sup>,  
S15 electropulsator, (Jouan, France):  
<sup>31</sup>, Cliniporator IGEA ESOPE<sup>214, 227</sup>,  
IQWave D-EECT Chemotech<sup>178</sup>.

### 6.1.4 BREAST CANCER

Complete remission appeared in a patient with breast adenocarcinoma who received i.v. Bleomycin, and after 8-26 minutes, it was followed by 10 sessions of 4-8 short (0.1ms) pulses of 1000 or 1300V/cm, delivered between 8-26 minutes at adjacent positions on the nodule to cover all the tumour surface.<sup>193</sup>

A Phase I/II trial for the treatment of cutaneous and subcutaneous tumours using electro-pulse enhanced chemotherapy was initiated to determine if this mode of treatment would be effective against certain primary and metastatic cutaneous malignancies. The study enrolled a group of six patients, one with metastatic breast adenocarcinoma. The patient received a 15,000 IU dose of Bleomycin administered intravenously at a rate of about 1500 IU per minute. Five to 15 minutes after the Bleomycin thoroughly infused and the patient is injected with a 1% lidocaine solution at around the treatment site. The treatment was followed by eight short (99  $\mu$ s) pulses at an amplitude of 1 300 V/cm administered directly to the tumours. The patient with metastatic breast adenocarcinoma showed complete responses in both treated nodules after *EpEChT*. The treatment tolerated well with no residual effects from the electric pulses. In conclusion the study indicated that *EpEChT* is an effective local treatment for metastatic breast and encourages further clinical studies.<sup>179</sup>

Five cancer centres have performed an independent clinical trial with a total of 291 cutaneous or subcutaneous tumours of which 2 were breast cancer with 10 nodules treated with electro-pulse enhanced chemotherapy. The tumours were measured, and the response to the treatment evaluated 30 days after the treatment. In the breast tumours treated with objective responses (OR) were recorded in only 2 nodules (20 %). The application of electric pulses to the patients was safe and well-tolerated.<sup>31</sup>

From November 1998 through to November 1999, 15 patients with 38 skin lesions participated in phase II prospective clinical trials, using intra-lesion Bleomycin (750-3500 IU). In the group of patients, there were two with totally 14 nodules of breast cancer. The treatment proceeds ten minutes after intra-tumour Bleomycin injection with six short electric pulses (0.1ms) delivered at a field strength of 1300V/cm, and with a frequency of 1Hz. The objective response of *EpEChT* treatment in this study was 100%, with 8 complete remissions (CR 58%) and 6 partial remissions (PR 42%). Although no complications appeared related to the treatment, more experience and longer follow-up were needed.<sup>158</sup>

A case report demonstrated that multiple applications of electro-chemotherapy could induce remission in a locally destructive breast cancer recurrence, which was refractory to other multimodal therapy.<sup>168</sup>

A two year long prospective non-randomised study in which four cancer centres enrolled patients evaluated the efficacy and safety of electro-pulse enhanced chemotherapy was carried out with Bleomycin or Cisplatin among 14 patients with breast cancer. The treatment of recurrent breast cancer performed out using intravenous or intra-tumour drug administration followed by application of electric pulses generated by a Cliniporator™ using plate or needle electrodes. In the 58 breast cancer nodules treated with electro-pulse enhanced chemotherapy, a complete response was recorded in 84 %, a partial response of 7 %, and stable disease of 10%, regardless of drug use or the route of its administration. The lack of detailed information makes it difficult to evaluate the outcome of this study further.<sup>162</sup>

Another study was performed to investigate the clinical utility of electro-pulse enhanced chemotherapy by treating 30 patients with cutaneous or subcutaneous recurrent tumours, which were inoperable, or progressive and refractory to systemic chemotherapy or radiotherapy. Of these patients, 12 had breast cancer with 99 nodules. After treatment with electro-pulse enhanced chemotherapy, 70 % of the breast tumours showed complete remission, 21% partial response and 9% no change.<sup>200</sup>

In a study of 52 consecutive patients with different type of cancer-histology, eleven were breast cancer, with 174 nodules treated with Bleomycin-based electro-chemotherapy. The treatment of breast tumours showed the objective response of 86%, with 50% complete remission, 36% a partial response and 14% with stable disease. None of the treated patients experienced a relapse in the treatment field. Thus *EpEChT* proved to be a safe, and effective treatment of breast cancer, that also preserves patients' quality of life.<sup>201</sup>

A phase II clinical study of electro-pulse enhanced chemotherapy engaged patients with cutaneous recurrent breast cancer nodules larger than 3 cm, for whom no further treatment options were available. The primary endpoint of the study was an objective response evaluated by clinical examination. Secondary endpoints included a response evaluated by PET/CT, a change in lung diffusion capacity, the patient reporting symptoms, and distress appearance. Treatment consisted of the i.v. injection of Bleomycin 15,000 IU/m<sup>2</sup>BSA followed by an application of electric pulses according to the ESOPe protocol. Of the 12 evaluable patients with a follow-up >8 weeks, computed tomography CT showed that 33% of patients were achieving over 50% tumour volume reduction. The objective response was 25% with 8% complete remission, and 17% partial response.

As much as 70% experienced a stable disease, and 8% experienced a relapse in the treatment field.<sup>228,206,229</sup>

Another study of 12 elderly breast cancer patient with 142 cutaneous metastases with a diameter > 3cm in only 2 patients, was treated with Bleomycin electro-pulse enhanced chemotherapy according to the ESOPE criteria. The objective response was 92.3 %, with a complete response of 75.3%, a partial response of 17%, and no change in 7.7% of the nodules. From these results *EpEChT* recommends as a primary local therapy in patients, and was not deemed suitable for surgical removal of a primary tumour < 3cm, even in the elderly.<sup>230</sup>

Between 2010 and 2013 a multicentre electro-pulse enhanced chemotherapy study enrolled 125 patients with metastases of breast cancer, and treatment was performed according to the ESOPE protocol in 113 patients with 214 evaluable nodules. After 2 months' follow-up, there was an objective response of 90.2% with 58.4%, complete response, 32% partial response, while 7% experienced a stable disease, and 2% suffered a relapse of disease in the treatment field. At a one year's follow-up, 96.4% of the patients experienced durable local control. The fraction of complete remissions varied with the size of a tumour: 80.3 % CR for diam. < 3 cm, and 46.1 % CR for diam. >3 cm. Thus *EpEChT* represents a valuable therapy for breast cancer, particularly for patients with tumours < 3 cm diameter.<sup>231</sup>

In a retrospective study, clinical features, treatment response, and side effects of electro-pulse enhanced chemotherapy were evaluated in 56 patients with various diagnoses, and were treated according to the ESOPE protocol at six German dermatology departments. In a cohort which included thirteen patients with metastasized breast cancer, complete remission appeared in 8%, a partial response in 39%, and in 15% there was no change of tumour growth, while 39% experienced tumour progression.<sup>190</sup>

A case report presented a 61-year-old woman with unresectable breast cancer recurrence to the skin and subcutaneous tissue, for which numerous lines of treatment were unsuccessful. After three treatments with electro-chemotherapy, however, a dramatic regression of the cutaneous metastatic foci was recorded, and after an actual observation period of 12 weeks, complete clinical remission was achieved.<sup>232</sup>

Between 2010 and 2013 a total of 125 patients with breast cancer skin metastases were enrolled onto a multicentre retrospective cohort study of electro-pulse enhanced chemotherapy.

In Table 6-10 the various subgroups in the study are displayed for oestrogen receptor (ER) positivity, and low Ki67 index after treatment of

109 patients with a Cliniporator™ device, following the European Standard Operative Protocol (ESOPE).<sup>233</sup>

**Table 6-10**

Tumour response to electro-pulse enhanced chemotherapy according to surrogate definition of breast cancer intrinsic subtypes.<sup>233</sup>

Subtype	No.	CR %	PR %	SD %	PD %	NE %	OR %	WR <sub>4</sub> %
A-like: ER.PgR+	23	73.9	17.4	4.3	4.3	0	91	79
B-like: HER2-	22	50	40.9	9.1	0	4.5	75	73
B-like: HER2 +.	17	58.8	29.4	5.9	5.9	0	88	69
Triple- HER2 +	35	57.1	31.4	11.4	0	0	89	76
	11	54.5	45.5	0	0	0	100	77
Sum/ Ave. /SD	108	58.9 9	32.9 10.9	6.1 4.4	2 2.9	0.9 2	92 5	75 4

NE% is percentage of patients not included in the evaluation

At a patient follow up after two months, 59% of the whole breast tumour cohort showed complete remission, 31 % showed partial response and 7.4% a stable disease, while 1.9% experienced relapse in the treatment field. One tumour, was not applicable for evaluation.<sup>233</sup> The weighted responses derived according to equation 6.2 and 6.3 were 68% for WR<sub>3</sub>, and 75% for WR<sub>4</sub> respectively.

Another study was a 10-year audit of a single centre experience of electro-pulse enhanced chemotherapy according to the European Standard Operating Procedures (ESOPE) with a Cliniporator™ device. In total, the patient cohort was 24 breast cancer patients who all had received prior multimodal therapy, and who had, or had developed 242 lesions. The objective response of *EpEChT* was 67 % with a complete response of 54 %, and a partial response of 13%, while 16 % experienced stable disease, and 1% experienced progressive disease. As smaller lesions were found to be more responsive, early treatment of *EpEChT* could apply within multimodal treatment strategies.<sup>234</sup>

A clinical study of seven breast cancer patients with 35 skin metastases treated with electro-pulse enhanced chemotherapy according to the ESOPE protocol resulted in 86% objective remissions, with 43% complete

remissions and 43% partial remissions, while 14 % experienced progressive disease. The results compare with the average results of 8 other published similar studies with a total average of objective response was estimated to 76% with 39 % complete remissions, while 16 % experienced stable disease and 8 % progressive disease.<sup>235,177</sup>

The results of the evaluation 90 patients with cutaneous recurrence from breast at two months after treatment with electro-pulse enhanced chemotherapy according to the ESOPE protocol at 10 European cancer centres, showed 74% objective remissions, with 52% complete remissions and 22% partial remissions, while 18% experienced stable and 8% progressive disease.<sup>236</sup> The only predictor variable considered related to the outcome of the treatment is the median diameter of the coetaneous metastases ranging from 1 to 550 mm. The results of the evaluable treatment of nodules <30 mm, and >30 mm summarized in Table 6-11a were derived from *table 5* in the publication of Matthiessen (2018).<sup>236</sup> Table 6-11b also shows the response parameters of the 83 evaluable patients at 2 months after the electro-pulse enhanced chemotherapy from *table 4* in the same publication.<sup>236</sup>

**Table 6-11a**

Tumour response to electro-pulse enhanced chemotherapy according to size of nodules < 30 mm. and > 30 mm. and at 2 months after treatment.<sup>236</sup>

	No. Pat.	No. Nodules	fCR	fPR	fSD	fPD	fNE
Nodules < 3cm		113	0.72	0.14	0.08	0.01	0.05
Nodules > 3cm		94	0.37	0.24	0.18	0.06	0.03
Average		207	0.57	0.20	0.13	0.03	0.04
Patients 2 months	90		0.52	0.22	0.18	0.08	0.03

fNE fraction of patients not included in the evaluation

**Table 6-11b**

The objective (fOR) and weighted responses fWR<sub>3</sub> and fWR<sub>4</sub> to electro-pulse enhanced chemotherapy according to size of nodules < 30 mm. and > 30 mm. and at 2 months after treatment.<sup>236</sup>

	No. Patients	No. Nodules	fOR	fWR <sub>3</sub>	fWR <sub>4</sub>
Nodules < 3cm		113	0.86	0.76	0.80
Nodules > 3cm		94	0.62	0.40	0.48
Average		207	0.76	0.60	0.67
Patients 2 months	90		0.74	0.51	0.60



### Summary of Breast Cancer

A summary of the results of electro enhanced chemotherapy treatment of breast cancer with Bleomycin by using various devices is given in Table 6-12 and Table 6-13.

**Table 6-12a**

Tumour response to electro-pulse enhanced chemotherapy with Bleomycin of breast cancer by using various devices.

Device Author <sup>Reference</sup>	No. Pat.	No. Tum.	fCR	fPR	fSD	fPD
<b>Medpulsar, (USA)</b>						
Heller,1996 <sup>179</sup>	1	2	1.00	0.00	0.00	0.00
Larkin,2007 <sup>200</sup>	12	99	0.70	0.21	0.09	0.00
<b>Home Made (Mexico)</b>						
Rodriguez- Cuevas,2001 <sup>158</sup>	2	14	0.58	0.42	0.00	0.00
<b>GTH 1287, Jouan (France).</b>						
Domenge, 996 <sup>193</sup>	1	1	0.00	1.00	0.00	0.00
Mir,1998 <sup>31</sup>	2	10	0.20	0.00	0.80	0.00
Rebersek,2004 <sup>237</sup>	6	12	0.33	0.42	0.25	0.00
<b>Cliniporator IGEA (Italy) ESOPE</b>						
Marty,2006 <sup>162</sup>	14	58	0.84	0.07	0.10	0.00
Campana,2009 <sup>201</sup>	11	174	0.50	0.36	0.14	0.00
Matthiessen,2012 <sup>229</sup>	12	12	0.08	0.08	0.75	0.08
Benevento,2012 <sup>230</sup>	12	142	0.75	0.17	0.08	0.00
Cabula,2015 <sup>231</sup>	112	214	0.59	0.32	0.07	0.02
Kreuter,2015 <sup>190</sup>	13	13	0.08	0.38	0.15	0.38
Wichtowski,2016 <sup>232</sup>	1	10	1.00	0.00	0.00	0.00
Bourke,2017 <sup>234</sup>	24	202	0.64	0.15	0.19	0.01
Campana,2017 <sup>233</sup>	108	239	0.59	0.31	0.07	0.02
Wichtowski,2017 <sup>177</sup>	7	35	0.43	0.43	0.00	0.14
Matthiessen,2018 <sup>236</sup>	90	207	0.52	0.22	0.18	0.08
<b>IQWave ChemoTech (Sweden) D-EECT</b>						
Kalavathy,2018 <sup>178</sup>	5	11	0.40	0.60	0.00	0.00
Sum	433	1455				
Average			0.51	0.29	0.16	0.04
SD			0.30	0.25	0.24	0.09
SE			0.07	0.06	0.06	0.02

**Table 6-12b**

The objective (fOR) and weighted responses fWR<sub>3</sub> and fWR<sub>4</sub> to electro-pulse enhanced chemotherapy with Bleomycin of breast cancer by using various devices.

<b>Device</b> Author <sup>Reference</sup>	No. Patients	No. Nodules	OR	WR <sub>3</sub>	WR <sub>4</sub>
<b>Medpulser, (USA)</b>					
Heller,1996 <sup>179</sup>	1	2	1.00	1.00	1.00
Larkin,2007 <sup>200</sup>	12	99	0.91	0.77	0.83
<b>Home Made (Mexico)</b>					
Rodriguez-Cuevas,2001 <sup>158</sup>	2	14	1.00	0.72	0.79
<b>GTH 1287, Jouan (France).</b>					
Domenge, 996 <sup>193</sup>	1	1	1.00	0.33	0.50
Mir,1998 <sup>31</sup>	2	10	0.20	0.20	0.40
Rebersek,2004 <sup>237</sup>	6	12	0.75	0.47	0.60
<b>Cliniporator IGEA (Italy)</b>					
Marty,2006 <sup>162</sup>	14	58	0.90	0.86	0.89
Campana,2009 <sup>201</sup>	11	174	0.86	0.62	0.72
Matthiessen,2012 <sup>229</sup>	12	12	0.17	0.03	0.23
Benevento,2012 <sup>230</sup>	12	142	0.92	0.81	0.86
Cabula,2015 <sup>231</sup>	112	214	0.91	0.68	0.75
Kreuter,2015 <sup>190</sup>	13	13	0.46	-0.18	-0.08
Wichtowski,2016 <sup>232</sup>	1	10	1.00	1.00	1.00
Bourke,2017 <sup>234</sup>	24	202	0.80	0.68	0.76
Campana,2017 <sup>233</sup>	108	239	0.91	0.68	0.75
Wichtowski,2017 <sup>177</sup>	7	35	0.86	0.43	0.51
Matthiessen,2018 <sup>236</sup>	90	207	0.74	0.51	0.59
<b>IQWave ChemoTech (Sweden)</b>					
Kalavathy, 2018 <sup>178</sup>	5	11	1.00	0.60	0.70
Sum	433	1455			
Average			0.80	0.57	0.66
SD			0.26	0.32	0.27
SE			0.06	0.08	0.07

**Table 6-13**

Summary of objective and weighted responses to electro-pulse enhanced chemotherapy with Bleomycin of breast cancer by using various devices.

Device	OR	SE	WR <sub>3</sub>	SE	WR <sub>4</sub>	SE
Medpulsar (USA)	0.96	0.18	0.89	0.11	0.91	0.08
Home Made (Mexico)	1.00	0.10	0.72	0.08	0.79	0.04
GTH 1287 Jouan, (France).	0.65	0.31	0.33	0.08	0.50	0.13
Cliniporator IGEA (Italy) ESOPE	0.78	0.09	0.56	0.10	0.63	0.10
IQWave ChemoTech, (Sweden) D-EECT	1.00	0.35	0.60	0.16	0.70	0.15
Over All Average	0.80	0.06	0.57	0.08	0.66	0.07

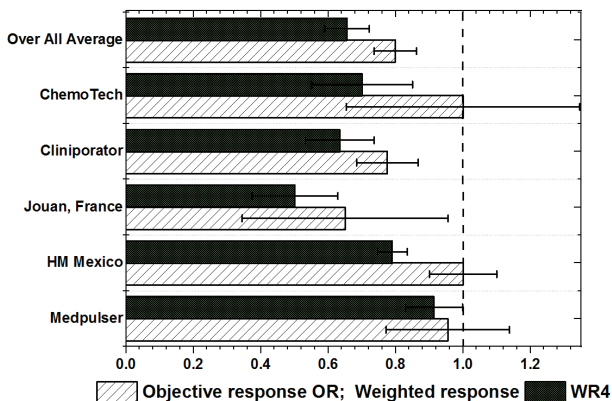


Figure 6-17

The objective responses and weighted response WR<sub>4</sub> of treating breast cancer with different devices

In treatment of Breast-cancer, the objective response was 100% for both the home-made Mexican device and the IQwave™ device closely followed by Medpulsar™ 91%. The Jouan device and Cliniporator™ deliver objective responses of 65% and 78% respectively.

The Medpulsar™ seems to deliver the best weighted response  $WR_4$  91% for breast cancer followed by the home-made Mexican device with  $WR_4$  79% and IQwave  $WR_4$  70%. The Jouan device and ESOPE protocol with Cliniporator™ had the lowest weighted response with  $WR_4$  50% and 63% respectively. In those judgements, however, the sizes of tumours treated with the different devices were not considered. In the next paragraph, the treatment response of tumours of various sizes will be considered.

Figure 6-18 shows the objective response of squamous-cell carcinoma SCC of different tumour diameter treated with various types of devices. The Medpulsar™ and IQwave™ seem both deliver 100% objective response, although the tumours treated with IQWave™ are twice as large. The electroporator-Jouan and Cliniporator™ seem both deliver an objective response of about 65%. Figure 6-19 shows the weighted response  $WR_4$  of breast-cancer of different tumour diameter treated with various types of devices. At large tumour treatment (diam.≈5cm) the iQWave™-device delivered the best weighted response,  $WR_4$ ≈60%, while the weighted response of Cliniporator™ was  $WR_4$ ≈40% for tumours of corresponding size. By treatment of small tumours (diam.<3cm) with Cliniporator™, Jouan or Medpulsar™, resulted in a weighted response  $WR_4$  of about 45-50%

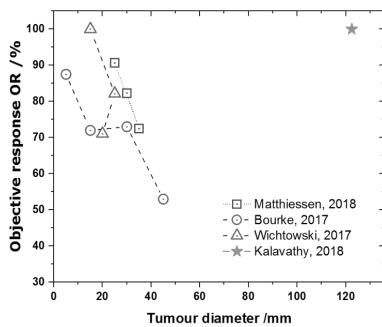


Figure 6-18  
Objective response of Breast cancer of various sizes treated with different devices.  
Cliniporator IGEA ESOPE:<sup>177, 234, 236</sup>  
IQWave D-EECT Chemotech.<sup>178</sup>

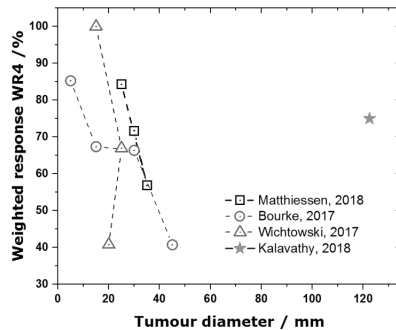


Figure 6-19  
Weighted response  $WR_4$  of Breast cancer of various sizes treated with different devices  
Cliniporator IGEA ESOPE:<sup>177, 234, 236</sup>  
IQWave D-EECT Chemotech.<sup>178</sup>

### 6.1.5. BASAL CELL CARCINOMA (BCC)

The first clinical trial that performed for the treatment of cutaneous and subcutaneous tumours using electro-pulse enhanced chemotherapy to be analysed here involved two patients with 6 nodules of basal cell carcinoma. The treatment resulted in 12 % complete remissions and an 88% partial response.<sup>179</sup>

A second clinical study was initiated by the same researchers to determine whether an intra-lesional injection of the drug in combination with electric pulses could provide an improved result. A total of 54 Basal Cell Carcinoma primary tumours in 20 patients received a complete *EpEChT* treatment that resulted in a 96% complete response and 6 % partial response.<sup>32</sup>

Another clinical study of the effects of *EpEChT* on 20 patients with 54 primary BCC tumours resulted in 94% complete responses after a single treatment. No recurrences appeared within a mean of 18 months of observation.<sup>238</sup>

Five cancer centres performed independent clinical trials of electro-pulse enhanced chemotherapy in a total 32 basal cell carcinoma in 10 patients. Complete responses appeared in 75% and a partial response in 25%, which gives an objective response of 100%.<sup>31</sup>

A review of the clinical data for electro-pulse enhanced chemotherapy presented results for intravenous (i.v.) as well as intra-tumour administration of Bleomycin. Treatment of 2 BCC patients with i.v., resulted in 17% complete remissions and 83 % partial remissions, while treatment of 20 BCC patients with i.t. resulted in 84 % complete remissions and 6 % partial remissions.<sup>194,239</sup>

Further studies were initiated to confirm whether an intra-lesional injection of Bleomycin in combination with electric pulses could provide an improved result of electro-pulse enhanced chemotherapy treatment of BCC. In a group of totally 34 patients, of whom twenty were patients with 54 BCC nodules, there was 100% objective response, with 94% complete remissions and 6% partial remissions.<sup>157</sup>

From November 1998 through November 1999, 15 patients with 38 skin lesions participated in phase II prospective clinical trial, using intra-lesional Bleomycin plus electric pulses delivered 10min after Bleomycin injection, which lasted 0.1ms each at a field strength of 1300V/cm and a frequency of 1Hz. The study involved nine patients with basal cell carcinomas (BCC). After a follow-up of about nine months there was a 77.7% complete response and a 22.3% partial response.<sup>158</sup>

A pulse-sequence for electro-chemotherapy, consisting of 16 biphasic pulses of 25+25 $\mu$ s duration and intra-tumour Bleomycin, was used for treatment of clinical stage one basal cell carcinoma lesions in 45 patients. 80% of the patients achieved a complete response, and 20 % of the patients experienced recurrences.<sup>196</sup>

A case of a 75-year-old man with a pigmented nodule manifesting as the basal cell was treated with electro-pulse enhanced chemotherapy, resulting in a rapid clinical and histologic regression of the treated lesions.<sup>240</sup>

Electro-pulse enhanced chemotherapy successfully treated a man affected by ulcerated basal cell carcinoma.<sup>241</sup>

Between June 2009 and January 2011, three patients with Gorlin-Goltz syndrome were treated with electro-pulse enhanced chemotherapy using intravenous Bleomycin, according to the ESOPe guidelines. The patients had a total of 99 nodules of basal cell carcinomas on the face and trunk. The treated nodules showed 99% objective clinical response, with 87% complete response without recurrence during 10 to 28 months of follow-up,<sup>242</sup>

A recent review of the literature concludes that electro-pulse enhanced chemotherapy is an alternative to treating advanced basal cell carcinoma. However, standardized treatment schedules and randomized clinical trials were not considered.<sup>174</sup>

### Summary of Basal Cell Carcinoma (BCC)

A summary of the results of treatment Basal Cell Carcinomas with Electro Enhanced Chemotherapy by using various devices reviewed in this section are given in Table 6-14a and 6-14b.

**Table 6-14a**  
Results of treatment Basal Cell Carcinomas with Electro Enhanced Chemotherapy using different devices

<b>Device</b> Author <sup>Reference</sup>	No. Pat.	No. Tum.	fCR	fPR	fSD	fPD
<b>Medpulsar BTX USA</b>						
Heller,1996 <sup>179</sup>	2	6	0.13	0.88	0	0
Glass,1997 <sup>238</sup>	10	32	0.75	0.25	0	0
Heller, 1998 <sup>32</sup>	20	54	0.94	0.06	0	0
Heller,1999 <sup>194</sup>	20	54	0.94	0.06	0	0
Heller,1999 <sup>194</sup>	2	6	0.17	0.83	0	0
Heller,2000 <sup>157</sup>	20	54	0.94	0.06	0	0
<b>Home Made, Mexico</b>						
Rodriguez-Cuevas,2001 <sup>158</sup> .	9	9	0.78	0.22	0	0

**Table 6-14a** continued

<b>Chemipulser III, Bulgaria</b>						
Peycheva,2004 <sup>196</sup> .	45	45	0.80	0.00	0	0.2
<b>Jouan France</b>						
Mir,1998 <sup>31</sup>	10	31	0.75	0.25	0	0
<b>ESOPE Cliniporator</b>						
Fantini,2008 <sup>240</sup>	1	3	1.00	0	0	0
Richetta,2011 <sup>241</sup>	1		1.00	0	0	0
Kis,2012 <sup>242</sup> .	3	99	0.87	0.12	0.01	0
Over all Average	143	393	0.75	0.23	0,00	0.02
SD			0.30	0,31	0,00	0.06
SE			0.09	0.09	0,00	0.02

**Table 6-14b**

The objective (fOR) and weighted responses fWR<sub>3</sub> and fWR<sub>4</sub> of treatment Basal Cell Carcinomas with Electro Enhanced Chemotherapy using different devices.

<b>Device</b> Author <sup>Reference</sup>	No. Patients	No. Nodules	OR	WR <sub>3</sub>	WR <sub>4</sub>
<b>Medpulser BTX USA</b>					
Heller,1996 <sup>179</sup>	2	6	1	0.42	0.56
Glass,1997 <sup>238</sup>	10	32	1	0.83	0.88
Heller, 1998 <sup>32</sup>	20	54	1	0.96	0.97
Heller,1999 <sup>194</sup>	20	54	1	0.96	0.97
Heller,1999 <sup>194</sup>	2	6	1	0.45	0.59
Heller,2000 <sup>157</sup>	20	54	1	0.96	0.97
<b>Home Made, Mexico</b>					
Rodriguez-Cuevas,2001 <sup>158</sup> .	9	9	1	0.85	0.89
<b>Chemipulser III, Bulgaria</b>					
Peycheva,2004 <sup>196</sup> .	45	45	0.8	0.60	0.60
<b>Jouan France</b>					
Mir,1998 <sup>31</sup>	10	31	1	0.83	0.88
<b>ESOPE Cliniporator</b>					
Fantini,2008 <sup>240</sup>	1	3	1	1	1
Richetta,2011 <sup>241</sup>	1		1	1	1
Kis,2012 <sup>242</sup> .	3	99	0.99	0.91	0.93
Sum					
Average	143	393	0.98	0.81	0.85
SD			0.06	0.21	0.17
SE			0.02	0.06	0.05

**Table 6-15**

Summary of Results of treatment Basal Cell Carcinomas with Electro Enhanced Chemotherapy by using different devices

Device	OR	SE	WR3	SE	WR4	SE
Medpulsar BTX USA	1.00	0	0.76	0.11	0.82	0.08
HM Mexico	1.00		0.85		0.85	
Chemipulsar III Bulgaria.	0.80		0.60		0.60	
Juan France	1.00		0.83		0.83	
ESOPE Cliniporator	1.00	0	0.79	0.03	0.79	0.02
Over all average	0.98	0.02	0.81	0.06	0,81	0,05

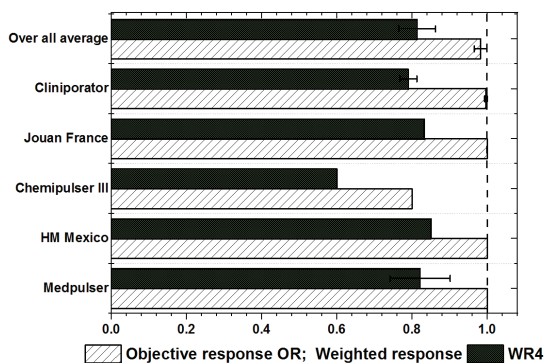


Figure 6-20

The objective responses and weighted response WR<sub>4</sub> of treating basal cell carcinoma by using different devices

### 6.1.6. KAPOSI'S SARCOMA

The first study of clinical applications of electro-pulse enhanced chemotherapy (*EpEChT*) involved one patient with four sites of Kaposi's sarcoma. *EpEChT* treatment with intra tumoural administration of Bleomycin resulted in partial response of one of the sites treated while the other three showed progressive disease

A review of electroporation therapy of Kaposi's sarcoma mentioned *EpEChT* as an indication for treatment, and in the following years, several case reports were published.<sup>243,244,160,245,246</sup>

One included a two-centre prospective phase II clinical trial of electro-pulse enhanced chemotherapy which involved 23 patients with a total of



541 Kaposi's sarcoma cutaneous nodules treated according to the ESOPE protocol. After a median follow up of 18 months, there were 65.2% complete remissions and 34.8% partial remissions, and at 24 months the survival rate was 74.4%.<sup>247</sup>

Clinical testing of newly developed electro-pulse enhanced chemotherapy equipment, with, heart QRS synchronizer, and the module for long-term recording of pulse parameters was carried out, involving 37 patients, some of whom had Kaposi's Sarcoma. The publication, however, does not specify the outcome of the treatment of the Kaposi patients specifically.<sup>248</sup>

One prospective clinical study aimed at evaluating electro-pulse enhanced chemotherapy (*EpEChT*) with the intravenous administration of Bleomycin on 18 patients with 63 nodules of Kaposi's sarcoma. The objective response was 100% with 89% complete remissions and 11 % partial remissions.<sup>249</sup>

A single-centre clinical study was performed to evaluate *EpEChT* in the local treatment of stage I-II Kaposi's sarcoma. At 4 weeks after the first treatment, a 73.6 % complete response was achieved. The three patients who didn't respond received a second treatment, and two of the patients got a third treatment until 100% complete remissions occurred.<sup>250,251</sup>

Between 2008 and 2013 a prospective, multicentre, observational study of electro-pulse enhanced chemotherapy enrolled 40 patients with Kaposi's sarcoma. The objective treatment results were 89%, with 44% complete remissions and 45% partial remissions, while 11 % experienced stable disease.<sup>175</sup>

A pilot study evaluating the effectiveness of electro-chemotherapy using reduced dosages of intravenous Bleomycin was carried out involving 40 patients with Kaposi's sarcoma. However, in the report, there is no specific data about the outcome of those patients.<sup>252</sup>

A total of 27 patients with classic Kaposi's sarcoma, were enrolled in a study aimed at evaluating the effect of *EpEChT* on HHV8 viral load. Tumour biopsies and blood samples were collected before and at six-month intervals for 12-48 months. The treatment resulted in 100% complete remissions that in the majority of cases was accompanied by clearance of the virus in the peripheral-blood mononuclear cells.<sup>253</sup>

### Summary of Kaposi's sarcoma

A summary of the results of treatment Kaposi's sarcoma with Electro Enhanced Chemotherapy as reviewed in this section is given in Table 6-16.

**Table 6-16a**

Fractional Responses to Electro-pulse enhanced chemotherapy treatments of Kaposi's sarcoma using various devices.

<b>Device</b> Author <sup>Reference</sup>	No pat	No. Tum	fCR	fPR	fSD	fPD
<b>BTX, Medpulsar</b>						
Heller, 1999 <sup>194</sup>	1	1	0	1.00	0	0
<b>Cliniporator, ESOPE</b>						
Garbay, 2006 <sup>160</sup>	1	8	1.00	0	0	0
Curatolo, 2008 <sup>245</sup>	1	1	1.00	0	0	0
Gualdi, 2010 <sup>246</sup>	1	1	1.00	0	0	0
Curatolo, 2012 <sup>247</sup>	23	10-36	0.65	0.35	0	0
Latini, 2012 <sup>249</sup>	18	63	0.89	0.11	0	0
Di Monta, 2014 <sup>251</sup>	19	19	1.00	0	0	0
Campana, 2016 <sup>175</sup>	40	40	0.44	0.45	0.11	0
Starita, 2017 <sup>253</sup>	27	27	1.00	0	0	0
Sum	131	182	0.87	0.11	0.01	0
Average,						
SD			0.20	0.17	0.04	0
SE			0.07	0.06	0.01	0

**Table 6-16b**

The objective (fOR) and weighted responses fWR<sub>3</sub> and fWR<sub>4</sub> to Electro-pulse enhanced chemotherapy treatments of Kaposi's sarcoma using various devices.

<b>Device</b> Author <sup>Reference</sup>	No patients	No. Nodules	OR	WR <sub>3</sub>	WR <sub>4</sub>
<b>BTX, Medpulsar</b>					
Heller, 1999 <sup>194</sup>	1	1	1.00	0.33	0.50
<b>Cliniporator, ESOPE</b>					
Garbay, 2006 <sup>160</sup>	1	8	1.00	1.00	1.00
Curatolo, 2008 <sup>245</sup>	1	1	1.00	1.00	1.00
Gualdi, 2010 <sup>246</sup>	1	1	1.00	1.00	1.00
Curatolo, 2012 <sup>247</sup>	23	10-36	1.00	0.77	0.83
Latini, 2012 <sup>249</sup>	18	63	1.00	0.93	0.94
Di Monta, 2014 <sup>251</sup>	19	19	1.00	1.00	1.00
Campana, 2016 <sup>175</sup>	40	40	0.89	0.59	0.69
Starita, 2017 <sup>253</sup>	27	27	1.00	1.00	1.00
Sum/Average,	131	182	0.99	0.91	0.93
/SD			0.04	0.14	0.11
/SE			0.01	0.05	0.04

### 6.1.7. SOFT-TISSUE SARCOMA

Between October 2006 and March 2012, a two-clinic phase II trial of electro-pulse enhanced chemotherapy was conducted on 34 patients with locally advanced or metastatic soft-tissue sarcomas. The objective response outcome after up to four treatments was 76% with 32.4% complete remissions and 44.1% partial remissions, while 8.8% experienced stable disease and 14.7% progress disease.<sup>254</sup>

Between 2008 and 2013, ten centres performed a clinical electro-pulse enhanced chemotherapy study that enrolled 376 eligible patients of whom 10 were soft-tissue sarcomas. There is, however, no specific data about the outcome of treatment of soft-tissue sarcomas.<sup>175</sup>

Table 6-17 shows the summary of the various results of soft-tissue sarcoma treated with electro-pulse enhanced chemotherapy.

**Table 6-17a**

Treatment results of Soft Tissue Sarcoma with electro-chemotherapy.						
Author <sup>Reference</sup>	No. patients	No. Nodules	fCR	fPR	fSD	fPD
Campana.2014 <sup>254</sup>	34		0.324	0.441	0.088	0.147

**Table 6-17b**

The objective (fOR) and weighted responses fWR <sub>3</sub> and fWR <sub>4</sub> of Soft Tissue Sarcoma treatment with electro-chemotherapy.					
Author <sup>Reference</sup>	No. patients	No. Nodules	fOR	fWR <sub>3</sub>	fWR <sub>4</sub>
Campana.2014 <sup>254</sup>	34		0.76	0.32	0.42

### 6.1.8. SKELETON

The first test of electro-pulse enhanced chemotherapy as a treatment of spinal metastasis was performed in a 51-year-old female patient with a 30-mm metastatic spinal melanoma treated according to the ESOPE protocol with Bleomycin. During a 48-month follow-up, the target tumour showed complete remission, and the patient's condition was noted as being in 'stable-disease'. Thus the treatment result of this single case of metastatic spinal melanoma with local control without adverse effects, indicates that electro-pulse enhanced chemotherapy has potential in the treatment of spinal metastasis.<sup>255</sup>

From July 2009 to July 2011, twenty-nine patients affected by painful bone metastases were treated with intravenous Bleomycin electro-pulse enhanced chemotherapy according to the ESOPE protocol. At 3 months after the treatment, 20 patients showed 5% a partial response, 85% stable disease, and 10% progression of disease. After 7-month follow-up of 18 patients, showed 61% a partial response, and 40% progression of the disease. After 12-months' follow-up of 11 patients, showed 64% a partial response and 36% progression of disease.<sup>256</sup>

Table 6-18 displays the treatment results of spinal and bone metastases with electro-pulse enhanced chemotherapy.

**Table 6-18a**

Treatment results of spinal and bone metastases with electro-pulse enhanced chemotherapy.

Author <sup>Reference</sup>	No.	Follow up	fCR	fPR	fSD	fPD
	Patients	month				
Gasbarrini,2015 <sup>255</sup>	1	48	1.00	0	0	0
Bianchi,2016-a <sup>256</sup>	20	3	0	0.05	0.85	0.10
Bianchi,2016-c <sup>256</sup>	18	7	0	0.61	0	0.39
Bianchi,2016-c <sup>256</sup>	11	12	0	0.64	0	0.36
Sum	50	18				
Average			0.25	0.32	0.21	0.21
/SD		18	0.43	0.30	0.37	0.17

**Table 6-18b**

The objective (fOR) and weighted responses fWR<sub>3</sub> and fWR<sub>4</sub> of spinal and bone metastasis's treatment with electro-pulse enhanced chemotherapy.

Author <sup>Reference</sup>	No.	Follow up	OR	WR <sub>3</sub>	WR <sub>4</sub>
	Patients	month			
Gasbarrini,2015 <sup>255</sup>	1	48	1.00	1.00	1
Bianchi,2016-a <sup>256</sup>	20	3	0.05	-0.08	0.14
Bianchi,2016-b <sup>256</sup>	18	7	0.61	-0.19	0.09
Bianchi,2016-c <sup>256</sup>	11	12	0.64	-0.15	0.04
Sum	50	18			
Average			0.57	0.14	0.25
/SD		18	0.34	0.50	0.25

### 6.1.9 LIVER

In a clinical phase I/II study of electro-pulse enhanced chemotherapy with Bleomycin during open surgery, by insertion of long needle electrodes in 29 colorectal liver metastases on 19 patients no, serious adverse events occurred. Radiological evaluation the treated metastases showed 85% complete responses and 15% partial responses.<sup>257</sup>

Histopathological findings in the colorectal liver metastases after electro-chemotherapy showed induced coagulation necrosis in the treated area encompassing both tumour and a narrow band of healthy tissue. Further evidence of disruption of vessels less than 5 mm in diameter and preservation of the larger vessels by electro-chemotherapy occurred. No viable tumour cells are found around the larger vessels in the treatment

volume. Around 9 weeks after electro-chemotherapy, regenerative changes occur.<sup>258</sup>

In a feasibility study of the treatment of portal-vein tumour thrombosis at the hepatic hilum in patients with hepatocellular carcinoma in cirrhosis, electro-pulse enhanced chemotherapy seems effective and safe for curative treatment.<sup>259</sup> The electro-pulse enhanced chemotherapy resulted in complete remissions in all treated nodules. Although 3 patients died within 1-14 months due to rupture of oesophageal varices or liver failure. The high risk of the occurrence of this complication might indicate that patients with gastric or oesophageal varices, it should be excluded from treatment with electro-pulse enhanced chemotherapy of the liver.<sup>259</sup>

Electro-chemotherapy with Bleomycin combined with open liver resection and performed with linear or hexagonal needle electrodes to 9 colorectal liver metastases in five patients according to the ESOPE protocol with 1-3 applications per nodule at 730V/cm resulted in 55.5% complete response, and 45.5% stable disease with no intraoperative complications. All five patients reached a 6 months' overall survival, and 4 out of 5 patients had 6 months' progression-free survival.<sup>260</sup>

## 6.1.10 OTHER DIAGNOSIS

### **Sweat gland carcinoma, *Eccrine poro-carcinoma***

A case of the patient with *Eccrine poro-carcinoma*, a rare type of skin cancer that arises from the intra-epidermal ductal portion of the eccrine sweat gland on the left arm with axillary nodal involvement, was treated by complete lymph node dissection and electro-pulse enhanced chemotherapy. After a follow-up of five months, complete response observed on a clinically macroscopic basis with no signs of axillary relapse or systemic disease.<sup>261</sup>

### **Gastric cancer**

A case of a 49-year-old man with advanced gastric cancer developed skin metastases around an ileostomy site was treated with electro-pulse enhanced chemotherapy according to the ESOPE protocol with i.v. Bleomycin. At one-month follow-up, partial tumour regression observed.<sup>262</sup>

### **Parotid gland**

In a case study, one metastasis in the left parotid gland and another metastasis in the neck was treated with electro-pulse enhanced chemotherapy performed using intravenous administration of Bleomycin and long single needle electrodes. The neck nodule got complete remission

while the parotid nodule got partial remission. Six weeks after electro-chemotherapy, fine-needle aspiration biopsy of the treated area revealed necrosis and inflammatory cells, without any viable tumour cells in the specimens from both of the treated lesions.<sup>263</sup>

### **Endometrial cancer**

The first case of cutaneous metastases from endometrial cancer treated with electro-pulse enhanced chemotherapy was a patient with multi-metastatic endometrial cancer. The patient received palliative systemic therapy, and electro-pulse enhanced chemotherapy according to the ESOPE guidelines. The treatment resulted in partial recovery, with necrosis at the treatment site and interruption of lesion bleeding.<sup>264</sup>

### **Prostate cancer**

A case report describes the successful electro-pulse enhanced chemotherapy treatment of a patient with prostate cancer with infiltration of the urethral sphincter. Four electrodes were inserted percutaneously through the perineum, each in pairs ventrally and dorsally of the sphincter externus arranged in a square. Electro-pulse enhanced chemotherapy performed according to the ESOPE protocol. Toxicity of the treatment was low, with only mild adverse events. At 6 months after the treatment, the patient was in complete remission with mild incontinence and mild erectile dysfunction.<sup>265</sup>

### **Pancreatic adenocarcinoma**

During the period 2011 - 2014 a clinical phase I/II study aimed to evaluate the effect of Electro-pulse enhanced chemotherapy in the treatment of locally advanced pancreatic adenocarcinoma enrolled 6 females and 5 male patients. Preliminary results show that for 5 patients no significant reduction of maximal tumour diameter appeared in CT and MR imaging procedures. However, after about one month from *EpEChT*, all patients showed a significant reduction of functional parameters value associated with a partial response.<sup>266</sup>

Eleven patients with locally advanced tumours of the head or the body of the pancreas managed treatment with electro-pulse enhanced chemotherapy compared to pre-operative status the patients with locally advanced pancreatic tumours reported pain reduction immediately after the electro-pulse enhanced chemotherapy treatment, and better quality of life without severe side effects or significant complication.<sup>267</sup>

In a clinical phase I/II study of electro-pulse enhanced chemotherapy functional MRI visualized significant reduction of advanced pancreatic

adenocarcinoma in the treated target area of patients at the National Cancer Institute, “G. Pascale Foundation” of Naples. During post-operative PET-examination, it was also indicated that the  $^{18}\text{F}$ FDG uptake was lower in respect to pre-operative evaluations.<sup>268</sup>

### Lung Cancer

Despite the high proportion of complete remissions of various types of cancer reported in the ESOPE study, there is no clinical study of electro-pulse enhance chemotherapy treatment of lung cancer reported.<sup>162</sup> But considering current attempts of thermal ablation for treatment of lung tumours indicates that electro-pulse enhanced chemotherapy might represent a significant breakthrough in the treatment of lung cancer.<sup>269</sup>

### Summary of various types of tumours

Table 6-19 shows a summary of the results of treatment various other types of tumours with electro-pulse enhanced chemotherapy reviewed in this section.

**Table 6-19a**

Results of electro pulse enhanced chemotherapy of various other types of tumours than above

Author <sup>Reference</sup>	Tumour type	Follow up month	fCR	fPR	fSD	fPD
Marone,2011 <sup>261</sup>	Sweat gland	5	1.00	0	0	0
Campana,2013 <sup>262</sup>	Gastric cancer	1	0	1.00	0	0
Groelj,2015 <sup>263</sup>	Parotid gland	1.5	1.00	0	0	0
Schiavii,2017 <sup>264</sup>	Endometrial ca.	4	0	1.00	0	0
Klein,2017 <sup>265</sup>	Prostate ca.	6	1.00	0	0	0
Granata,2014 <sup>266</sup>	Pancreatic ad.ca.	1	0	1.00	0	0
Tafuto,2015 <sup>267</sup>	Pancreatic ad.ca.	1	0	1.00	0	0
Bimonte,2016 <sup>268</sup>	Pancreatic ad.ca.	3	0	1.00	0	0
Jahangeer,2013 <sup>269</sup>	Lung cancer	-	-	-	-	-
Average		21	0.38	0.63	0	0



**Table 6-19b**

The objective (fOR) and weighted responses fWR<sub>3</sub> and fWR<sub>4</sub> to electro pulse enhanced chemotherapy of various other types of tumours than above.

Author <sup>Reference</sup>	Tumour type	Follow up month	OR	WR <sub>3</sub>	WR <sub>4</sub>
Marone,2011 <sup>261</sup>	Sweat gland	5	1.00	1.00	1.00
Campana,2013 <sup>262</sup>	Gastric cancer	1	1.00	0.33	0.50
Groselj,2015 <sup>263</sup>	Parotid gland	1.5	1.00	1.00	1.00
Schiavii,2017 <sup>264</sup>	Endometrial cancer	4	1.00	0.33	0.50
Klein,2017 <sup>265</sup>	Prostate cancer	6	1.00	1.00	1.00
Granata,2014 <sup>266</sup>	Pancreatic ad.ca.	1	1.00	0.33	0.50
Tafuto,2015 <sup>267</sup>	Pancreatic ad.ca	1	1.00	0.33	0.50
Bimonte,2016 <sup>268</sup>	Pancreatic ad.c.a	3	1.00	0.33	0.50
Jahangeer,2013 <sup>269</sup>	Lung cancer	-	-	-	-
Average		21	1.00	0.58	0.61
SD		2		0.35	0.33
SE		0.8		0.13	0.11

### 6.1.11 SUMMARY OF ALL *EpEChT* CLINICAL STUDIES WITH BLEOMYCIN

Table 6-20 gives a summary of the results all electro-pulse enhanced chemotherapy clinical studies with Bleomycin reviewed in this chapter.

**Table 6-20a**

Summary of all results of clinical studies with Bleomycin electro-enhanced chemotherapy of various other types of tumours.

Type of Ca.	fCR	fPR	fSD	fPD
Malignant Melanoma	0.49±0.08	0.30±0.06	0.16±0.3	0.04±0.02
Squamous cell carcinoma	0.38±0.05	0.35±0.05	0.15±0.03	0.12±0.04
Breast Cancer	0.51±0.07	0.29±0.06	0.16±0.06	0.04±0.02
Basal Cell Carcinoma	0.75±0.09	0.23±0.09	0	0.02±0.02
Kaposi's sarcoma	0.87±0.07	0.11±0.01	0.01±0.04	0.00±0.00

Table 6-20a continued

Soft Tissue <i>Sarco-sarcoma</i>	0.32	0.44	0.09	0.15
Skeleton metastases	0.25±0.20	0.32±0.15	0.21±0.19	0.21±0.09
Liver metastases	0.57±0.40	0.14±0.24	0.11±0.19	0.18±0.26
Other tumours	0.38±0.20	0.63±0.20	0	0
Average±SD	0.50±0.20	0.31±0.16	0.10±0.08	0.08±0.08
Average±SE	0.50±0.07	0.32±0.05	0.10±0.03	0.08±0.03

Table 6-20b

The objective (fOR) and weighted responses fWR<sub>3</sub> and fWR<sub>4</sub> to all results of clinical studies with Bleomycin electro-enhanced chemotherapy of various other types of tumours.

Type of Ca.	No. Patients	No. Nodules	fOR	fWR <sub>4</sub>
Malignant Melanoma	376	1799	0.80±0.5	0.55±0.07
Squamous cell carcinoma	562	669	0.73±0.04	0.48±0.06
Breast Cancer	433	1455	0.80±0.06	0.66±0.07
Basal Cell Carcinoma	143	393	0.98±0.02	0.85±0.05
Kaposi's sarcoma	131	1182	0.99±0.01	0.93±0.04
Soft Tissue <i>Sarco-sarcoma</i>	34	34	0.76	0.42
Skeleton metastases	50	50	0.57±0.16	0.25±0.12
Liver metastases	17	9	0.71±0.29	0.49±0.51
Other tumours	9	9	1.00	0.61±0.11
Sum	1755	5600		
Average±SD			0.82±0.15	0.58±0.21
Average±SE			0.82±0.05	0.58±0.07

Kaposi's sarcoma, and Basal Cell Carcinoma are the types of tumours most successfully treated with Bleomycin electro-pulse enhanced chemotherapy, with objective responses close to 100% and weighted response WR<sub>4</sub> close to 90%.

The second most successful treatment of malignant melanoma and breast cancer achieved an objective response of about 80% with weighted response 60% due to about 4% of progressive disease. Thus more effort should be focused to improve the treatment of malignant melanoma and breast cancer.

The treatment results for liver metastases is also promising with an objective response of treatment about 70%. The weighted response is, however, only about 40% due to a high percentage of about 20% progressive

disease. Thus more effort should be focused to improve the treatment of liver metastases.

The overall result of electro-pulse enhanced chemotherapy is auspicious with an average objective response of 82% and an average weighted response of about 60%. The future development should be focused to enhance the response of complete remissions and reduce the fraction of progressive disease.

## 6.2 CLINICAL STUDIES OF *EpEChT* WITH CIS-PLATIN

### 6.2.1 INTRODUCTION

The first study performed to study electro-pulse enhanced chemotherapy with Cisplatin was cutaneous tumour nodules in four patients with 19 nodules of malignant melanoma, squamous-cell carcinoma, and basal cell carcinoma. Cisplatin was administered intra-tumoural at doses depending on the size of the tumour nodule according to Figure 6-21.

The variation of the administrated intra-tumour dose of Cisplatin(Pt) with the size of the tumour nodule is represented by the values given in *Table 2* of the publication by Sersa.1998<sup>270</sup> follows the equation:

$$\text{Cis-Pt dose (mg)} = 0.2 + 0.01 \times \text{TV}(\text{mm}^3)$$

in the interval  $1 < \text{TV}(\text{mm}^3) < 1000$

Electric pulses were delivered one per second, through two parallel stainless steel electrodes, with a constant amplitude of 1300V per cm of electrode distance (910V/cm) and 0.1ms in duration. At a four-weeks follow-up, a complete response (CR) occurred in all 19 electro-chemotherapy treated nodules, and they all remained without progression up to 7-11 months.<sup>270</sup>

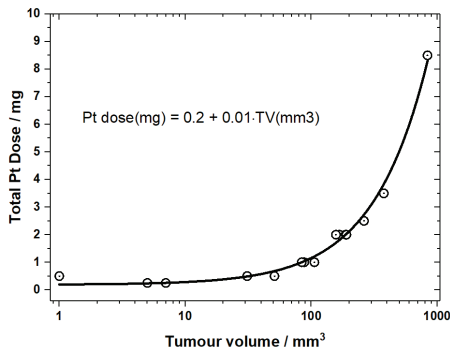


Figure 6-21

The administrated intra-tumour dose of cisplatin(Pt) extracted of the values given in *Table 2* of the publication by Sersa 1998.<sup>270</sup>

A two year-long prospective non-randomised study with four cancer centres enrolled 14 patients with breast cancer to evaluate and confirm the efficacy and safety of electro-pulse enhanced chemotherapy with Bleomycin or Cisplatin. The treatment of recurrent breast cancer was performed using an intravenous or intra-tumoural drug, followed by application of electric pulses generated by a Cliniporator™ using plate or needle electrodes. In the 58 breast cancer nodules treated with electro-pulse enhanced chemotherapy, a complete response appeared in 84 % of the nodules, partial response in 7 %, and stable disease in 10%, regardless use of drug or route of its administration.<sup>162</sup>

Intra-tumour administration of Cisplatin is recommended by *European Standard Operating Procedures of Electro chemotherapy* (ESOPE) to depend on tumour volume according to the follow rules:

**Cisplatin.** dissolved at a concentration of 2 mg/ml given intratumoural only.

- For tumour > 1 cm<sup>3</sup> 0.5 mg/cm<sup>3</sup> CisPt i.t Dose = 0.5 ×TV [mg]
- For tumour 1 - 0.5 cm<sup>3</sup> 1 mg/cm<sup>3</sup> CisPt i.t Dose = 1 ×TV [mg]
- For tumour < 0.5 cm<sup>3</sup> 2 mg/cm<sup>3</sup> CisPt i.t Dose = 2 ×TV [mg]

Electric pulses were applied to the tumour nodules as soon as possible within 2min after the intra-tumoural injection of Cisplatin.<sup>165</sup>

## 6.2.2 MALIGNANT MELANOMA

A Phase II clinical study was performed to evaluate the antitumor effectiveness of electro-pulse enhanced chemotherapy using intra-tumour Cisplatin administration on cutaneous tumour nodules in 10 malignant melanoma patients with 133 tumour nodules of different sizes.<sup>271</sup>

Cisplatin was administered intra-tumorally at doses depending on the size of the tumour nodule according to the equation:

$$\text{Pt-dose (mg)} = 0.01 \times \text{TV}(\text{mm}^3)$$

up to 200 mm<sup>3</sup>, then 2 mg for all volumes above 200 mm<sup>3</sup>.

Eighty-two tumour nodules treated with cisplatin electro-chemotherapy; 27 tumour nodules were treated with cisplatin only; 2 tumour nodules were treated. with electric pulses only; and 22 tumour nodules were untreated. After four weeks the fraction of complete response in the electro-pulse enhanced chemotherapy group was 68% and partial response was 10%, which corresponds to 78 % objective responses, and 15% experienced stable disease and 5% progressive disease, while in the objective response in the

cisplatin group was 38%, and in the electric pulses only there was no response.<sup>271</sup> In a previous study of 4 patients with 19 nodules the complete response was 100 %.<sup>270</sup> Thus electro-pulse enhanced chemotherapy with cisplatin was judged to be a highly effective approach for treatment of cutaneous malignant melanoma nodules.<sup>271,272</sup>

A case with a large anorectal malignant melanoma was preoperatively treated by electro-pulse enhanced chemotherapy with Cisplatin to reduce the tumour size, to enable Sphincter-saving local excision. After surgery, radiation-brachytherapy was delivered to the excision site, and at 14 months' follow-up there, was no sign of recurrence.<sup>273</sup>

Another case of melanoma on the calf with multiple cutaneous and subcutaneous metastases treated by electro-pulse enhanced chemotherapy with Cisplatin showed a long-lasting complete response.<sup>167</sup>

**Table 6-21a**

The reported responses of cis-Pt *EpEChT* of Malignant Melanoma.

Author <sup>Reference</sup>	No. Patients	No. nodules	<i>f</i> CR	<i>f</i> PR	<i>f</i> SD	<i>f</i> PD
Sersa,1998 <sup>270</sup>	4	19	1	0	0	0
Sersa,2000 <sup>271</sup>	10	82	0.68	0.10	0.15	0.05
Sersa,2003 <sup>274</sup>	3	10	0.50	0.20	0.30	0
Snoj,2005 <sup>273</sup>	1	1	1	0	0	0
Snoj,2006 <sup>167</sup>	1	16	0.81	0	0	0.23
Sum	19	128				
Average			0.80	0.06	0.09	0.06
SD			0.21	0.09	0.13	0.10
SE			0.10	0.04	0.06	0.04

**Table 6-21b**

Objective (*f*OR) and weighted responses *f*WR<sub>3</sub> and *f*WR<sub>4</sub> to Cis-Pt *EpEChT* of Malignant Melanoma.

Author <sup>Reference</sup>	No. Patients	No. nodules	<i>f</i> OR	<i>f</i> WR <sub>3</sub>	<i>f</i> WR <sub>4</sub>
Sersa,1998 <sup>270</sup>	4	19	1	1	1
Sersa,2000 <sup>271</sup>	10	82	0.78	0.70	0.72
Sersa,2003 <sup>274</sup>	3	10	0.70	0.57	0.68
Snoj,2005 <sup>273</sup>	1	1	1	1	1
Snoj,2006 <sup>167</sup>	1	16	0.81	0.58	0.58
Sum/Average	19	128	0.86	0.77	0.79
/SD			0.14	0.22	0.19
/SE			0.06	0.10	0.09

### 6.2.3 BREAST CANCER BC

In a study treating two patients with 12 cutaneous breast cancer lesions of by electro-pulse enhance chemo-therapy with Cisplatin, a complete response appeared in 33% and partial response in 67 %, while no complete responses occurred with i.t. application of Cisplatin alone.<sup>237</sup>

**Table 6-22a**

Reported responses of Cis-Pt <i>EpEChT</i> treatment of Breast Cancer						
Author <sup>Reference</sup>	No. Patients	No. nodules	fCR	fPR	fSD	fPD
Rebersek,2004 <sup>237</sup>	2	12	0.33	0.67	0	0

**Table 6-22b**

Objective (fOR) and weighted responses fWR<sub>3</sub> and fWR<sub>4</sub> to Cis-Pt *EpEChT* treatment of Brest Cancer

Author <sup>Reference</sup>	No. Patients	No. nodules	fOR	fWR <sub>3</sub>	fWR <sub>4</sub>
Rebersek,2004 <sup>237</sup>	2	12	1	0.55	0.67

### 6.2.4 SUMMARY OF ALL *EpEChT* CLINICAL STUDIES WITH CIS-PLATIN

**Table 6-23a**

The reported responses of cis-Pt *EpEChT* treatment of various types of tumours

Diagnosis	No. Pat.	No. Tum.	fCR	fPR	fSD	fPD
Malignant Melanoma	19	128	0.80	0.06	0.09	0.06
Squamous Cell Ca	1	2	1	0	0	0
Basal Cell Ca.	1	9	1	0	0	0
Breast cancer	2	12	0.33	0.67	0	0
Sum	23	151				
Average			<b>0.78</b>	<b>0.18</b>	<b>0.02</b>	<b>0.01</b>
SD			0.32	0.33	0.05	0.03
SE			0.22	0.23	0.03	0.02

**Table 6-23b**

Objective (fOR) and weighted responses fWR<sub>3</sub> and fWR<sub>4</sub> to cis-Pt  
*EpEChT* treatment of various types of tumours

Diagnosis	No. Patients	No. nodules	fOR	fWR <sub>3</sub>	fWR <sub>4</sub>
Malignant Melanoma	19	128	0.86	0.77	0.79
Squamous Cell Ca	1	2	1	1	1
Basal Cell Ca.	1	9	1	1	1
Breast cancer	2	12	1	0.55	0.67
Sum	23	151			
Average			0.96	0.83	0.86
SD			0.07	0.22	0.17
SE			0.05	0.15	0.08

**Table 6-24a**

The response ratios to Cis-Pt *EpEChT* / Bleomycin *EpEChT* treatments of  
various types of tumours

Diagnosis	Pt/Bleo CR	Pt/Bleo. PR	Pt/Bleo. SD	Pt/Bleo. PD
Malignant Melanoma	1.76	0.18	0.54	1.29
Squamous Cell Ca.	2.37	0	0	0
Basal Cell Ca.	1.32	0	0	0
Breast cancer	0.63	2.53	0	0
Average	1.52	0.68	0.14	0.32

**Table 6-24b**

Objective OR and weighted WR<sub>3</sub> and WR<sub>4</sub> response-ratios to Cis-Pt  
*EpEChT* / Bleomycin *EpEChT* treatments of various types of tumours

Diagnosis	Pt/Bleo. OR	Pt/Bleo. WR <sub>3</sub>	Pt/Bleo. WR <sub>4</sub>
Malignant Melanoma	1.10	1.48	1.44
Squamous Cell Ca	1.34	2.44	1.82
Basal Cell Carcinoma	1.02	1.23	1.18
Breast cancer	1.24	0.97	1.01
Average	1.18	1.53	1.36

In Table 6-24 are given the ratios of the average responses for treatment of various types of tumours with Cis-Pt *EpEChT* (Table 6-23) and corresponding tumours with Bleomycin *EpEChT* (Table 6-20). The corresponding ratios for objective and the WR<sub>4</sub> weighted responses are displayed in Figure 6-22. Although the number of cases are sparse, squamous-cell carcinoma seems to respond much better, and malignant melanoma seems to respond slightly better with Cis-Pt *EpEChT* than with Bleomycin *EpEChT*. For Basal cell carcinoma and breast cancer there seems to be no difference.

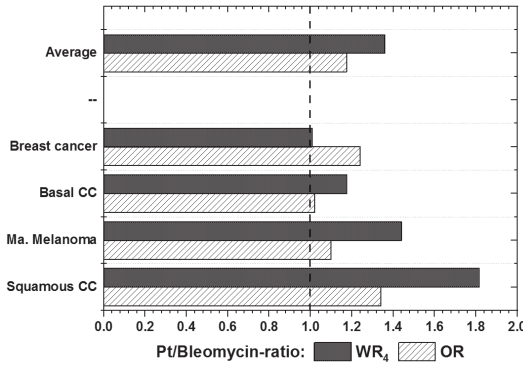


Figure 6-22  
Response ratios of Cis-Pt *EpEChT* versus Bleomycin *EpEChT* objective OR and weighted WR<sub>4</sub> responses for treatment of various types of tumours.

According to the ESOPE recommendation, Cisplatin should only be administered at a concentration of 2 mg/ml, although the total administered dose varies with the tumour volume and the number of therapy sessions as shown in Figure 6-23.

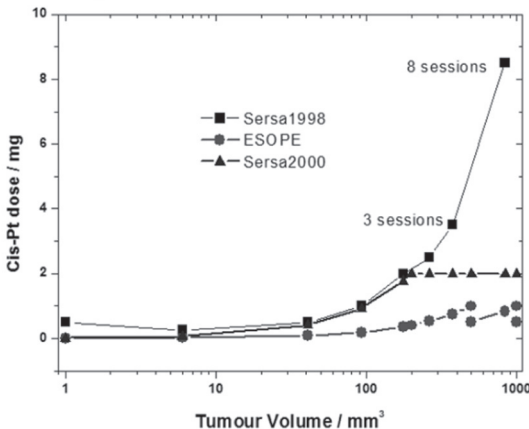


Figure 6-23  
Variation of total administered dose of Cis-Pt with the tumour volume and the number therapy sessions as used in clinical studies.<sup>270,271,272</sup> and recommended by ESOPE.<sup>165</sup>



## 6.3 CLINICAL STUDIES OF *EpEChT* WITH OTHER PHARMACEUTICALS

### 6.3.1 CLINICAL STUDIES OF *EpEChT* WITH INTERLEUKINS

Treatment regimens combining electro-pulse enhanced cancer therapy (EpECT) to biological response modifiers (interleukin-2, interferon) and immunotherapeutic compounds is presently intensively explored in animal and human cancer models. The hope is that immunotherapy combined to EpECT could broaden the therapeutic indications of EpECT to deep-seated and spread disease.

In an attempt to analyse anti-tumour immune response in patients treated with IL-2 based immunotherapy systemic anti-tumour cytotoxic T lymphocyte (CTL) responses was studied against known tumour antigens in melanoma patients over the course of IL-2 based immunotherapy combined with electrochemotherapy.<sup>275,276,277</sup> Surprisingly, they found that anti-tumour CTL responses significantly declined upon initiation of therapy, but reappeared when pausing IL-2 administration. Molecular analyses of the clono-typic composition of responding T cells demonstrated that new clones emerged during the treatment, and that tumour-specific T cells left the peripheral blood and could subsequently localize at the tumour site. This underlines the importance to gain detailed information on the interactions between cancer cells and cells of the immune system.

The US company *OncoSec Medical* has three ongoing Phase 2 trials in treating metastatic melanoma, which support that electro-pulse treatment combined with the agent IL-12 (*ImmunoPulse*) to 47 melanoma patients showed a systematic immune response with tumour shrinkage.

Merkel-cell carcinoma (MCC) is an orphan disease with no Food and Drug Administration-approved treatments so far. However, *OncoSec Medical* is conducting trials in treating MCC with '*ImmunoPulse*,' in which they record an uptake of IL-12 of at least 100-fold, and some as high as the 1,000-fold increase in patients treated.<sup>278</sup>

### 6.3.2 CLINICAL STUDIES OF *EpE*-DELIVERY OF DNA VACCINES

In a review, the use of electro-pulse enhanced DNA delivery to enhance the immune responses, the cancer antigens, and the escape mechanism(s) used by tumour cells are discussed, with a focus on the progress of clinical trials using cancer DNA vaccines.<sup>279</sup>

In phase I/II trial a DNA vaccine, SCIB1, incorporating two CD8 and two CD4 epitopes from TRP-2/gp100 has evaluated in patients with metastatic melanoma. The patient tolerated the delivery of the DNA vaccine well, and the vaccine stimulated potent T cell responses in melanoma patients.<sup>280</sup>

**6.3.3 *EpEChT* WITH PD-1, CTLA-4 IMMUNE CHECKPOINT BLOCKADE**

Anti-PD-1 agents and anti-CTLA-4 agents have been shown to improve progression-free survival and objective response rate as monotherapy in patients with advanced melanoma. However, they are not adequate for all cases and associated with significant toxicity.<sup>281</sup>

Table 6-25 displays the results of a retrospective study ipilimumab in combination with electro-pulse enhanced chemo-therapy *EpEChT* which involved fifteen patients with previously treated metastatic melanoma. The patients included in the analysis received ipilimumab 3mg/kg every three weeks for 4 cycles. After the first Ipilimumab infusion, they underwent *EpEChT* with Bleomycin 15mg/m<sup>2</sup>.<sup>282</sup>

**Table 6-25a**

Treatment response to melanoma patients with a combination of Bleomycin *EpEChT* and the anti-CTLA-4 agent Ipilimumab.

Diagnosis	No. Patients	Response	fCR	fPR	fSD	fPD
Malignant Melanoma	15	Local	0.27	0.40	0.33	0
Malignant Melanoma	9	Systemic	0	0.30	0.26	0

**Table 6-25b**

The objective OR and weighted WR<sub>3</sub> and WR<sub>4</sub> treatment response to melanoma patients with a combination of Bleomycin *EpEChT* and the anti-CTLA-4 agent Ipilimumab.

Diagnosis	No. Patients	Response	fOR	fWR <sub>3</sub>	fWR <sub>4</sub>
Malignant Melanoma	15	Local	0.67	0.40	0.55
Malignant Melanoma	9	Systemic	0.56	0.30	0.22

Another clinical evaluation of the use of electro-pulse enhanced chemotherapy (EEChT) combined with CTLA-4 or PD-1 inhibitors involved 33 patients with unresectable or metastatic melanoma. The patients received combination of *EpEChT* and immune checkpoint blockade for distant or cutaneous metastases within 4 weeks. Table 6-26 shows a

summary of the treatment results. The anti-CTLA-4 agent Ipilimumab combined with *EpEChT* showed a high systemic response rate. The local response, however, was lower than reported for electro-pulse enhanced chemotherapy *EpEChT* only.<sup>283</sup>

A case history reports a complete response after electro enhanced chemotherapy on a progressive mass of metastatic melanoma (MM), while anti-PD-1 treatment with Nivolumab, with no evidence of disease at 4 years since previous local recurrence, combined with anti-PD-1 treatment exhibited induced durable complete response in the heavily pre-treated metastatic melanoma patient.<sup>284</sup>

**Table 6.26**

The response of combination of Bleomycin EpECT treatment with anti PD-1 and anti-CTLA-4 agents.

No. Pat.	Agent	Local response %	Systemic response %	Time to progression month	Toxicity Event %
28	Anti CTLA-4	66.7	19.2	2	25
5	Anti PD-1	66.7	40	5	

### 6.3.4 ELECTRO ENHANCED THERAPEUTIC EFFICIENCY OF CALCIUM

A double-blinded randomized study was performed to compare calcium electroporation to electro-chemotherapy concerning the response measured 6 months after treatment.<sup>285</sup> The study protocol included seven patients with a total of 47 cutaneous metastases from breast cancer and malignant melanoma with a total of 37 metastases randomized for treatment. The patients received intratumoural administered calcium ( $\approx 50\mu\text{mol}$ ) or Bleomycin ( $\approx 200\text{IU}$ ) followed by application of electric pulses at average electro- doses of respectively 700 and 400J/g respective to the tumour site. Table 6-27 shows the treatment results, which do not indicate any significant difference between the two treatments.

**Table 6-27a**The fractional responses of Calcium and Bleomycin *EpEChT* treatment

Drug	Dose	CR	PR	SD	PD
Bleomycin (1000IU)	i.t 0.2 ml	0.68	0.15	0	0.15
CaCl <sub>2</sub> (220mM)	i.t 0.2 ml	0.66	0.05	0.16	0.11

**Table 6-27b**Objective OR and weighted WR<sub>3</sub> and WR<sub>4</sub> treatment response to Calcium and Bleomycin *EpEChT* treatments

Drug	Dose	OR	WR <sub>3</sub>	WR <sub>4</sub>
Bleomycin (1000IU)	i.t 0.2 ml	0.83	0.58	0.61
CaCl <sub>2</sub> (220mM)	i.t 0.2 ml	0.71	0.57	0.62

Since the patients who received calcium treatment on average received larger deposited electric energy, their responses are not entirely comparable with the Bleomycin treatment. This study, however, clearly show the benefit of using Ca in electro enhanced cancer-therapy, like in electro enhanced weed control (see 4.6.1).

# CHAPTER VII

## SAFETY OF ELECTRO ENHANCED CHEMOTHERAPY

### 7.1 BIOLOGICAL EFFECTS OF ELECTRIC SHOCK

#### 7.1.1 TOLERANCE OF ELECTRICAL SENSATION INDUCED BY ELECTRIC FIELDS

Exposure of patients to intense electric pulses is known to affect cell membranes in the exposed tissues. At exposure to a strong electric current and high absorbed electric energy, denaturation of macromolecules and complex biochemical reactions occur.

The field-induced transmembrane potential can produce electro-conformational changes of ion channels and ion pumps in the cell membranes. If the potential exceeds the dielectric strength of the cell membrane (approximately 0.5 V for a pulse width of a few ms), electro conformational changes of membrane lipid bilayers create electroporation. These events cause the electric current to pass through the porated cell membrane and affect the cytoplasmic contents of the cells. Besides electroporation of cell membranes and denaturation, cytoplasmic macromolecule brings about many complex biochemical reactions such as oxidation of proteins and lipids. The combined effects of all these events may damage the cells beyond possible repair. Lipid peroxidation and the subsequent loss of the energy-transducing ability of the cells may occur even at moderate temperatures between 40°C and 45°C.<sup>286</sup>

A clinical study enrolled 20 patients in order to evaluate the safety and human tolerance of electrical sensation induced by electric fields with non-invasive electrodes. The patients were subjected during 3ms to single pulses of 50–80 V amplitude escalating in 10-V increments. Table 7-1 shows the patients' rating of the pulse sensation on a scale of 0, no pain, to 10, excruciating pain.

The summary of the results displayed in Figure 7-1 indicates that the tolerability starts to decrease above 80 V. Thus, exposure to higher amplitudes requires local anaesthesia to be applied.<sup>287,288</sup>

In addition to the sensation of pain caused by high voltage pulse delivery, muscle contractions present other unpleasant sensations for patients undergoing electro-chemotherapy. Since each single pulse that was delivered was associated with muscle contractions, studies have been conducted in an attempt to reduce the number of unpleasant sensations by increasing the frequency of electric pulses over the frequency of tetanic contraction. Measurements of muscle torque in rats showed that exposure to electric fields of pulse frequencies above the frequency of sustained muscle contraction ( $> 100$  Hz) reduces the number of individual contractions to a single muscle contraction.<sup>289</sup>

Summary of the results displayed in Figure 7-1 indicates that the tolerability starts to decrease above 80 V. Thus, exposure to higher amplitudes requires local anaesthesia to be applied.<sup>287,288</sup>

Regardless of the pulse amplitude, with increasing pulse frequency, muscle torque increases up to the frequency of 100 or 200 Hz and then decreases to a value similar to that after application of a 1 Hz pulse train. Electro-chemotherapy in vivo with higher repetition frequencies inhibits tumour growth and is efficient at all pulse frequencies examined (1 Hz - 5 kHz). These results suggest that there is considerable potential for clinical use of high-frequency pulses in electro-chemotherapy.<sup>289</sup>

According to their results, the muscle torque grows with an increase of the repetition frequency, and at the frequency 5 kHz the muscle torque was two times higher than at 1 Hz. They also found that electro-pulse-enhanced chemotherapy of a tumour model in mice at 1 Hz or 5 kHz has about the same efficiency (at 32% versus 22% complete remissions respectively). Thus, application of a 5 kHz pulse train with 8 pulses instead of 8 individual pulses at 1 Hz has the advantage of only one sensation instead of eight with the same outcome of the treatment.<sup>289</sup>

**Table 7-1**  
Score table of the electric pulse sensation

Score	Sensation
0	No pain
1-2	Mild
2-4	Discomforting
5	BETWEEN
6-7	Distressing
8-9	Horrible
10	Excruciating

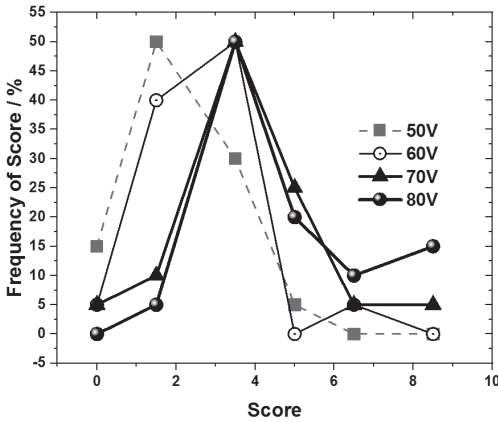


Figure 7-1  
Frequency of score for pain sensation at exposure to cutaneous electric fields during 3 ms at various amplitudes.

### 7.1.2 TOLERANCE OF PAIN AND MUSCLE CONTRACTIONS INDUCED BY ELECTRIC FIELDS

A clinical study was designed to analyse the safety of electro-pulsed-enhanced chemotherapy, and involved 61 patients. The use of low doses of the chemotherapeutic preparations limits adverse reactions related to treatment with Bleomycin or Cisplatin.

For the relief of symptoms associated with the application of electrical pulses, 60% of the patients used local anaesthesia, and 40% used general anaesthesia. In patients with local anaesthesia, the median level of pain immediately after treatment was 35 units in a range 0-100 of visual assessment. Two days after treatment, the median pain level had dropped to 20 units. Patients treated with general anaesthesia reported significantly lower pain than those treated with local anaesthesia. The pain was assessed as acceptable and was limited to the area of the treated tumour. In connection with the application of electrical pulses, no or low muscle contractions were observed with needle electrodes while strong muscle contractions were observed with surface platelets.

No serious incidents associated with pulse therapies were noted, and the majority of patients treated were willing to accept treatment again if needed.<sup>162</sup>

### 7.1.3 SIDE EFFECTS OF ELECTRIC FIELD TREATMENT IN THE HEAD AND NECK REGION

Table 7-2 displays various forms of adverse events that might occur after the treatment of mucosa in the head/throat area with pulsed electric fields. The most common event (25%) was to feel the “smell of odours”, with one serious case. Another serious side effect was “ulceration” (9%). In addition, there were less serious side effects such as “hyperpigmentation” (16%) and flu-like symptoms (14%).<sup>227</sup>

**Table 7-2**

Side effects of electric field treatment in the Head and Neck region.<sup>227</sup>

Type	Grade I/II		Grade III/IV	
	N	%	N	%
Odour smelling	10	23.3	1	2.3
Ulceration	4	9.3	4	9.3
Hyperpigmentation	7	16.3		
Flu - symptoms	6	14.0		
Suppuration	3	7.0		
Nausea	3	7.0		
Swelling	2	4.7		
Dysphagia	1	2.3		
Sensitive tongue, saliva stasis in the floor of the mouth	1	2.3		
Large defect of the lip, incontinency for saliva	1	2.3		

N = number of cases

## 7.2 THE EFFECT OF ELECTRIC PULSES ON THE FUNCTIONING OF THE HEART

### 7.2.1 NORMAL CONDITIONS

Figure 7-2 describes the electrophysiology of the heart with the different waveforms of the electrocardiogram (ECG) of the healthy heart. The P-wave represents the depolarization of the muscle cells in both the left and right atria from -80 mV to +20 mV, leading to a contraction in the atria. The QRS complex represents the depolarization of muscle cells in the heart's chamber also from -80 mV to +20 mV. The T-wave represents the repolarization of the muscle cells of the heart back to -80 mV.



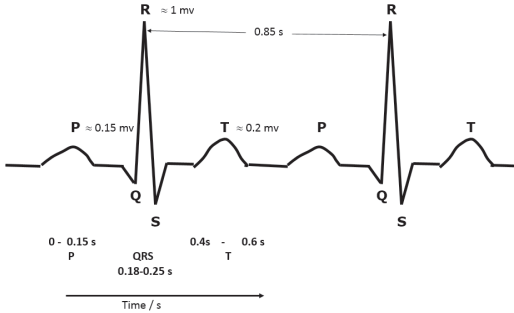


Figure 7-2  
Electro-physiology of the heart. The different waveforms of the usually recorded ECG of the healthy heart.

In a study of the influence of electro-pulse-enhanced therapy on the functioning of the heart of human patients, no pathological morphological changes occurred. However, a detailed analysis of the electrocardiogram after application of electro-pulse enhanced therapy, showed a decrease in transient RR intervals, although this was not significant.<sup>290</sup>

Figure 7-3 displays the ratio of various ECG parameters in patients exposed to electroporation (EP) and in healthy condition (no pulses).<sup>290</sup>

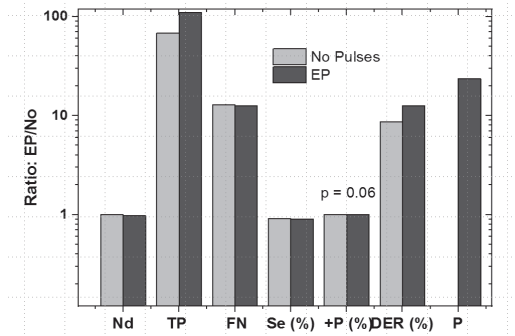


Figure 7-3

Ratio of various ECG parameters in patients exposed to electro-pulse enhanced therapy (EP) and in normal condition (no pulses)

Nd = total number of possible detected QRS complexes (normal and abnormal), the sum of TP and FN;

TP = true positive for QRS detection (the number of correctly detected QRS complexes);

FN = false negative for QRS detection (the number of missed QRS complexes);

Se = sensitivity (%) for QRS detection; %

+P = positive predictivity (%) for QRS detection;

DER = detection error rate (%) for QRS detection;

P = premature heartbeats of ventricular, supraventricular or ectopic origin;

### 7.2.2 *EpEChT* THERAPY OF LIVER METASTASES

In 2015, Mali et al. studied the effects of intra-abdominal *EpEChT* of colorectal liver metastases on the functioning of the heart during the early post-operative care period.<sup>291</sup> Although the deep-seated tumours were located close to the heart, no significant heart rhythm changes (i.e., induction of extra systoles, ventricular tachycardia or fibrillation) or pathological morphological changes (i.e., ST-segment changes) indicating myocardial ischemia occurred. However, they found several minor statistically significant but clinically irrelevant changes in HRV parameters after *EpEChT* procedures: a decrease in median values of the mean NN interval, a decrease in the low-frequency and the normalized low-frequency component, and an increase in the normalized high-frequency component.

The conclusions here are thus that intra-abdominal *EpChT* treatment does not cause any relevant changing of the heart function. They expressed, however, statistically significant but clinically irrelevant changes in heart-rate and long-term HRV parameters. The nature of these changes is not related to the known effects of the drugs given to the patients in post-operative care.<sup>291</sup>

### 7.2.3 IRREVERSIBLE ELECTROPORATION ON THE FUNCTIONING OF THE HEART

Between September 2011 and September 2014, a single-centre nonrandomized clinical trial of irreversible electroporation (IRE) was performed at the department of surgery at Uppsala University Hospital, Sweden. The study aimed to assess the safety and efficacy in IRE ablation of 38 malignant liver tumours on 30 patients. In one patient, ECG changes occurred during IRE, and chest pain required morphine. Minor complications occurred in 6 patients, ranging from increased blood pressure to a self-limiting hematoma in the ablated zone requiring no further action.<sup>292</sup>

A study of demographic and intraoperative data for patients (n = 43) undergoing irreversible electroporation for *hepato-pancreato-biliary* and retroperitoneal malignancies during 2012 to 2015 was performed to describe the intraoperative adverse events associated with irreversible electroporation in patients undergoing solid tumour ablation. It revealed that there was about 20% adverse events, of which 90% were primarily cardiac, including 77% related to blood pressure elevation, and 16% to arrhythmia. One patient with arrhythmia required the termination of ablation.<sup>293</sup>

A study of the safety of treatment with irreversible electro-ablation involved 26 New Zealand white rabbits with VX2 tumours implanted adjacent to the sciatic nerves. After the treatment, the sciatic nerves were removed for histopathologic evaluation and showed preserved endo-neural architecture after treatment with irreversible electro-ablation.<sup>294</sup>

#### 7.2.4 MICROWAVE ABLATION AND FUNCTIONING OF THE HEART

A safety and efficacy study of liver microwave (MW) ablations performed between June 2010 and August 2015 involved 118 cases of percutaneous ablation at zone margins within 5mm of the liver capsule near the heart.<sup>295</sup> The risk group comprised 27 cases with ablation zones extended to less than or equal to 5 mm from the myocardium, and the remaining ablation cases formed the control group.

After the treatment, there was no difference between the groups in terms of frequency of alterations in peri-procedural blood pressure (25.9% vs 29.6%.  $p=0.81$ ) or heart rate (18.5% vs 24.2%.  $P = 0.61$ ) or rate of LTP (12.0% vs 10.8%.  $P = 1.0$ ). Thus, percutaneous MW ablation near the heart may be considered safe and effective, without increased risk of cardiac complications and with similar rates of LTP, compared with a control group of peripheral liver ablations.<sup>295</sup>

#### 7.2.5 ELECTROSHOCK WEAPON ON FUNCTIONING OF THE HEART

TASER is an electroshock weapon which fires two small dart-like electrodes, which stay connected to the central unit by conductors, to deliver an electric shock to voluntary disrupt control of muscles, resulting in strong involuntary long muscle contractions.

**Table 7-3**

Specifications of electroshock weapon TASER type M26 and X26

Specification	Taser M26	Taser X26
Output pulse amplitude	3800 V	600 V
Pulse length	40 $\mu$ s	100 $\mu$ s
Pulses delivered in a shot	100	95
Duration	5 s	5 s
Pulse delivery frequency	20 Hz	19 Hz

Table 7-3 shows the specification of the TASER X26 pulse, which is very similar to the pulses from an electroporation device. The probability of triggering cardiac arrhythmias in the use of electroshock weapon depends on the currents that occur in the heart and surrounding organs.<sup>296,297</sup>

A single coarse mesh finite element model using the time-duration threshold of approximately  $2.98 \cdot 10^{-3}$  (V×/m) for nerve stimulation, shows that TASER would not stimulate regions farther than roughly 19 cm away from the darts.<sup>297</sup>

Thus electroporation devices that deliver pulses with a short duration and low duty cycle similar to TASER should not cause any risk of triggering cardiac arrhythmias (VF) at treatment locations about 20 cm away from the heart.

## **7.3 SAFETY AND EFFICACY OF IRREVERSIBLE ELECTROPORATION (IRE)**

### **7.3.1 IRE ABLATION OF LIVER TUMOURS**

In irreversible electroporation (IRE), the applied field-strength is higher than in electro-chemotherapy in order to kill (ablate) the tumour cell instantly without adding any chemotherapy drugs. Thus, the safety matter of IRE has been carefully studied in several clinical trials.

A single-centre nonrandomized clinical trial of the safety and efficacy of IRE ablation involved 30 patients with 38 liver tumours.<sup>292</sup> At six months after the IRE treatment, there was no evidence of a tumour in the ablated area in 66% of the patients. In six patients, minor complications appeared, and, in one patient, bile duct dilatation and stricture of the portal vein and bile duct occurred.

All publications reporting clinical responses from IRE ablation of liver tumours demonstrate the need for the conducting of more clinical studies in order to establish full safety and efficacy for IRE treatment of primary and metastatic hepatic malignancies.<sup>298</sup>

### **7.3.2 NERVES ADJACENT TO IRE ABLATION OF TUMOURS**

A study of the safety of IRE ablation on the sciatic nerve involved 26 New Zealand white rabbits VX2 with tumours implanted adjacent to the sciatic nerves.<sup>298</sup> After IRE ablation, severe damage appeared on nerves adjacent to the tumour. However, in a short time, their function and structure repaired. The control rabbits also showed nerve damage but with no signs of repair and rapid tumour progression. Thus, irreversible electro pulse

treatment of tumours located adjacent to nerves seems not to cause severe nerve damage.

## CHAPTER VIII

# NEW DIMENSIONS FOR ELECTRO-PULSE- ENHANCED CANCER-THERAPY

### 8.1 CLINICAL *EpECT* STUDIES

#### 8.1.1 RECENT CLINICAL *EpECT* STUDIES

Most clinical studies so far have used the ESOPe protocol with pulses of constant voltage amplitude applied in a train of 8 pulses at an interval of 0.2ms. By successively decreasing voltage for each pulse, a new treatment concept called dynamic electro-enhanced chemotherapy (D-EECT<sup>TM</sup>) developed. A clinical case study in India recently applied the D-EECT concept.<sup>178</sup> The study involved 23 patients treated in a total of 38 sessions of D-EECT<sup>TM</sup> at four different cancer centres. Table 8-1 shows the treatment responses for a total of 66 tumours of various sizes and various histological types. In all of the evaluable tumours, the objective responses were found to be 100% with complete remissions 18%, and partial remissions 82%. No progressive disease was recorded and the average weighted ( $WR_4$ ) response became  $58 \pm 4(SE)\%$ .

The objective responses of 100% squamous cell carcinomas in Kalavathy's study are better than the overall average of 78% for the objective response estimated from all reported clinical studies of SCC reviewed in Chapter 6. The weighted ( $WR_4$ ) response of 61% was greater than the overall average of 48% for the weighted ( $WR_4$ ) response estimated from all reported clinical studies of SCC reviewed in Chapter 6. No cases with progressive disease appeared in Kalavathy's study, which might indicate a better immune response than the clinical studies of SCC reviewed in Chapter 6 with an estimated fraction progress disease of 12%.

**Table 8-1**

Type of tumours and the percentage of tumours' response to D-EECT treatment.<sup>178</sup>

Tumour Type	Histology	CR %	PR %	OR %	WR <sub>4</sub> %
Squamous cell ca.	HN SCC	21	79	100	61
Breast cancer	Adeno carcinoma	14	86	100	57
Breast cancer	Infiltrated ductal	50	50	100	75
Breast cancer	Poorly diff.	0	100	100	50
Rectal cancer	Adeno carcinoma	0	100	100	50
Vaginal vault ca.	Squamous	0	100	100	50
Soft tissue sarcoma		0	100	100	50
Fibro sarcoma		67	33	100	84
Spindle cell ca.		0	100	100	50
Average		18	82	100	58
SE		8	8		4

Table 8-2 shows the summary of another recent report of 43 patients with recurrent mucosal head and neck tumours treated according to the ESOPE protocol.<sup>227</sup> A cohort of 34 patients had evaluable SCC tumours, and 3 were adenocarcinoma patients. The SCC patients were split into one group with nodule diameter less than 3 cm, and another group with nodules larger than 3 cm. Table 8-2 shows the summary of the averages of the various responses of the total number of patients and the two groups separately.

There was no remarkable variation of responses in the various groups of patients shown in Table 8-2, except that the weighted (WR<sub>4</sub>) response was greater in the group with small tumours than in the group with large tumours. In Kalavathy's work, however, the size of the SCC nodules was in the range of 5-6 cm with 61% weighted (WR<sub>4</sub>) response, which is greater than corresponding value of 38% for tumours larger than 3 cm treated according to the ESOPE protocol.<sup>178</sup>

**Table 8-2a**

Summary of the results of EpEChT according to ESOPE in treatment of head and neck cancer.<sup>227</sup>

Type of patients	No. of patients	No. patients evaluable	fCR	fPR	fSD	fPD
All	43	37	0.22	0.43	0.27	0.08
All SCC 91%		34	0.21	0.44	0.26	0.09
SCC<3 cm		14	0.21	0.50	0.21	0.07
SCC>3 cm		20	0.20	0.40	0.30	0.10
Tot AD 9 %	4	3	0.2	0.4	0.3	0.1

**Table 8-2b**

Summary of objective OR and weighted WR<sub>4</sub> treatment response to EpEChT according to ESOPE in treatment of head and neck cancer.<sup>227</sup>

Type of patients	No. of patients	No. patients evaluable	fOR	fWR <sub>4</sub>
All	43	37	0.65	0.42
All SCC 91%		34	0.65	0.41
SCC<3 cm		14	0.71	0.44
SCC>3 cm		20	0.60	0.38
Tot AD 9 %	4	3	0.6	0.38

The objective responses of 100% for breast cancer in Kalavathy's study are better than the overall average of 80% for the objective response estimated from all reported clinical studies of SCC reviewed in Chapter 6. However, the ratio of complete to partial remissions is 0.25 in Kalavathy's study, which is much smaller than the ratio of 2 for corresponding averages estimated from all reported clinical studies of breast cancer reviewed in Chapter 6.

Table 8-3 shows a summary of another recent report on electro-pulse enhanced chemotherapy treatment of 90 patients with cutaneous recurrence from breast tumours according to the ESOPE protocol at 10 European cancer centres. The table shows the response to electro-pulse-enhanced chemotherapy for breast tumours according to the size of nodules less than 3cm in size, or larger than 3cm, and at the bottom of the table the average patient response at 2 months after treatment is given.<sup>236</sup> The weighted (WR<sub>4</sub>) response was 80% in the group with small tumours and 48% in the group of large tumours.



**Table 8-3a**

Tumour response to electro-chemotherapy according to ESOPE for a size of nodules < 3 cm, and > 3cm, and the average patient response at 2 months after treatment.<sup>236</sup>

	No. Nodules	fCR	fPR	fSD	fPD	fNE
Nodules < 3 cm	113	0.72	0.14	0.08	0.01	0.05
Nodules > 3 cm	94	0.37	0.24	0.18	0.06	0.03
Average	207	0.57	0.20	0.13	0.03	0.04

fNE is the fraction of patients not included in the evaluation.

**Table 8-3b**

Summary of objective OR and weighted  $WR_4$  tumour response to electro-chemotherapy according to ESOPE for a size of nodules < 3 cm, and > 3cm, and the average patient response at 2 months after treatment.<sup>236</sup>

	No. Nodules	fOR	f $WR_4$
Nodules < 3 cm	113	0.86	0.80
Nodules > 3 cm	94	0.62	0.48
Average	207	0.76	0.67

In Kalavathy's study<sup>178</sup> of breast cancer patients with nodules in the range of 7-8 cm, the weighted response is about the same as it is for tumours larger than 3 cm in the ESOPE study. Her treatment of patients with breast-infiltrated ductal carcinoma with even larger tumours (10-15 cm) resulted in a weighted ( $WR_4$ ) response of 75%, which is better than the 48% weighted ( $WR_4$ ) response for tumours larger than 3cm in the ESOPE study.<sup>236</sup>

### 8.1.2 *EpEChT* AND CYCLOPHOSPHAMIDE (CTX)

Cyclophosphamide has been found to induce beneficial immunomodulatory effects in adaptive immunotherapy with the following mechanisms involved in the creation of this immunologic effect.<sup>116</sup>

1. Elimination of  $CD4^+$ , and  $CD25^+$  T-cells in naive and tumour-bearing hosts;
2. Induction of T- cell growth factors such as type-I interferons (IFNs);
3. Enhanced grafting of adoptively transferred, tumour-killing effector T-cells (CTL).

Thus, cyclophosphamide preconditioning of recipient hosts (for donor T-cells) might be used to enhance immunity in naïve hosts and to enhance adaptive immunotherapy.

A recent *in vitro* study showed that electro-enhanced chemotherapy with cyclophosphamide (CTX) has a similar anti-tumoural effect as Bleomycin.<sup>117</sup>

Kalavathy successfully treated one patient with locally advanced breast cancer, but with no secondary deposits anywhere, by using the routine chemotherapy combination of Adriamycin, and Cyclophosphamide (with a dose according to the BSA) followed by *EpEChT* within 24 hours of intravenous administration of chemotherapy drugs.<sup>178</sup>

The combination of electro-enhanced gene therapy with Vasostatin-gene and cyclophosphamide administration was found to improve the therapeutic effects in melanoma tumours. Both significant inhibition of tumour growth and extended survival of treated mice were observed.<sup>118</sup>

### 8.1.3 *EpEChT* AND TAMOXIFEN?

Studies of MCF-7 human breast adenocarcinoma cells with tamoxifen in combination with pulsed electric fields resulted in enhanced uptake of Tamoxifen and decreased tumour cell growth compared to treatment with tamoxifen alone.<sup>299,300</sup> These results suggest that clinical use of electro-pulse-enhanced therapy combined with tamoxifen could lead to a more effective anti-tumour response than tamoxifen alone.<sup>299</sup> Reducing Tamoxifen dosage for the treatment of Estrogen receptor-positive breast cancer might also become a consequence of treatment with pulsed electric fields.<sup>300</sup>

## 8.2. ELECTRO-PULSE ENHANCED IMMUNO THERAPY

### 8.2.1 *EpEGT* AND INTERLEUKIN-2 (IL-2)

In animal experiments conducted by Mir and colleagues in 1992, systemic, anti-metastatic immune responses were achieved through a combination of electro-pulse enhanced chemotherapy and delivering histoincompatible cells secreting interleukin-2 (IL-2).<sup>164,120,301,302,119</sup>

Later, Heller discussed the clinical potential of the use of electro-pulse enhanced gene-therapy (*EpEGT*) in the treatment of melanoma.<sup>303</sup> Delivery of a plasmid DNA encoding interleukin-12 (IL-12) or interleukin-2 (IL-2) using *EpEGT* proved to be safe with no severe toxicities reported, while *EpEGT* with the delivery of IL-12 plasmid DNA resulted in significant necrosis of melanoma cells in the majority of treated tumours. Biopsies from

the treated tumours showed significant lymphocytic infiltration. Following this treatment, a systemic response in untreated melanoma lesions also appeared.<sup>303</sup>

In a recent review, Calvet and Mir (2016) noted the promising outcome of combining electro-enhanced chemotherapy with immunotherapy.<sup>124</sup> By the end of 2015, about 140 cancer treatment centres in Europe practiced electro-pulse-enhanced chemotherapy for local treatment of skin metastases in about 13,000 cancer patients. By combining DNA vaccination and cytokine-based immunotherapy to stimulate anti-tumour immunity in combination with electro-pulse enhanced chemotherapy, a systemic anti-metastatic response of clinical significance might occur.<sup>124</sup>

### **8.2.2 *EpECT* AND IMMUNOMODULATING ANTIBODIES (CTLA-4 AND PD-1)**

The use of the anti-CTLA-4 drug Ipilimumab and the anti-PD-1 drug Nivolumab in patients with advanced melanoma has been shown to improve progression-free survival and objective response. However, the use of these drugs might cause such severe toxicity that some patients discontinue the treatment.<sup>281</sup>

A retrospective multicentre program to study a combination of electro-pulse-enhanced chemotherapy according to the ESOPE protocol with 15000 IU Bleomycin, and immune therapy using either the anti-CTLA-4 drug Ipilimumab or the anti-PD-1 drugs Nivolumab or Pembrolizumab, involved 33 patients with distant cutaneous melanoma metastases.<sup>304</sup>

Table 8-4 shows the summary of responses of the various treatments derived from the published data. The local objective (OR) and weighted (WR<sub>4</sub>) responses of the combination are, however, much lower than those for *EpEChT* alone, as reviewed in Chapter 6. The systemic responses of the combination are quite low, and due to common progressive disease (PD), the weighted (WR<sub>4</sub>) response is strongly negative for Ipilimumab and close to zero for anti-PD-1. The toxicity of Ipilimumab in the combined treatment was found to be more severe than it was for treatment using Ipilimumab alone.<sup>304</sup>

A case of massive skin metastasis from melanoma that relapsed after repeated electro-pulse enhanced chemotherapy, received further treatments with checkpoint immune therapy. At 6 months after treatment with anti-PD-1 Nivolumab, the complete response appeared.<sup>305</sup>

Another case with a relapsed progressive mass of malignant melanoma was treated with electro-pulse-enhanced chemotherapy using an IGEA Cliniporator device through a hexagonal electrode on the progressive mass,

while on anti-PD-1 Nivolumab treatment. Complete response was achieved, with no evidence of disease at 4 years after the local recurrence.<sup>284</sup>

**Table 8-4a**

The response of combining electro-pulse-enhanced chemotherapy and checkpoint immune therapy.<sup>304</sup>

Drug	Response	No. patients	CR	PR	SD	PD
Ipilimumab	Local	28	0.18	0.50	0.11	0.21
Ipilimumab	Systemic	26	0.08	0.12	0.08	0.73
anti-PD-1	Local	5	0	0.09	0	0.06
anti-PD-1	Systemic	5	0	0.06	0	0.09

**Table 8-4b**

Summary of objective OR and weighted WR<sub>4</sub> response of combining electro-pulse-enhanced chemotherapy and checkpoint immune therapy.<sup>304</sup>

Drug	Response	No. patients	OR	WR <sub>4</sub>
Ipilimumab	Local	28	0.68	0,25
Ipilimumab	Systemic	26	0.19	-0,57
anti-PD-1	Local	5	0.09	-0,02
anti-PD-1	Systemic	5	0.06	-0,06

The contradictory results of the multicentre study and the case reports require more studies to examine the timing and dosage of immunomodulation antibodies in combination with electro-pulse therapy.

## 8.4 ELECTRO-PULSE ENHANCED RADIATION THERAPY “EPERT”

### 8.4.1 EPERT OF FIBROBLAST CELLS AND SUBCUTANEOUS IMPLANTED TUMOURS IN RAT

Radiation therapy alone is known to have limited therapeutic effects on brain tumours, in contrast to when it is used in combination with high voltage pulses. Effective killing of V-79 fibroblast cells remarkably occurred after combined exposure with 2Gy gamma-radiation and exponential shaped pulsed electric fields with an amplitude of 1600V/cm and a time-constant of 1ms at 1Hz repetition.<sup>128,77,129,130</sup>

The encouraging results from the experiments with V79-cells raised the idea of combining treatment of pulsed electric fields and gamma-radiation in Fischer rats with N32 tumours implanted on their flanks.

Each experiment was performed on four different groups with 6 animals in each:

- Untreated Controls (Ctrl);
- Radiation therapy only (RAD);
- Pulsed electric field only (PEF);
- Combined radiation therapy and pulsed electric field, (RAD + PEF)

Lead blocks surrounded the tumour to focus the radiation from the source at a distance (SSD) of 80 cm. A pulsed electric field applied by an isolated slide-calliper with plane electrodes (15x15 mm) was mounted on the blades enclosing the tumour. The tumour volume was estimated as an ellipsoid by measuring the length, width, and thickness with the slide-calliper.

A dramatic decrease of the tumour volume appeared on subcutaneously implanted tumours through the combed treatment of pulsed electric fields and gamma-radiation. Since the radiation dose used in the combined treatment is low (15-30Gy), it might be possible to treat recurrent tumours which already received a full dose with conventional radiation therapy. It is, thus, worthwhile to further explore this combined type of treatment. It might be of particular interest to apply high voltage impulses combined with brachy-therapy where the radioactive source (e.g. Iridium-192) can serve as an electrode.<sup>133</sup>

#### **8.4.2 EpEChT COMBINED WITH RADIATION THERAPY**

##### **EpECT of EAT tumours in mice with Cisplatin and RT**

Sersa and colleagues performed a study of combined modality therapy with Cisplatin and radiation using electroporation of subcutaneous Ehrlich ascites tumours (EATs) in CBA mice.<sup>134,135</sup> The mice were treated either by Cisplatin (CDDP), electric pulses (EP), or ionizing radiation (RT). Figure 8-1 displays the results of the single (CDDP 4 mg/kg body weight, EP 8 pulses of 1300V/cm and 0.1ms, RT 15 Gy single fraction), and combined treatments (EP+CDDP, EP+RT, RT+CDDP, and EP+CDDP+RT) recorded 100 days after treatment. These results show that delivery of Cisplatin into the cells through electroporation of tumours increases the radio-sensitizing effect of Cisplatin. However, the enhanced therapeutic effect may also be due to radiation-reduced tumour immunosuppression.

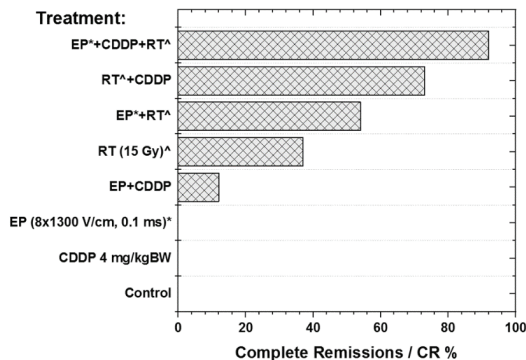


Figure 8-1  
Treatment results at  
100 days after the  
various types of  
treatment.<sup>134,135</sup>

### ***EpEChT* of LPB sarcoma in mice with Cisplatin and RT**

In a 2003 study, Kranjc and collaborators treated LPB murine sarcoma cells and tumours in mice, either with Cisplatin, electroporation or ionizing radiation alone, as well as combinations of these. In vitro response was determined by colony forming assay, while in vivo treatment effectiveness was determined by the values of the 50% tumour control dose (TCD50).

They found that exposure of cells in vitro to a combination of Cisplatin and electroporation increased accumulation of Cisplatin, and reduced tumour perfusion. In combination with ionizing radiation, the treatment effect was significantly enhanced by 60%, compared to irradiation only and by 40% compared to tumours treated with Cisplatin and irradiation.<sup>136</sup>

### ***EpEChT* of LPB sarcoma in mice with Bleomycin and RT**

In a 1995 study, Okunieff and colleagues studied the effect of EpECT using Bleomycin combined with radiation therapy on subcutaneous murine sarcoma LPB cells, syngeneic to the C57Bl/6 mice used in the experiments. Three minutes after intravenous injection of Bleomycin (BLM) in a volume of 150  $\mu$ l, they exposed a tumour to 8 electric pulses of 1300 V/cm with 0.1ms duration at 1 Hz, using plate electrodes placed on the skin overlying the tumour.<sup>137</sup>

Table 8-5 shows the values of the TCD50 for various combinations of treatment, and the relative tumour control (RTC), as opposed to radiotherapy only (RT). Neither treatment of animals with radiation alone (RT) nor the application of electric pulses or Bleomycin on the tumours before irradiation (EpE+RT and Bleo+RT) had any effect on the TCD50. However, the application of electric pulses with Bleomycin simultaneously combined with radiation therapy (EpEBleo+RT), decreased the TCD50

value of tumours by a factor of 1.9 compared to any other treatment. Hence, it is evident that radiation therapy of tumours significantly contributed to the therapeutic effect of EpEChT on tumours with BLM.<sup>138</sup>

**Table 8-5**

The values of the 50% tumour control dose (TCD<sub>50</sub>) and the relative tumour control for various combinations of treatment.<sup>138</sup>

Treatment	TCD <sub>50</sub>	SD	RTC
RT	23.1	0.3	1.0
EpE+RT	22.1	0.3	1.0
Bleo+RT	22.8	0.3	1.0
EpEBleo+RT	12.4	0.3	1.9

### EpECT using Bleomycin and RT

As shown in the previous paragraph, radiation therapy two-fold increased the therapeutic effect of electro-chemotherapy with Bleomycin.<sup>138</sup> Further studies in two murine tumour models with different histology showed that electro-pulse-enhanced chemotherapy before radiotherapy of the tumours and a single fraction of ionizing radiation of 10 Gy reduced the tumour volume by 98%, and five daily fractions of 2 Gy reduced the volume by 85%.<sup>139</sup>

The mechanism behind the effect of the combination of EpECT and RT is probably similar to the enhancement of the effect of tumour vaccine achieved by a single fraction of radiation therapy (RT).<sup>143,142,141,306</sup> The creation of a bolus of dead tumour cells as a result of the EpECT treatment is similar to the administration of a bolus of dead tumour cells that activates the tumour immune-suppression by an accumulation of Myeloid-derived suppressor cells (MDSC) in the tumour microenvironment. A single fraction of ionizing radiation of about 8 Gy deactivates the immune-suppressive effect over 10-14 days. If there are surviving tumour cells present after the treatment, the tumour starts growing again. Thus, a few repeated treatment regimens are required to achieve a complete cure.

The results of the combination of EpEChT and radiation therapy suggest a therapy regime with repeated treatments of EpEBleo. + RT (6-10 Gy) once a week until complete remission occurs. The absorbed dose and number of treatments required might vary with the histology of a tumour and from patient to patient. To bring this therapy regime to clinical practice is a challenge to the oncology community with clinical trials and efforts to standardize the treatment parameters.

## 8.5 IRREVERSIBLE ELECTROPORATION IRE

Irreversible electroporation (IRE) is a technique for the treatment of tumours with high-voltage (2-3 kV/cm) electrical pulses.<sup>307</sup> In liver and pancreatic cancer surgery, irreversible electroporation IRE is used as an alternative to the more established method of HF thermal ablation.

**Table 8-6**

Results from five clinical studies of liver cancer (CRLM: colorectal liver metastasis. HCC: hepatocellular carcinoma) treatment with IRE.

Reference	HCC	CRLM	Other	CR %	Com %	FT
	No.	No.	No.			
Cannon,2013 <sup>309</sup>	14	20	10	97	9	12
Cheung,2013 <sup>310</sup>	18			67	34	18
Kingham,2012 <sup>311</sup>	11	21	5	96	14	6
Scheffer,2014 <sup>312</sup>		10		90	0	1
Sugimoto,2015 <sup>313</sup>	6			83	0	9
Average $\pm$ SD				87 $\pm$ 12	11 $\pm$ 11	9

CRLM: colorectal liver metastasis; HCC: hepatocellular carcinoma

CR: Primary efficiency, Com: Complications, FT: Followup time in months

The IRE method has similar treatment results to thermal ablation, but has the advantage of avoiding severe thermal complications.<sup>308</sup>

Table 8-6 shows that the mean total remissions in five clinical studies of liver cancer treatment with IRE are 87 $\pm$ 12%.<sup>309,310,311,312,313</sup> The levels of local recurrence and minimal complications are both, on average, about 11% at a follow-up time of around 9 months.

IRE treatment of pancreatic cancer results in increased survival time but with more complications compared to the treatment of liver cancer. Table 8-7 shows the results of 5 clinical studies,<sup>314,315,316,317,318,319</sup> and one single patient.<sup>314</sup> Despite the risk of significant complications, the IRE is considered to be a possible alternative for the treatment of pancreatic cancer.<sup>319</sup>

However, clinical randomized studies and development of treatment protocols are required to establish the method in clinical routine.<sup>308</sup>



**Table 8-7**

Results from five clinical studies of pancreatic treatment with IRE.

Author <sup>Reference</sup>	Patient No.	CR	Com. No.	FT
		%		
Bagla,2012 <sup>314</sup>	1	100	0	6
Martin,2012 <sup>315</sup>	27	96	4	3
Martin,2013 <sup>316</sup>	54	94	32	12
Narayanan,2012 <sup>317</sup>	14	100	4	14
Paiella,2015 <sup>318</sup>	10	100	3	15
Sugimoto, 2018 <sup>319</sup>	8	NR	6/8	12 <sup>*</sup> )

CR: Primary efficiency, Com: Complications FT: Follow-up time in months  
 NR: not reported, <sup>\*</sup>)Progression free survival time

Sano reported in 2018 of an *in vitro* experiment on cell cultures, combining IRE treatment with 500 ns pulses and radiation therapy in single dose fractions of 2 or 20Gy.<sup>320</sup> IRE and radiation therapy (RT) appear to induce different delayed cell death mechanisms. After 14 days, the combinatorial therapy resulted in the lowest cell survival. These results are in agreement with the findings reported above (8.4), and indicate an *in vivo* antitumor efficacy of combined H-FIRE and RT as well.<sup>320</sup>

## 8.6 NANOSECOND HIGH VOLTAGE ELECTRIC PULSES

High voltage electric pulses of nanosecond (1ns =10<sup>-9</sup> s) pulse length interact with several biological targets, such as plasma membranes, intracellular structures, calcium ions, cell nuclei, and mitochondria. A review of the effects of ns-pulses on eukaryotic cells summarizes and analyses the published data for assessing the use of ns-pulses in electroporation therapy.<sup>321</sup>

A recent study of the effect of ns-pulses on the inhibition of oral cancer growth *in vitro* and *in vivo* revealed their potential use in oral cancer therapy.<sup>322</sup> However, the most intriguing effect of ns-pulse treatment is the eradicating of local breast cancer while reducing distant metastases recently demonstrated by Guo (2018).<sup>323</sup> A single ns-pulse treatment with 600 pulses, with a field strength of 50 kV/cm and 100ns pulse length at 1Hz, results in complete regression of a poorly immunogenic, metastatic 4T1-Luc mouse mammary carcinoma. Secondary tumour cell challenge demonstrated a vaccine-like effect of the ns-pulse treatment, which suggests a potent antitumor immunity effect on distant metastases in addition to a local tumour eradication.<sup>323</sup>

## **8.7 CONCLUSION *EpECT***

In summary, there are great clinical potentials in applying electro-pulse treatment to enhance the effect of established cancer therapy regimes.

### **8.7.1 CHEMOTHERAPY *EpEChT***

Electro-pulse-enhanced chemotherapy (EpEChT), as reviewed in Chapter 6, is already clinically established in the treatment of tumours. However, with further experience, and with improvements such as the development of new drugs, pulse-sequences and protocols, we should be able to approve the EpEChT method treatment for primary tumours.

### **8.7.2 RADIATION THERAPY *EpERT***

Preclinical studies indicate excessive potential in a combination of electro-pulse treatment and radiation therapy.<sup>142,143</sup>

A few clinical studies have been performed with the combination of electro-pulse-enhanced chemotherapy and radiation therapy, with great success.<sup>138,139</sup>

### **8.7.3 IMMUNE THERAPY *EpEIT***

DNA vaccination and cytokine-based immunotherapy stimulate anti-tumour immunity which, in combination with electro-pulse-enhanced chemotherapy, creates a systemic anti-metastatic response with vast clinical potential. The use of EpECT in combination with immune-modulating antibodies (CTLA-4 and PD-1), however, results in clinical outcomes which require more studies to examine the timing and dosage. In summary, there is great clinical potential in applying electro-pulse treatment to enhance the effect of established cancer therapy regimes. However, the best regime appears to be the combination of electro-pulse enhanced immunotherapy combined with a single fraction of radiation therapy.<sup>142,141,306,143</sup>

## REFERENCES

1. Sale AJH, Hamilton WA. Effects of high electric fields on microorganisms .1. Killing of bacteria and yeasts. *Biochimica Et Biophysica Acta*. 1967;148(3):781-&.
2. Sale AJH, Hamilton WA. Effects of high electric fields on microorganisms .3. Lysis of erythrocytes and protoplasts. *Biochimica Et Biophysica Acta*. 1968;163(1):37-&.
3. Neumann E, Rosenheck K. Permeability changes induced by electric impulses in vesicular membranes. *Journal of Membrane Biology*. 1972;10(3-4):279-90.
4. Zimmermann U, Schulz J, Pilwat G. transcellular ion flow in escherichia-coli b and electrical sizing of bacterias. *Biophysical Journal*. 1973;13(10):1005-13.
5. Zimmermann U, Pilwat G, Riemann F. Dielectric breakdown of cell membranes *Biophysical Journal* 1974;14,(11):881-99.
6. Rosenheck K, Lindner P, Pecht I. Effect of electric-fields on light-scattering and fluorescence of chromaffin granules. *Journal of Membrane Biology*. 1975;20(1-2):1-12.
7. Kinoshita K, Tsong TY. Voltage-induced pore formation and hemolysis of human erythrocytes. *Biochimica Et Biophysica Acta*. 1977;471(2):227-42.
8. Lindner P, Neumann E, Rosenheck K. Kinetics of permeability changes induced by electric impulses in chromaffin granules. *Journal of Membrane Biology*. 1977;32(3-4):231-54.
9. Benz R, Zimmermann U. Pulse-length dependence of the electrical breakdown in lipid bilayer-membranes. *Biochimica Et Biophysica Acta*. 1980;597(3):637-42.
10. Zimmermann U, Vienken J, Pilwat G. Development of drug carrier systems - electrical-field induced effects in cell-membranes. *Bioelectrochemistry and Bioenergetics*. 1980;7(3):553-74.
11. Neumann E, Gerisch G, Opatz K. Cell-fusion induced by high electric impulses applied to dictyostelium. *Naturwissenschaften*. 1980;67(8):414-5.
12. Scheurich P, Zimmermann U, Mischel M, Lamprecht I. Membrane-fusion and deformation of red-blood-cells by electric-fields.

- Zeitschrift Fur Naturforschung Section C-a Journal of Biosciences. 1980;35(11-1):1081-5.
13. Richter HP, Scheurich P, Zimmermann U. Electric field-induced fusion of sea-urchin eggs. *Development Growth & Differentiation*. 1981;23(5):479-86.
  14. Scheurich P, Zimmermann U. Giant human-erythrocytes by electric-field-induced cell-to-cell fusion. *Naturwissenschaften*. 1981;68(1):45-6.
  15. Scheurich P, Zimmermann U, Schnabl H. Electrically stimulated fusion of different plant-cell protoplasts - mesophyll cell and guard-cell protoplasts of vicia-faba. *Plant Physiology*. 1981;67(4):849-53.
  16. Zimmermann U, Scheurich P. Fusion of avena-sativa mesophyll cell protoplasts by electrical breakdown. *Biochimica Et Biophysica Acta*. 1981;641(1):160-5.
  17. Zimmermann U, Scheurich P. High-frequency fusion of plant-protoplasts by electric-fields. *Planta*. 1981;151(1):26-32.
  18. Zimmermann U, Scheurich P, Pilwat G, Benz R. Cells with manipulated functions - new perspectives for cell biology, medicine, and technology. *Angewandte Chemie-International Edition in English*. 1981;20(4):325-44.
  19. Zimmermann U, Friedrich U, Mussauer H, Gessner P, Hamel K, Sukhoruhov V. Electromanipulation of mammalian cells: Fundamentals and application. *Ieee Transactions on Plasma Science*. 2000;28(1):72-82.
  20. Weber H, Forster W, Berg H, Jacob HE. Parasexual hybridization of yeasts by electric-field stimulated fusion of protoplasts. *Current Genetics*. 1981;4(2):165-6.
  21. Weber H, Forster W, Jacob HE, Berg H. Microbiological implications of electric-field effects .3. Stimulation of yeast protoplast fusion by electric-field pulses. *Zeitschrift Fur Allgemeine Mikrobiologie*. 1981;21(7):555-62.
  22. Wong TK, Nicolau C, Hofschneider PH. Appearance of beta-lactamase activity in animal-cells upon liposome-mediated gene-transfer. *Gene*. 1980;10(2):87-94.
  23. Neumann E, Schaefferridder M, Wang Y, Hofschneider PH. Gene-transfer into mouse lyoma cells by electroporation in high electric-fields. *Embo Journal*. 1982;1(7):841-5.
  24. Neumann E. Membrane electroporation and direct gene-transfer. . *Bioelectrochemistry and Bioenergetics*. 1992;28(1-2):247-67.

25. Lo MMS, Tsong TY, Conrad MK, Strittmatter SM, Hester LD, Snyder SH. Monoclonal-antibody production by receptor-mediated electrically induced cell-fusion. *Nature*. 1984;310(5980):792-4.
26. Okino M, Mohri H. Effects of a high-voltage electrical impulse and an anticancer drug on in vivo growing tumors. *JpnJCancer Res.* 1987;78,(12):1319-21.
27. Okino M, Tomie H, Kanesada H, Marumoto M, Esato K, Suzuki H. Optimal electric conditions in electrical impulse chemotherapy. *Japanese Journal of Cancer Research*. 1992;83(10):1095-101.
28. Mir LM, Belehradek M, Domenge C, Orlowski S, Poddevin B, Belehradek J, Schwaab G, Luboinski B, Paoletti C. Electrochemotherapy, A Novel Antitumor Treatment - 1st Clinical-Trial. *Comptes Rendus De L Academie Des Sciences Serie Iii-Sciences De La Vie-Life Sciences*. 1991;313(13):613-8.
29. Nordenstrom BEW. *Biologically Closed Electric Circuits: Clinical, Experimental and Theoretical Evidence for an Additional Circulatory System* Stockholm, Sweden: Nordic Medical Publications; First edition 1983.
30. Heller R, Jaroszeski M, Glass F, Puleo C, Deconti R, Reintgen D, Gilbert R. Enhanced delivery of bleomycin using electric fields for the effective treatment of skin malignancies. *Proceedings of the American Association for Cancer Research Annual Meeting*. 1997;38(0):259-.
31. Mir LM, Glass LF, Sersa G, Teissie J, Domenge C, Miklavcic D, Jaroszeski MJ, Orlowski S, Reintgen DS, Rudolf Z, Belehradek M, Gilbert R, Rols MP, Belehradek J, Bachaud JM, DeConti R, Stabuc B, Cemazar M, Coninx P, Heller R. Effective treatment of cutaneous and subcutaneous malignant tumours by electrochemotherapy. *British Journal of Cancer*. 1998;77(12):2336-42.
32. Heller R, Jaroszeski MJ, Reintgen DS, Puleo CA, DeConti RC, Gilbert RA, Glass LF. Treatment of cutaneous and subcutaneous tumors with electrochemotherapy using intralesional bleomycin. *Cancer*. 1998;83(1):148-57.
33. Hyacinthe M, Jaroszeski MJ, Dang VV, Coppola D, Karl RC, Gilbert RA, Heller R. Electrically enhanced drug delivery for the treatment of soft tissue sarcoma. *Cancer*. 1999;85(2):409-17.
34. Salford LG, Persson BRR, Brun A, Ceberg CP, Kongstad PC, Mir LM. A new Brain Tumour Therapy Combining Bleomycin with in vivo Electroporation. *Biochemical and Biophysical Research Communications*. 1993;194(2):938-43.

35. Jaroszeski M, Gilbert R, Dang V, Hickey J, Heller R. In vivo electroporation for drug delivery to rat hepatomas. Proceedings of the American Association for Cancer Research Annual Meeting. 1997;38(0):259-60.
36. Jaroszeski MJ, Gilbert RA, Heller R. In vivo antitumor effects of electrochemotherapy in a hepatoma model. *Biochimica Et Biophysica Acta-General Subjects*. 1997;1334(1):15-8.
37. Chazal M, Benchimol D, Bague P, Pierrefite V, Milano G, & , Bourgeon A. Treatment of hepatic metastases of colorectal cancer by electrochemotherapy: an experimental study in the rat 1998;124,(3):536-40.
38. Jaroszeski MJ, Illingworth P, Pottinger C, Hyacinthe M, Heller R. Electrically mediated drug delivery for treating subcutaneous and orthotopic pancreatic adenocarcinoma in a hamster model. *Anticancer Research*. 1999;19(2A):989-94.
39. Kuksin D, ,, Chan LL. Analyzing NCI-60 Cancer Cell Lines. <http://www.nexcelom.com/Applications/Cancer-Cells.html>. 2013.
40. Dolfi SC, Chan LL, Qiu J, . ea. The metabolic demands of cancer cells are coupled to their size and protein synthesis rates. *Cancer & Metabolism*. 2013;1(1).
41. Schwan HP. Biophysics of the interaction of electromagnetic energy with cells and membranes. . In: Grandolfo M, Michaelson SM, Rindi A, editors. *Biological Effects and Dosimetry of Nonionizing Radiation* New York,: Plenum Press; 1983. p. 213-31.
42. Grosse C, Schwan HP. Cellular membrane-potentials induced by alternating-fields. *Biophysical Journal*. 1992;63(6):1632-42.
43. Haemmerich D, Schutt DJ, Wright AW, Webster JG, Mahvi DM. Electrical conductivity measurement of excised human metastatic liver tumours before and after thermal ablation. *Physiological Measurement*. 2009;30(5):459-66.
44. Jossinet J. Variability of impedivity in normal and pathological breast tissue. 1996;- 34(- 5):- 350.
45. Marszalek P, Liu DS, Tsong TY. Schwan equation and transmembrane potential induced by alternating electric field. *Biophysical Journal*. 1990;58(4):1053-8.
46. Chen C, Evans JA, Robinson MP, Smye SW, O'Toole P. Measurement of the efficiency of cell membrane electroporation using pulsed ac fields. *Physics in Medicine and Biology*. 2008;53(17):4747-57.
47. Garcia-Sanchez T, Merla C, Fontaine J, Muscat A, Mir LM. Sine wave electroporation reveals the frequency-dependent

- response of the biological membranes. *Biochimica et biophysica acta*. 2018;1860(5):1022-34.
48. Weaver JC. Molecular basis for cell membrane electroporation. In: Lee RC, Capelli-Schellpfeffer M, Kelley KM, editors. *Annals of the New York Academy of Sciences; Electrical injury: A multidisciplinary approach to therapy, prevention, and rehabilitation*. Annals of the New York Academy of Sciences. 7201994. p. 141-52.
49. Weaver JC, Chizmadzhev YA. Theory of electroporation: A review. *Bioelectrochemistry and Bioenergetics*. 1996;41(2):135-60.
50. Weaver JC, Smith KC, Esser AT, Son RS, Gowrishankar TR. A brief overview of electroporation pulse strength-duration space: A region where additional intracellular effects are expected. *Bioelectrochemistry*. 2012;87:236-43.
51. Neu JC, Krassowska W. Asymptotic model of electroporation. *Physical Review E*. 1999;59(3):3471-82.
52. DeBruin KA, Krassowska W. Modeling electroporation in a single cell. I. Effects of field strength and rest potential. *Biophysical Journal*. 1999;77(3):1213-24.
53. Smith KC, Neu JC, Krassowska W. Model of creation and evolution of stable electropores for DNA delivery. *Biophysical Journal*. 2004;86(5):2813-26.
54. Neu JC, Smith KC, Krassowska W. Electrical energy required to form large conducting pores. *Bioelectrochemistry*. 2003;60(1-2):107-14.
55. Krassowska W, Filev PD. Modeling Electroporation in a Single Cell. *Biophysical Journal*. 2007;92(2):404-17.
56. Persson BRR. Exploration of Electro-Enhanced-Chemotherapy II. Uptake of radioactive tracer in rat Muscle tissue at 6 and 24 hours after applied electric pulses of 1000 V/cm field-strength, 100  $\mu$ s pulse-length, and various number of pulses. *Acta Scientiarum Lundsensia*, ISSN 1651-5013. 2017;2017(003):1-21.
57. Neumann E, Toensing K, Kakorin S, Budde P, Frey J. Mechanism of electroporative dye uptake by mouse B cells. *Biophysical Journal*. 1998;74(1):98-108.
58. Persson BRR. Exploration of Electro-Enhanced-Chemotherapy I. Exploration of the uptake of radioactive tracer in rat Muscle tissue of 2 - 12 applied electric pulses of 600;800;1000;1200 V/cm field-strength, 100;250;500  $\mu$ s pulse-length, and 2,4,6,8,10,12 number of pulses. *Acta Scientiarum Lundsensia*, ISSN 1651-5013. 2017;2017(002):1-20.

59. Tanforde C. *Physical Chemistry of Macromolecules*. New York: John Wiley, ; 1961.
60. Nishida K, Ando Y, Kawamura H. Diffusion coefficients of anticancer drugs and compounds having a similar structure at 30 °C. *Colloid and Polymer Science*. 1983;261(1):70-3.
61. Groselj A, Krzan M, Kosjek T, Bosnjak M, Sersa G, Cemazar M. Bleomycin pharmacokinetics of bolus bleomycin dose in elderly cancer patients treated with electrochemotherapy. *Cancer Chemotherapy and Pharmacology*. 2016;77(5):939-47.
62. Glaser RW, Leikin SL, Chernomordik LV, Pastushenko VF, Sokirko AI. Reversible electrical breakdown of lipid bilayers - formation and evolution of pores. *Biochimica Et Biophysica Acta*. 1988;940(2): 275-87.
63. Neumann E, Sowers AE, Jordan C. *Electroporation and Electrofusion in Cell Biology*:. New York: Plenum Press; 1989.
64. Jeong WC, Meng ZJ, Kim HJ, Kwon OI, Woo EJ. Experimental Validations of In Vivo Human Musculoskeletal Tissue Conductivity Images Using MR-Based Electrical Impedance Tomography. *Bioelectromagnetics*. 2014;35(5):363-72.
65. Gabriel C, Peyman A, Grant EH. Electrical conductivity of tissue at frequencies below 1 MHz. *Physics in Medicine and Biology*. 2009;54(16):4863-78.
66. Gabriel C, Gabriel S, Corthout E. The dielectric properties of biological tissues .1. Literature survey. *Physics in Medicine and Biology*. 1996;41(11):2231-49.
67. Andreuccetti D, Fossi R. Dielectric properties of human tissues: definitions, parametric model, computing codes. Firenze, Italy: Istituto di Ricerca Sulle Onde Elettromagnetiche, Consiglio Nazionale delle Ricerche. IROE-CNR; 2000.
68. Gabriel S, Lau RW, Gabriel C. The dielectric properties of biological tissues .2. Measurements in the frequency range 10 Hz to 20 GHz. *Physics in Medicine and Biology*. 1996;41(11):2251-69.
69. Gabriel S, Lau RW, Gabriel C. The dielectric properties of biological tissues .3. Parametric models for the dielectric spectrum of tissues. *Physics in Medicine and Biology*. 1996;41(11):2271-93.
70. Gabriel C. Compilation of the dielectric properties of body tissues at RF and microwave frequencies. Report N.AL/OE-TR- 1996-0037. Radiofrequency Radiation Division, Brooks Air Force Base, Texas (USA), ; 1996. Contract No.: N.AL/OE-TR- 1996-0037,.



71. Cole KS, Cole RH. Dispersion and absorption in dielectrics I. Alternating current characteristics. *Journal of Chemical Physics*. 1941;9(4):341-51.
72. Andreuccetti D, Fossi: R. Proprietà dielettriche dei tessuti umani: definizioni, modello parametrico, codici di calcolo, Report N.TR/ICEMM/13.00, IFAC-CNR, Firenze (I), . 2000.
73. Persson BRR. Application of High Voltage Impulses in vivo for Tumor Therapy and Gene Therapy. In: Lin JC, editor. *Advances in Electromagnetic Fields In Living system*. 3: Kluwer Academic/Plenum Published,; 2000. p. 121-46.
74. Hasgall PA, Di Gennaro F, Baumgartner C, Neufeld E, Gosselin MC, Payne D, Klingenböck A, Kuster N. IT'IS Database for thermal and electromagnetic parameters of biological tissues, Version 3.0. In: [www.itis.ethz.ch/database](http://www.itis.ethz.ch/database), editor. ETH, Zürich: IT'IS Foundation; 2015.
75. Persson BRR. QF Modelling of Electro-Pulse-Enhanced-Cancer-Therapy. *Acta Scientiarum Lundensia*. 2019;2019(001):1-16.
76. Engstrom PE, Ivarsson K, Tranberg KG, Stenram U, Salford LG, Persson BRR. Electrically mediated drug delivery for treatment of an adenocarcinoma transplanted into rat liver. *Anticancer Research*. 2001;21(3B):1817-22.
77. Engstrom PE, Persson BRR, Salford LG. Effect of high voltage electrical pulses on subcutaneous glioma tumours on rats. *Bioelectrochemistry and Bioenergetics*. 1998;47(1):163-6.
78. Engstrom PE, Persson BRR, Salford LG. Dynamic gamma camera studies of In-111-bleomycin complex in normal and glioma bearing rats after in vivo electropermeabilization using exponential high-voltage pulses. *Bioelectrochemistry and Bioenergetics*. 1998;46(2): 241-8.
79. Engstrom P, Salford LG, Persson BR. Distribution of bleomycin in a rat model. *Methods in molecular medicine*. 2000;37:285-92.
80. Engström PE, Persson RBR, Brun A, Salford LG, Engström PE. A new antitumor treatment combining radiation and electric pulses. PhD Thesis. 1999-12-17. Lund: Lund University, Radiation Physics Dept, S-221 85 LUND, Sweden; 1999. p. 1-15.
81. Kempf V, Persson RBR. <sup>99m</sup>Tc-DTPA(Sn) dry-kit preparation - quality-control and clearance studies. *Nuclear Medicine-Nuklearmedizin*. 1975;13(4):389-99.
82. Wold HOA. Soft modelling: the basic design and some extensions. In: Jöreskog KG, Wold HOA, editors. *Systems under indirect observation, Part II*. Amsterdam: . Northholland; 1982. p. 1-5.

83. Wold S, Martens H, Wold H. The multivariate calibration-problem in chemistry solved by the PLS method. *Lecture Notes in Mathematics*. 1983;973:286-93.
84. Wold S, Kettaneh N, Tjessem K. Hierarchical multiblock PLS and PC models for easier model interpretation and as an alternative to variable selection. *Journal of Chemometrics*. 1996;10(5-6):463-82.
85. Wold S, Sjostrom M, Eriksson L. PLS-regression: a basic tool of chemometrics. *Chemometrics and Intelligent Laboratory Systems*. 2001;58(2):109-30.
86. Mir LM, Banoun H, Paoletti C. Introduction of definite amounts of nonpermeant molecules into living cells after electropermeabilization: Direct access to the cytosol. *Experimental Cell Research*. 1988;175(1):15-25.
87. Orłowski S, Belehradek J, Paoletti C, Mir L. Transient electropermeabilization of cells in culture. Increase of the cytotoxicity of anticancer drugs. *BiochemPharmacol*. 1988;37(24):4727-33.
88. Orłowski S, Belehradek J, Paoletti C, Mir LM. Transient electropermeabilization of cells in culture - increase of the cytotoxicity of anticancer drugs. *Biochemical Pharmacology*. 1988;37(24):4727-33.
89. Orłowski S, Belehradek JJ, Paoletti C, Mir LM. Electropermeabilization of Living Cells. Adolphe, M And A Guillouzo. *Colloque INSERM*1988. p. 255.
90. Engstrom PE, Persson BRR, Salford LG. Studies of in vivo electropermeabilization by gamma camera measurements of Tc-99m-DTPA. *Biochimica Et Biophysica Acta-General Subjects*. 1999;1473(2-3):321-8.
91. Grafstrom G, Engstrom P, Salford LG, Persson BRR. Tc-99m-DTPA uptake and electrical impedance measurements in verification of in vivo electropermeabilization efficiency in rat muscle. *Cancer Biotherapy and Radiopharmaceuticals*. 2006;21(6):623-35.
92. Gehl J, Mir LM. Determination of optimal parameters for in vivo gene transfer by electroporation, using a rapid in vivo test for cell permeabilization. *Biochemical and Biophysical Research Communications*. 1999;261(2):377-80.
93. Mir LM, Bureau MF, Gehl J, Rangara R, Rouy D, Caillaud JM, Delaere P, Branellec D, Schwartz B, Scherman D. High-efficiency gene transfer into skeletal muscle mediated by electric pulses. *Proceedings of the National Academy of Sciences of the United States of America*. 1999;96(8):4262-7.

94. Belehraddek J, Orlowski S, Poddevin B, Paoletti C, Mir LM. Electrochemotherapy of spontaneous mammary-tumors in mice. *European Journal of Cancer*. 1991;27(1):73-6.
95. Heller R, Jaroszeski M, Deconti R, Reintgen D, Gilbert R, Glass F. Electrochemotherapy as a treatment for melanoma and other cutaneous malignancies. *Melanoma Research*. 1997;7(SUPPL. 1):S32-S.
96. Heller R, Jaroszeski M, Perrott R, Messina J, Gilbert R. Effective treatment of B16 melanoma by direct delivery of bleomycin using electrochemotherapy. *Melanoma Research*. 1997;7(1):10-8.
97. Mir LM, Devauchelle P, Quintin-Colonna F, Delisle F, Doliger S, Fradelizi D, Belehraddek J, Orlowski S. First clinical trial of cat soft-tissue sarcomas treatment by electrochemotherapy. *British Journal of Cancer*. 1997;76(12):1617-22.
98. Mir LM, Devauchelle P, Quintin-Colonna F, Delisle F, Doliger S, Fradelizi D, Orlowski JJBaS. First clinical trial of cat soft-tissue sarcomas treatment by electrochemotherapy. *British Journal of Cancer*. 1997;76(12):1617-22.
99. Kubota Y, Nakada T, Yanai H, Itoh K, Sasagawa I, Kawai K. Histological evaluation of the effects of electroporabilization after administration of bleomycin on bladder cancer in the rat. *European Urology*. 1998;34(4):372-6.
100. Kubota Y, Nakada T, Yanai H, Kakizaki H, Sasagawa I, Watanabe M. Electroporabilization in bladder cancer chemotherapy. *Cancer Chemotherapy and Pharmacology*. 1996;39(1-2):67-70.
101. Ceberg CP, Brun A, Mir LM, Persson BRR, Salford LG. Enhanced boron uptake in RG 2 rat gliomas by electroporabilization in vivo - a new possibility in boron neutron capture therapy. *Anti-Cancer Drugs*. 1994;5:463-6.
102. Jaroszeski MJ, Gilbert R, Perrott R, Heller R. Enhanced effects of multiple treatment electrochemotherapy. *Melanoma Research*. 1996;6(6):427-33.
103. Mir LM, Orlowski S, Belehraddek J, Paoletti C. Electrochemotherapy Potentiation of Antitumor Effect of Bleomycin by local electric pulses. *European Journal of Cancer*. 1991;27(1):68-72.
104. Donelli MG, Zucchetti M, D'Incalci M. Do anticancer agents reach the tumor target in the human brain? *Cancer ChemotherPharmacol*. 1992;30(4):251-60.
105. Hou DY, Hoch H, Johnston GS, Tsou KC, Farkas RJ, Miller EE. Use of <sup>111</sup>In-bleomycin for combining radiotherapy and chemotherapy on glioma-bearing mice. *J Surg Oncol*. 1985;29(2):71-7.

106. Hou DY, Hoch H, Johnston GS, Tsou KC, Jones AE, Farkas RJ, Miller EE. A new <sup>111</sup>In-bleomycin complex for tumor imaging: preparation, stability, and distribution in glioma-bearing mice. *J Surg Oncol.* 1984;25,( 3):168-75.
107. Hou DY, Hoch H, Johnston GS, Tsou KC, Jones AE, Farkas RJ, Miller EE, Larson SM. A new <sup>111</sup>In-bleomycin complex for combined radiotherapy and chemotherapy. *J Surg Oncol.* 1985; 29(2):91-8.
108. Hou DY, Hoch H, J, ohnston GS, Tsou KC, Jones AE, Miller EE, Larson SM. A new tumor imaging agent--<sup>111</sup>In-bleomycin complex. Comparison with <sup>67</sup>Ga-citrate and <sup>57</sup>Co-bleomycin in tumor-bearing animals. *J Surg Oncol.* 1984; 27(3):189-95.
109. Kuriyama S, Matsumoto M, Mitoro A, Tsujinoue H, Toyokawa Y, Nakatani T, Yamazaki M, Okamoto S, Fukui H. Electrochemotherapy against colorectal carcinoma: comparison of in vitro cytotoxicity of 5-fluorouracil, cisplatin and bleomycin. *Int J Oncol* 1999;15(1):89-94.
110. Ramirez LH, Orłowski S, An D, Bindoula G, Dzodic R, Ardouin P, Bognel C, Belehradek J, Munck JN, Mir LM. Electrochemotherapy on liver tumours in rabbits. *British Journal of Cancer.* 1998;77(12):2104-11.
111. Kambe M, Arita D, Kikuchi H, Funato T, Tezuka F, Gamo M, Murakawa Y, Kanamaru R. Enhancing the effect of anticancer drugs against the colorectal cancer cell line with electroporation. *Tohoku Journal of Experimental Medicine.* 1996;180(2):161-71.
112. Kambe M, Arita D, Kikuchi H, Funato T, Tezuka F, Gamo M, Murakawa Y, Kanamaru R. Enhancement of the efficacy of anticancer drugs with electroporation: Successful electrochemotherapy against gastric cancer cell lines in vivo and in vitro. *International Journal of Clinical Oncology.* 1997;2(2):111-7.
113. Cemazar M, Sersa G, Miklavcic D. Electrochemotherapy with cisplatin in the treatment of tumor cells resistant to cisplatin. *Anticancer Research.* 1998;18(6A):4463-6.
114. Cemazar M, Milacic R, Miklavcic D, Dolzan V, Sersa G. Intratumoral cisplatin administration in electrochemotherapy: antitumor effectiveness, sequence dependence and platinum content. *Anti-Cancer Drugs.* 1998;9(6):525-30.
115. Ursic K, Kos S, Kamensek U, Cemazar M, Scancar J, Bucek S, Kranjc S, Staresinic B, Sersa G. Comparable effectiveness and immunomodulatory actions of oxaliplatin and cisplatin in

- electrochemotherapy of murine melanoma. *Bioelectrochemistry*. 2018;119:161-71.
116. Sistigu A, Viaud S, Chaput N, Bracci L, Proietti E, Zitvogel L. Immunomodulatory effects of cyclophosphamide and implementations for vaccine design. *Seminars in Immunopathology*. 2011;33(4):369-83.
  117. Xu BQ, Sun Y, Zhao JF, Tong ZG, Yuan QP, Gong YY, Sun Q, Wang SX, *ieee*. The study on the treatment of mice inoculated S-180 with electrochemotherapy2007. 495-8 p.
  118. Jazowiecka-Rakus J, Jarosz M, Szala S. Combination of vasostatin gene therapy with cyclophosphamide inhibits growth of B16(F10) melanoma tumours. *Acta Biochimica Polonica*. 2006;53(1):199-202.
  119. Mir LM, Orlowski S, Poddevin B, Belehradek J, Jr. Electrochemotherapy tumor treatment is improved by interleukin-2 stimulation of the host's defenses. *European cytokine network*. 1992;3(3):331-4.
  120. Mir LM, Roth C, Orlowski S, Quintincolonna F, Fradelizi D, Belehradek J, Kourilsky P. Systemic antitumor effects of electrochemotherapy combined with histoincompatible cells secreting Interleukin-2. *Journal of Immunotherapy*. 1995;17(1):30-8.
  121. Sersa G, Kotnik V, Cemazar M, Miklavcic D, Kotnik A. Electrochemotherapy with bleomycin in SA-1 tumor-bearing mice - Natural resistance and immune responsiveness. *Anti-Cancer Drugs*. 1996;7(7):785-91.
  122. Orlowski S, An DJ, Belehradek J, Mir LM. Antimetastatic effects of electrochemotherapy and of histoincompatible interleukin-2-secreting cells in the murine Lewis lung tumor. *Anti-Cancer Drugs*. 1998;9(6):551-6.
  123. Calvet CY, Famin D, Andre FM, Mir LM. Electrochemotherapy with bleomycin induces hallmarks of immunogenic cell death in murine colon cancer cells. *Oncoimmunology*. 2014;3(4).
  124. Calvet CY, Mir LM. The promising alliance of anti-cancer electrochemotherapy with immunotherapy. *Cancer and Metastasis Reviews*. 2016;35(2):165-77.
  125. Siesjö P, Visse E, Lindvall M, Salford LG, Sjögren H-O. Immunization with mutagen-treated (tum-) cells causes rejection of nonimmunogenic rat glioma isografts. *Cancer Immunol Immunother*. 1993;37:67-74.
  126. Engström P, Bengt Widegren\* B, Persson BRR. Electro Enhanced Gen Tumour Therapy with IL-18 and IFN $\gamma$  transfected tumour cell

- vaccine..\*In memory of Beng Widegren □2014, ISSN 1651-5013. Acta Scientiarum Lundensia ISSN 1651-5013. 2018; 2018(005):1-x.
127. Persson BRR, Baureus Koch CB, Grafstrom G, Engstrom PE, Salford LG. A model for evaluating therapeutic response of combined cancer treatment modalities: Applied to treatment of subcutaneously implanted brain tumors (N32 and N29) in Fischer rats with pulsed electric fields (PEF) and (CO)-C-60-gamma radiation (RT). *Technology in Cancer Research & Treatment*. 2003;2(5):459-70.
  128. Danfelter M, Engstrom P, Persson BRR, Salford LG. Effect of high voltage pulses on survival of Chinese hamster V79 lung fibroblast cells. *Bioelectrochemistry and Bioenergetics*. 1998;47(1):97-101.
  129. Persson B, inventor; Bertil Persson, assignee. Anordningar för elektrodynamisk strålterapi av tumörsjukdomar ( in swedish). Sweden patent C3 509 204. 1998 19961001.
  130. Persson B, inventor; Bertil Persson, assignee. A Method and an apparatus for treating tumoural diseases (cancer). International patent WO98/14238. 1998 Apr. 9, 1998.
  131. Engstrom PE, Persson BRR, Brun A, Salford LG. A new antitumour treatment combining radiation and electric pulses. *Anticancer Research*. 2001;21(3B):1809-15.
  132. Engström P, Danfelter M, Persson BRR, Salford LG. Effect of in vivo electroporation with exponential pulses, as single treatment of subcutaneously implanted rat gliomas. EANO, Verseailles, Sept 12-17, 1998. 1998.
  133. Persson BRR. Treating tumoral diseases (cancer) with a combination of ionizing radiation and pulsed electric fields. *Acta Scientiarum Lundensia*. 2011;2011-001(001):1-20.
  134. Sersa G, Cemazar M, Rudolf Z, Fras AP. Adenocarcinoma skin metastases treated by electrochemotherapy with cisplatin combined with radiation. . *Radiol Oncol*. 1999;33(291–296).
  135. Sersa G, Kranjc S, Cemazar M. Improvement of combined modality therapy with cisplatin and radiation using electroporation of tumors. *International Journal of Radiation Oncology Biology Physics*. 2000;46(4):1037-41.
  136. Kranjc S, Cemazar M, Grosel A, Scancar J, Sersa G. Electroporation of LPB sarcoma cells in vitro and tumors in vivo increases the radiosensitizing effect of cisplatin. *Anticancer Research*. 2003;23(1A):275-81.

137. Okunieff P, Morgan D, Niemierko A, Suit HD. Radiation dose-response of human tumors. *International Journal of Radiation Oncology Biology Physics*. 1995;32(4):1227-37.
138. Kranjc S, Cemazar M, Grosel A, Sentjurc M, Sersa G. Radiosensitising effect of electrochemotherapy with bleomycin in LPB sarcoma cells and tumors in mice. *Bmc Cancer*. 2005;5.
139. Kranjc S, Tevz G, Kamensek U, Vidic S, Cemazar M, Sersa G. Radiosensitizing Effect of Electrochemotherapy in a Fractionated Radiation Regimen in Radiosensitive Murine Sarcoma and Radioresistant Adenocarcinoma Tumor Model. *Radiation Research*. 2009;172(6):677-85.
140. Persson BRR, Bauréus Koch C, Grafström G, Ceberg C, Nittby H, Widegren B, Salford LG. Tumour response from immunization with interferon-gamma (IFN $\gamma$ ) transfected syngeneic tumour cells combined with radiation therapy in rats with contra-lateral tumours. *Cancer Therapy* 2010;8A (on line [www.cancer-therapy.org](http://www.cancer-therapy.org))).
141. Persson BRR, Koch CB, Grafstrom G, Ceberg C, Af Rosenschold PM, Nittby H, Widegren B, Salford LG. Radiation Immunomodulatory Gene Tumor Therapy of Rats with Intracerebral Glioma Tumors. *Radiation Research*. 2010;173(4):433-40.
142. Persson BRR. Radiation Immune Modulation Therapy of Glioma, . In: Chen CC, editor. *Advances in the Biology, Imaging and Therapies for Glioblastoma*,. Vienna: InTech; 2011. p. 363-86.
143. Ceberg C, Persson BRR. Co-operative radio-immune-stimulating cancer therapy. *Trends in Cancer Reseach*. 2013;9:87 - 108.
144. Kass GE, Orrenius S. Calcium signaling and cytotoxicity. *Environmental health perspectives*. 1999;107 Suppl 1(Suppl 1):25-35.
145. Orrenius S, Gogvadze V, Zhivotovsky B. Calcium and mitochondria in the regulation of cell death. *Biochemical and Biophysical Research Communications*. 2015;460(1):72-81.
146. Persson BRR. The effect of high voltage pulses at various calcium concentrations in seeds of *Sinapsus* Unpublished results. 1995.
147. Persson B, Henriksson P, Nybrant T, Mattsson B, inventors; Zero Weed AB, assignee. Method and device for weed control (US 6,237,278 B1, 2001) Sweden patent PTC/ SE 96/01068. 1996 2/20/1995
148. Hofmann F, Ohnimus H, Scheller C, Strupp W, Zimmermann U, Jassoy C. Electric field pulses can induce apoptosis. *Journal of Membrane Biology*. 1999;169(2):103-9.

149. Frandsen SK, Gissel H, Hojman P, Eriksen J, Gehl J. Calcium electroporation in three cell lines: a comparison of bleomycin and calcium, calcium compounds, and pulsing conditions. *Biochimica Et Biophysica Acta-General Subjects*. 2014;1840(3):1204-8.
150. Frandsen SK, Gissel H, Hojman P, Tramm T, Eriksen J, Gehl J. Direct Therapeutic Applications of Calcium Electroporation to Effectively Induce Tumor Necrosis. *Cancer Research*. 2012;72(6):1336-41.
151. Frandsen SK, Kruger MB, Mangalanathan UM, Tramm T, Mahmood F, Novak I, Gehl J. Normal and Malignant Cells Exhibit Differential Responses to Calcium Electroporation. *Cancer Research*. 2017;77(16):4389-401.
152. Nanda GS, Sun FX, Hofmann GA, Hoffman RM, Dev SB. Electroporation enhances therapeutic efficacy of anticancer drugs: Treatment of human pancreatic tumor in animal model. *Anticancer Research*. 1998;18(3A):1361-6.
153. Vasquez JL, Gehl J, Hermann GG. Electroporation enhances mitomycin C cytotoxicity on T24 bladder cancer cell line: A potential improvement of intravesical chemotherapy in bladder cancer. *Bioelectrochemistry*. 2012;88:127-33.
154. Vasquez JL, Ibsen P, Lindberg H, Gehl J. In Vitro and In Vivo Experiments on Electrochemotherapy for Bladder Cancer. *Journal of Urology*. 2015;193(3):1009-15.
155. Belehradec JJ, Orłowski S, Poddevin B, Mir LM. Electrochemotherapy potentiation of Bleomycin by local electric pulses. *Journal of Cancer Research and Clinical Oncology*. 1990;116(SUPPL. PART 1):620-.
156. Belehradec M, Domenge C, Luboinski B, Orłowski S, Belehradec J, Mir LM. Electrochemotherapy, A New Antitumor Treatment - 1st Clinical Phase-I-II Trial. *Cancer*. 1993;72:3694-700.
157. Heller R, Jaroszeski MJ, Reintgen DS, Puleo CA, DeConti RC, Gilbert RA, Glass LF. Treatment of cutaneous and subcutaneous tumors with electrochemotherapy using intralesional bleomycin. *Cancer*. 2000;83(1):148-57.
158. Rodriguez-Cuevas S, Barroso-Bravo S, Almanza-Estrada J, Cristobal-Martinez L, Gonzalez-Rodriguez E. Electrochemotherapy in primary and metastatic skin tumors: Phase II trial using intralesional bleomycin. *Archives of Medical Research*. 2001;32(4):273-6.
159. Gothelf A, Mir LM, Gehl J. Electrochemotherapy: results of cancer treatment using enhanced delivery of bleomycin by electroporation. *Cancer Treatment Reviews*. 2003;29(5):371-87.



160. Garbay J-R, Billard V, Bernat C, Mir LM, Morsli N, Robert C. Successful repetitive treatments by electrochemotherapy of multiple unresectable Kaposi sarcoma nodules. *Ejc Supplements*. 2006;4(11):29-31.
161. Gehl J, Sersa G, Garbay J, Soden D, Rudolf Z, Marty M, O'Sullivan G, Geertsen PF, Mir LM. Results of the ESOPE (European Standard Operating Procedures on Electrochemotherapy) study: Efficient, highly tolerable and simple palliative treatment of cutaneous and subcutaneous metastases from cancers of any histology. *Journal of Clinical Oncology*. 2006;24(18):464S-S.
162. Marty M, Sersa G, Garbay JR, Gehl J, Collins CG, Snoj M, Billard V, Geertsen PF, Larkin JO, Miklavcic D, Pavlovic I, Paulin-Kosir SM, Cemazar M, Morsli N, Rudolf Z, Robert C, O'Sullivan GC, Mir LM. Electrochemotherapy - An easy, highly effective and safe treatment of cutaneous and subcutaneous metastases: Results of ESOPE (European Standard Operating Procedures of Electrochemotherapy) study. *Ejc Supplements*. 2006;4(11):3-13.
163. Miklavcic D, Corovic S, Pucihar G, Pavselj N. Importance of tumour coverage by sufficiently high local electric field for effective electrochemotherapy. *Ejc Supplements*. 2006;4(11):45-51.
164. Mir LM. Bases and rationale of the electrochemotherapy. *Ejc Supplements*. 2006;4(11):38-44.
165. Mir LM, Gehl J, Sersa G, Collins CG, Garbay J-R, Billard V, Geertsen PF, Rudolf Z, O'Sullivan GC, Marty M. Standard operating procedures of the electrochemotherapy: Instructions for the use of bleomycin or cisplatin administered either systemically or locally and electric pulses delivered by the Cliniporator (TM) by means of invasive or non-invasive electrodes. *Ejc Supplements*. 2006;4(11):14-25.
166. Sersa G. The state-of-the-art of electrochemotherapy before the ESOPE study; advantages and clinical uses. *Ejc Supplements*. 2006;4(11):52-9.
167. Snoj M, Rudolf Z, Paulin-Kosir SM, Cemazar M, Snoj R, Sersa G. Long lasting complete response in melanoma treated by electrochemotherapy. *Ejc Supplements*. 2006;4(11):26-8.
168. Whelan MC, Larkin JO, Collins CG, Cashman J, Breathnach O, Soden DM, O'Sullivan GC. Effective treatment of an extensive recurrent breast cancer which was refractory to multimodal therapy by multiple applications of electrochemotherapy. *Ejc Supplements*. 2006;4(11):32-4.

169. Gehl J, Sersa G, Matthiessen LW, Muir T, Soden D, Occhini A, Quaglino P, Curatolo P, Campana LG, Kunte C, Clover AJP, Bertino G, Farricha V, Odili J, Dahlstrom K, Benazzo M, Mir LM. Updated standard operating procedures for electrochemotherapy of cutaneous tumours and skin metastases. *Acta Oncologica*. 2018;57(7):874-82.
170. Reinhold U. Electrochemotherapy for primary skin cancer and skin metastasis related to other malignancies. *Anti-Cancer Drugs*. 2011;22(8):711-8.
171. Testori A, Rossi CR, Tosti G. Utility of electrochemotherapy in melanoma treatment. *Current Opinion in Oncology*. 2012;24(2):155-61.
172. Mali B, Jarm T, Snoj M, Sersa G, Miklavcic D. Antitumor effectiveness of electrochemotherapy: A systematic review and meta-analysis. *Ejso*. 2013;39(1):4-16.
173. Schmidt G, Juhasz-Boss I, Solomayer EF, Herr D. Electrochemotherapy in Breast Cancer: A Review of References. *Geburtshilfe Und Frauenheilkunde*. 2014;74(6):557-62.
174. Peris K, Tambone S, Kostaki D, Varrassi E, Fagnoli MC. Treatments of advanced basal cell carcinoma: a review of the literature. *Giornale Italiano Di Dermatologia E Venereologia*. 2016;151(1):77-86.
175. Campana LG, Testori A, Curatolo P, Quaglino P, Mocellin S, Framarini M, Borgognoni L, Ascierio PA, Mozzillo N, Guida M, Bucher S, Rotunno R, Marengo F, De Salvo GL, De Paoli A, Rossi CR, Bonadies A. Treatment efficacy with electrochemotherapy: A multi-institutional prospective observational study on 376 patients with superficial tumors. *Ejso*. 2016;42(12):1914-23.
176. Campana LG, Marconato R, Valpione S, Galuppo S, Alaibac M, Rossi CR, Mocellin S. Basal cell carcinoma: 10-year experience with electrochemotherapy. *Journal of translational medicine*. 2017; 15(122):1-12.
177. Wichtowski M, Murawa D, Kulcenty K, Zaleska K. Electrochemotherapy in Breast Cancer - Discussion of the Method and Literature Review. *Breast Care*. 2017;12(6):409-14.
178. Kalavathy G, Gurumurthy. G., Rajesh K, Saravanan, Asoke M, Persson BRR. Dynamic-ElectroEnhanced Chemotherapy brings relief to palliative patients with large tumour burden. *Trends in Cancer Research*. 2018;13:29-41.
179. Heller R, Jaroszeski MJ, Glass LF, Messina JL, Rapaport DP, DeConti RC, Fenske NA, Gilbert RA, Mir LM, Reintgen DS. Phase

- I/II trial for the treatment of cutaneous and subcutaneous tumors using electrochemotherapy. *Cancer*. 1996;77(5):964-71.
180. Glass LF, Pepine ML, Fenske NA, Jaroszeski M, Reintgen DS, Heller R. Bleomycin-mediated electrochemotherapy of metastatic melanoma. *Archives of Dermatology*. 1996;132(11):1353-7.
  181. Barre FX, Mir LM, Lecluse Y, Harel-Bellan A. Highly efficient oligonucleotide transfer into intact yeast cells using square-wave pulse electroporation. *Biotechniques*. 1998;25(2):294-6.
  182. Rols MP, Bachaud JM, Giraud P, Chevreau C, Roche H, Teissie J. Electrochemotherapy of cutaneous metastases in malignant melanoma. *Melanoma Research*. 2000;10(5):468-74.
  183. Gehl J, Geertsen PF. Efficient palliation of haemorrhaging malignant melanoma skin metastases by electrochemotherapy. *Melanoma Research*. 2000;10(6):585-9.
  184. Gehl J, Geertsen PF. Palliation of haemorrhaging and ulcerated cutaneous tumours using electrochemotherapy. *Ejc Supplements*. 2006;4(11):35-7.
  185. Byrne CM, Thompson JF. Role of electrochemotherapy in the treatment of metastatic melanoma and other metastatic and primary skin tumors. *Expert Review of Anticancer Therapy*. 2006;6(5):671-8.
  186. Byrne CM, Thompson JF, Johnston H, Hersey P, Quinn MJ, Hughes TM, McCarthy WH. Treatment of metastatic melanoma using electroporation therapy with bleomycin (electrochemotherapy). *Melanoma Research*. 2005;15(1):45-51.
  187. Snoj M, Cemazar M, Kolar BS, Sersa G. Effective treatment of multiple unresectable skin melanoma Metastases by electrochemotherapy. *Croatian Medical Journal*. 2007;48(3):391-5.
  188. Kis E, Szegesi I, Ocsai H, Gyulai R, Kemeny L, Olah J. Electrochemotherapy of melanoma cutaneous metastases. *Orvosi Hetilap*. 2010;151(3):96-101.
  189. Kis E, Olah J, Ocsai H, Baltas E, Gyulai R, Kemeny L, Horvath AR. Electrochemotherapy of Cutaneous Metastases of Melanoma-A Case Series Study and Systematic Review of the Evidence. *Dermatologic Surgery*. 2011;37(6):816-24.
  190. Kreuter A, van Eijk T, Lehmann P, Fischer M, Horn T, Assaf C, Schley G, Herbst R, Kellner I, Weisbrich C, Hyun J, Wieland U, Schlaak M, Rubben A, Lommel K. Electrochemotherapy in advanced skin tumors and cutaneous metastases - a retrospective multicenter analysis. *Journal Der Deutschen Dermatologischen Gesellschaft*. 2015;13(4):308-16.

191. Kunte C, Letule V, Gehl J, Dahlstroem K, Curatolo P, Rotunno R, Muir T, Occhini A, Bertino G, Powell B, Saxinger W, Lechner G, Liew SH, Pritchard-Jones R, Rutkowski P, Zdzienicki M, Mowatt D, Sykes AJ, Orlando A, Mitsala G, Rossi CR, Campana L, Brizio M, de Terlizzi F, Quaglino P, Odili J, Insp ECTINS. Electrochemotherapy in the treatment of metastatic malignant melanoma: a prospective cohort study by InspECT. *British Journal of Dermatology*. 2017;176(6):1475-85.
192. Domenge C, Orlowski S, Belehradek J, Jr., De Baere T, Schwaab G, Luboinski B, Mir LM. Phase I-II treatment of large permeation nodules of head and neck squamous cell carcinoma (HNSCC) and breast adenocarcinoma (BA) by electrochemotherapy (ECT). *Proceedings of the American Association for Cancer Research Annual Meeting*. 1995;36(0):248-.
193. Domenge C, Orlowski S, Luboinski B, DeBaere T, Schwaab G, Belehradek J, Mir LM. Antitumor electrochemotherapy - New advances in the clinical protocol. *Cancer*. 1996;77(5):956-63.
194. Heller R, Gilbert R, Jaroszeski MJ. Clinical applications of electrochemotherapy. *Advanced Drug Delivery Reviews*. 1999;35(1):119-29.
195. Burian M, Formanek M, Regele H. Electroporation therapy in head and neck cancer. *Acta Oto-Laryngologica*. 2003;123(2):264-8.
196. Peycheva E, Daskalov I. Electrochemotherapy of skin tumours: comparison of two electroporation protocols. *Journal of BUON : official journal of the Balkan Union of Oncology*. 2004;9(1):47-50.
197. Bloom DC, Goldfarb PM. The role of intratumour therapy with electroporation and bleomycin in the management of advanced squamous cell carcinoma of the head and neck. *Ejso*. 2005;31(9):1029-35.
198. Tijink BM, De Bree R, Van D, Leemans CR. How we do it: Chemo-electroporation in the head and neck for otherwise untreatable patients. *Clinical Otolaryngology*. 2006;31(5):447-51.
199. Burian M, Plath T. Electrochemotherapy for treatment of oral squamous cell carcinoma - a phase IV study. *Oral Oncology*. 2007;117-8.
200. Larkin JO, Collins CG, Aarons S, Tangney M, Whelan M, O'Reily S, Breathnach O, Soden DM, O'Sullivan GC. Electrochemotherapy - Aspects of preclinical development and early clinical experience. *Annals of Surgery*. 2007;245(3):469-79.
201. Campana LG, Mocellin S, Basso M, Puccetti O, De Salvo GL, Chiarion-Sileni V, Vecchiato A, Corti L, Rossi CR, Nitti D.

- Bleomycin-Based Electrochemotherapy: Clinical Outcome from a Single Institution's Experience with 52 Patients. *Annals of Surgical Oncology*. 2009;16(1):191-9.
202. Gargiulo M, Moio M, Monda G, Parascandolo S, Cubicciotti G. Electrochemotherapy: Actual Considerations and Clinical Experience in Head and Neck Cancers. *Annals of Surgery*. 2010;251(4):773-.
203. Landstrom FJ, Nilsson COS, Crafoord S, Reizenstein JA, Adamsson G-BM, Lofgren LA. Electroporation Therapy of Skin Cancer in the Head and Neck Area. *Dermatologic Surgery*. 2010;36(8):1245-50.
204. Landstrom FJ, Nilsson COS, Reizenstein JA, Nordqvist K, Adamsson G-B, Lofgren AL. Electroporation therapy for T1 and T2 oral tongue cancer. *Acta Oto-Laryngologica*. 2011;131(6):660-4.
205. Matthiessen LW, Chalmers RL, Sainsbury DCG, Veeramani S, Kessell G, Humphreys AC, Bond JE, Muir T, Gehl J. Management of cutaneous metastases using electrochemotherapy. *Acta Oncologica*. 2011;50(5):621-9.
206. Matthiessen LW, Johannesen HH, Hendel HW, Moss T, Kamby C, Gehl J. Electrochemotherapy for large locoregional recurrence of breast cancer: Results from a phase II clinical trial showing efficacy in heavily pretreated patients. *Journal of Clinical Oncology*. 2011;29(15).
207. Marengo F, Nardo T, Savoia P, Bernengo MG. Effectiveness of electrochemotherapy in treatment of a recurrent squamous cell carcinoma of the scalp. *European Journal of Dermatology*. 2011;21(4):618-9.
208. Skarlatos I, Kyrgias G, Mosa E, Provatopoulou X, Spyrou M, Theodorou K, Lepouras A, Gounaris A, Koukourakis M. Electrochemotherapy in Cancer Patients: First Clinical Trial in Greece. *In Vivo*. 2011;25(2):265-74.
209. Mevio N, Bertino G, Occhini A, Scelsi D, Tagliabue M, Mura F, Benazzo M. Electrochemotherapy for the treatment of recurrent head and neck cancers: preliminary results. *Tumori*. 2012;98(3):308-13.
210. Gargiulo M, Papa A, Capasso P, Moio M, Cubicciotti E, Parascandolo S. Electrochemotherapy for Non-Melanoma Head and Neck Cancers Clinical Outcomes in 25 Patients. *Annals of Surgery*. 2012;255(6):1158-64.
211. Benevento R, Vicidomin iA, Padovano SV, Renzulli M, Di Nardo D, Canonico S, Santoriello A. Electrochemotherapy of head and neck cancer in elderly patients: a preliminary report. *BMC Surg*;13(Suppl 1):A5. 2013;13(Suppl 1):A5.((Suppl 1 :A5).

212. Macri GF, Greco A, Gallo A, Fusconi M, Marinelli C, de Vincentiis M. Use of electrochemotherapy in a case of neck skin metastasis of oral squamous cell carcinoma: Case report and considerations. *Head and Neck-Journal for the Sciences and Specialties of the Head and Neck*. 2014;36(9):E86-E90.
213. Solari N, Spagnolo F, Ponte E, Quaglia A, Lillini R, Battista M, Queirolo P, Cafiero F. Electrochemotherapy for the Management of Cutaneous and Subcutaneous Metastasis: A Series of 39 Patients Treated With Palliative Intent. *J Surg Oncol*. 2014;109(3):270-4.
214. Seccia V, Muscatello L, Dallan I, Bajraktari A, Briganti T, Ursino S, Galli L, Falcone A, Sellari-Franceschini S. Electrochemotherapy and Its Controversial Results in Patients with Head and Neck Cancer. *Anticancer Research*. 2014;34(2):967-72.
215. Campana LG, Mali B, Sersa G, Valpione S, Giorgi CA, Strojan P, Miklavcic D, Rossi CR. Electrochemotherapy in non-melanoma head and neck cancers: a retrospective analysis of the treated cases. *British Journal of Oral & Maxillofacial Surgery*. 2014;52(10):957-64.
216. Landstrom FJ, Reizenstein JA, Nilsson COS, von Beckerath M, Lofgren AL, Adamsson GB, Moller C. Electrochemotherapy - possible benefits and limitations to its use in the head and neck region. *Acta Oto-Laryngologica*. 2015;135(1):90-5.
217. Landstrom FJ, Reizenstein J, Adamsson GB, Von Beckerath M, Moller C. Long-term follow-up in patients treated with curative electrochemotherapy for cancer in the oral cavity and oropharynx. *Acta Oto-Laryngologica*. 2015;135(10):1070-8.
218. Domanico R, Trapasso S, Santoro M, Pingitore D, Allegra E. Electrochemotherapy in combination with chemoradiotherapy in the treatment of oral carcinomas in advanced stages of disease: efficacy, safety, and clinical outcomes in a small number of selected cases. *Drug Design Development and Therapy*. 2015;9:1185-91.
219. Quaglino P, Matthiessen LW, Curatolo P, Muir T, Bertino G, Kunte C, Odili J, Rotunno R, Humphreys AC, Letul V, Marengo F, Cuthbert C, Albret R, Benazzo M, De Terlizzi F, Gehl J. Predicting patients at risk for pain associated with electrochemotherapy. *Acta Oncologica*. 2015;54(3):298-306.
220. Campana LG, Bonadies A, Curatolo P, Quaglino P, Mocellin S, Framarini M, Gerlini G, Ascierio P, Guida M, Bucher S, Rotunno R, Marengo F, De Salvo GL, Testori A, Angela DP, Rossi CR, Intergp I-GIM. Treatment efficacy with electrochemotherapy: a multi-

- institutional prospective observational study on 376 patients with superficial tumors. *Melanoma Research*. 2016;26:E9-E.
221. Rotunno R, Marengo F, Ribero S, Calvieri S, Amerio P, Curatolo P, Quaglino P. Electrochemotherapy in non-melanoma head and neck skin cancers: a three-center experience and review of the literature. *Giornale Italiano Di Dermatologia E Venereologia*. 2016;151(6): 610-8.
222. Bertino G, Sersa G, De Terlizzi F, Occhini A, Plaschke CC, Groselj A, Langdon C, Grau JJ, McCaul JA, Heuveling D, Cemazar M, Stojan P, de Bree R, Leemans CR, Wessel I, Gehl J, Benazzo M. European Research on Electrochemotherapy in Head and Neck Cancer (EURECA) project: Results of the treatment of skin cancer. *European Journal of Cancer*. 2016;63:41-52.
223. Di Monta G, Caraco C, Simeone E, Grimaldi AM, Marone U, Di Marzo M, Vanella V, Festino L, Palla M, Mori S, Mozzillo N, Ascierto PA. Electrochemotherapy efficacy evaluation for treatment of locally advanced stage III cutaneous squamous cell carcinoma: a 22-cases retrospective analysis. *Journal of Translational Medicine*. 2017;15.
224. Plaschke CC, Johannesen HH, Hansen RH, Hendel HW, Kiss K, Gehl J, Wessel I. The DAHANCA 32 study: Electrochemotherapy for recurrent mucosal head and neck cancer. *Head and Neck-Journal for the Sciences and Specialties of the Head and Neck*. 2019;41(2):329-39.
225. Wahl RL, Jacene H, Kasamon Y, Lodge MA. From RECIST to PERCIST: Evolving Considerations for PET response criteria in solid tumors. *J Nucl Med* 2009;50(Suppl 1):122S–50S.
226. Allegretti JP, Panje W-H. Electroporation Therapy for Head and Neck Cancer Including Carotid Artery Involvement The *Laryngoscope*. 2001;111(1):54-6.
227. Plaschke CC, Bertino G, McCaul JA, Grau JJ, de Bree R, Sersa G, Occhini A, Groselj A, Langdon C, Heuveling DA, Cemazar M, Stojan P, Leemans CR, Benazzo M, De Terlizzi F, Wessel I, Gehl J. European Research on Electrochemotherapy in Head and Neck Cancer (EURECA) project: Results from the treatment of mucosal cancers. *European Journal of Cancer*. 2017;87:172-81.
228. Matthiessen LW, Kamby C, Hendel HW, Johannesen HH, Gehl J. Ongoing trial of electrochemotherapy as palliative treatment for chest wall recurrence of breast cancer. *Journal of Clinical Oncology*. 2010;28(15).

229. Matthiessen LW, Johannesen HH, Hendel HW, Moss T, Kamby C, Gehl J. Electrochemotherapy for large cutaneous recurrence of breast cancer: A phase II clinical trial. *Acta Oncologica*. 2012;51(6):713-21.
230. Benevento R, Santoriello A, Perna G, Canonico S. Electrochemotherapy of cutaneous metastases from breast cancer in elderly patients: a preliminary report. *Bmc Surgery*. 2012;12.
231. Cabula C, Campana LG, Grilz G, Galuppo S, Bussone R, De Meo L, Bonadies A, Curatolo P, De Laurentiis M, Renne M, Valpione S, Fabrizio T, Solari N, Guida M, Santoriello A, D'Aiuto M, Agresti R. Electrochemotherapy in the Treatment of Cutaneous Metastases from Breast Cancer: A Multicenter Cohort Analysis. *Annals of Surgical Oncology*. 2015;22:S442-S50.
232. Wichtowski M, Potocki P, Kufel-Grabowska J, Streb J, Murawa D. Electrochemotherapy in the Treatment of Massive, Multisite Breast Cancer Metastasis to the Skin and Subcutaneous Tissue: A Case Report. *Breast Care*. 2016;11(5):353-5.
233. Campana LG, Galuppo S, Valpione S. Treatment of cutaneous metastases of breast cancer with electrochemotherapy: what is the magnitude of clinical benefit? *Breast Cancer Research and Treatment*. 2017;163(2):399-401.
234. Bourke MG, Salwa SP, Sadadcharam M, Whelan MC, Forde PF, Larkin JO, Collins CG, O'Reilly S, O'Sullivan GC, Clover AJ, Soden DM. Effective treatment of intractable cutaneous metastases of breast cancer with electrochemotherapy: Ten-year audit of single centre experience. *Breast Cancer Research and Treatment*. 2017;161(2):289-97.
235. Wichtowski M, Nowaczyk P, Kocur J, Murawa D. Irreversible electroporation in the treatment of locally advanced pancreas and liver metastases of colorectal carcinoma. *Wspolczesna Onkologia-Contemporary Oncology*. 2016;20(1):39-44.
236. Matthiessen LW, Keshtgar M, Curatolo P, Kunte C, Grischke E-M, Odili J, Muir T, Mowatt D, Clover JP, Liew SH, Dahlstroem K, Newby J, Letulé V, Stauss E, Humphreys A, Banerjee S, Klein A, Rotunno R, de Terlizzi F, Gehl J. Original Study: Electrochemotherapy for Breast Cancer—Results From the INSPECT Database. *Clinical Breast Cancer*. 2018; 18(5): E909-E917.
237. Rebersek M, Cufer T, Cemazar M, Kranjc S, Sersa G. Electrochemotherapy with cisplatin of cutaneous tumor lesions in breast cancer. *Anti-Cancer Drugs*. 2004;15(6):593-7.



238. Glass LF, Jaroszeski M, Gilbert R, Reintgen DS, Heller R. Intralesional bleomycin-mediated electrochemotherapy in 20 patients with basal cell carcinoma. *Journal of the American Academy of Dermatology*. 1997;37(4):596-9.
239. Heller R, Gilbert R, Jaroszeski MJ. Clinical trials for solid tumors using electrochemotherapy. *Methods in molecular medicine*. 2000;37:137-56.
240. Fantini F, Gualdi G, Cimitan A, Giannetti A. Metastatic basal cell carcinoma with squamous differentiation - Report of a case with response of cutaneous metastases to electrochemotherapy. *Archives of Dermatology*. 2008;144(9):1186-8.
241. Richetta AG, Curatolo R, D'Epiro S, Mancini M, Mattozzi C, Giancristoforo S, Rotunno R, Calvieri S. Efficacy of electrochemotherapy in ulcerated basal cell carcinoma. *Clinica Terapeutica*. 2011;162(5):443-5.
242. Kis E, Baltas E, Kinyo A, Varga E, Nagy N, Gyulai R, Kemeny L, Olah J. Successful Treatment of Multiple Basaliomas with Bleomycin-based Electrochemotherapy: A Case Series of Three Patients with Gorlin-Goltz Syndrome. *Acta Dermato-Venereologica*. 2012;92(6):648-51.
243. Orr RM. Technology evaluation: Electroporation therapy, Genetronics Inc. *Current Opinion in Molecular Therapeutics*. 2000;2(2):205-10.
244. Peycheva E. Electrochemotherapy of Sarcoma Kaposi (HIV-negative first clinical stage). *Dokladi na B"lgarskata Akademiya na Naukite*. 2001;54(12):101-2.
245. Curatolo P, Mancini M, Ruggiero A, Clerico R, Di Marco P, Calvieri S. Successful treatment of penile Kaposi's sarcoma with electrochemotherapy. *Dermatologic Surgery*. 2008;34(6):839-43.
246. Gualdi G, Monari P, Fantini F, Cesinaro AM, Cimitan A. Electrochemotherapy-induced virus disappearance in HHV-8-positive skin nodules of Kaposi sarcoma: first histological and immunohistochemical demonstration of efficacy. *Journal of the European Academy of Dermatology and Venereology*. 2010;24(2):239-41.
247. Curatolo P, Quaglini P, Marengo F, Mancini M, Nardo T, Mortera C, Rotunno R, Calvieri S, Bernengo MG. Electrochemotherapy in the Treatment of Kaposi Sarcoma Cutaneous Lesions: A Two-Center Prospective Phase II Trial. *Annals of Surgical Oncology*. 2012;19(1):192-8.

248. Dotsinsky I, Nikolova B, Peycheva E, Tsoneva I. New modality for electrochemotherapy of surface tumors. *Biotechnology & Biotechnological Equipment*. 2012;26(6):3402-6.
249. Latini A, Bonadies A, Trento E, Bultrini S, Cota C, Solivetti FM, Ferraro C, Ardigo M, Amorosi B, Palamara G, Bucher S, Giuliani M, Cordiali-Fei P, Ensoli F, Di Carlo A. Effective treatment of Kaposi's sarcoma by electrochemotherapy and intravenous bleomycin administration. *Dermatologic Therapy*. 2012;25(2):214-8.
250. Caraco C, Di Monta G, Marone U, Benedetto L, Buonaguro F, Tornesello M, Mozzillo N. Cutaneous Kaposi Sarcoma Correlated with HHV-8 virus KSHV Infection Treated with Electrochemotherapy: A Single Institution Experience. *Annals of Surgical Oncology*. 2013;20:S125-S.
251. Di Monta G, Caraco C, Benedetto L, La Padula S, Marone U, Tornesello ML, Buonaguro FM, Simeone E, Ascierio PA, Mozzillo N. Electrochemotherapy as "new standard of care" treatment for cutaneous Kaposi's sarcoma. *Ejso*. 2014;40(1):61-6.
252. Rotunno R, Deterlizzi F, Ribero S, Campana L, Quaglino P, Kunte C, Liew SH, Odili J, Gehl J, Curatolo P. Prospective pilot study evaluating the effectiveness of electrochemotherapy using reduced dosages of intravenous bleomycin. *Journal of the European Academy of Dermatology and Venereology*. 2017;31:36-7.
253. Starita N, Di Monta G, Cerasuolo A, Marone U, Anniciello AM, Botti G, Buonaguro L, Buonaguro FM, Tornesello ML. Effect of electrochemotherapy on human herpesvirus 8 kinetics in classic Kaposi sarcoma. *Infectious Agents and Cancer*. 2017;12.
254. Campana LG, Bianchi G, Mocellin S, Valpione S, Campanacci L, Brunello A, Donati D, Sieni E, Rossi CR. Electrochemotherapy Treatment of Locally Advanced and Metastatic Soft Tissue Sarcomas: Results of a Non-Comparative Phase II Study. *World Journal of Surgery*. 2014;38(4):813-22.
255. Gasbarrini A, Campos WK, Campanacci L, Boriani S. Electrochemotherapy to Metastatic Spinal Melanoma A Novel Treatment of Spinal Metastasis? *Spine*. 2015;40(24):E1340-E6.
256. Bianchi G, Campanacci L, Ronchetti M, Donati D. Electrochemotherapy in the Treatment of Bone Metastases: A Phase II Trial. *World Journal of Surgery*. 2016;40(12):3088-94.
257. Edhemovic I, Brecelj E, Gasljevic G, Music MM, Gorjup V, Mali B, Jarm T, Kos B, Pavliha D, Kuzmanov BG, Cemazar M, Snoj M, Miklavcic D, Gadzijev EM, Sersa G. Intraoperative

- Electrochemotherapy of Colorectal Liver Metastases. *J Surg Oncol*. 2014;110(3):320-7.
258. Gasljevic G, Edhemovic I, Cemazar M, Breclj E, Gadzijev EM, Music MM, Sersa G. Histopathological findings in colorectal liver metastases after electrochemotherapy. *Plos One*. 2017;12(7).
259. Tarantino L, Busto G, Nasto A, Fristachi R, Cacace L, Talamo M, Accardo C, Bortone S, Gallo P, Tarantino P, Nasto RA, Di Minno MND, Ambrosino P. Percutaneous electrochemotherapy in the treatment of portal vein tumor thrombosis at hepatic hilum in patients with hepatocellular carcinoma in cirrhosis: A feasibility study. *World Journal of Gastroenterology*. 2017;23(5):906-18.
260. Coletti L, Battaglia V, De Simone P, Turturici L, Bartolozzi C, Filipponi F. Safety and feasibility of electrochemotherapy in patients with unresectable colorectal liver metastases: A pilot study. *International Journal of Surgery*. 2017;44:26-32.
261. Marone U, Caraco C, Anniciello AM, Di Monta G, Chiofalo MG, Di Cecilia ML, Mozzillo N. Metastatic eccrine porocarcinoma: report of a case and review of the literature. *World Journal of Surgical Oncology*. 2011;9.
262. Campana LG, Scarpa M, Sommariva A, Bonandini E, Valpione S, Sartore L, Rossi CR. Minimally invasive treatment of peristomal metastases from gastric cancer at an ileostomy site by electrochemotherapy. *Radiology and Oncology*. 2013;47(4):370-5.
263. Grosej A, Kos B, Cemazar M, Urbancic J, Kragelj G, Bosnjak M, Veberic B, Strojjan P, Miklavcic D, Sersa G. Coupling treatment planning with navigation system: a new technological approach in treatment of head and neck tumors by electrochemotherapy. *Biomedical Engineering Online*. 2015;14.
264. Schiavii MC, Di Tucci C, Rotunno R, Palaia I, Di Donato V, Marchetti C, Colagiovanni V, Salerno L, Curatolo P, Muzii L, Monti M, Panici PB. Skin metastases from endometrial cancer treated with electrochemotherapy: case report and review of literature. *European Journal of Gynaecological Oncology*. 2017;38(5):800-5.
265. Klein N, Gunther E, Zapf S, El-Idrissi R, Atta J, Stehling M. Prostate cancer infiltrating the bladder sphincter successfully treated with Electrochemotherapy: a case report. *Clinical Case Reports*. 2017;5(12):2127-32.
266. Granata V, Fusco R, Piccirillo M, Palaia R, Lastoria S, Petrillo A, Izzo F. Feasibility and safety of intraoperative electrochemotherapy in locally advanced pancreatic tumor: a preliminary experience. *European Journal of Inflammation*. 2014;12(3):467-77.

267. Tafuto S, von Arx C, De Divitiis C, Maura CT, Palaia R, Albino V, Fusco R, Membrini M, Petrillo A, Granata V, Izzo F, Multidiscipli ECE. Electrochemotherapy as a new approach on pancreatic cancer and on liver metastases. *International Journal of Surgery*. 2015;21:S78-S82.
268. Bimonte S, Leongito M, Granata V, Barbieri A, del Vecchio V, Falco M, Nasto A, Albino V, Piccirillo M, Palaia R, Amore A, di Giacomo R, Lastoria S, Setola SV, Fusco R, Petrillo A, Izzo F. Electrochemotherapy in pancreatic adenocarcinoma treatment: pre-clinical and clinical studies. *Radiology and Oncology*. 2016;50(1): 14-20.
269. Jahangeer S, Forde P, Soden D, Hinchion J. Review of current thermal ablation treatment for lung cancer and the potential of electrochemotherapy as a means for treatment of lung tumours. *Cancer Treatment Reviews*. 2013;39(8):862-71.
270. Sersa G, Stabuc B, Cemazar M, Jancar B, Miklavcic D, Rudolf Z. Electrochemotherapy with cisplatin: Potentiation of local cisplatin antitumour effectiveness by application of electric pulses in cancer patients. *European Journal of Cancer*. 1998;34(8):1213-8.
271. Sersa G, Stabuc B, Cemazar M, Miklavcic D, Rudolf Z. Electrochemotherapy with cisplatin: Clinical experience in malignant melanoma patients. *Clinical Cancer Research*. 2000;6(3): 863-7.
272. Sersa G, Stabuc B, Cemazar M, Miklavcic D, Rudolf Z. Electrochemotherapy with cisplatin: the systemic antitumour effectiveness of cisplatin can be potentiated locally by the application of electric pulses in the treatment of malignant melanoma skin metastases. *Melanoma Research*. 2000;10(4):381-5.
273. Snoj M, Rudolf Z, Cemazar M, Jancar B, Sersa G. Successful sphincter-saving treatment of anorectal malignant melanoma with electrochemotherapy, local excision and adjuvant brachytherapy. *Anti-Cancer Drugs*. 2005;16(3):345-8.
274. Sersa G, Cemazar M., Rudolf Z. Electrochemotherapy: advantages and drawbacks in treatment of cancer patients. *Cancer Therapy*. 2003;1:133-42.
275. Andersen MH, Gehl J, Reker S, Geertsen P, Becker JC, Straten PT. Concomitant administration of interleukin-2 during therapeutic vaccinations against cancer: The good, the bad or the evil? (vol 23, pg 5265, 2005). *Journal of Clinical Oncology*. 2005;23(27):6812-.
276. Andersen MH, Reker S, Straten PT, Gehl J, Geertsen P, Becker JC. Concomitant administration of interleukin-2 during therapeutic

- vaccinations against cancer: The good, the bad, or the evil? *Journal of Clinical Oncology*. 2005;23(22):5265-7.
277. Andersen MH, Gehl J, Reker S, Pedersen LO, Becker JC, Geertsen P, Straten PT. Dynamic changes of specific T cell responses to melanoma correlate with IL-2 administration. *Seminars in Cancer Biology*. 2003;13(6):449-59.
278. Dhillon P. OncoSec Medical Incorporated. *Human Vaccines & Immunotherapeutics*. 2016;12(10):2488-90.
279. Lee SH, Danishmalik SN, Sin JI. DNA vaccines, electroporation and their applications in cancer treatment. *Human Vaccines & Immunotherapeutics*. 2015;11(8):1889-900.
280. Patel PM, Ottensmeier CH, Mulatero C, Lorigan P, Plummer R, Pandha H, Elsheikh S, Hadjimichael E, Villasanti N, Adams SE, Cunnell M, Metheringham RL, Brentville VA, Machado L, Daniels I, Gijon M, Hannaman D, Durrant LG. Targeting gp100 and TRP-2 with a DNA vaccine: Incorporating T cell epitopes with a human IgG1 antibody induces potent T cell responses that are associated with favourable clinical outcome in a phase I/II trial. *Oncoimmunology*. 2018;7(6).
281. Grimaldi AM, Marincola FM, Ascierto PA. Single versus combination immunotherapy drug treatment in melanoma. *Expert Opinion on Biological Therapy*. 2016;16(4):433-41.
282. Mozzillo N, Simeone E, Benedetto L, Curvietto M, Giannarelli D, Gentilcore G, Camerlingo R, Capone M, Madonna G, Festino L, Caraco C, Di Monta G, Marone U, Di Marzo M, Grimaldi AM, Mori S, Ciliberto G, Ascierto PA. Assessing a novel immuno-oncology-based combination therapy: Ipilimumab plus electrochemotherapy. *Oncoimmunology*. 2015;4(6).
283. Heppt MV, Eigentler TK, Kahler KC, Herbst RA, Goppner D, Gambichler T, Ulrich J, Dippel E, Loquai C, Schell B, Schilling B, Schad SG, Schultz ES, Matheis F, Tietze JK, Berking C. Immune checkpoint blockade with concurrent electrochemotherapy in advanced melanoma: a retrospective multicenter analysis. *Cancer Immunology Immunotherapy*. 2016;65(8):951-9.
284. Karaca B, Yayla G, Erdem M, Gürler T. Electrochemotherapy with anti-PD-1 treatment induced durable complete response in heavily pretreated Metastatic melanoma patient. *Anti-Cancer Drugs*. 2018;29(2):190-6.
285. Falk H, Matthiessen LW, Wooler G, Gehl J. Calcium electroporation for treatment of cutaneous metastases; a randomized double-blinded

- phase II study, comparing the effect of calcium electroporation with electrochemotherapy. *Acta Oncologica*. 2018;57(3):311-9.
286. Tsong TY, Su ZD. Biological effects of electric shock and heat denaturation and oxidation of molecules, membranes, and cellular functions. In: Chen CT, Lee RC, Shih JX, Zhong MH, editors. *Occupational Electrical Injury: An International Symposium*. Annals of the New York Academy of Sciences. 8881999. p. 211-32.
287. Zhang L, Rabussay DP. Clinical evaluation of safety and human tolerance of electrical sensation induced by electric fields with non-invasive electrodes. *Bioelectrochemistry*. 2002;56(1-2):233-6.
288. Wallace MS, Ridgeway B, Jun E, Schulteis G, Rabussay D, Zhang L. Topical delivery of lidocaine in healthy volunteers by electroporation, electroincorporation. or iontophoresis: An evaluation of skin anesthesia. *Region Anesth Pain Med*. 2001;26(3):229-38.
289. Miklavcic D, Cemazar M. The effect of high frequency electric pulses on muscle contractions and antitumor efficiency in vivo for a potential use in clinical electrochemotherapy. *Bioelectrochemistry*. 2005;65(2):121-8.
290. Mali B, Jarm T, Corovic S, Paulin-Kosir MS, Cemazar M, Sersa G, Miklavcic D. The effect of electroporation pulses on functioning of the heart. *Medical & Biological Engineering & Computing*. 2008;46(8):745-57.
291. Mali B, Gorjup V, Edhemovic I, Brecej E, Cemazar M, Sersa G, Strazisar B, Miklavcic D, Jarm T. Electrochemotherapy of colorectal liver metastases - an observational study of its effects on the electrocardiogram. *Biomedical Engineering Online*. 2015;14.
292. Frühling P, Nilsson A, Duraj F, Haglund U, Norén A. Single-center nonrandomized clinical trial to assess the safety and efficacy of irreversible electroporation (IRE) ablation of liver tumors in humans: Short to mid-term results. *European Journal of Surgical Oncology*. 2017;43:751-7.
293. Kambakamba P, Bonvini JM, Glenck M, Lopez LC, Pfammatter T, Clavien PA, DeOliveira ML. Intraoperative adverse events during irreversible electroporation-a call for caution. *American Journal of Surgery*. 2016;212(4):715-21.
294. Luo X, Qin Z, Tao H, Shi J, Fang G, Li Z, Zhou X, Chen J, Xu K, Zeng J, Niu L. Original Article: The Safety of Irreversible Electroporation on Nerves Adjacent to Treated Tumors. *World Neurosurgery*. 2017;108:642-9.
295. Carberry GA, Smolock AR, Cristescu M, Wells SA, Ziemlewicz TJ, Lubner MG, Hinshaw JL, Brace CL, Lee FT. Safety and Efficacy of

- Percutaneous Microwave Hepatic Ablation Near the Heart. *Journal of Vascular and Interventional Radiology*. 2017;28(4):490-7.
296. Panescu D, Kroll MW, Stratbucker RA. Medical safety of TASER conducted energy weapon in a hybrid 3-point deployment mode. Conference proceedings : Annual International Conference of the IEEE Engineering in Medicine and Biology Society IEEE Engineering in Medicine and Biology Society Conference. 2009;2009:3191-4.
297. Sun H. Models of ventricular fibrillation probability and neuromuscular stimulation after Taser® use in humans. Madison, Wisconsin, USA: University of Wisconsin; 2007.
298. Lyu T, Wang X, Su Z, Shangguan J, Sun C, Figini M, Wang J, Yaghmai V, Larson AC, Zhang Z. Irreversible electroporation in primary and metastatic hepatic malignancies A review. *Medicine*. 2017;96(17).
299. Camarillo IG, Nichols M, Zheng MM, Sonnenburg D, Sundararajan R. Electro-endocrine combination therapy for aggressive breast tumors. *Journal of Electrostatics*. 2008;66(1-2):99-106.
300. Esmekaya MA, Kayhan H, Yagci M, Coskun A, Canseven AG. Effects of Electroporation on Tamoxifen Delivery in Estrogen Receptor Positive (ER plus ) Human Breast Carcinoma Cells. *Cell Biochemistry and Biophysics*. 2017;75(1):103-9.
301. Mir LM, Roth C, Orłowski S, Quintin-Colonna F, Fradelizi D, Belehradec J, Jr., Kourilsky P. Local and systemic antitumor effects in mice of the combination of electrochemotherapy and an immunotherapy with histoincompatible cells secreting interleukin-2. *Proceedings of the American Association for Cancer Research Annual Meeting*. 1993;34(0):461-.
302. Mir LM, Roth C, Orłowski S, Belehradec J, Fradelizi D, Paoletti C, Kourilsky P. Potentiation of the Antitumoral Effect of Electrochemotherapy by an Immunotherapy with Allogeneic Cells producing Interleukin-2. *Comptes Rendus De L Academie Des Sciences Serie Iii-Sciences De La Vie-Life Sciences*. 1992;314(12): 539-44.
303. Heller LC, Heller R. Electroporation Gene Therapy Preclinical and Clinical Trials for Melanoma. *Current Gene Therapy*. 2010;10(4):312-7.
304. Heppt MV, Eigentler TK, Kaehler KC, Herbst RA, Goepfner D, Gambichler T, Ulrich J, Dippel E, Loquai C, Schell B, Schilling B, Schaed SG, Schultz ES, Matheis F, Tietze JK, Berking C. Immune checkpoint blockade with concurrent electrochemotherapy in

- advanced melanoma: a retrospective multicenter analysis. *Cancer Immunology Immunotherapy*. 2016;65(8):951-9.
305. Sponghini A, Patrucco F, Giorgione R, Farinelli P, Zottarelli F, Rondonotti D, Savoia P. Complete response to anti-PD-1 nivolumab in massive skin metastasis from melanoma: efficacy and tolerability in an elderly patient. *Anti-cancer drugs*. 2017;28(7):808-10
  306. Persson BRR, Koch CB, Grafström G, Ceberg C, af Rosenschöld PM, Widegren B, Salford LG. Survival of rats with N29 brain tumours after irradiation with 5 or 15 Gy and immunization with IFN-gamma secreting tumour cells. *Bmei 2008: Proceedings of the International Conference on Biomedical Engineering and Informatics, Vol 2*. 2008:243-7.
  307. Davalos RV, Mir LM, Rubinsky B. Tissue ablation with irreversible electroporation. *Annals of Biomedical Engineering*. 2005;33(2):223-31.
  308. Kourounis G, Tabet PP, Moris D, Papalambros A, Felekouras E, Georgiades F, Astras G, Petrou A. Irreversible electroporation (Nanoknife (R) treatment) in the field of hepatobiliary surgery: Current status and future perspectives. *Journal of Buon*. 2017;22(1):141-9.
  309. Cannon R, Ellis S, Hayes D, Narayanan G, Martin RCG. Safety and early efficacy of irreversible electroporation for hepatic tumors in proximity to vital structures. *J Surg Oncol*. 2013;107(5):544-9.
  310. Cheung W, Kavnaudias H, Roberts S, Szkandera B, Kemp W, Thomson KR. Irreversible Electroporation for Unresectable Hepatocellular Carcinoma: Initial Experience and Review of Safety and Outcomes. *Technology in Cancer Research & Treatment*. 2013;12(3):233-41.
  311. Kingham TP, Karkar AM, D'Angelica MI, Allen PJ, DeMatteo RP, Getrajdman GI, Sofocleous CT, Solomon SB, Jarnagin WR, Fong YM. Ablation of Perivascular Hepatic Malignant Tumors with Irreversible Electroporation. *J Am Coll Surg*. 2012;215(3):379-87.
  312. Scheffer HJ, Nielsen K, van Tilborg A, Vieveen JM, Bouwman RA, Kazemier G, Niessen HWM, Meijer S, van Kuijk C, van den Tol MP, Meijerink MR. Ablation of colorectal liver metastases by irreversible electroporation: results of the COLDFIRE-I ablate-and-resect study. *European Radiology*. 2014;24(10):2467-75.
  313. Sugimoto K, Moriyasu F, Kobayashi Y, Saito K, Takeuchi H, Ogawa S, Ando M, Sano T, Mori T, Furuichi Y, Nakamura I. Irreversible electroporation for nonthermal tumor ablation in patients with



- hepatocellular carcinoma: initial clinical experience in Japan. *Japanese Journal of Radiology*. 2015;33(7):424-32.
314. Bagla S, Papadouris D. Percutaneous Irreversible Electroporation of Surgically Unresectable Pancreatic Cancer: A Case Report. *Journal of Vascular and Interventional Radiology*. 2012;23(1):142-5.
315. Martin RCG, McFarland K, Ellis S, Velanovich V. Irreversible Electroporation Therapy in the Management of Locally Advanced Pancreatic Adenocarcinoma. *J Am Coll Surg*. 2012;215(3):361-9.
316. Martin RCG, II, McFarland K, Ellis S, Velanovich V. Irreversible Electroporation in Locally Advanced Pancreatic Cancer: Potential Improved Overall Survival. *Annals of Surgical Oncology*. 2013;20:S443-S9.
317. Narayanan G, Hosein PJ, Arora G, Barbery KJ, Froud T, Livingstone AS, Franceschi D, Lima CMR, Yrizarry J. Percutaneous Irreversible Electroporation for Downstaging and Control of Unresectable Pancreatic Adenocarcinoma. *Journal of Vascular and Interventional Radiology*. 2012;23(12):1613-21.
318. Paiella S, Butturini G, Frigerio I, Salvia R, Armatura G, Bacchion M, Fontana M, D'Onofrio M, Martone E, Bassi C. Safety and Feasibility of Irreversible Electroporation (IRE) in Patients with Locally Advanced Pancreatic Cancer: Results of a Prospective Study. *Digestive Surgery*. 2015;32(2):90-7.
319. Sugimoto K, Moriyasu F, Tsuchiya T, Nagakawa Y, Hosokawa Y, Saito K, Tsuchida A, Itoi T. Irreversible Electroporation for Nonthermal Tumor Ablation in Patients with Locally Advanced Pancreatic Cancer: Initial Clinical Experience in Japan. *Internal Medicine*. 2018;57(22):3225-31.
320. Sano MB, Volotskova O, Xing L. Treatment of Cancer In Vitro Using Radiation and High-Frequency Bursts of Submicrosecond Electrical Pulses. *Ieee Transactions on Biomedical Engineering*. 2018;65(4):928-35.
321. Napotnik TB, Rebersek M, Vernier PT, Mali B, Miklavcic D. Effects of high voltage nanosecond electric pulses on eukaryotic cells (in vitro): A systematic review. *Bioelectrochemistry*. 2016;110:1-12.
322. Guo JS, Dong FH, Ding L, Wang KL, Zhang J, Fang J. A novel drug-free strategy of nano-pulse stimulation sequence (NPSS) in oral cancer therapy: In vitro and in vivo study. *Bioelectrochemistry*. 2018;123:26-33.
323. Guo SQ, Jing Y, Burcus NI, Lassiter BP, Tanaz R, Heller R, Beebe SJ. Nano-pulse stimulation induces potent immune responses,

eradicating local breast cancer while reducing distant metastases.  
International Journal of Cancer. 2018;142(3):629-40.

# INDEX

<sup>18</sup>FDG-PET 105, 135

<sup>60</sup>Co-gamma 78, 79

<sup>99m</sup>Tc-DTPA 22, 56, 57, 58

<sup>111</sup>In-Bleomycin 55, 56, 71

## A

Ablation 135, 153, 154, 155, 156,  
167

absorbed energy 4, 19, 45, 46, 52,  
53, 63, 64, 65

AC 2, 14, 34

AC field 10, 11, 14

Adenocarcinoma 54, 70, 90, 115,  
134, 135, 158, 161

Administration 3, 24, 35, 55, 57, 73-  
75, 85, 90-93, 103, 104, 116,  
124, 127, 128, 133, 139, 144,  
161, 166

Admittance 12, 27, 28, 32

Anaesthesia 91, 96, 97, 104, 148,  
149, 150

anticancer drug 3, 69, 72, 75

anti-PD-1 145, 146, 162, 163

## B

Basal cell carcinoma 69, 90, 91, 93,  
124, 125, 127, 136, 137, 138,  
142, 143

Bladder 57, 70, 88

Bleomycin 3, 4, 24, 25, 55, 56, 66,  
69, 70, 71-75, 82-85, 87, 89, 90-  
93, 95, 96, 100-104, 115-117,  
120-122, 124, 125, 127-129,  
131-133, 136, 137, 139, 142,  
145-147, 150, 161, 162, 165,  
166

blood-brain barrier 71

Boron 70

brain tumour 75-78

breast cancer 69, 91, 93, 112, 115-  
123, 136, 137, 139-143, 146,  
158-161, 168

BTX 98, 111-114, 125-127, 129,  
130

## C

Calcium 6, 8, 86, 87, 146, 147, 168

CaCl<sub>2</sub> 147

Cancer therapy 3, 4, 70, 75, 87, 110,  
144, 147, 149, 168, 169

Capacitance 11, 26, 27, 28, 29, 30

Carboplatin 87

CD25 73, 160

CD4 73, 75, 80, 81, 145, 160

Cliniporator 98, 99, 102, 112-114,  
116, 118, 120-123, 126, 127,  
129, 130, 139, 162

Colon 71, 75

Colorectal 70-72, 74, 132, 133, 153,  
167

Complete response 89-97, 100, 102,  
104, 106, 110, 116-118, 124,  
125, 128, 133, 138-141, 146,  
162, 163

Conductance 12, 22, 23, 27, 28, 31,  
32, 36-41, 62

conductance relaxation 23, 38-40

conductivity 9, 10, 12-14, 16, 17,  
19, 22, 28, 29, 36, 41-53, 62, 65

conformational changes 1, 148

correlation 59-66, 108

CT 105, 106, 107, 108, 109, 116

CTL 73, 144, 160

CTLA-4 145, 146, 162, 169

CTX 73, 74, 160, 161

current density 44, 45, 47, 49-51,  
63-65

Cyclophosphamide 73, 74, 160, 161

Cytoplasm 9-11, 26, 148

## D

DAC 76, 77

DC 8, 14, 34, 40, 42

DC field 8

D-EECT 104, 112-114, 120, 122, 123, 157, 158

Dielectric 1, 9, 10, 12, 26, 32, 42, 70, 87, 148

Diffusion 23, 24, 116

diffusion coefficient 23

distribution 44, 47-52, 55, 57

DNA 2, 26, 76, 144, 145, 161, 162, 169

Drug 3, 19, 21, 23, 24, 35, 55, 56, 70, 72, 103, 116, 124, 139, 144, 147, 162, 163

drug delivery 19, 21

drug uptake 11, 55, 57, 66, 72

DTPA 22, 56, 57, 58

## E

ECG 151, 152, 153

ECT 3, 69, 96, 103,

EECT 104, 112-114, 120, 122, 123, 157, 158

electric current 44, 50, 51, 148

electric field 1-3, 4, 7-12, 14, 29, 33, 36, 44, 45, 48, 49, 53, 54, 69, 76, 77, 79, 80, 86, 87, 151, 164

electric potential 7, 8, 9, 48

electric pulses 1-3, 22, 55, 57, 70, 75, 76, 82, 83, 89-92, 95, 96, 100, 115, 116,

124, 138-140, 146, 148, 149, 151, 164, 165, 168

Electrode 44, 48-53, 81, 89, 90, 92, 95, 138, 162, 164

electro-dosimetry 4, 26-54

electrofusion 2

electroporation 1-3, 10-26, 29, 33, 35, 37, 41, 46, 47, 53, 57, 62, 66, 69, 72, 73, 82, 101, 127, 146, 148, 152, 153, 155, 164, 165, 167, 168

electroshock weapon 154, 155

electro-pores 19, 20, 21

endometrial 134, 135, 136

EpECT 3-25, 83, 85, 95, 144, 146, 157, 162, 164-166, 169

EpEChT 3, 69, 73-75, 81, 82, 84, 85, 89-147, 153, 159, 160-166, 169

equivalent circuit 27, 30, 32

Escherichia coli 1

ESOPE 15, 24, 91, 92, 93, 101-104, 112-114, 116-120, 122, 123, 125-131, 133-135, 139, 143, 157-160, 162

ethyl-N-nitrosourea 75

exponential growth 84, 85

exponential pulses 35, 36, 72, 86, 87, 77

exponentially decreasing pulse 16, 17, 18, 54, 69

extracellular space 10, 23, 34

## F

Fibroblast 77, 87, 163

Fibrosarcoma 74

field strength 1, 10-12, 14, 21, 22, 24, 36, 44, 45, 47-50, 53, 57, 58, 60, 62, 64-67, 70, 91, 96, 100, 115, 124, 155, 168

Fischer rat 78, 79, 163

Fourier analysis 15-19

Frequency 10-19, 27-29, 31-37, 42, 43, 91, 92, 96, 100, 115, 124, 149, 150, 153, 154

Fusion 2

## G

gamma camera 55-68

Gastric 133, 135, 136

Glioma 3, 55, 70, 71, 75, 76

Goldman equation 8

GTH 1287 120, 121, 122

## H

Haemoglobin 1, 10

head and neck 3, 69, 89, 90, 100-104, 151, 158, 159  
 healthy tissue 41, 43, 72, 132  
 heart 128, 151, 152, 153, 154, 155  
 hepatic tumours 70, 71  
 hexagonal 92, 133, 162  
 high voltage 1, 2, 26, 77, 78, 81, 86, 149, 163, 164, 167, 168  
 hydrophilic 3, 5, 6, 20

## I

IFN- $\gamma$  75, 76, 77  
 IL-2 74, 144, 161  
 IL-12 144, 161  
 IL-18 75, 76  
 immune therapy 76, 162, 163, 169  
 immune-suppression 77, 166  
 immunomodulating 162  
 Immuno therapy 74, 161  
 Impedance 22, 26-32, 34-37, 41  
 impedance of tissue 26, 29, 35, 36  
 Interleukin 74, 76, 144, 161  
 intra-tumoural 73, 92, 93, 100, 138, 139  
 intravenous 24, 25, 55, 71, 83, 89, 91, 92, 96, 100, 104, 116, 124, 125, 128, 131, 133, 139, 161, 165  
 Ipilimumab 145, 146, 162, 163  
 IRE 2, 22, 26, 39, 153, 154, 155, 167, 168  
 Iridium-192 81, 164  
 Irreversible 2, 22, 26, 39, 153, 154, 155, 167  
 ITIS 12, 13, 42, 43  
 IQWave 112-114, 120-123

## J

Jouan 111-114, 120-123, 126

## K

Kaposi's sarcoma 69, 90, 127, 128, 129, 130, 136  
 Kidney 55, 56, 57

## L

Laplace equation 9, 10  
 Latent Structures 59, 60, 62, 63, 65, 66  
 LCI 33, 62, 63, 66, 67, 68  
 LD50 71, 73  
 Liver 3, 12, 54, 71, 74, 132, 133, 137, 138, 153-155, 167  
 liver metastases 132, 133, 137, 138, 153  
 Loss Change Index 33, 34, 37, 38, 62, 63  
 loss factor 33  
 loss tangent 32, 33, 34, 37, 38, 42  
 lung 74, 87, 116, 135, 136  
 lung cancer 135, 136

## M

malignant melanoma 69, 90, 94-99, 136-143, 145, 146, 162  
 mechanism 73, 85, 144, 160, 168  
 Medpulsar 98, 99, 111, 113, 114, 120-123, 125-127, 129, 130  
 membrane potential 1, 6-12, 20, 87, 148  
 metastases 75, 90, 91, 95, 96, 102, 117, 118, 119, 131-134, 137, 138, 140, 146, 153, 162, 168  
 methyl 71, 76  
 Mexico 98-100, 111, 113, 120-122, 125-127  
 Mir 3, 2, 52, 69, 74, 90, 98, 111, 120, 121, 126, 161, 162  
 Mitomycin 87, 88  
 Modelling 26, 34, 47, 48, 50, 59, 60-62, 64-68  
 molecular weight 24  
 Mr 52  
 MRI 41, 105, 106, 109, 134  
 Muscle 8, 12, 13, 16, 17, 19, 22, 23, 37, 40, 42, 43, 45-49, 51-53, 57, 62, 70, 149-151, 154  
 N  
 N29 75, 76, 78, 79, 80  
 N32 55, 71, 75, 78, 163

- Nanosecond 168  
Nernst potential 6, 7  
Nerve 8, 15, 154, 155, 156  
needle electrode 11, 22, 44, 45, 47,  
48, 51, 62, 92, 100, 116, 132-  
134, 139, 150  
Nivolumab 146, 162, 163  
nude mice 72, 73, 74, 87  
Nyquist Plot 28, 29, 32
- O
- objective response 89, 91, 94-97,  
99-105, 113-119, 122-124, 127,  
128, 130, 137-139, 145, 157,  
159, 162  
oestrogen receptor (ER) 117  
Oxaliplatin 73
- P
- Pain 15, 101, 104, 105, 134, 148,  
149, 150, 153  
Papilloma 71  
Parotid 133-136  
Pancreas 3, 134  
Pancreatic 70, 87, 134, 135, 136,  
167, 168  
Partial Least Square Regression 59  
partial response 90, 94-97, 100, 103,  
104, 109, 111, 116, 117, 118,  
124, 127, 131, 132, 134, 139,  
140, 141  
PCA 59, 107, 108, 109  
PD-1 145, 146, 162, 163, 169  
Permeabilization 1, 14, 26, 34, 39,  
46, 47, 65, 70, 74  
PET 105, 106, 110, 111, 116  
phase angle 32, 33, 34, 62  
Phosphorous 5, 6  
Plate electrode 28, 83, 92, 116, 139,  
165  
PLS 59-68  
Poisson's equation 8  
Potassium 1, 6, 7, 8  
Power 32, 33, 44, 46, 51, 52  
Preclinical 4, 69-88, 169  
primary pulse 48-51
- Principal Component Analysis 59,  
108  
Progressive disease 94, 96, 97, 100-  
102, 108, 118, 119, 127, 137,  
138, 139, 157, 162  
Projection 59, 60, 62, 63, 64, 65, 66,  
67  
Prostate 134-136  
pulse parameters 10, 71, 128  
pulse-train 15-19, 54, 149
- R
- Rabbit 71, 74, 154, 155  
Radiation 52, 69, 76-85, 140, 163-  
169  
radiation therapy 52, 69, 77, 79-85,  
163-166, 168, 169  
rat liver 54, 71  
rectangular pulse 15, 16, 19, 37, 38  
relaxation 10, 22, 23, 38, 39, 40, 41,  
62, 65, 66  
remission 70, 71, 80, 81, 91, 94, 95,  
100-104, 108, 111, 116-119,  
124, 128, 130, 131, 133-135,  
138, 149, 157, 159, 161, 166,  
167  
Resistivity 11-13, 26, 27, 30, 31, 37,  
62  
Resistivity Change Index 37, 62  
Reversible 1, 22, 23, 26, 38, 39, 65,  
66
- S
- Sarcoma 69, 82, 83, 90, 127-131,  
136, 137, 158, 165  
Squamous cell carcinoma 69, 90,  
100-104, 111-114, 123, 136-  
138, 143, 157  
Secreting 74, 75, 76, 77, 161  
Side effects 96, 117, 134, 151  
sinusoidal pulse 18, 19  
skeleton 131, 137  
Sodium 6, 7, 8  
specific absorbed energy 45, 46, 53,  
63, 64, 65  
specific therapeutic effect 76, 77

- specific therapeutic response (STR)
  - 105, 106, 108, 109, 110
- Spindle cell 158
- square wave pulses 69, 72
- Stable disease 91, 94, -97, 102-104,
  - 106, 108-111, 116-119, 128,
  - 130-133, 139
- Statistics 79
- Subcutaneous 3, 55, 69, 70, 75, 76,
  - 79, 80, 81, 89, 96, 100, 102,
  - 103, 115-117, 124, 140, 163,
  - 164, 165
- survival time 70, 79, 167, 168
- sweat gland 133, 134, 135
  
- T
- Tamoxifen 160
- TCD50 82, 83, 165, 166
- Temperature 1, 7, 45, 46, 53, 148
- tension energy 20
- thermal 46, 135, 167
  
- time-constant 28, 35, 86, 87, 167
- T-lymphocyte 74, 80
- Transfection 2
- tumour tissue 12, 13, 14, 16, 17, 43
  
- U
  
- V
- Vaccine 144, 145
- Variable Importance 60, 63, 65, 66,
  - 67
- Vasostatin 74, 161
- VIP 60, 62, 63, 64, 65, 66, 67
  
- W
- Weed 86, 147
- Weighted response 94, 97, 99, 108,
  - 113, 114, 118, 119, 121-123,
  - 126, 127, 130-132, 135-138,
  - 140-143, 160